Evidence-Based Complementary and Alternative Medicine

Standardization and Biological Properties of Functional Herbal Food 2021

Lead Guest Editor: Jianping Chen
Guest Editors: Li Zhang, Miranda Li Xu, and Xiaolong Ji

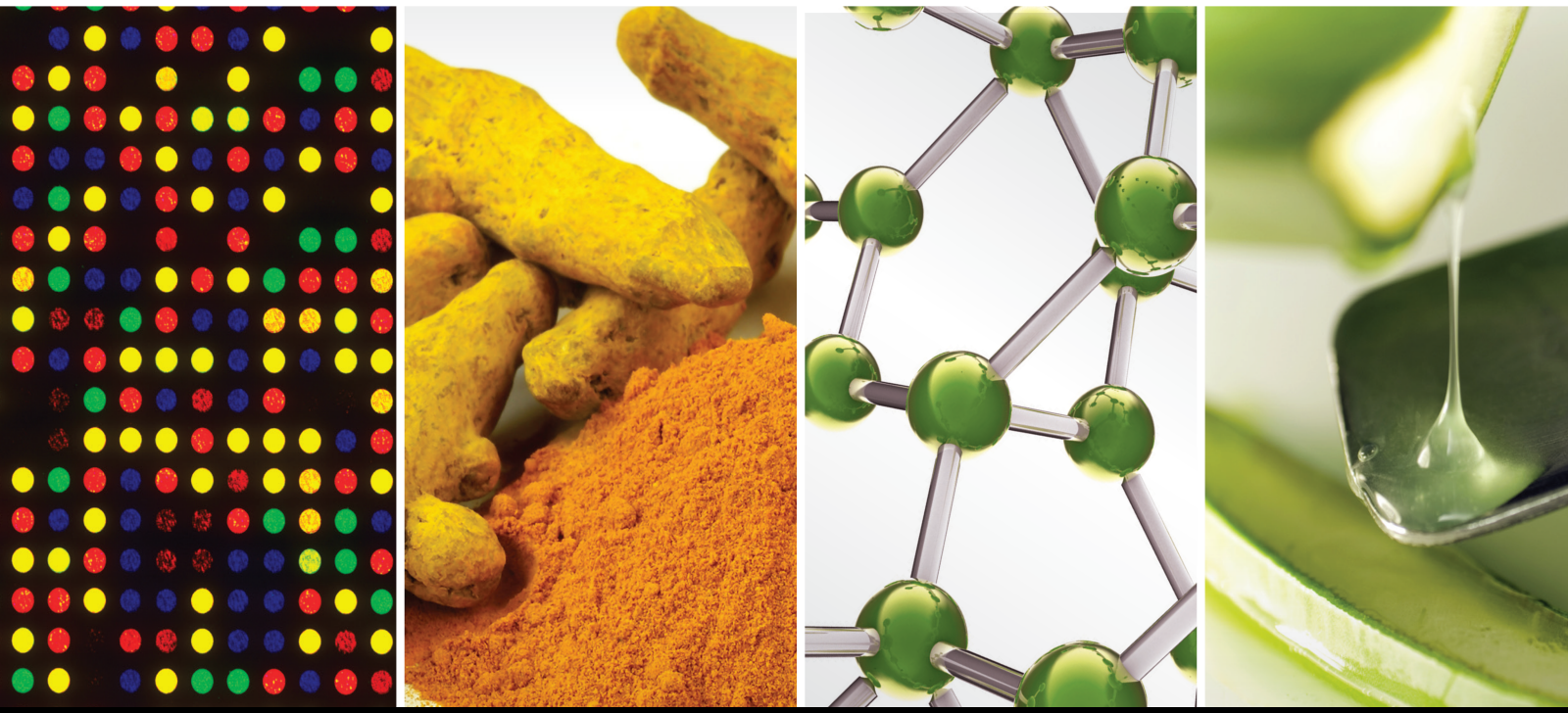

Standardization and Biological Properties of Functional Herbal Food 2021

Evidence-Based Complementary and Alternative Medicine

Standardization and Biological Properties of Functional Herbal Food 2021

Lead Guest Editor: Jianping Chen
Guest Editors: Li Zhang, Miranda Li Xu, and Xiaolong Ji

Copyright © 2021 Hindawi Limited. All rights reserved.

This is a special issue published in “Evidence-Based Complementary and Alternative Medicine.” All articles are open access articles distributed under the Creative Commons Attribution License, which permits unrestricted use, distribution, and reproduction in any medium, provided the original work is properly cited.

Chief Editor

Jian-Li Gao, China

Associate Editors

Hyunsu Bae, Republic of Korea
Raffaele Capasso, Italy
Jae Youl Cho, Republic of Korea
Caigan Du, Canada
Yuewen Gong, Canada
Hai-dong Guo, China
Kuzhuvelil B. Harikumar, India
Ching-Liang Hsieh, Taiwan
Cheorl-Ho Kim, Republic of Korea
Victor Kuete, Cameroon
Hajime Nakae, Japan
Yoshiji Ohta, Japan
Olumayokun A. Olajide, United Kingdom
Chang G. Son, Republic of Korea
Shan-Yu Su, Taiwan
Michał Tomczyk, Poland
Jenny M. Wilkinson, Australia

Academic Editors

Eman A. Mahmoud, Egypt
Ammar AL-Farga, Saudi Arabia
Smail Aazza, Morocco
Nahla S. Abdel-Azim, Egypt
Ana Lúcia Abreu-Silva, Brazil
Gustavo J. Acevedo-Hernández, Mexico
Mohd Adnan, Saudi Arabia
Jose C Adsuar, Spain
Sayeed Ahmad, India
Touqeer Ahmed, Pakistan
Basiru Ajiboye, Nigeria
Bushra Akhtar, Pakistan
Fahmida Alam, Malaysia
Mohammad Jahoor Alam, Saudi Arabia
Clara Albani, Argentina
Ulysses Paulino Albuquerque, Brazil
Mohammed S. Ali-Shtayeh, Palestinian Authority
Ekram Alias, Malaysia
Terje Alraek, Norway
Adolfo Andrade-Cetto, Mexico
Letizia Angiolella, Italy
Makoto Arai, Japan
Daniel Dias Rufino Arcanjo, Brazil
Duygu AĞAGÜNDÜZ, Turkey
Neda Baghban, Iran
Samra Bashir, Pakistan
Rusliza Basir, Malaysia
Jairo Kenupp Bastos, Brazil
Arpita Basu, USA
Mateus R. Beguelini, Brazil
Juana Benedí, Spain
Samira Boulbaroud, Morocco
Mohammed Bourhia, Morocco
Abdelhakim Bouyahya, Morocco
Nunzio Antonio Cacciola, Italy
Francesco Cardini, Italy
María C. Carpinella, Argentina
Harish Chandra, India
Guang Chen, China
Jianping Chen, China
Kevin Chen, USA
Mei-Chih Chen, Taiwan
Xiaojia Chen, Macau
Evan P. Cherniack, USA
Giuseppina Chianese, Italy
Kok-Yong Chin, Malaysia
Lin China, China
Salvatore Chirumbolo, Italy
Hwi-Young Cho, Republic of Korea
Jeong June Choi, Republic of Korea
Jun-Yong Choi, Republic of Korea
Kathrine Bisgaard Christensen, Denmark
Shuang-En Chuang, Taiwan
Ying-Chien Chung, Taiwan
Francisco José Cidral-Filho, Brazil
Daniel Collado-Mateo, Spain
Lisa A. Conboy, USA
Kieran Cooley, Canada
Edwin L. Cooper, USA
José Otávio do Amaral Corrêa, Brazil
Maria T. Cruz, Portugal
Huantian Cui, China
Giuseppe D'Antona, Italy
Ademar A. Da Silva Filho, Brazil
Chongshan Dai, China
Laura De Martino, Italy
Josué De Moraes, Brazil

Arthur De Sá Ferreira, Brazil
Nunziatina De Tommasi, Italy
Marinella De leo, Italy
Gourav Dey, India
Dinesh Dhamecha, USA
Claudia Di Giacomo, Italy
Antonella Di Sotto, Italy
Mario Dioguardi, Italy
Jeng-Ren Duann, USA
Thomas Efferth, Germany
Abir El-Alfy, USA
Mohamed Ahmed El-Esawi, Egypt
Mohd Ramli Elvy Suhana, Malaysia
Talha Bin Emran, Japan
Roger Engel, Australia
Karim Ennouri, Tunisia
Giuseppe Esposito, Italy
Tahereh Eteraf-Oskouei, Iran
Robson Xavier Faria, Brazil
Mohammad Fattahi, Iran
Keturah R. Faurot, USA
Piergiorgio Fedeli, Italy
Laura Ferraro, Italy
Antonella Fioravanti, Italy
Carmen Formisano, Italy
Hua-Lin Fu, China
Liz G Müller, Brazil
Gabino Garrido, Chile
Safoora Gharibzadeh, Iran
Muhammad N. Ghayur, USA
Angelica Gomes, Brazil
Elena González-Burgos, Spain
Susana Gorzalczany, Argentina
Jiangyong Gu, China
Maruti Ram Gudavalli, USA
Jian-You Guo, China
Shanshan Guo, China
Narcís Gusi, Spain
Svein Haavik, Norway
Fernando Hallwass, Brazil
Gajin Han, Republic of Korea
Ihsan Ul Haq, Pakistan
Hicham Harhar, Morocco
Mohammad Hashem Hashempur, Iran
Muhammad Ali Hashmi, Pakistan
Waseem Hassan, Pakistan
Sandrina A. Heleno, Portugal
Pablo Herrero, Spain
Soon S. Hong, Republic of Korea
Md. Akil Hossain, Republic of Korea
Muhammad Jahangir Hossen, Bangladesh
Shih-Min Hsia, Taiwan
Changmin Hu, China
Tao Hu, China
Weicheng Hu, China
Wen-Long Hu, Taiwan
Xiao-Yang (Mio) Hu, United Kingdom
Sheng-Teng Huang, Taiwan
Ciara Hughes, Ireland
Attila Hunyadi, Hungary
Liaqat Hussain, Pakistan
Maria-Carmen Iglesias-Osma, Spain
Amjad Iqbal, Pakistan
Chie Ishikawa, Japan
Angelo A. Izzo, Italy
Satveer Jagwani, USA
Rana Jamous, Palestinian Authority
Muhammad Saeed Jan, Pakistan
G. K. Jayaprakasha, USA
Kyu Shik Jeong, Republic of Korea
Leopold Jirovetz, Austria
Jeeyoun Jung, Republic of Korea
Nurkhalida Kamal, Saint Vincent and the Grenadines
Atsushi Kameyama, Japan
Kyungsu Kang, Republic of Korea
Wenyi Kang, China
Shao-Hsuan Kao, Taiwan
Nasiara Karim, Pakistan
Morimasa Kato, Japan
Kumar Katragunta, USA
Deborah A. Kennedy, Canada
Washim Khan, USA
Bonglee Kim, Republic of Korea
Dong Hyun Kim, Republic of Korea
Junghyun Kim, Republic of Korea
Kyungho Kim, Republic of Korea
Yun Jin Kim, Malaysia
Yoshiyuki Kimura, Japan

Nebojša Kladar, Serbia
Mi Mi Ko, Republic of Korea
Toshiaki Kogure, Japan
Malcolm Koo, Taiwan
Yu-Hsiang Kuan, Taiwan
Robert Kubina, Poland
Chan-Yen Kuo, Taiwan
Kuang C. Lai, Taiwan
King Hei Stanley Lam, Hong Kong
Fanuel Lampiao, Malawi
Ilaria Lampronti, Italy
Mario Ledda, Italy
Harry Lee, China
Jeong-Sang Lee, Republic of Korea
Ju Ah Lee, Republic of Korea
Kyu Pil Lee, Republic of Korea
Namhun Lee, Republic of Korea
Sang Yeoup Lee, Republic of Korea
Ankita Leekha, USA
Christian Lehmann, Canada
George B. Lenon, Australia
Marco Leonti, Italy
Hua Li, China
Min Li, China
Xing Li, China
Xuqi Li, China
Yi-Rong Li, Taiwan
Vuanghao Lim, Malaysia
Bi-Fong Lin, Taiwan
Ho Lin, Taiwan
Shuibin Lin, China
Kuo-Tong Liou, Taiwan
I-Min Liu, Taiwan
Suhuan Liu, China
Xiaosong Liu, Australia
Yujun Liu, China
Emilio Lizarraga, Argentina
Monica Loizzo, Italy
Nguyen Phuoc Long, Republic of Korea
Zaira López , Mexico
Chunhua Lu, China
Ângelo Luís, Portugal
Anderson Luiz-Ferreira, Brazil
Ivan Luzardo Luzardo-Ocampo, Mexico
Michel Mansur Machado, Brazil
Filippo Maggi, Italy
Juraj Majtan, Slovakia
Toshiaki Makino, Japan
Nicola Malafronte, Italy
Giuseppe Malfa, Italy
Francesca Mancianti, Italy
Carmen Mannucci, Italy
Juan M. Manzaneque, Spain
Fatima Martel, Portugal
Carlos H. G. Martins, Brazil
Maulidiani Maulidiani, Malaysia
Andrea Maxia, Italy
Avijit Mazumder, India
Isac Medeiros, Brazil
Ahmed Mediani, Malaysia
Lewis Mehl-Madrona, USA
Ayikoé Guy Mensah-Nyagan, France
Oliver Micke, Germany
Maria G. Miguel, Portugal
Luigi Milella, Italy
Roberto Miniero, Italy
Letteria Minutoli, Italy
Prashant Modi, India
Daniel Kam-Wah Mok, Hong Kong
Changjong Moon, Republic of Korea
Albert Moraska, USA
Mark Moss, United Kingdom
Yoshiharu Motoo, Japan
Yoshiki Mukudai, Japan
Sakthivel Muniyan, USA
Saima Muzammil, Pakistan
Benoit Banga N'guessan, Ghana
Massimo Nabissi, Italy
Siddavaram Nagini, India
Takao Namiki, Japan
Srinivas Nammi, Australia
Krishnadas Nandakumar, India
Vitaly Napadow, USA
Edoardo Napoli, Italy
Jorddy Neves Cruz, Brazil
Marcello Nicoletti, Italy
Eliud Nyaga Mwaniki Njagi, Kenya
Cristina Nogueira, Brazil

Sakineh Kazemi Noureini, Iran
Rômulo Dias Novaes, Brazil
Martin Offenbaecher, Germany
Oluwafemi Adeleke Ojo, Nigeria
Olufunmiso Olusola Olajuyigbe, Nigeria
Luís Flávio Oliveira, Brazil
Mozaniel Oliveira, Brazil
Atolani Olubunmi, Nigeria
Abimbola Peter Oluyori, Nigeria
Timothy Omara, Austria
Chiagoziem Anariochi Otuechere, Nigeria
Sokcheon Pak, Australia
Antônio Palumbo Jr, Brazil
Zongfu Pan, China
Siyaram Pandey, Canada
Niranjan Parajuli, Nepal
Gunhyuk Park, Republic of Korea
Wansu Park, Republic of Korea
Rodolfo Parreira, Brazil
Mohammad Mahdi Parvizi, Iran
Luiz Felipe Passero, Brazil
Mitesh Patel, India
Claudia Helena Pellizzon, Brazil
Cheng Peng, Australia
Weijun Peng, China
Sonia Piacente, Italy
Andrea Pieroni, Italy
Haifa Qiao, USA
Cláudia Quintino Rocha, Brazil
DANIELA RUSSO, Italy
Muralidharan Arumugam Ramachandran, Singapore
Manzoor Rather, India
Miguel Rebollo-Hernanz, Spain
Gauhar Rehman, Pakistan
Daniela Rigano, Italy
José L. Rios, Spain
Francisca Rius Diaz, Spain
Eliana Rodrigues, Brazil
Maan Bahadur Rokaya, Czech Republic
Mariangela Rondanelli, Italy
Antonietta Rossi, Italy
Mi Heon Ryu, Republic of Korea
Bashar Saad, Palestinian Authority
Sabiu Saheed, South Africa
Mohamed Z.M. Salem, Egypt
Avni Sali, Australia
Andreas Sandner-Kiesling, Austria
Manel Santafe, Spain
José Roberto Santin, Brazil
Tadaaki Satou, Japan
Roland Schoop, Switzerland
Sindy Seara-Paz, Spain
Veronique Seidel, United Kingdom
Vijayakumar Sekar, China
Terry Selfe, USA
Arham Shabbir, Pakistan
Suzana Shahar, Malaysia
Wen-Bin Shang, China
Xiaofei Shang, China
Ali Sharif, Pakistan
Karen J. Sherman, USA
San-Jun Shi, China
Insop Shim, Republic of Korea
Maria Im Hee Shin, China
Yukihiro Shoyama, Japan
Morry Silberstein, Australia
Samuel Martins Silvestre, Portugal
Preet Amol Singh, India
Rajeev K Singla, China
Kuttulebbai N. S. Sirajudeen, Malaysia
Slim Smaoui, Tunisia
Eun Jung Sohn, Republic of Korea
Maxim A. Solovchuk, Taiwan
Young-Jin Son, Republic of Korea
Chengwu Song, China
Vanessa Steenkamp, South Africa
Annarita Stringaro, Italy
Keiichiro Sugimoto, Japan
Valeria Sulsen, Argentina
Zewei Sun, China
Sharifah S. Syed Alwi, United Kingdom
Orazio Taglialatela-Scafati, Italy
Takashi Takeda, Japan
Gianluca Tamagno, Ireland
Hongxun Tao, China
Jun-Yan Tao, China
Lay Kek Teh, Malaysia
Norman Temple, Canada

Kamani H. Tennekoon, Sri Lanka
Seong Lin Teoh, Malaysia
Menaka Thounaojam, USA
Jinhui Tian, China
Zipora Tietel, Israel
Loren Toussaint, USA
Riaz Ullah, Saudi Arabia
Philip F. Uzor, Nigeria
Luca Vanella, Italy
Antonio Vassallo, Italy
Cristian Vergallo, Italy
Miguel Vilas-Boas, Portugal
Aristo Vojdani, USA
Yun WANG, China
QIBIAO WU, Macau
Abraham Wall-Medrano, Mexico
Chong-Zhi Wang, USA
Guang-Jun Wang, China
Jinan Wang, China
Qi-Rui Wang, China
Ru-Feng Wang, China
Shu-Ming Wang, USA
Ting-Yu Wang, China
Xue-Rui Wang, China
Youhua Wang, China
Kenji Watanabe, Japan
Jintanaporn Wattanathorn, Thailand
Silvia Wein, Germany
Katarzyna Winska, Poland
Sok Kuan Wong, Malaysia
Christopher Worsnop, Australia
Jih-Huah Wu, Taiwan
Sijin Wu, China
Xian Wu, USA
Zuoqi Xiao, China
Rafael M. Ximenes, Brazil
Guoqiang Xing, USA
JiaTuo Xu, China
Mei Xue, China
Yong-Bo Xue, China
Haruki Yamada, Japan
Nobuo Yamaguchi, Japan
Junqing Yang, China
Longfei Yang, China
Mingxiao Yang, Hong Kong
Qin Yang, China
Wei-Hsiung Yang, USA
Swee Keong Yeap, Malaysia
Albert S. Yeung, USA
Ebrahim M. Yimer, Ethiopia
Yoke Keong Yong, Malaysia
Fadia S. Youssef, Egypt
Zhilong Yu, Canada
RONGJIE ZHAO, China
Sultan Zahiruddin, USA
Armando Zarrelli, Italy
Xiaobin Zeng, China
Y Zeng, China
Fangbo Zhang, China
Jianliang Zhang, China
Jiu-Liang Zhang, China
Mingbo Zhang, China
Jing Zhao, China
Zhangfeng Zhong, Macau
Guoqi Zhu, China
Yan Zhu, USA
Suzanna M. Zick, USA
Stephane Zingue, Cameroon

Contents

Characterization of a Tumor-Microenvironment-Relevant Gene Set Based on Tumor Severity in Colon Cancer and Evaluation of Its Potential for Dihydroartemisinin Targeting

Bo Liang, Biao Zheng, Yan Zhou, Zheng-Quan Lai, Citing Zhang, Zilong Yan, Zhangfu Li, Xuefei Li, Peng Gong, Jianhua Qu, and Jikui Liu

Research Article (10 pages), Article ID 4812068, Volume 2021 (2021)

Hindawi
Evidence-Based Complementary and Alternative Medicine
Volume 2021, Article ID 9658638, 10 pages
https://doi.org/10.1155/2021/9658638

Research Article

Benefit Effect of *Dendrobium officinale* Ultrafine Powder on DSS-Induced Ulcerative Colitis Rats by Improving Colon Mucosal Barrier

Xiang Zheng,[1] **Tao-Xiu Xiong**,[1] **Ke Zhang**,[1] **Fu-Chen Zhou**,[1] **Hui-Ying Wang**,[1] **Bo Li**,[1,2] **Ying-Jie Dong**,[1] **Xinglishang He**,[1] **Lin-Zi Li**,[1] **Qiao-Xian Yu**,[3] **Gui-Yuan Lv**,[4] **and Su-Hong Chen**[1,2]

[1]*Zhejiang University of Technology, Hangzhou 310014, Zhejiang, China*
[2]*Zhejiang Synergetic Traditional Chinese Medicine Research and Development Co., Ltd., Deqing 322099, Zhejiang, China*
[3]*Zhejiang Senyu Co., Ltd., Yiwu 322099, Zhejiang, China*
[4]*Zhejiang Chinese Medical University, Hangzhou 310053, Zhejiang, China*

Correspondence should be addressed to Qiao-Xian Yu; sstpfd@126.com, Gui-Yuan Lv; zjtcmlgy@163.com, and Su-Hong Chen; chensuhong@zjut.edu.cn

Received 24 April 2021; Revised 26 September 2021; Accepted 9 October 2021; Published 30 December 2021

Academic Editor: Xiaolong Ji

Copyright © 2021 Xiang Zheng et al. This is an open access article distributed under the Creative Commons Attribution License, which permits unrestricted use, distribution, and reproduction in any medium, provided the original work is properly cited.

Aim and Objective. To study the effect of *Dendrobium officinale* ultrafine powder (DOFP) on the intestinal mucosal barrier in rats with ulcerative colitis (UC) induced by dextran sulfate sodium (DSS). *Materials and Methods*. After intragastric administration of DOFP for 3 weeks, the rat UC model was made by the administration of 4% oral DSS solution for one week, and the drug was given at the same time. During the experiment, the disease activity index (DAI) score of the rats was regularly computed. At the end of the experiment, the blood routine indexes of rats were obtained. The histopathological changes in the colon were monitored by hematoxylin-eosin (H&E) and PAS staining and observation of ultrastructural changes in the colon by transmission electron microscope. Occludin expression in the colon was monitored by Western blot, the expression of claudin-1 and ZO-1 in the colon was detected by immunofluorescence, and the expression of TNF-α, IL-6, and IL-1β in the colon was detected by immunohistochemistry. *Results*. The results firstly indicated that DOFP could significantly alleviate the signs and symptoms of the DSS-induced rats UC model, which manifested as improvement of body weight loss, increase of colon length, and improvement of the symptoms of diarrhea and hematochezia. Then, results from histopathology, blood routine examination, and transmission electron microscope analysis further implied that DOFP could dramatically reduce inflammatory cell infiltration and restore intestinal epithelial barrier integrity. In addition, the experiments of Western Blot analysis, immunofluorescence, and PAS staining also further confirmed that DOFP could markedly increase related protein expressions of the intestinal barrier and mucus barrier, as the expression of occludin, claudin-1, and ZO-1 in the colon significantly decreased. The experiments of immunohistochemistry confirmed that DOFP could markedly decrease protein expression levels of inflammatory cytokines TNF-α, IL-6, and IL-1β. *Conclusion*. DOFP notably alleviated inflammatory lesions, repaired the colon mucosa damage by promoting the expression of tight junction proteins occludin, claudin-1, and ZO-1 and inhibiting the release of inflammatory factors TNF-α, IL-6, and IL-1β, and finally achieved the purpose of treating UC.

1. Introduction

Ulcerative colitis (UC) is an inflammatory bowel disease characterized by inflammatory cell infiltration into the colonic mucosa. The etiology and pathogenesis of ulcerative colitis are not clear [1, 2]. This disorder severely affects the normal life of patients and also increases the risk of secondary infections and colon cancer [3]. At present, the drugs used to treat UC are corticosteroids, 5-aminosalicylic acid (5-ASA), immunosuppressants, and biological agents or

their derivatives [4]. However, the side effects of these drugs have a negative impact upon the liver, as well as psychological functions and other body systems [5]. Therefore, there is an urgent need to obtain therapeutic drugs with definite curative effects and few side effects.

Although the exact pathophysiological mechanism of UC is not clear, studies suggest that diet, environment, and intestinal mucosal injury are closely related to the occurrence of UC [6–8]. Tight junctions (TJs) mainly include transmembrane proteins, occludins, claudins, cytoplasmic, and attachment proteins of the ZO family proteins. In-depth studies have found that the expression of TJ protein is abnormal in UC, and this directly affects the intestinal mucosal barrier function and plays a key role in promoting the occurrence and development of UC [9]. Intestinal epithelial TJ protein can not only block the abnormal immune response caused by pathogenic intestinal microorganisms but also alleviate the inflammatory response caused by excessive leakage of bacteria and antigens through the mucous membrane [8]. Therefore, when there is a decrease in TJs, intestinal permeability increases, and this can cause celiac disease, diabetes, UC, and other diseases [10].

Dendrobium officinale Kimura et Migo *(D. officinale)* is a plant that has the effect of "benefiting the stomach and promoting fluid" [11], and its uses were recorded in the Shennong Materia Medica over 2000 years ago. The dried stem is the plant part of *D. officinale* that is medicinally used, and modern pharmacological studies have shown that *D. officinale* has a variety of biological activities, such as hepatoprotective, anticancer, hypoglycemic, antifatigue, and gastric ulcer protection [12]. *D. officinale* has a variety of active principles, such as polysaccharides, flavonoids, alkaloids, and essential oils. And polysaccharides are the dominant substances [13]. It has been reported that *D. officinale* and its polysaccharides have many beneficial effects on UC, such as decreasing colonic inflammation and regulating intestinal flora [14–16]. Ultrafine grinding technology uses mechanical or hydrodynamic methods to crush raw materials into a nanopowder or micropowder. After ultrafine pulverization, the particle size of a drug can reach 1–10 μm as an ultrafine powder [17]. The powder has the advantages of convenient transportation and storage, excellent water solubility, low loss of functional components, high utilization rate, and beneficial dietary fiber [18, 19].

Previous laboratory studies have shown that *D. officinale* ultrafine powder (DOFP) could increase the expression of intestinal ZO-1 in convalescent nonalcoholic fatty liver model mice and regulate the abnormality of the intestinal-liver axis by inhibiting LPS-TLR4-related inflammation [18]. However, whether *D. officinale* can inhibit intestinal inflammation by regulating TJ protein in the UC model requires further study. We speculated that DOFP might act on the TJ proteins of the intestinal mucosal barrier to subsequently ameliorate UC. Therefore, in this study, dextran sulfate sodium (DSS) was used to induce UC in rats, and the focus was on the TJ proteins occludin, claudin-l, and ZO-1 to explore the efficacy and mechanism of DOFP in the prevention and treatment of ulcerative colitis.

2. Materials and Methods

2.1. Materials and Reagents. DSS (relative molecular weight 40000, Hubei Xinghengkang Chemical Technology Co., Ltd.) and the reagents of hematoxylin and eosin were purchased from the Institute of Biological Engineering of Nanjing Jiancheng Co. Ltd. (Nanjing, China).

2.2. Animal Treatment. Forty healthy male SD rats (200 ± 20 *g*) were purchased from the Zhejiang Experimental Animal Center (Hangzhou, China), license number: SCXK (Zhejiang) 2014–0001. All the animals were housed at room temperature of 25°C and at 45–55% relative humidity with a 12-hour light-dark cycle. All rats were fed a standard pellet chow diet, and the gastric volume was 1 mL/100 g. All animal experiments were conducted with the approval of the Animal Care and Use Committee of Zhejiang University of Technology (ethical approval number: 20200603038).

2.3. DOFP Preparation. Dried *D. officinale* was purchased from Zhejiang Senyu Co., Ltd. (Zhejiang, China). The dried herb was crushed to create *D. officinale* coarse powder (DOFC) and *D. officinale* ultrafine powder (DOFP). The DOFP and DOFC were observed by scanning electron microscope (JEOL JSM-IT100, Beijing, China), the samples were fixed on scanning electron microscopy stubs using double-sided adhesive tape and then coated with Au at 50 mA for 3 min through a sputter coater, and a scanning electron microscope with a secondary electron detector was used to obtain digital images of the samples at an accelerating voltage of 20 kV.

The content of polysaccharides was determined by the phenol sulfuric acid method, and the maximum absorbance was found at 488 nm [18]. With standard glucose (Shanghai Yuanye Bio-Technology Co., Ltd., Shanghai, China) as the control substance, 1 mL extract sample or glucose standard solution was added to a 10 mL plugged test tube, and water was added to 1 mL, mixed with 1 mL 5% phenol (Shanghai Yuanye Bio-Technology Co., Ltd., Shanghai, China), then mixed with 5 mL sulfuric acid (Sinopharm Chemical Reagent Co., Ltd, Shanghai, China), reacted in a boiling water bath for 20 min, and cooled in an ice bath for 5 min to stop the reaction. The absorbance was measured at 488 nm. The standard regression equation for glucose is $y = 0.0364x - 0.0027$; $R = 0.9984$ (y denotes absorbance, while x denotes the concentration of glucose).

2.4. Animal Groups. Rats were randomly divided into four groups, the normal group (NG), model group (MG), DOFP low-dose group (DOFP-L, at a dose of 0.3 g/kg), and DOFP high-dose group (DOFP-H, at a dose of 0.6 g/kg), with ten animals in each group. The DOFP-L and DOFP-H rats received the corresponding drugs on a daily basis (p.o.) for 4 weeks. After 3 weeks of treatment, except for the NG, 4% DSS solution was added to all other groups of rats drinking water ad libitum to induce ulcerative colitis (UC). For the 4 weeks experiment, all rats were fed with the standard diet,

Table 1: Scoring standard of the disease activity index (DAI) [20].

Score	Body weight decrease rate (%)	Fecal property	Hematochezia status
0	0	Normal	Normal
1	1–5	Semiloose (+)	Feces with occult blood (+)
2	6–10	Semiloose (++)	Feces with occult blood (++)
3	11–15	Loose (+)	Bloody feces (+)
4	>15	Loose (++)	Bloody feces (++)

and the rats in the NG and MG were provided with water every day (p.o.). Referring to the Pharmacopoeia of the People's Republic of China (2020 Edition), the recommended daily dosage of *Dendrobium officinale* is 6–12 g. The administration dosage for the rats was converted according to the surface area of a 60 kg human body, the high-dose *Dendrobium officinale* ultrafine powder is 0.6 g/kg, and the low dose is 0.3 g/kg in this study. In addition, previous laboratory studies have shown that the 0.6 g/kg dose group of *Dendrobium officinale* ultrafine powder can increase the expression of tight junction protein in the intestine of nonalcoholic fatty liver model mice during the recovery period, inhibit LPS-TLR4 related inflammation, and regulate the abnormality of the intestinal-liver axis [18].

2.5. Disease Activity Score. After the establishment of the model, the body weight, bleeding, and fecal consistency of the rats were measured and recorded every day (Table 1) [20].

2.6. Blood Routine Index Detection. On the last day of the experiment, 12 hours after fasting, retroorbital blood was sampled and placed in an EP tube pretreated with Ethylene Diamine Tetraacetic Acid (EDTA) to prepare whole blood. The white blood corpuscles (WBC), red blood corpuscles (RBC), hemoglobin (HGB), hematocrit (HCT), mean cell volume (MCV), mean corpuscular hemoglobin (MCH), mean erythrocyte hemoglobin concentration (MCHC), platelet count (PLT), mean platelet volume (MPV), and eosinophil (EO) counts were analyzed using an automatic hematology analyzer (Sysmex Corporation, XT-2000i, Shanghai, China).

2.7. Colonic Length Measurement and Tissue Preservation. After anesthetization with pentobarbital sodium (Chengdu Huaxia Chemical Reagent Co., Ltd., Sichuan, China), blood samples were removed from the abdominal aorta of rats, then the colon was dissected and quickly separated, and the length of colon was measured. Part of the colon was stored at −80°C for Western blot examination; another part was cut into small pieces and fixed in 2.5% glutaraldehyde solution to be observed by transmission electron microscope; and the remainder was fixed in 4% neutral formalin for H&E staining, PAS staining, and immunofluorescence analysis.

2.8. Colon Tissue H&E Staining and Histopathological Score. The fixed colon tissue was embedded in paraffin after dehydration, and 4 μm paraffin sections were prepared. After dewaxing and hydration, H&E staining was performed. The paraffin sections were observed and photographed by optical biological microscope and scored according to a standard procedure (Table 2) [21].

2.9. PAS Staining. For staining, 4 μm paraffin sections were prepared. After dewaxing and hydration, the samples were treated with periodic acid dye, and incubation was performed for 6.5 min. After rinsing with distilled water, the samples were treated with Schiff reagent and were incubated away from light for 15 min and then rinsed with running water. Then, hematoxylin staining was performed for 1.5 min, and the samples were subsequently rinsed with running water and then dried. The tissues were observed, and images were recorded with an optical biological microscope.

2.10. Ultrastructural Observation of Colon in UC Rats. For structural examination, 2–3 pieces of colon tissue were submerged in 2.5% glutaraldehyde fixative solution for more than 24 hours. Then, ultrathin sections were created, and the ultrastructure of colonic epithelial cells was observed by transmission electron microscope (HITACHI, HT7700, 80 kV, China).

2.11. Western Blot Analysis. Liquid nitrogen was used for the mechanical lysis of 50–100 mg frozen colon tissues. Then, the tissues were lysed in RAPI buffer with protease/phosphatase inhibitor for 30 min on ice. The lysates were clarified by centrifugation at 10,000 rpm for 20 min at 4°C, and the protein concentrations were determined using BCA protein analysis kits (Shanghai Beyotime Biotechnology Co., Ltd., Shanghai, China). After adjusting the concentration, electrophoretic separation and membrane transfer were carried out. The membrane was incubated in 5% milk at room temperature for 2 hours, and the first antibody of occludin or GAPDH (Proteintech Group, Shanghai, China) was incubated with the membrane overnight at 4°C. After three washes in TBST for 5 min each, the second antibody was incubated with the membrane at room temperature for 2 hours. After rinsing with TBST, the bands were identified by chemiluminescence, and the gray value of the corresponding protein band was analyzed by ImageJ software.

2.12. Immunofluorescence. For immunofluorescence staining, 4 μm paraffin sections were prepared, and after dewaxing and hydration, the samples were incubated in 3% H_2O_2 for 15 min at room temperature. After three washes in

Table 2: Histological scoring system [21].

Score	Inflammation	Mucosal damage	Crypt damage	Range of lesions (%)
0	None	None	None	0
1	Mild	Mucous layer	1/3	1–25
2	Moderate	Submucosa	2/3	26–50
3	Severe	Muscularis and serosa	100%	51–75
4	—	—	100% + epithelium	76–100

PBS for 5 min each, the samples were incubated in 5% BSA at room temperature for 2 hours. The first antibody of claudin-1 and ZO-1 was incubated with the sections overnight at 4°C. The second fluorescent antibody was incubated with the sections at room temperature for 30 min. After rinsing with PBS and then staining with DAPI, the paraffin sections were observed and photographed under a fluorescence microscope (Olympus BX43, China).

2.13. Immunohistochemistry. 4 μm paraffin sections were used for immunohistochemistry, and following the elimination of the endogenous peroxidase activity and antigen reparation, the tissues were sealed with blocking buffer. Then, the tissues were incubated with anti-TNF-α, anti-IL-6, and anti-IL-1β (Proteintech Group, Shanghai, China) overnight at 4°C and subsequently with the secondary antibody. The DAB chromogen was used for incubation, and then hematoxylin was used for counterstaining. After dehydration of gradient ethanol and sealing slices with neutral gum, slices were observed under a microscope. The positive results were stained in yellow. The images were analyzed using Image-Pro Plus software.

2.14. Statistical Method. All the data were statistically analyzed by SPSS 22 software, and the data were expressed as mean ± SD. The comparison between groups was performed by single-factor analysis of variance (ANOVA).

3. Results

3.1. Quality Control of DOFP. The DOFP and DOFC were observed and photographed under a scanning electron microscope. There were many intact cells in the DOFC (Figure 1(b)), while DOFP (Figure 1(a)) had fewer intact cells, and most of them were cell fragments. DOFC and DOFP contained 46.50% and 56.67% polysaccharides, respectively, as determined by the phenol sulfuric acid method, which indicated that there was greater polysaccharide dissolution of DOFP as compared to DOFC.

3.2. DOFP Relieved the Signs and Symptoms of UC in Rats Induced by DSS. The rats in each group showed different degrees of colitis via symptoms such as weight loss, diarrhea, and hematochezia. Compared with the normal group, the length of colon in the model group was shorter (Figures 2(a) and 2(b)), and the disease activity index (DAI) scores were significantly increased ($P < 0.05$) (Figure 2(c)), suggesting that the model of colitis induced by DSS was successful. Compared with the model group, both high and low doses of DOFP improved the symptoms of colon shortening in model rats, and it significantly improved the DAI score in model rats ($P < 0.05$). The above data indicated that DOFP treatment improved DSS-induced colitis in rats.

3.3. The Effect of DOFP on Routine Blood Indexes of DSS-Induced Colitis Model Rats. The results of the blood routine examination of rats showed that WBC, HGB, and PLT in the model group were significantly higher than those in the normal group ($P < 0.05$), and MCV of the model group was significantly lower than that in the normal group (Table 3). Compared with the model group, the levels of WBC, HGB, and PLT in the DOFP-H group were significantly decreased ($P < 0.05$), while the MCV in the DOFP-L and DOFP-H groups was significantly increased ($P < 0.05$). It is suggested that DOFP can reduce WBC and other inflammatory indexes and decrease inflammatory lesions in UC model rats.

3.4. The Effect of DOFP on the Pathological Changes in Colon Tissue in DSS-Induced Colitis Model Rats. The results of H&E staining showed that, compared with the normal group, the colonic mucosa of the model group was severely damaged, a large number of inflammatory cells infiltrated, and the crypt and glandular structures were severely damaged. Compared with the model group, the DOFP-L and DOFP-H groups exhibited decreased colonic mucosal injury, inflammatory cell infiltration, and crypt and glandular structure destruction and other pathological changes of the model rats (Figure 3(a)). The histopathological score of the model group was significantly higher than that of the normal group ($P < 0.01$), and the histopathological score of the DOFP-L and DOFP-H groups was significantly lower than that of the model group ($P < 0.05$, 0.01) (Figure 3(b)).

3.5. The Effect of DOFP on Goblet Cells and Mucus in the Colons of DSS-Induced Colitis Model Rats. The results of PAS staining showed that the shape of colonic goblet cells in the normal group was full and round, mucus secretion was abundant, and the mucosal surface was covered with mixed mucus. Compared with the normal group, the goblet cells in the model group atrophied to varying degrees, and the mucus cover on the mucous membrane was decreased. Compared with the model group, the atrophy of intestinal mucosal epithelial cells and goblet cells in the DOFP-L and DOFP-H groups was reversed by varying degrees, and the mucus secretion increased (Figure 3(c)).

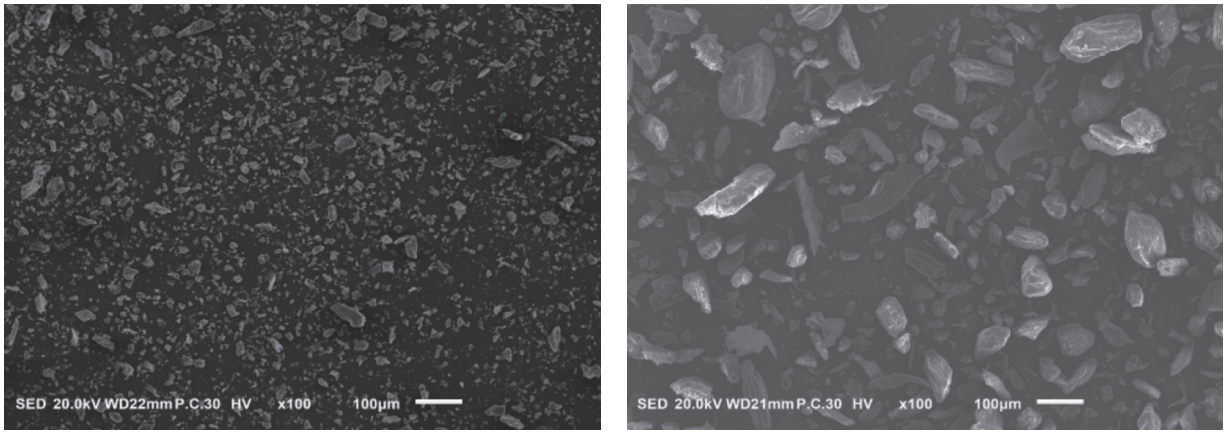

(a) (b)

Figure 1: Characteristics of DOFC and DOFP. (a) SEM micrographs of DOFP. (b) SEM micrographs of DOFC.

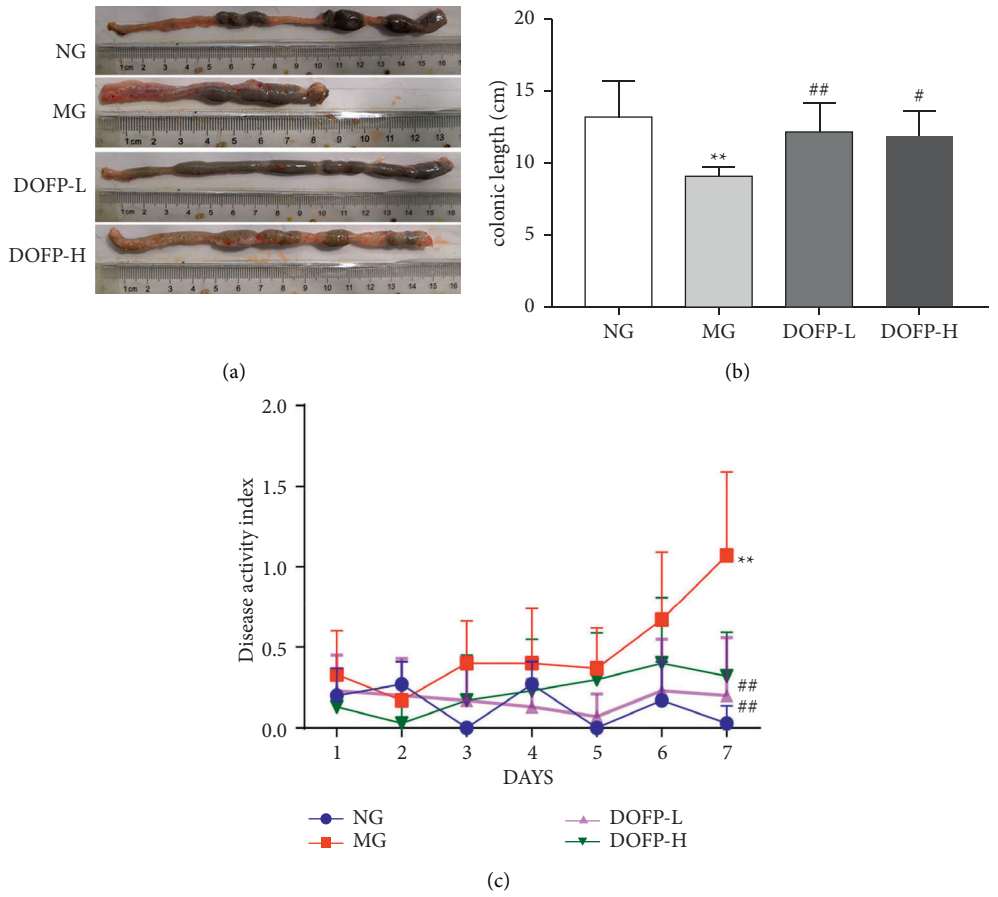

Figure 2: DOFP treatment improves DSS-induced colitis in rats. (a) Representative photos of colon length. (b) Colon length. (c) Disease activity score. $^{**}P < 0.01$, compared with the normal group; $^{\#}P < 0.05$ and $^{\#\#}P < 0.01$, compared with the model group.

3.6. Transmission Electron Microscope Observation. The results of TEM showed that the microvilli on the surface of the colonic mucosa epithelial cells in the normal group were intact, the epithelial cells were tightly connected, and the intercellular space exhibited no obvious abnormal changes. In the model group, the rat colonic mucosal epithelial cells

Table 3: Effect of DOFP on blood indexes of rats.

Project	NG	MG	DOFP-L	DOFP-H
WBC (10^9/L)	8.95 ± 1.31	12.35 ± 3.49*	10.39 ± 1.14	9.87 ± 1.82#
RBC (10^{12}/L)	10.26 ± 0.52	10.80 ± 0.90	10.65 ± 0.60	10.13 ± 0.80
HGB (g/L)	185.11 ± 6.25	193.89 ± 11.49*	194.70 ± 9.93	181.00 ± 11.80#
HCT (%)	54.38 ± 2.70	56.70 ± 3.23	56.57 ± 2.90	54.41 ± 3.30
MCV (Fl)	54.63 ± 2.92	51.91 ± 2.00*	53.80 ± 1.55#	54.32 ± 2.17#
MCH (pg)	18.23 ± 0.87	17.99 ± 0.65	18.29 ± 0.64	18.25 ± 0.59
MCHC (g/L)	343.80 ± 6.66	342.00 ± 4.18	344.20 ± 5.25	339.00 ± 8.25
PLT (10^9/L)	853.00 ± 153.72	1011.57 ± 123.19*	961.88 ± 179.04	837.86 ± 214.65#
MPV (fL)	7.61 ± 0.31	7.68 ± 0.24	7.44 ± 0.34#	7.55 ± 0.42
EO (%)	0.10 ± 0.02	0.10 ± 0.04	0.11 ± 0.05	0.12 ± 0.04

*$P < 0.05$ and **$P < 0.01$, compared with the normal group; #$P < 0.05$ and ##$P < 0.01$, compared with the model group.

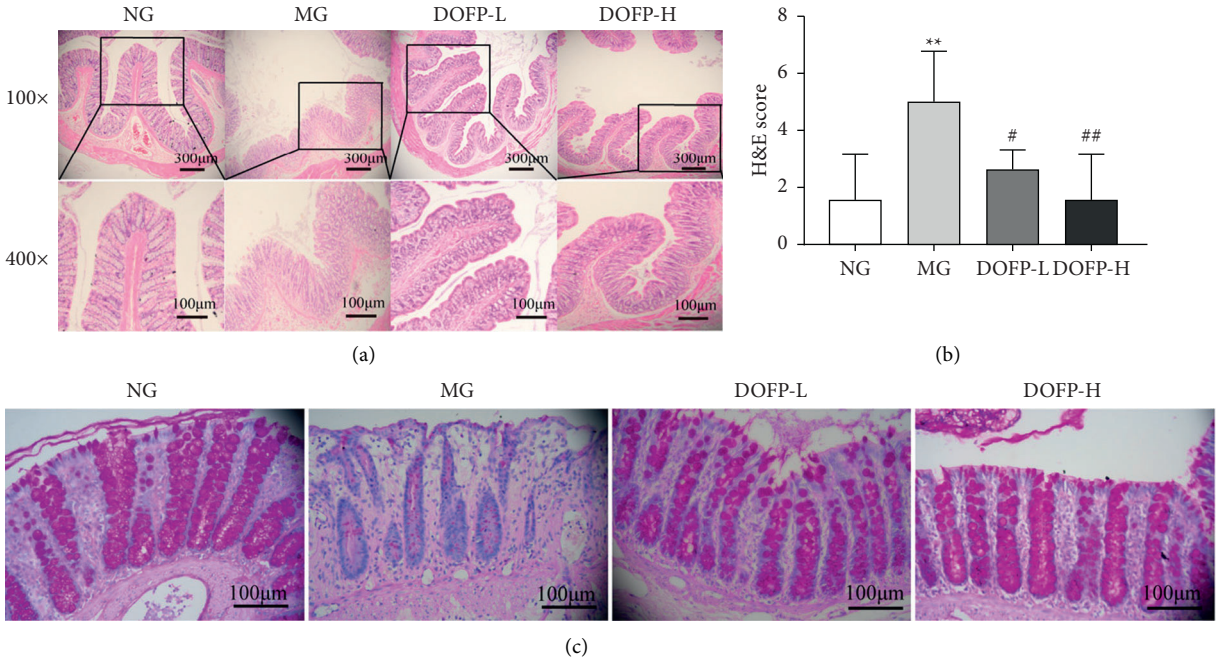

Figure 3: Effects of DOFP on histopathology of colitis rats. (a) Representative picture of colonic H&E staining (100×, 400×). (b) Colonic H&E staining score. (c) Representative picture of colonic PAS staining (400×). *$P < 0.05$ and **$P < 0.01$, compared with the normal group; #$P < 0.05$ and ##$P < 0.01$, compared with the model group.

lost microvilli, the intercellular space widened, the endoplasmic reticulum expanded, the mitochondria were swollen, part of the cytoplasm was dissolved, and apoptosis was visible. The colonic mucosal epithelial cells in rats from the DOFP group exhibited additional thick and short microvilli that were neatly arranged and uniform in size, the cells were neatly arranged, the degree of intercellular widening was significantly reduced, the glandular epithelia were closely connected to each other, and there was no expanded endoplasmic reticulum or swollen mitochondria (Figure 4(a)).

3.7. The Effect of DOFP on the Expression of Occludin Protein in Colon Tissue. Tight junction (TJ) protein plays an important role in maintaining a normal intestinal barrier. In order to clarify the effect of DOFP on TJ protein, the expression of occludin protein in the rat colon was detected by Western blot. The results showed that, compared with the normal group, the model group exhibited significantly decreased expression of occludin in colon tissue ($P < 0.05$). Compared with the model group, the DOFP-L group exhibited significantly increased expression of occludin protein in colon tissue ($P < 0.05$) (Figure 4(b)).

3.8. The Effect of DOFP on the Expression of Claudin-1 and ZO-1 Protein in Colon Tissue. The results of immunofluorescence showed that the expression of claudin-1 and ZO-1 protein in the colon tissue of the model group was lower than that of the normal group. Compared with the model group, the expression of claudin-1 and ZO-1 protein in the colon tissue of rats in the DOFP-L group increased (Figures 4(c) and 4(d)). It is suggested that the DOFP can increase the expression of occludin, claudin-1, ZO-1, and other tight junctions in the colon of UC model rats, and this subsequently acts to strengthen the intestinal mucosal barrier.

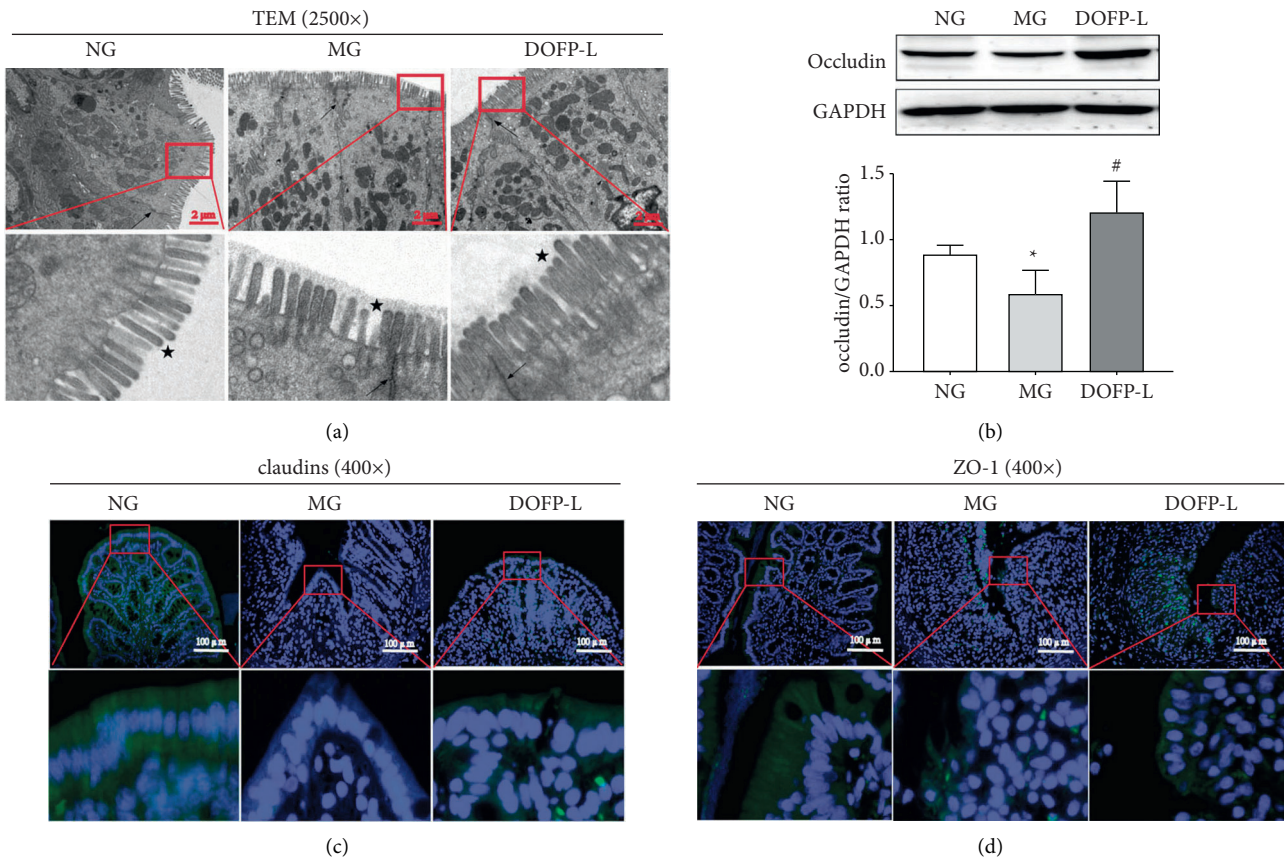

Figure 4: Effects of DOFP on TJ barrier function of colonic mucosa in UC rats. (a) Representative picture of the ultrastructure of colonic mucosa in colon. The arrow points to the tight junction, and the asterisk indicates microvilli. (b) Representative picture and semiquantitative statistical map of occludin protein bands in colon. (c) Representative picture of claudin-1 proteins expression with immunofluorescence in colon (400×). (d) Representative picture of ZO-1 proteins expression with immunofluorescence in colon (400×). $^{*}P < 0.05$ and $^{**}P < 0.01$, compared with the normal group; $^{\#}P < 0.05$ and $^{\#\#}P < 0.01$, compared with the model group.

3.9. The Effect of DOFP on the Expression of TNF-α, IL-6, and IL-1β Protein in Colon Tissue. The results of immunohistochemistry showed that the expression of TNF-α, IL-6, and IL-1β protein in the colon tissue of the model group was higher than that of the normal group. Compared with the model group, the expression of TNF-α, IL-6, and IL-1β protein in the colon tissue of rats in the DOFP-L group decreased (Figures 5(a) and 5(b)). It is suggested that the DOFP can decrease the expression of TNF-α, IL-6, and IL-1β in the colon of UC model rats and play a role in inhibiting the intestinal inflammatory response.

4. Discussion

UC is a chronic inflammatory bowel disease, and its incidence has been increasing worldwide for many years [22]. Increasing evidence shows that the use of Chinese herbal medicine is effective for diseases, especially inflammatory diseases [23]. In the treatment of DSS-induced UC model mice with Lizhong decoction, colonic lesions were decreased in all dose groups, the disease activity index (DAI) score was decreased, and the expression of TJ proteins was upregulated [7]. *Dendrobium officinale* contains a variety of active ingredients, including polysaccharides, alkaloids, glycosides, phenanthrene, bibenzyl, and amino acids, among which polysaccharides have the highest content in *D. officinale*. Our previous literature showed that the total polysaccharide content (47.96%, w/w) and monosaccharide contents (consisted of D-mannose, glucose, galactose, and arabinose at 42.2%, 12.3%, 0.4%, and 0.4%, w/w) were detected in DOFP [18]. The total flavonoid content ($3.78 \pm 0.48\%$) and the content of naringenin (0.3601 ± 0.014 mg/g) in DOFP were detected in a sodium hydroxide-aluminum sulfate method and high-performance liquid chromatograph (HPLC) system (1260, Agilent, Germany), respectively, as described in our previous report [19]. Modern pharmacological studies have shown that polysaccharides have anti-inflammatory, antioxidant, antitumor, and other pharmacological effects, enhance immunity, and regulate intestinal flora [24].

D. officinale has antifatigue, anti-inflammation, and antioxidation effects, reduces night sweats and dizziness, enhances immunity, and has been used in traditional Chinese medicine for more than 1000 years [23, 25]. *D. officinale* and its polysaccharides have many beneficial anti-UC effects, such as decreasing colonic inflammation and regulating intestinal flora [14, 15].

There are a large number of symbiotic bacteria in the colon. The intestinal mucosal barrier consists of closely

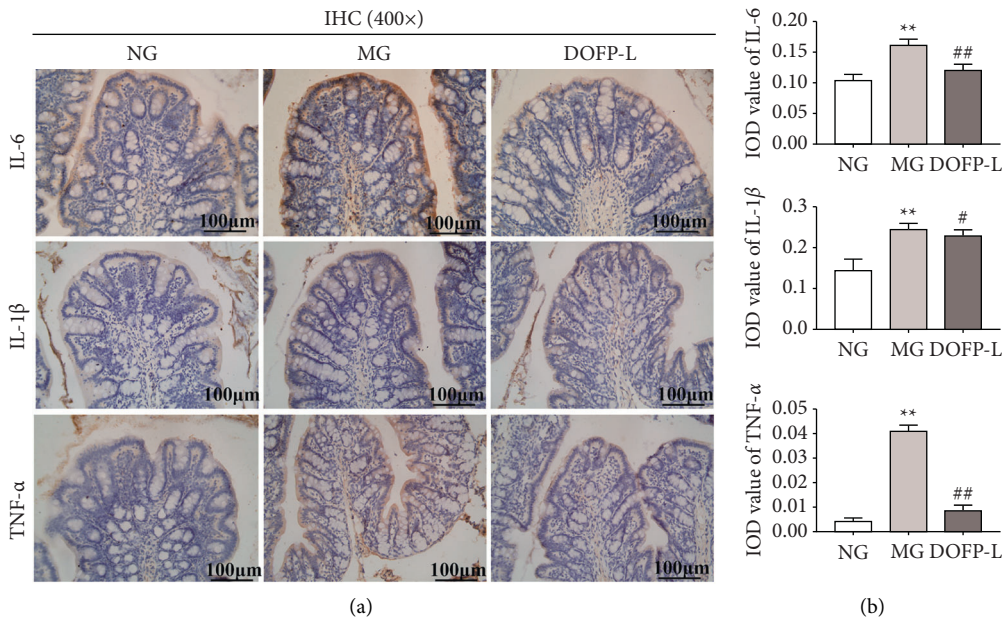

FIGURE 5: Effects of DOFP on the inflammatory factors TNF-α, IL-6, and IL-1β of colonic mucosa in UC rats. (a) Representative picture of colonic IHC staining (400×). (b) Colon IHC average optical density statistics chart. $^{*}P < 0.05$ and $^{**}P < 0.01$, compared with the normal group; $^{\#}P < 0.05$ and $^{\#\#}P < 0.01$, compared with the model group.

arranged colonic epithelial cells that act as an important physical and immune obstacle between the intestinal flora and the body. It is the key factor for the body to maintain the stability of the intestinal environment [26]. Although the exact pathophysiological mechanism of UC is not clear, it has been proposed that the decrease in intestinal mucosal barrier permeability can cause severe inflammation and lead to the development of UC. Therefore, maintaining the integrity of the intestinal mucosal barrier is an important strategy for the treatment of UC [27]. Intestinal mucosal epithelial cells and their TJs form a complete epithelial barrier, which is an important part of the intestinal mucosal mechanical barrier [7].

The barrier function of the intestinal epithelium is partially maintained by the TJs between adjacent epithelial cells. The TJs are composed of a series of proteins with multiple functions, including occludins, claudins, and ZO family proteins. Studies have shown that downregulation of TJs may cause ectopic invasion of intestinal pathogens, antigens, and toxins through the colonic mucosal barrier, resulting in the activation of immune cells and abnormal immune response of the intestinal mucosa. This can destroy the mucosal barrier function and increase intestinal permeability, which can then promote the occurrence and development of UC [28].

Occludins protein is a direct component of the TJ protein structure, and because of its adhesion characteristics, it can form an intercellular barrier through multimerization. For example, with increasing levels of occludins protein, the intercellular adhesion increases, the transmembrane resistance increases, and the permeability of the intestinal mucosal barrier decreases [29]. Both claudins and occludins are cell membrane proteins that are the functional and structural basis of the TJ complex.

Small molecular transmembrane proteins with a relative molecular weight of approximately 22,000 can directly affect the transmembrane resistance of epithelial and endothelial tissues, determine the ion selectivity of the TJ complex, and regulate the TJ permeability [30]. ZO proteins are cytoplasmic proteins that contain PDZ domains, which contribute to the anchoring of TJ proteins such as claudins and occludins to the cytoplasm [31]. Therefore, occludins, claudins, ZO, and other family proteins are often used as indicators to evaluate TJ barrier function and permeability function in tissues and are also important indicators for monitoring the degree of intestinal mucosal barrier injury in UC.

In the current study, it was found that the expression of occludin, claudin-1, ZO-1, and other TJ proteins decreased in DSS-induced UC model rats, and the intestinal mucosal barrier was damaged. In a study on the effect of patchouli extract on DSS-induced UC model rats, the expression of occludin, claudin-1, ZO-1, and other TJ proteins decreased in the model group [23]. In the current study, we found that, after the intervention of DOFP, the protein expression of occludin, claudin-1, and ZO-1 in the colon of model rats was significantly increased, and the colonic mucosal barrier did not degrade. Some studies have shown that *D. officinale* polysaccharides can protect the intestinal mucosal barrier, reduce intestinal cell permeability, maintain intestinal balance, restore intestinal villus damage, and effectively improve intestinal barrier function by upregulating the expression of TJ proteins such as occludin, claudin-1, and ZO-1 and reducing apoptosis [14, 32]. The previous study of

our group showed that DOFP significantly increased the expression of occludin, claudin-1, and ZO-1 mRNA, tightened the loose arrangement of intestinal villi, protected the intestinal barrier function, and reduced the liver damage caused by lipopolysaccharide (LPS) in convalescent nonalcoholic fatty liver model mice (induced by a high-sugar and high-fat diet) [18]. DOFP repaired the damaged colonic mucosal barrier by upregulating the expression of occludin, claudin-1, and ZO-1TJ proteins.

DSS-induced UC model rats possess a disease pathology that is similar to that of human UC, including weight loss, diarrhea, hematochezia, intestinal mucosal injury, and other symptoms, in which the severity of hematochezia is one of the important indicators to evaluate the degree of mucosal barrier damage [5]. In the current study, the results of hematoxylin-eosin (H&E) staining and periodic Acid-Schiff (PAS) staining showed that the colon of model rats sustained a mucosal injury, with inflammatory cell infiltration, an increase in goblet cells and mucus, the appearance of other histological lesions, and an increase in the DAI score. Some studies have shown that *D. officinale* polysaccharides can significantly reduce the DAI score of mice with UC induced by DSS and effectively ameliorate the hematochezia and weight loss [14, 33].

Mucosal barrier damage and inflammation are important pathological changes in the course of UC. DSS mainly develops intestinal inflammation by increasing intestinal permeability and damaging the intestinal barrier. It mainly affects the tight junction proteins of epithelial cells such as ZO-1 and occludin to damage the intestinal barrier, thereby increasing TNF-α and IL-6 expression of inflammatory factors [34].

In this study, we found that DOFP significantly reduced the DAI score of model rats, reduced the occurrence of hematochezia, reduced the shortening of the colon, improved the disappearance of microvilli of colonic mucosal epithelial cells and expansion of the endoplasmic reticulum, normalized the appearance of the mitochondria, upregulated the expression of TJ protein, downregulated the expression of inflammatory factors, effectively alleviated the injury of the intestinal mucosa, and improved the quality of life of the rats.

5. Conclusions

In a word, our results show that DOFP can improve DSS-induced colitis in model rats. It increases the expression of TJ proteins such as occludin, claudin-l, and ZO-1 in colon, inhibits the release of inflammatory factors TNF-α, IL-6, and IL-1β, repairs intestinal mucosal injury, reduces intestinal cell permeability, and maintain intestinal balance, so as to achieve the purpose of treating UC. These results suggest that *D. officinale* may be developed as a potential drug for the treatment of UC. However, *D. officinale* has a variety of active constituents, such as polysaccharides, flavonoids, alkaloids, and essential oils, which may be the possible active principle of this plant. We can further study it in the future.

5.1. Statement of Human and Animal Rights. All of the experimental procedures involving animals were conducted in accordance with the Institutional Animal Care guidelines of Zhejiang University of Technology, China, and approved by the Animal Care and Use Committee of Zhejiang University of Technology, China.

Data Availability

The data to support the findings of this study are included within the article. Other data used to support the findings of this study are available from the corresponding author upon request.

Ethical Approval

All animal experiments were conducted with the approval of the Animal Care and Use Committee of Zhejiang University of Technology (ethical approval number: 20200603038).

Conflicts of Interest

The authors declare that they have no conflicts of interest.

Authors' Contributions

Xiang Zheng, Tao-Xiu Xiong, and Ke Zhang contributed equally to this paper.

Acknowledgments

This study was supported by the National Key Research and Development Program (no. 2017YFC1702200), the National Science Foundation of China (nos. 81874352, 81873036, 81673638, and 81803760), the Project of Zhejiang Research Institute of China Engineering Science and Technology Development Strategy (no. 2019-ZJ-JS-05), the Key Research and Development Program of Zhejiang Province (2017C03052), and the General Project Foundation of the Zhejiang Provincial Department of Education (Y202043163).

References

[1] H. Chu, X. Tao, Z. Sun, W. Hao, and X. Wei, "Galactooligosaccharides protects against DSS-induced murine colitis through regulating intestinal flora and inhibiting NF-κB pathway," *Life Sciences*, vol. 242, Article ID 117220, 2020.

[2] Z. Lu, W. Xiong, S. Xiao et al., "Huanglian Jiedu Decoction ameliorates DSS-induced colitis in mice via the JAK2/STAT3 signalling pathway," *Chinese Medicine*, vol. 15, no. 1, 2020.

[3] Z. Yuan, L. Yang, X. Zhang, P. Ji, Y. Hua, and Y. Wei, "Huanglian-jie-du decoction ameliorates acute ulcerative colitis in mice via regulating NF-κB and Nrf2 signaling pathways and enhancing intestinal barrier function," *Frontiers in Pharmacology*, vol. 10, no. 10, Article ID 1354, 2019.

[4] N. Jiang, Y. Wei, Y. Cen et al., "Andrographolide derivative al-1 reduces intestinal permeability in dextran sulfate sodium (dss)-induced mice colitis model," *Life Sciences*, vol. 241, Article ID 117164, 2020.

[5] Z.-F. Zhang, H.-W. Zhao, X. Chai et al., "Effect of Hedyotis Diffusae Herba on dextran sulphate sodium-induced chronic ulcerative colitis in mice," *Chinese Traditional and Herbal Drugs*, vol. 46, no. 23, pp. 83–88, 2015.

[6] Y. Sheng, T. Wu, Y. Dai, K. Ji, Y. Zhong, and Y. Xue, "The effect of 6-gingerol on inflammatory response and Th17/Treg balance in DSS-induced ulcerative colitis mice," *Annals of Translational Medicine*, vol. 8, no. 7, p. 442, 2020.

[7] Y. Shen, J. Zou, M. Chen et al., "Protective effects of Lizhong decoction on ulcerative colitis in mice by suppressing inflammation and ameliorating gut barrier," *Journal of Ethnopharmacology*, vol. 259, Article ID 112919, 2020.

[8] S. Huang, Y. Fu, B. Xu et al., "Wogonoside alleviates colitis by improving intestinal epithelial barrier function via the MLCK/pMLC2 pathway," *Phytomedicine*, vol. 68, Article ID 153179, 2020.

[9] J. Wang, C. Zhang, C. Guo, and X. Li, "Chitosan ameliorates DSS-induced ulcerative colitis mice by enhancing intestinal barrier function and improving microflora," *International Journal of Molecular Sciences*, vol. 20, no. 22, Article ID 5751, 2019.

[10] S.-T. Wu, "Studies on chemical constituents and pharmacological effect of active fraction compound in treating ulcerative colitis in compound kushen decoction," Master thesis, Hubei University of Chinese Medicine, Wuhan, China, 2017.

[11] L. Gui-yuan, M.-Q. Yan, and S.-H. Chen, "Review of pharmacological activities of *Dendrobium officinale* based on traditional functions," *China Journal of Chinese Materia Medica*, vol. 38, no. 4, pp. 489–493, 2013.

[12] H. Zhao, X. Chen, X. Chen et al., "New peptidendrocins and anticancer chartreusin from an endophytic bacterium of Dendrobium officinale," *Annals of Translational Medicine*, vol. 8, no. 7, p. 455, 2020.

[13] H. Tang, T. Zhao, Y. Sheng, T. Zheng, L. Fu, and Y. Zhang, "*Dendrobium officinale* Kimura et Migo: a Review on Its Ethnopharmacology, Phytochemistry, Pharmacology, and Industrialization," *Evidence-based Complementary and Alternative Medicine*, vol. 2017, Article ID 7436259, 19 pages, 2017.

[14] J. Liang, H. Li, J. Chen et al., "*Dendrobium officinale* polysaccharides alleviate colon tumorigenesis via restoring intestinal barrier function and enhancing anti-tumor immune response," *Pharmacological Research*, vol. 148, Article ID 104417, 2019.

[15] L. Li, H. Yao, X. Li et al., "Destiny of *Dendrobium officinale* polysaccharide after oral administration: indigestible and nonabsorbing, ends in modulating gut microbiota," *Journal of Agricultural and Food Chemistry*, vol. 67, no. 21, pp. 5968–5977, 2019.

[16] Y. Yuan, J. Zhang, X. Liu, M. Meng, J. Wang, and J. Lin, "Tissue-specific transcriptome for *Dendrobium officinale* reveals genes involved in flavonoid biosynthesis," *Genomics*, vol. 112, no. 2, pp. 1781–1794, 2020.

[17] Y.-J. Yang, "Research progress on superfine grinding technique in field of Chinese materia medica," *Chinese herbal medicine*, vol. 50, no. 23, pp. 5887–5891, 2019.

[18] S.-S. Lei, B. Li, Y.-H. Chen et al., "*Dendrobii Officinalis*, a traditional Chinese edible and officinal plant, accelerates liver recovery by regulating the gut-liver axis in NAFLD mice," *Journal of Functional Foods*, vol. 61, Article ID 103458, 2019.

[19] S.-S. Lei, N.-Y. Zhang, F.-C. Zhou et al., "*Dendrobium officinale* regulates fatty acid metabolism to ameliorate liver lipid accumulation in NAFLD mice," *Evidence-based Complementary and Alternative Medicine*, vol. 2021, Article ID 6689727, 12 pages, 2021.

[20] Z. Liu, F. Liu, W. Wang et al., "Study of the alleviation effects of a combination of Lactobacillus rhamnosus and inulin on mice with colitis," *Food & Function*, vol. 11, no. 5, pp. 3823–3837, 2020.

[21] Z. Zhang, S. Li, H. Cao et al., "The protective role of phloretin against dextran sulfate sodium-induced ulcerative colitis in mice," *Food and Function*, vol. 10, no. 1, pp. 422–431, 2019.

[22] F. Xie, H. Zhang, C. Zheng, and X.-f. Shen, "Costunolide improved dextran sulfate sodium-induced acute ulcerative colitis in mice through NF-κB, STAT1/3, and Akt signaling pathways," *International Immunopharmacology*, vol. 84, Article ID 106567, 2020.

[23] Z. Wu, H. Zeng, L. Zhang et al., "Patchouli alcohol: a natural sesquiterpene against both inflammation and intestinal barrier damage of ulcerative colitis," *Inflammation*, vol. 43, no. 4, pp. 1423–1435, 2020.

[24] X. Ji, C. Hou, Y. Gao, Y. Xue, Y. Yan, and X. Guo, "Metagenomic analysis of gut microbiota modulatory effects of jujube (*Ziziphus jujuba* Mill.) polysaccharides in a colorectal cancer mouse model," *Food & Function*, vol. 11, no. 1, pp. 163–173, 2020.

[25] Z. Yu, Y. Liao, J. Teixeira da Silva, Z. Yang, and J. Duan, "Differential accumulation of anthocyanins in *Dendrobium officinale* stems with red and green peels," *International Journal of Molecular Sciences*, vol. 19, no. 10, Article ID 2857, 2018.

[26] S. Y. Salim and J. D. Söderholm, "Importance of disrupted intestinal barrier in inflammatory bowel diseases," *Inflammatory Bowel Diseases*, vol. 17, no. 1, pp. 362–381, 2011.

[27] H. Lee, Y. S. Son, M.-O. Lee et al., "Low-dose interleukin-2 alleviates dextran sodium sulfate-induced colitis in mice by recovering intestinal integrity and inhibiting AKT-dependent pathways," *Theranostics*, vol. 10, no. 11, pp. 5048–5063, 2020.

[28] S. Yin, H. Yang, Y. Tao et al., "Artesunate ameliorates DSS-induced ulcerative colitis by protecting intestinal barrier and inhibiting inflammatory response," *Inflammation*, vol. 43, no. 2, pp. 765–776, 2020.

[29] W. Fries, A. Belvedere, and S. Vetrano, "Sealing the broken barrier in IBD: intestinal permeability, epithelial cells and junctions," *Current Drug Targets*, vol. 14, no. 12, pp. 1460–1470, 2013.

[30] Y.-X. Rao, J. Chen, and Y.-D. Wu, "Changes in the expression of liver tight junction protein in dextran sulfate sodium induced ulcerative colitis rat model," *Journal of pediatrics*, vol. 30, no. 10, pp. 967–972, 2012.

[31] S. Shastri, T. Shinde, K. L. Woolley, J. A. Smith, N. Gueven, and R. Eri, "Short-chain naphthoquinone protects against both acute and spontaneous chronic murine colitis by alleviating inflammatory responses," *Frontiers in Pharmacology*, vol. 12, Article ID 709973, 2021.

[32] K. Wang, X. Yang, Z. Wu et al., "Dendrobium officinale polysaccharide protected CCl4-induced liver fibrosis through intestinal homeostasis and the LPS-TLR4-NF-κb signaling pathway," *Frontiers in Pharmacology*, vol. 11, Article ID 240, 2020.

[33] J. Liang, S. Chen, J. Chen et al., "Therapeutic roles of polysaccharides from *Dendrobium Officinaleon* colitis and its underlying mechanisms," *Carbohydrate Polymers*, vol. 185, pp. 159–168, 2018.

[34] C.-L. Zhu, J.-J. Mu, and J.-W. Xu, "Repair effect of purple sweet potato anthocyanin on intestinal barrier injury in mice with ulcerative colitis induced by DSS," *Chinese Journal of Pathophysiology*, vol. 36, no. 10, pp. 1844–1853, 2020.

Hindawi
Evidence-Based Complementary and Alternative Medicine
Volume 2021, Article ID 6622981, 13 pages
https://doi.org/10.1155/2021/6622981

Review Article

Effects of Sesame Consumption on Inflammatory Biomarkers in Humans: A Systematic Review and Meta-Analysis of Randomized Controlled Trials

Shabnam Rafiee,[1] **Roghaye Faryabi**,[1] **Alireza Yargholi**,[1] **Mohammad Ali Zareian**,[1] **Jessie Hawkins**,[2] **Nitin Shivappa**,[3,4] **and Laila Shirbeigi**[1]

[1]*Department of Traditional Medicine, School of Persian Medicine, Tehran University of Medical Sciences (TUMS), Tehran, Iran*
[2]*Integrative Health, Franklin School of Integrative Health Sciences, Franklin, TN, USA*
[3]*Cancer Prevention and Control Program, University of South Carolina, Columbia, SC 29208, USA*
[4]*Department of Epidemiology and Biostatistics, Arnold School of Public Health, University of South Carolina, Columbia, SC 29208, USA*

Correspondence should be addressed to Laila Shirbeigi; l.shirbeigi@yahoo.com

Received 5 May 2021; Revised 4 October 2021; Accepted 15 October 2021; Published 1 November 2021

Academic Editor: Xiaolong Ji

Copyright © 2021 Shabnam Rafiee et al. This is an open access article distributed under the Creative Commons Attribution License, which permits unrestricted use, distribution, and reproduction in any medium, provided the original work is properly cited.

Objectives. Existing evidence produces conflicting findings regarding the effect of sesame intake on inflammatory biomarkers; this knowledge gap has yet to be met through systematic review and meta-analysis. This meta-analysis of randomized, controlled clinical trials (RCTs) was conducted to evaluate the effects of sesame consumption on markers of inflammation in humans. *Methods*. PubMed, Scopus, and the Cochrane Database of Systematic Reviews were searched through August 2020 to identify relevant papers for inclusion. Using the random-effects model, data were evaluated as weighted mean differences (WMD) with 95% confidence intervals (CI). Cochrane's Q and I-squared (I^2) tests were used to identify within-studies heterogeneity. *Results*. Seven RCTs with 310 participants (157 intervention and 153 control) were included in the meta-analysis. Sesame consumption reduced serum level interleukin-6 (IL-6) (WMD − 0.90; 95% CI (−1.71, −0.09), $I^2 = 80.4\%$) compared to the control group. However, sesame intake had no significant effects on C-reactive protein (CRP) and tumor necrosis factor-α (TNF-α) compared to the control group. Subgroup analysis identified a reduction in serum CRP, TNF-α, and IL-6 concentration among studies with participants who had a higher level of these biomarkers at baseline, those which used sesamin capsules, and those with a bigger sample size, those conducted in Asia, and studies on females. *Conclusion*. Sesame consumption reduced serum levels of IL-6 but did not affect CRP and TNF-α in humans. Additional trials should be conducted utilizing a larger and longer treatment duration, along with studies using different sesame formulations (capsule, oil, and seed) and conducting on participants with varied health conditions.

1. Introduction

Low-grade chronic inflammation, characterized by the chronically low levels of inflammatory biomarkers, is associated with type 2 diabetes, cardiovascular disease, aging, obesity, and different kinds of cancer [1–3]. Interleukin-6 (IL-6), tumor necrosis factor-α (TNF-α), and C-reactive protein (CRP) are among the most commonly studied inflammatory biomarkers [4]. IL-6, with both anti-inflammatory and pro-inflammatory properties, is produced by macrophages and T-cells [5, 6]. TNF-α is a pro-inflammatory cytokine produced by macrophages following inflammatory stimuli [7]. CRP, an acute-phase protein, is secreted from the liver [8] as a response to elevated concentrations of IL-6 and TNF-α [9]. Given the role of inflammation in the pathogenesis of chronic illness, anti-inflammatory agents such as exercise, antioxidants, and nonsteroidal drugs are practical preventive measures for

chronic diseases [10, 11]. Dietary factors are also considered the main alternative treatments for low-grade inflammation [12, 13]. Among dietary factors, nutraceuticals and plant oils have garnered great attention due to the adverse effects and high cost of many medications [14, 15]. Several studies indicated anti-inflammatory effects of oil crop intake including flaxseed, olive, and canola oils both in Asian [16, 17] and Western countries [18, 19].

Sesame (*Sesamum indicum*) is a culinary ingredient that has been used in food preparation for thousands of years, especially in Asian countries [20]. The seeds contain an abundance of polyunsaturated fatty acids (PUFA), vitamin E, phytosterol, fiber, and bioactive lignans (*sesamin*, *sesamol*, *sesamolin*, and *episesamin*), which produce antioxidant and anti-inflammatory activity [21–23]. One of the most abundant lignans in sesame (*sesamin*) has been found to exhibit beneficial effects on inflammatory markers [24], hyperglycemia [25], hypertension [26], and hyperlipidemia [27] in humans. Sesamin is found in many sesame-containing products, including sesame oil, sesame seeds, sesame meals, and sesame-based supplements [28].

Evidence from animal studies reveals that sesamin improves hyperglycemia, reduces inflammation, and improves insulin resistance in diabetic mice [29]. However, human studies have produced conflicting results [24, 30–35]. While some studies found that sesame consumption reduces inflammatory biomarkers levels [33, 35], others did not find the same benefits [24, 34]. This study is the first systematic review and meta-analysis of randomized controlled trials, with the purpose of quantifying the overall effect of sesame consumption on inflammatory biomarkers in humans.

2. Materials and Methods

This systematic review and meta-analysis utilize the Preferred Reporting Items for Systematic Reviews and Meta-Analyses (PRISMA) guidelines [36]. The protocol was registered at the Center for Open Science Framework (OSF) database (https://www.osf.io, DOI: 10.17605/OSF.IO/TJ4N8).

2.1. Search Strategy. The search included online databases of PubMed, Scopus, and the Cochrane Database of Systematic Reviews continued until August 2020. It was conducted using medical subject headings (MESH) and relevant keywords of the following terms: ("Sesame*" OR "Sesame Oil" OR "Sesame Seed" OR "*Sesamum*" OR "*Sesamin* supplement") AND ("adiponectin" OR "leptin" OR "TGF-β" OR "high sensitive CRP" OR "IL-10" OR "IL-8" OR "TNF" OR "IL-6" OR "hs-CRP" OR "CRP" OR "Biological marker" OR "Systemic inflammation" OR "Interleukin" OR "Interleukin-1β" OR "adipokines" OR "myokine" OR "Neurogenic Inflammation" OR "Inflammation Mediator" OR "Monocyte chemotactic protein 1" OR "Intercellular adhesion molecule-1" OR "p-selectin" OR" eselectin" OR "Matrix metalloproteinase" OR "Acute phase reactant" OR "Cytokine" OR "Transforming growth factor beta" OR "C- Reactive protein" OR "Tumor necrosis factor" OR "Interleukin-6" OR "Interleukin-8" OR "Interleukin-10" OR "Inflammatory biomarker" OR "inflame"*). Database search restrictions were not utilized. The Google Scholar, reference lists of the eligible RCTs, and related review articles were also assessed to identify RCTs that were not found in the online database search.

2.2. Eligibility Criteria. Randomized controlled clinical trials were included if they met the following criteria: (1) studies which evaluated the effects of consuming sesame or its products (sesame seed, sesame oil, or *sesamin* supplement) on serum concentrations of inflammatory biomarkers, including CRP, TNF-α, and IL-6; (2) studies which reported mean or median, standard deviation (SD), and 95% confidence interval on inflammatory biomarkers. Both parallel and crossover designs were included. It was excluded if a study did not evaluate serum inflammatory markers or included sesame in a combination of active ingredients. Two separate investigators (SR and AY) evaluated each article's title and abstract based on the inclusion/exclusion criteria. Discrepancies in data extraction were resolved by the principal investigator (LS).

2.3. Data Extraction. Data were extracted independently by two researchers (MAZ and RF) and included the following information: first author's surname, publication year, study location, participants health status, age (mean/range) and sex, number of participants, study design, duration of intervention, sesame product and dosage, characteristics of the placebo/control group, mean and standard deviation (SD) both at baseline and post-intervention. Data from studies that did not report inflammatory measures as SI units were converted to these measures.

2.4. Risk of Bias Assessment. The potential risk of bias for each included study was assessed using the Cochrane Collaboration's tool [37]. This tool evaluates factors such as blinding, loss of follow-up, random sequence generation, selective reporting of outcomes, and other potential sources of bias. Studies were ranked as having a high, unclear, or low risk of bias based on those criteria.

2.5. Statistical Analysis. Effect sizes, which were calculated from the mean and standard deviations of the change in inflammatory markers, were pooled using a random-effects model and reported as weighted mean difference (WMD) and 95% confidence interval. Mean changes were calculated if the study did not provide those data. The formula used for calculating mean changes was as follows: final mean value minus baseline mean value. Standard deviations were calculated as $\mathrm{SD}_{\mathrm{Change}} = \sqrt{\mathrm{SD}^2_{\mathrm{Baseline}} + \mathrm{SD}^2_{\mathrm{Final}} - (2 \times r \times \mathrm{SD}_{\mathrm{Baseline}} \times \mathrm{SD}_{\mathrm{Final}})}$ [38]. A correlation coefficient equal to 0.8 was considered as R-value when calculating SD change [38]. Data that was reported as median and interquartile ranges was converted to means and standard deviations with the method described by Hozo et al. [39]. If required, confidence

intervals were converted to standard deviations using the formula $\text{SD} = \sqrt{n} \times \text{upper limit (UL)} - \text{lower limit (LL)}/3.92$ [38]. To identify heterogeneity, we calculated I^2, and values above 50% were interpreted as evidence of heterogeneity. We also conducted subgroup analysis using predefined factors. These included the type of sesame product (i.e., seed, oil, and supplement), baseline serum values, study size, duration, geographic region, sex, and baseline BMI. Sensitivity analyses were conducted to assess the role of each study in the final effect size. Egger's test and visual inspection of funnel plots were used to identify the potential for publication bias [40]. All statistical procedures were conducted using STATA (Version 12.0, Stata Corp, College Station, TX, USA), and statistical significance was defined as $P < 0.05$.

3. Results

3.1. Study Selection. The online database search produced 632 relevant manuscripts, and no additional documents were identified through the evaluation of reference lists. Removal of 210 duplicate manuscripts left 422 abstracts to screen. After screening, 28 studies remained for full-text evaluation. This process eliminated an additional 21 studies: irrelevant outcomes ($n = 14$); review articles ($n = 2$); animal research ($n = 3$); a combination of sesame with other substances ($n = 1$); and failure to evaluate serum biomarkers ($n = 1$). A total of seven studies remained for this analysis (Figure 1).

3.2. Study Characteristics. All the identified studies were RCTs published between 2009 and 2019 (see Table 1). The studies reflected 157 participants in treatment groups and 153 participants in control groups and had interventions ranging from 4 weeks to 8 weeks. The 310 participants were aged 16 to 70 years. Two of the seven trials only included males [30, 34], one only included females [33], and the other four trials included both sexes [24, 31, 32, 35]. Four studies were conducted in Iran [31, 33, 35], one in Brazil [30], one in Greece [34], and one study in Australia [24]. Different sesame products were used for the intervention: sesame oil was used in two studies [31, 34], three studies used sesame seeds [24, 30, 32], and two studies used *sesamin*-based supplement [33, 35]. Placebo materials also varied; options included starch capsules [33, 35], sunflower oil [31], a combination of honey, maltodextrin, milk, and caramel coloring [30], and glucosamine [32]. One study did not identify which placebo materials were used [24], and another study did not use the standard of care (regular diet) rather than a placebo [34]. None of the studies reported any significant side effects. Patient's health among the studies varied, one study used patients with type 2 diabetes [35], one used patients with hypertension [34], one used patients with metabolic syndrome [31], one used overweight patients [24], one used semiprofessional athletes [30], one used patients with rheumatoid arthritis [33], and one used patients with knee osteoarthritis [32]. Six of the trials used a parallel design [30–35], and the other used a crossover design [24].

3.3. Assessment of the Risk of Bias. After assessing the quality of studies using the six domains of the Cochrane Collaboration's tool, five studies were found to be of high quality, while the others were classified as fair. All studies described which method was used for randomization. Two studies had poor allocation concealment, and five studies were single- or double-blinding (Table 2).

3.4. Meta-Analysis

3.4.1. Findings on the Effect of Sesame on CRP. Combining the effect sizes from 7 studies, we did not find a significant reduction in serum CRP concentrations after sesame consumption, as compared to control group [weighted mean difference [Weighted Mean Difference (WMD) – 0.55; 95% CI (−1.22, 0.12), $I^2 = 75.3\%$] (Figure 2). The subgroup analysis found that baseline serum CRP levels, baseline BMI, intervention type, duration of treatment, geographic region, sample size, and sex are all sources of heterogeneity. Subgroup analysis also found that CRP was significantly reduced in studies which were conducted in Iran [WMD – 1.38; 95% CI (−2.70, −0.06), $P = 0.039$], studies in which participants had higher baseline serum CRP (≥10 mg/L) [WMD – 5.91; 95% CI (−8.25, −3.58), $P < 0.01$], studies conducted on females [WMD – 6.12; 95% CI (−8.63, −3.61), $P < 0.001$], and studies with a larger sample size (≥40) [WMD – 1.38; 95% CI (−2.70, −0.06), $P = 0.039$] (Table 3).

3.4.2. Effect of Sesame on IL-6. Based on the findings of 4 studies, a significant reduction in serum IL-6 was found after sesame consumption [WMD – 0.90; 95% CI (−1.71, −0.09), $I^2 = 80.4\%$] (Figure 3). According to subgroup analyses, intervention type, baseline serum values of IL-6, geographic region, baseline BMI, duration of treatment, and sample size are all sources of heterogeneity. Subgroup analysis also found that sesame consumption decreased serum IL-6 in studies which used *sesamin* capsule and in studies of participants with higher baseline serum IL-6 (≥2 ng/L) [WMD – 1.94; 95% CI (−3.57, −0.30), $P = 0.020$], studies conducted in Iran, studies with larger sample sizes (≥40) [WMD – 1.23; 95% CI (−1.95, −0.52), $P < 0.001$], and studies conducted on females [WMD – 1.59; 95% CI (−2.84, −0.33), $P = 0.013$] (Table 3).

3.4.3. Effect of Sesame on TNF-α. Pooling the effect sizes from 4 studies, we failed to find a significant reduction in serum TNF-α concentrations after sesame consumption [WMD – 0.35; 95% CI (−0.78, 0.08), $I^2 = 88.4\%$] (Figure 4). Subgroup analysis identified intervention type, geographic region, and sample size as the sources of heterogeneity. Subgroup analysis also found that sesame consumption had a significant effect on TNF-α in studies which were conducted in Iran, used *sesamin* supplementation, had larger samples (≥40) [WMD – 0.67; 95% CI (−0.95, −0.38), $P < 0.001$], and studies conducted on females [(WMD) – 0.53; 95% CI (−0.82, −0.23), $P = 0.001$] (Table 3).

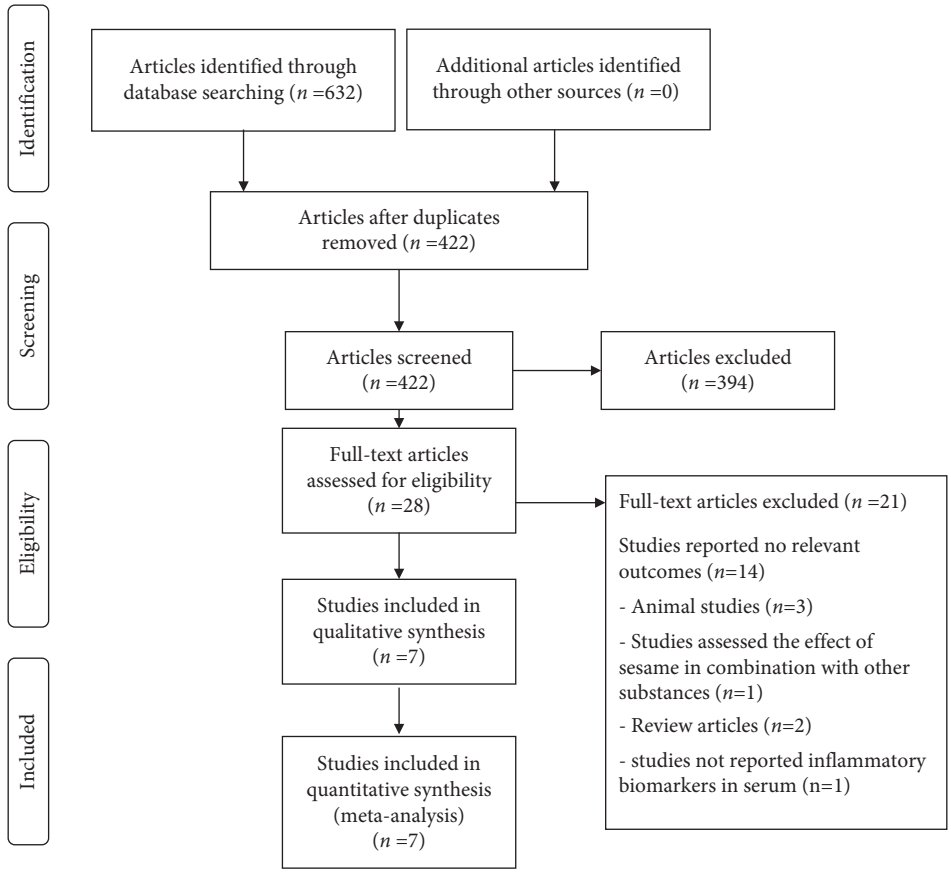

Figure 1: Study selection diagram.

3.5. Sensitivity Analysis. A sensitivity analysis was conducted to identify the size of the influence of each study on the overall effect size produced. This analysis found that none of the studies significantly affected the outcome (Supplementary Figures 1–3).

3.6. Publication Bias. Publication bias was assessed using visual inspection of funnel plots and the Egger test. Inspection of the funnel plots did not provide any evidence of publication bias (Supplementary Figures 4–6). These observations were confirmed by Egger's linear regression for CRP ($P = 0.12$), IL-6 ($P = 0.31$), and TNF-α ($P = 0.44$).

4. Discussion

The present meta-analysis showed that sesame and the consumption of its products could lower serum IL-6 levels but did not affect serum concentrations of CRP and TNF-α in humans. Besides, a significant reduction was identified in serum CRP, TNF-α, and IL-6 concentration among studies with participants who had a higher level of these biomarkers at baseline, used *sesamin* capsules, had a larger sample size, were conducted in Asia, and studies with female participants. This is the first systematic review and meta-analysis to identify the effects of sesame supplementation on serum inflammatory biomarkers.

We found that serum IL-6 decreased followed by sesame consumption. In line with our result, Hsu et al. [41] revealed that administration of different dosages of sesame oil (0, 1, 2, or 4 mL/kg, orally) decreased IL-6 and TNF-α in the rat. Another study in microglia cells showed neuroprotective influences of sesamin supplementation by its effects on lowering mRNA levels of IL-6 [42]. Chaval and Forse indicated that mice fed the diet that contained 1% sesamol had lower serum levels of IL-6 and PGES2 in comparison to the control mice [43]. One randomized double-blind, placebo-controlled showed daily consumption of a low-fat muffin plus flaxseed lignan complex (500 mg/d of secoisolariciresinol diglucoside) for 6 weeks did not decrease IL-6 compared to a low-fat muffin in 22 healthy postmenopausal women [44]. The level of lignans in sesame is even higher than in flaxseed, which was previously considered the richest source of lignans [45]. One animal study indicated more beneficial effects of the sesame seed lignan in lowering breast tumor growth compared to flaxseed lignan [46].

We did not find significant effects of total sesame consumption on serum CRP and TNF-α concentrations. In consistency with our results, an in vitro study showed supplementation for 12 weeks with 18 g/d of sesame oil did not have a significant effect on TNF-α and PGE-2 in cultured blood of healthy male volunteers [47]. In addition, supplementation with 25 g/day sesame seeds for 5 weeks had no beneficial effects on CRP, TNF-α, and IL-6 in overweight or

Table 1: Characteristics of randomized trials on the effects of sesame consumption on inflammatory biomarkers in humans included in the meta-analysis.

Reference	Location	Subjects and gender	Age, y[1]	Design	Intervention type		Duration (wk)	Outcomes	Outcome[2]		Notes about subjects
					Intervention	Control (name and composition)			Intervention	Control	
Helli et al. [33]	Iran	F : 44 S : 22 C : 22	S + C: 55.49 ± 5.98	Parallel	Sesamin capsule (200 mg/d)	Placebo capsules (starch)	6	hs-CRP TNF-α IL-6	hs-CRP (mg/L) : before: 22.28 ± 5.85; after: 17.33 ± 4.05 TNF (ng/L) : before: 2.17 ± 0.71; after: 1.67 ± 0.58 IL-6 (ng/L) : before: 4.84 ± 3.67 after: 3.45 ± 1.69	hs-CRP (mg/L) : before: 20.74 ± 7.43; after: 21.91 ± 7.81 TNF (ng/L) : before: 2.03 ± 0.82; after: 2.06 ± 0.36 IL-6 (ng/L) : before: 4.38 ± 2.67; after: 4.58 ± 1.85	44 patients with rheumatoid arthritis
Farajbaksh et al. [31]	Iran	M : 16 F : 31 S : 24 (7/17) C : 23 (9/14)	30–70 yrs S : 48.04 ± 7.67 C : 50.17 ± 7.6	Parallel	Sesame oil (30 mL/d)	Placebo (sunflower oil)	8	hs-CRP	hs-CRP (mg/L) : before: 43.8 ± 13.4; after: 39.6 ± 17	Hs-CRP (mg/L) : before: 43.5 ± 17.4; after: 43.9 ± 20.1	47 patients with metabolic syndrome
Da silva barbosa et al. [30]	Brazil	M : 20 S : 10 C : 10	16–18 yrs		Sesame seed (40 g/d)	Placebo (honey, maltodextrin, cow milk, and artificial caramel food coloring)	4	hs-CRP	hs-CRP (mg/L) : before: 3.66 ± 1.4; after: 0.8 ± 1.0	hs-CRP (mg/L) : before: 3.31 ± 1.8; after: 0.6 ± 0.4	20 semiprofessional soccer players

Table 1: Continued.

Reference	Location	Subjects and gender	Age, y[1]	Design	Intervention type		Duration (wk)	Outcomes	Outcome[2]		Notes about subjects
					Intervention	Control (name and composition)			Intervention	Control	
Mohammad Shahi et al. [35]	Iran	F + M: 48 S: 24 C: 24	30–60 yrs S: 50 ± 12.3 C: 51.72 ± 12.24	Parallel	Sesamin capsule (200 mg/d)	Placebo capsules (starch)	8	hs-CRP TNF-α IL-6 IL-6	hs-crp (mg/L): before: 2.83 ± 1.35; after: 2.53 ± 1.44 TNF (ng/L) before: 1.92 ± 0.76; after: 1.3 ± 0.27 IL-6 (ng/L): before: 20.19 ± 12.1; after: 17.2 ± 9.13 Adiponectin (μg/mL): before: 6.21 ± 1.33; after: 7.34 ± 2.88	Hs-CRP (mg/L): before: 2.80 ± 1.25; after: 2.92 ± 1.3 TNF (ng/L): before: 1.66 ± 0.76; after: 1.86 ± 0.9 IL-6 (ng/L): before: 21.26 ± 10.73 after: 22.19 ± 11.14 Adiponectin (μg/L): before: 6.60 ± 1.62; after: 6.19 ± 1.10	44 type 2 diabetes mellitus
Haghighian et al. [32]	Iran	F + M: 45 S: 22 C: 23	50–70 yrs S: 56.90 ± 6.39 C: 58.27 ± 7.84	Parallel	Sesame seed (40 g/d) + acetaminophen	Placebo (glucosamine) + acetaminophen	8	hs-CRP IL-6	hs-CRP (mg/L): before: 1.45 ± 1.12; after: 1.42 ± 1.32 IL-6 (ng/L): before: 2.29 ± 0.82; after: 0.38 ± 0.05	hs-CRP (mg/L): before: 1.64 ± 1.19; after: 1.68 ± 0.87 IL-6 (ng/L): before: 2.43 ± 0.68; after: 1.53 ± 0.04	45 patients with knee osteoarthritis

Table 1: Continued.

Reference	Location	Subjects and gender	Age, y[1]	Design	Intervention type		Duration (wk)	Outcomes	Outcome[2]		Notes about subjects
					Intervention	Control (name and composition)			Intervention	Control	
Karatzi et al. [34]	Greece	M : 30 S : 17 C : 13	S : 49.8 ± 8.46 C : 56.8 ± 12	Parallel	Sesame oil (35 g/d)	Control	8	CRP TNF-α	CRP (mg/L) : before: 1.8 ± 1.8; after: 2.0 ± 2.3 TNF (ng/L) : before: 0.77 ± 1.0; after: 0.96 ± 1.5	CRP (mg/L) : before: 1.9 ± 2.3; after: 2.0 ± 2.5 TNF (ng/L) : before: 0.31 ± 0.51; after: 0.54 ± 0.61	30 hypertension men
Wu et al. [24]	Australia	F + M: 3 S : 38 C : 38	S: 54.7 ± 8.6 C : 54.7 ± 8.6	Crossover	Sesame seed (25 g/d)	Placebo	5	hs-CRP TNF-α IL-6	hs-CRP (mg/L) : before: 2.1 ± 2.5; after: 1.89 ± 2.06 TNF-α (ng/L) : before: 1.85 ± 0.59; after: 1.83 ± 0.58 IL-6 (ng/L) : before: 2.08 ± 1.16; after: 2.05 ± 1.03	hs-CRP (mg/L) : before: 1.98 ± 2.29; after: 2.02 ± 2.42 TNF-α (ng/L) : before: 1.83 ± 0.61; after: 1.8 ± 0.59 IL-6 (ng/L) : before: 2.14 ± 1.3; after: 2.25 ± 1.33	38 overweight men and women

[1]Values are overall ranges and means ± SDs in each group. [2]Values are means ± SDs. C: control; CRP: C-reactive protein; F: female; hs-CRP: highly sensitive C-reactive protein; IL-6: interleukin-6; M: male; S: sesame; and TNF-α: tumor necrosis factor-α.

Table 2: Cochrane's risk of bias assessment for randomized controlled trials on the effect of sesame consumption on inflammatory biomarkers in human[1].

Reference	Random sequence generation	Allocation concealment	Blinding of participants, personnel, and outcome assessors	Incomplete outcome data	Selective outcome reporting	Other sources of bias
Helli et al. [33]	L	L	L	L	L	L
Farajbakhsh et al. [31]	L	H	L	L	L	L
Da Silva Barbosa et al. [30]	L	H	L	L	L	L
Mohammad Shahi al. [35]	L	H	L	L	L	L
Haghighian et al. [32]	L	H	H	L	L	L
Karatzi et al. [34]	L	H	H	L	L	L
Wu et al. [24]	L	L	L	L	L	L

[1]H: high risk of bias; L: low risk of bias; and U: unclear risk of bias.

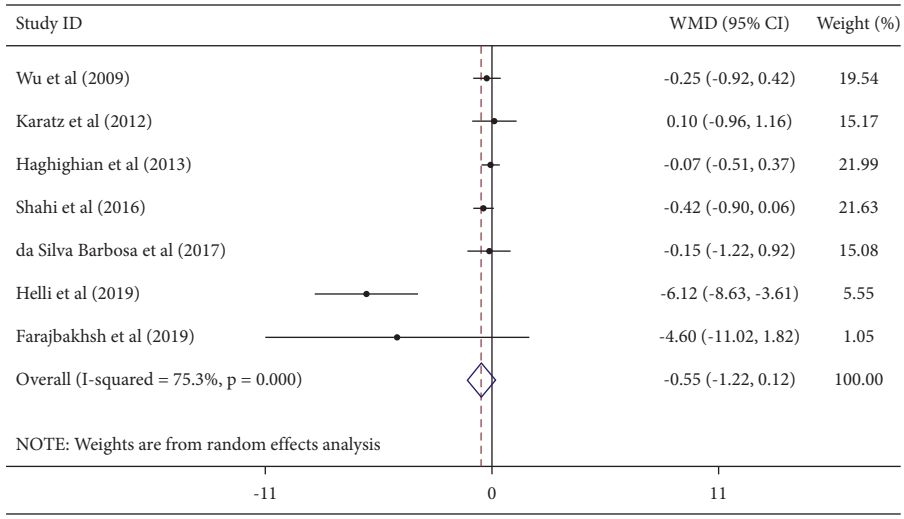

Figure 2: Forest plot showing the effects of sesame consumption on circulating CRP (WMDs and 95% CIs) in humans using the random-effects model. CI: confidence interval; CRP: C-reactive protein; and WMD: weighted mean difference.

men and women [24]. In contrast to our findings, one RCT study indicated that 0.5 mL/kg/day sesame oil consumption along with interferon beta-1a decreased TNF-α measured in supernatants of peripheral blood mononuclear cells in patients with multiple sclerosis compared to patients who only received interferon beta-1a [48]. In one randomized clinical trial study, supplementation with 360 mg/d flaxseed-derived lignin for twelve weeks decreased C-reactive protein in 39 diabetic women [49]. In an animal study conducted by Chiang et al., sesamin significantly reduced the serum CRP, TNF-α, and IL-6 levels in the rat with liver injury received 10 mg/kg sesamin orally [50]. These inconsistent findings might be partially due to different sources of sesame, geographic region, sex, and study sample size.

Using sesame as sesamin capsule decreases CRP, IL-6, and TNF-α significantly. This may be due to the high bioavailability of sesame lignan in sesamin capsules compared to sesame seed or sesame oil. In addition, our study also showed that sesame intake lowered CRP, IL-6, and TNF-α in studies in which participants had higher baseline serum levels of these markers. Rheumatoid arthritis, knee osteoarthritis, lupus erythematosus, and multiple sclerosis are chronic inflammatory systemic diseases (CIDs) with high serum inflammatory biomarkers [51].

The participants of most included studies had normal serum levels of inflammatory markers at the baseline. Therefore, this may be a reason for observing no significant effects in the meta-analysis. Besides, this study also indicated that sesame intake lowers CRP and IL-6 among participants with high baseline serum levels of these markers. Because nearly all participants had normal serum TNF-α, we could not perform subgroup analysis for this biomarker. Although obese individuals have higher concentrations of inflammatory biomarkers than normal weight subjects, this study did not show any anti-inflammatory effects of sesame in both obese (BMI $\geq 30\ Kg/m^2$) and non-obese (BMI $< 30\ Kg/m^2$) persons due to a limited number of studies in each subgroup. Furthermore, the duration of

Table 3: Pooled estimates of the effects of sesame consumption on inflammatory biomarkers within different subgroups[3].

	Number of trials			WMD (95% CI)			*P* value			*P*-heterogeneity			I^2 (%)		
	CRP	TNF	IL-6	CRP	TNF	IL-6	CRP	TNF	IL-6	CRP	TNF	IL-6	CRP	TNF	IL-6
Total	7	4	4	−0.55 (−1.22, 0.12)	−0.34 (−0.77, 0.08)	−0.90 (−1.71, −0.09)	0.109	0.111	0.029	<0.001	<0.001	0.002	75.1	88.4	80.4
Baseline serum biomarker[1]															
<10 mg/L	5	—	2	−0.20 (−0.48, 0.06)	—	−0.56 (−1.41, 0.28)	0.138	—	0.193	0.831	—	0.158	0	—	49.8
≥10 mg/L	2	—	2	−5.91 (−8.25, −3.58)	—	−1.94 (−3.57, −0.30)	<0.001	—	0.020	0.666	—	0.029	0	—	78.9
Baseline BMI															
≥30 kg/m^2	3	2	1	−3.40 (−8.16, 1.35)	−0.24 (−0.77, 0.28)	−0.73 (−2.13, 0.66)	0.161	0.363	0.303	<0.001	0.002	—	90.5	89.5	—
<30 kg/m^2	4	2	3	−0.19 (−0.49, 0.10)	−0.45 (−1.21, 0.31)	−1.75 (−4.23, 0.73)	0.193	0.245	0.167	0.693	0.008	0.266	0	85.9	24.5
Type of intervention															
Sesame capsule	2	2	2	−0.62 (−1.09, −0.15)	−0.67 (−0.95, −0.38)	−1.94 (−3.57, −0.30)	0.271	<0.001	0.020	<0.001	0.190	0.020	94.8	41.9	14.9
Sesame seed	3	1	2	−0.12 (−0.47, 0.22)	0.01 (−0.15, 0.17)	−0.56 (−1.41, 0.28)	0.476	0.907	0.193	0.908	—	0.193	0	—	89.8
Sesame oil	2	1	—	−0.02 (−1.07, 1.02)	−0.04 (−0.52, 0.44)	—	0.582	0.871	—	0.157	—	—	50.1	—	—
Duration of treatment															
<8 wk	3	2	2	−1.73 (−3.92, 0.45)	−0.24 (−0.77, 0.28)	−0.73 (−2.13, 0.66)	0.120	0.363	0.303	<0.001	0.002	0.029	90.1	89.5	78.9
=8 wk	4	2	2	−0.21 (−0.55, 0.12)	−0.45 (−1.21, 0.31)	−1.75 (−4.23, 0.73)	0.216	0.245	0.167	0.356	0.008	0.158	7.5	85.9	49.8
Geographic region															
Asia	4	2	3	−1.38 (−2.70, −0.06)	−0.67 (−0.95, −0.38)	−1.23 (−1.95, −0.52)	0.039	<0.001	0.001	<0.001	0.190	0.266	87.3	41.9	24.5
Non-Asia	3	2	1	−0.14 (−0.65, 0.35)	0.005 (−0.15, 0.16)	−0.14 (−0.48, 0.20)	0.559	0.955	0.428	0.861	0.848	—	0	0	—
Sample size															
<40	3	2	1	−0.14 (−0.65, 0.35)	0.005 (−0.15, 0.16)	−0.14 (−0.48, 0.20)	0.559	0.955	0.428	0.861	0.848	0.428	0	0	—
≥40	4	2	3	−1.38 (−2.70, −0.06)	−0.67 (−0.95, −0.38)	−1.23 (−1.95, −0.52)	0.039	<0.001	<0.001	<0.001	0.190	0.001	87.3	41.9	24.5
Sex															
Men	2	1	–	−0.02 (−0.77, 0.72)	−0.04 (−0.52, 0.44)	—	0.950	0.871	—	—	—	—	0	—	—
Women	1	1	1	-6.12 (−8.63, −3.61)	−0.53 (−0.82, −0.23)	−1.59 (−2.84, −0.33)	<0.001	0.001	0.013	0.411	—	—	—	—	—
Both	4	2	3	−0.24 (−0.53, 0.04)	−0.39 (−1.20, 0.41)	−0.72 (−1.62, 0.17)	0.103	0.342	0.116	0.745	<0.001	0.002	0	95.2	84.1

[1]<10 mg/L, ≥10 mg/L for CRP, <2 ng/L, ≥2 ng/L for TNF, <3 ng/L, ≥3 ng/L for IL-6, [2]BMI: body mass index; CI: confidence interval; CRP: C-reactive protein; IL-6: interleukin-6; TNF-*α*: tumor necrosis factor-*α*; and WMD: weighted mean difference.

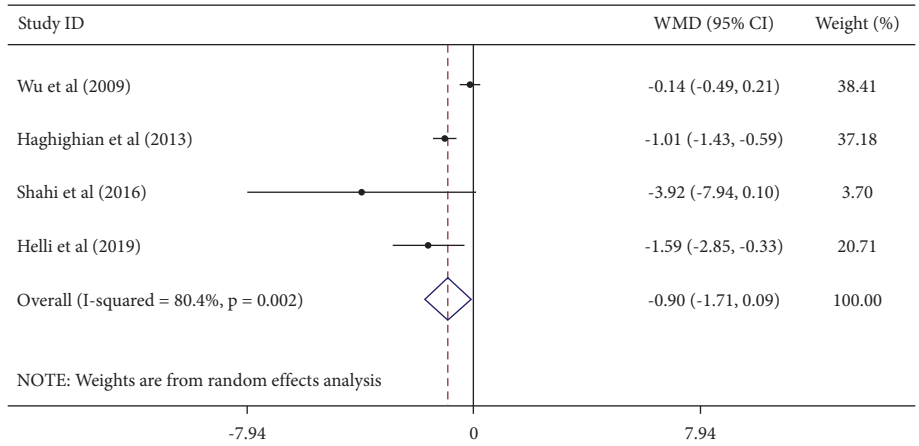

Figure 3: Forest plot showing the effects of garlic supplementation on circulating IL-6 (WMDs and 95% CIs) in adults using the random-effects model. CI: confidence interval; IL-6: interleukin-6; and WMD: weighted mean difference.

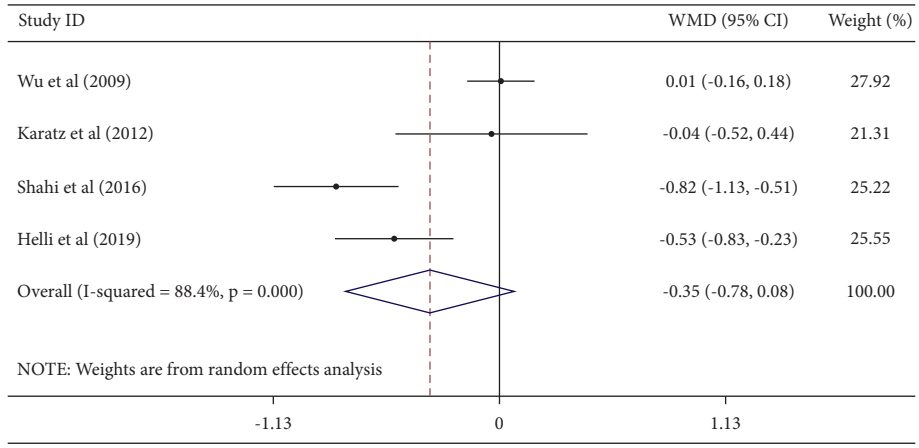

Figure 4: Forest plot showing the effects of sesame consumption on circulating TNF-α (WMDs and 95% CIs) in humans using the random-effects model. CI: confidence interval; TNF-α: tumor necrosis factor-α; and WMD: weighted mean difference.

eligible studies (≤8 weeks) might not be long enough to see the possible effects on inflammatory markers. Moreover, sesame is a commonly used oil, especially in Asian countries [20]. The studies conducted in Iran show that sesame consumption declined inflammatory biomarkers. Another reason for failing to find a significant association may be a low number of participants.

Several mechanisms of action have been identified as responsible for the anti-inflammatory effects. Sesamol (3–100 μM) was found to lessen the production of nitric oxide (NO) and pro-inflammatory cytokines, suppress the expression of inducible nitric oxide synthase (iNOS) and cyclooxygenase-2 (COX-2), and promote Nrf2, an antioxidant pathway. It was also found to block the mitogen-activated protein kinase (MAPK) and NF-κB pathways and decrease reactive oxygen species production, which decreased the inflammatory response [52]. In a study by Chu and colleagues, one subcutaneous injection of sesamol (10 mg/kg, s.c.) was found to significantly reduce the levels of NF-κB, iNOS, and interleukin 1β (IL-1β) [53]. Another study revealed that sesamol (5–20 μM) significantly inhibits the expression of several matrix metalloproteinases (MMPs), TNFα- and IL-1β-induced gelatinolysis of MMP-9, MMP-1, and MMP-13 expression, IL-1β- and phosphorylation of ERK1/2 or p38 MAPKs in SW1353 cells, a human chondrosarcoma cell line [54]. The same study revealed that oral administration of sesamol (30 mg/kg, p.o.) for 2 weeks attenuated MMP-1 and MMP-9 expression in the cartilage of monosodium iodoacetate (MIA)-induced osteoarthritis in male Wistar rats [54]. Sesamol (0.1–1.0 mg/kg, p.o.) also inhibited the activation of mucosal NF-κB and attenuated the recruitment of inflammatory cells, including CD68 + Kupffer cells and neutrophils [55]. Noteworthy, Chang and colleagues demonstrated that sesamol (2.5–25 μM) treatment in platelets significantly decreased collagen-induced phosphorylation of IκB kinase β (IKKβ) [56] (Figure 5).

This study has several limitations. The total number of clinical trials that qualified for this analysis was small, and more studies are required to deepen our understanding. Additionally, this analysis includes studies conducted on a wide range of dosing protocols, participant ages, underlying health status, and duration. We tried to detect the source of heterogeneity by subgroup analysis. However, because studies were performed in participants with a different

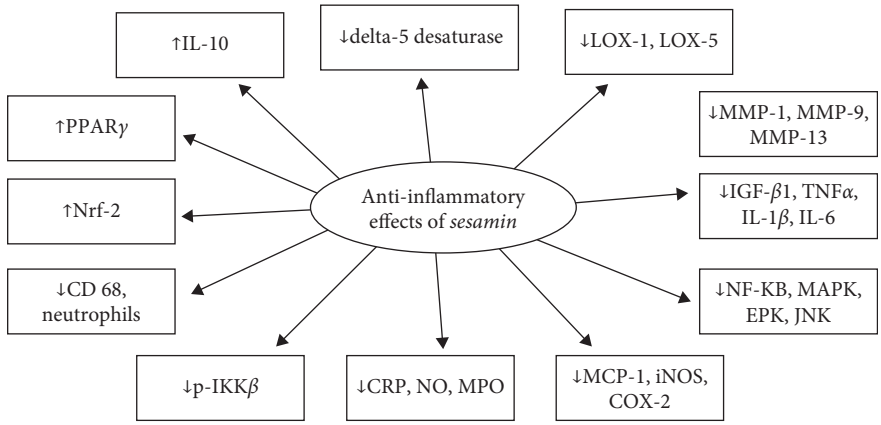

Figure 5: The mechanism of sesame reducing inflammation.

health condition and limited number of studies for each subgroup, we could not perform subgroup analysis according to health status. The overall result may have been influenced by the differences in dosing and sourcing of sesame. Subgroup analysis to identify dose-dependence or contrast groups by dosing was not feasible due to variations in the sesame preparations and the difficulty of obtaining accurate dose conversions. In addition, most of the trials included in this analysis were conducted in Asian countries and were small-scale studies assessing effects elsewhere. Finally, the high risk of random allocation and blinding biases found in some studies resulted in lower scientific evidence.

5. Conclusion

In conclusion, the consumption of sesame can significantly reduce serum IL-6 levels without any effects on CRP and IL-6. The small numbers of related RCTs and high amounts of heterogeneity among these studies limit generalizability. We recommend that additional high-quality RCTs be conducted on participants with different health conditions, varying the duration of intervention, and multiple forms and dosages of sesame consumption to confirm our findings.

Data Availability

Data will be made available if deemed necessary upon request to the corresponding author.

Conflicts of Interest

The authors declare that they have no conflicts of interest regarding the publication of this paper.

Authors' Contributions

Shabnam Rafiee and Laila Shirbeigi conceptualized and designed the study. Shabnam Rafiee, Roghaye Faryabi, and Alireza Yargholi drafted the manuscript and collected data. Mohammad Ali Zareian analyzed the data. Laila Shirbeigi and Shabnam Rafiee reviewed the protocol for important intellectual content. Jessie Hawkins and Nitin Shivappa as natives did English language editing. All authors read and approved the final manuscript.

Supplementary Materials

Supplementary Figure 1. Analysis of the influence of sesame consumption on serum CRP concentrations in humans. CI: confidence interval; CRP: C-reactive protein. *Supplementary Figure 2*. Analysis of the influence of sesame consumption on serum IL-6 concentrations in humans. CI: confidence interval; IL-6: interleukin-6. *Supplementary Figure 3*. Analysis of the influence of sesame consumption on serum TNF concentrations in humans. CI: confidence interval; TNF: tumor necrosis factor. *Supplementary Figure 4*. Funnel plot for assessing publication bias in the studies reporting the effects of sesame consumption on serum CRP concentrations in humans. CRP: C-reactive protein; SE: standard error; WMD: weighted mean difference. *Supplementary Figure 5*. Funnel plot for assessing publication bias in the studies reporting the effects of sesame consumption on serum IL-6 concentrations in humans. IL-6: interleukin-6; SE: standard error; and WMD: weighted mean difference. *Supplementary Figure 6*. Funnel plot for assessing publication bias in the studies reporting the effects of sesame consumption on serum TNF concentrations in humans. TNF: tumor necrosis factor; SE: standard error; and WMD: weighted mean difference. (*Supplementary Materials*)

References

[1] V. Guarner and M. E. Rubio-Ruiz, "Low-grade systemic inflammation connects aging, metabolic syndrome and cardiovascular disease," *Aging and Health-A Systems Biology Perspective*, Karger Publishers, vol. 40, pp. 99–106, 2015.

[2] A. Pradhan, "Obesity, metabolic syndrome, and type 2 diabetes: inflammatory basis of glucose metabolic disorders," *Nutrition Reviews*, vol. 65, no. suppl_3, pp. S152–S156, 2007.

[3] B. Zhou, B. Shu, J. Yang, J. Liu, T. Xi, and Y. Xing, "C-reactive protein, interleukin-6 and the risk of colorectal cancer: a meta-analysis," *Cancer Causes & Control*, vol. 25, no. 10, pp. 1397–1405, 2014.

[4] G. S. Hotamisligil, "Inflammation and metabolic disorders," *Nature*, vol. 444, no. 7121, pp. 860–867, 2006.

[5] A. C. Ferguson-Smith, Y.-F. Chen, M. S. Newman, L. T. May, P. B. Sehgal, and F. H. Ruddle, "Regional localization of the interferon-β2B-cell stimulatory factor 2/hepatocyte stimulating factor gene to human chromosome 7p15-p21," *Genomics*, vol. 2, no. 3, pp. 203–208, 1988.

[6] T. Van Der Poll, C. V. Keogh, X. Guirao, W. A. Buurman, M. Kopf, and S. F. Lowry, "Interleukin-6 gene-deficient mice show impaired defense against pneumococcal pneumonia," *The Journal of Infectious Diseases*, vol. 176, no. 2, pp. 439–444, 1997.

[7] M. Cesari, B. W. J. H. Penninx, A. B. Newman et al., "Inflammatory markers and onset of cardiovascular events," *Circulation*, vol. 108, no. 19, pp. 2317–2322, 2003.

[8] M. Pepys, "The acute phase response and C-reactive protein," *Oxford textbook of medicine*, vol. 2, pp. 1527–1533, 1995.

[9] M. B. Pepys and G. M. Hirschfield, "C-reactive protein: a critical update," *Journal of Clinical Investigation*, vol. 111, no. 12, pp. 1805–1812, 2003.

[10] N. Esser, N. Paquot, and A. J. Scheen, "Anti-inflammatory agents to treat or prevent type 2 diabetes, metabolic syndrome and cardiovascular disease," *Expert Opinion on Investigational Drugs*, vol. 24, no. 3, pp. 283–307, 2015.

[11] M. Askari, R. Faryabi, H. Mozaffari, and M. Darooghegi Mofrad, "The effects of N-Acetylcysteine on serum level of inflammatory biomarkers in adults. Findings from a systematic review and meta-analysis of randomized clinical trials," *Cytokine*, vol. 135, Article ID 155239, 2020.

[12] L. Galland, "Diet and inflammation," *Nutrition in Clinical Practice*, vol. 25, no. 6, pp. 634–640, 2010.

[13] F. Eichelmann, L. Schwingshackl, V. Fedirko, and K. Aleksandrova, "Effect of plant-based diets on obesity-related inflammatory profiles: a systematic review and meta-analysis of intervention trials," *Obesity Reviews*, vol. 17, no. 11, pp. 1067–1079, 2016.

[14] M. Darooghegi Mofrad, A. Milajerdi, F. Koohdani, P. J. Surkan, and L. Azadbakht, "Garlic supplementation reduces circulating C-reactive protein, tumor necrosis factor, and Interleukin-6 in adults: a systematic review and meta-analysis of randomized controlled trials," *Journal of Nutrition*, vol. 149, no. 4, pp. 605–618, 2019.

[15] M. Rahimlou, N. B. Jahromi, N. Hasanyani, and A. R. Ahmadi, "Effects of flaxseed interventions on circulating inflammatory biomarkers: a systematic review and meta-analysis of randomized controlled trials," *Advances in Nutrition*, vol. 10, no. 6, pp. 1108–1119, 2019.

[16] N. Morshedzadeh, S. Shahrokh, H. A. Aghdaei et al., "Effects of flaxseed and flaxseed oil supplement on serum levels of inflammatory markers, metabolic parameters and severity of disease in patients with ulcerative colitis," *Complementary Therapies in Medicine*, vol. 46, pp. 36–43, 2019.

[17] G. Zong, W. Demark-Wahnefried, H. Wu, and X. Lin, "Effects of flaxseed supplementation on erythrocyte fatty acids and multiple cardiometabolic biomarkers among Chinese with risk factors of metabolic syndrome," *European Journal of Nutrition*, vol. 52, no. 5, pp. 1547–1551, 2013.

[18] E. Sanchez-Rodriguez, S. Biel-Glesson, J. R. Fernandez-Navarro et al., "Effects of virgin olive oils differing in their bioactive compound contents on biomarkers of oxidative stress and inflammation in healthy adults: a randomized double-blind controlled trial," *Nutrients*, vol. 11, no. 3, 2019.

[19] M. Kruse, C. Von Loeffelholz, D. Hoffmann et al., "Dietary rapeseed/canola-oil supplementation reduces serum lipids and liver enzymes and alters postprandial inflammatory responses in adipose tissue compared to olive-oil supplementation in obese men," *Molecular Nutrition & Food Research*, vol. 59, no. 3, pp. 507–519, 2015.

[20] M. Namiki, "Nutraceutical functions of sesame: a review," *Critical Reviews in Food Science and Nutrition*, vol. 47, no. 7, pp. 651–673, 2007.

[21] Q. Jin, Y. Liu, X. Wang, and H. Dai, "Sesamin as a natural antioxidant," *Journal of the Chinese Cereals and Oils Association*, vol. 20, pp. 89–93, 2005.

[22] A. Kamal-Eldin, A. Moazzami, and S. Washi, "Sesame seed lignans: potent physiological modulators and possible ingredients in functional foods & nutraceuticals," *Recent Patents on Food, Nutrition & Agriculture*, vol. 3, no. 1, pp. 17–29, 2011.

[23] M. Elleuch, S. Besbes, O. Roiseux, C. Blecker, and H. Attia, "Quality characteristics of sesame seeds and by-products," *Food Chemistry*, vol. 103, no. 2, pp. 641–650, 2007.

[24] J. H. Y. Wu, J. M. Hodgson, I. B. Puddey, R. Belski, V. Burke, and K. D. Croft, "Sesame supplementation does not improve cardiovascular disease risk markers in overweight men and women," *Nutrition, Metabolism, and Cardiovascular Diseases*, vol. 19, no. 11, pp. 774–780, 2009.

[25] D. Sankar, A. Ali, G. Sambandam, and R. Rao, "Sesame oil exhibits synergistic effect with anti-diabetic medication in patients with type 2 diabetes mellitus," *Clinical Nutrition*, vol. 30, no. 3, pp. 351–358, 2011.

[26] H. Khosravi-Boroujeni, E. Nikbakht, E. Natanelov, and S. Khalesi, "Can sesame consumption improve blood pressure? A systematic review and meta-analysis of controlled trials," *Journal of the Science of Food and Agriculture*, vol. 97, no. 10, pp. 3087–3094, 2017.

[27] S. Khalesi, E. Paukste, E. Nikbakht, and H. Khosravi-Boroujeni, "Sesame fractions and lipid profiles: a systematic review and meta-analysis of controlled trials," *British Journal of Nutrition*, vol. 115, no. 5, pp. 764–773, 2016.

[28] J.-C. Zhou, D.-W. Feng, and G.-S. Zheng, "Extraction of sesamin from sesame oil using macroporous resin," *Journal of Food Engineering*, vol. 100, no. 2, pp. 289–293, 2010.

[29] L. Hong, W. Yi, C. Liangliang, H. Juncheng, W. Qin, and Z. Xiaoxiang, "Hypoglycaemic and hypolipidaemic activities of sesamin from sesame meal and its ability to ameliorate insulin resistance in KK-Ay mice," *Journal of the Science of Food and Agriculture*, vol. 93, no. 8, pp. 1833–1838, 2013.

[30] C. V. d. S. Barbosa, A. S. Silva, C. V. C. de Oliveira et al., "Effects of sesame (*Sesamum indicum* L.) supplementation on creatine kinase, lactate dehydrogenase, oxidative stress markers, and aerobic capacity in semi-professional soccer players," *Frontiers in Physiology*, vol. 8, p. 196, 2017.

[31] A. Farajbakhsh, S. M. Mazloomi, M. Mazidi et al., "Sesame oil and vitamin E co-administration may improve cardio metabolic risk factors in patients with metabolic syndrome: a randomized clinical trial," *European Journal of Clinical Nutrition*, vol. 73, no. 10, pp. 1403–1411, 2019.

[32] M. K. Haghighian, B. Alipoor, A. M. Mahdavi, B. E. Sadat, M. A. Jafarabadi, and A. Moghaddam, "Effects of sesame seed supplementation on inflammatory factors and oxidative stress biomarkers in patients with knee osteoarthritis," *Acta Medica Iranica*, vol. 53, no. 4, pp. 207–213, 2015.

[33] B. Helli, M. M. Shahi, K. Mowla, M. T. Jalali, and H. K. Haghighian, "A randomized, triple-blind, placebo-controlled clinical trial, evaluating the sesamin supplement effects on proteolytic enzymes, inflammatory markers, and clinical indices in women with rheumatoid arthritis," *Phytotherapy Research*, vol. 33, no. 9, pp. 2421–2428, 2019.

[34] K. Karatzi, K. Stamatelopoulos, M. Lykka et al., "Acute and long-term hemodynamic effects of sesame oil consumption in hypertensive men," *Journal of Clinical Hypertension*, vol. 14, no. 9, pp. 630–636, 2012.

[35] M. Mohammad Shahi, M. Zakerzadeh, M. Zakerkish, M. Zarei, and A. Saki, "Effect of sesamin supplementation on glycemic status, inflammatory markers, and adiponectin levels in patients with type 2 diabetes mellitus," *Journal of Dietary Supplements*, vol. 14, no. 1, pp. 65–75, 2017.

[36] D. Moher, L. Shamseer, L. Shamseer et al., "Preferred reporting items for systematic review and meta-analysis protocols (PRISMA-P) 2015 statement," *Systematic Reviews*, vol. 4, no. 1, p. 1, 2015.

[37] J. P. Higgins, J. Thomas, J. Chandler et al., *Cochrane Handbook for Systematic Reviews of Interventions*, John Wiley & Sons, New Jersey, USA, 2019.

[38] M. Borenstein, L. V. Hedges, J. P. Higgins, and H. R. Rothstein, *Introduction to Meta-Analysis*, John Wiley & Sons, New Jersey, USA, 2011.

[39] S. P. Hozo, B. Djulbegovic, and I. Hozo, "Estimating the mean and variance from the median, range, and the size of a sample," *BMC Medical Research Methodology*, vol. 5, no. 1, p. 13, 2005.

[40] M. Egger, G. D. Smith, M. Schneider, and C. Minder, "Bias in meta-analysis detected by a simple, graphical test," *BMJ*, vol. 315, no. 7109, pp. 629–634, 1997.

[41] D.-Z. Hsu, S.-J. Chen, P.-Y. Chu, and M.-Y. Liu, "Therapeutic effects of sesame oil on monosodium urate crystal-induced acute inflammatory response in rats," *Springer Plus*, vol. 2, no. 1, p. 659, 2013.

[42] K.-C. G. Jeng, R. C. W. Hou, J.-C. Wang, and L.-I. Ping, "Sesamin inhibits lipopolysaccharide-induced cytokine production by suppression of p38 mitogen-activated protein kinase and nuclear factor-κB," *Immunology Letters*, vol. 97, no. 1, pp. 101–106, 2005.

[43] S. R. Chavali and R. A. Forse, "Decreased production of interleukin-6 and prostaglandin E2 associated with inhibition of delta5 desaturation of ω6 fatty acids in mice fed safflower oil diets supplemented with sesamol," *Prostaglandins, Leukotrienes and Essential Fatty Acids*, vol. 61, no. 6, pp. 347–352, 1999.

[44] J. Hallund, I. Tetens, S. Bügel, T. Tholstrup, and J. M. Bruun, "The effect of a lignan complex isolated from flaxseed on inflammation markers in healthy postmenopausal women," *Nutrition, Metabolism, and Cardiovascular Diseases*, vol. 18, no. 7, pp. 497–502, 2008.

[45] I. E. J. Milder, I. C. W. Arts, B. V. D. Putte, D. P. Venema, and P. C. H. Hollman, "Lignan contents of Dutch plant foods: a database including lariciresinol, pinoresinol, secoisolariciresinol and matairesinol," *British Journal of Nutrition*, vol. 93, no. 3, pp. 393–402, 2005.

[46] J. S. Truan, J.-M. Chen, and L. U. Thompson, "Comparative effects of sesame seed lignan and flaxseed lignan in reducing the growth of human breast tumors (MCF-7) at high levels of circulating estrogen in athymic mice," *Nutrition and Cancer*, vol. 64, no. 1, pp. 65–71, 2012.

[47] S. Ten Wolde, F. Engels, A. M. Miltenburg, E. A. Kuijpers, G. I. Struijk-Wielinga, and B. A. Dijkmans, "Sesame oil in injectable gold: two drugs in one?" *Rheumatology*, vol. 36, no. 9, pp. 1012–1015, 1997.

[48] F. Faraji, M. Hashemi, A. Ghiasabadi et al., "Combination therapy with interferon beta-1a and sesame oil in multiple sclerosis," *Complementary Therapies in Medicine*, vol. 45, pp. 275–279, 2019.

[49] A. Pan, W. Demark-Wahnefried, X. Ye et al., "Effects of a flaxseed-derived lignan supplement on C-reactive protein, IL-6 and retinol-binding protein 4 in type 2 diabetic patients," *British Journal of Nutrition*, vol. 101, no. 8, pp. 1145–1149, 2009.

[50] H.-M. Chiang, H. Chang, P.-W. Yao et al., "Sesamin reduces acute hepatic injury induced by lead coupled with lipopolysaccharide," *Journal of the Chinese Medical Association*, vol. 77, no. 5, pp. 227–233, 2014.

[51] R. H. Straub and C. Schradin, "Chronic inflammatory systemic diseases: an evolutionary trade-off between acutely beneficial but chronically harmful programs," *Evolution, Medicine, and Public Health*, vol. 2016, no. 1, pp. 37–51, 2016.

[52] X.-L. Wu, C.-J. Liou, Z.-Y. Li, X.-Y. Lai, L.-W. Fang, and W.-C. Huang, "Sesamol suppresses the inflammatory response by inhibiting NF-κB/MAPK activation and upregulating AMP kinase signaling in RAW 264.7 macrophages," *Inflammation Research*, vol. 64, no. 8, pp. 577–588, 2015.

[53] P.-Y. Chu, D.-Z. Hsu, P.-Y. Hsu, and M.-Y. Liu, "Sesamol down-regulates the lipopolysaccharide-induced inflammatory response by inhibiting nuclear factor-kappa B activation," *Innate Immunity*, vol. 16, no. 5, pp. 333–339, 2010.

[54] Y.-C. Lu, T. Jayakumar, Y.-F. Duann et al., "Chondroprotective role of sesamol by inhibiting MMPs expression via retaining NF-κB signaling in activated SW1353 cells," *Journal of Agricultural and Food Chemistry*, vol. 59, no. 9, pp. 4969–4978, 2011.

[55] D. Z. Hsu, Y. W. Chen, P. Y. Chu, S. Periasamy, and M. Y. Liu, "Protective effect of 3, 4-methylenedioxyphenol (sesamol) on stress-related mucosal disease in rats," *BioMed Research International*, vol. 2013, Article ID 481827, 8 pages, 2013.

[56] C. C. Chang, W. J. Lu, E. T. Ong et al., "A novel role of sesamol in inhibiting NF-κB-mediated signaling in platelet activation," *Journal of Biomedical Science*, vol. 18, no. 1, pp. 93–10, 2011.

Hindawi
Evidence-Based Complementary and Alternative Medicine
Volume 2021, Article ID 1464027, 7 pages
https://doi.org/10.1155/2021/1464027

Research Article

Explore the Lipid-Lowering and Weight-Reducing Mechanism of Lotus Leaf Based on Network Pharmacology and Molecular Docking

Guangjiao Zhou,[1] **Xuehua Feng**,[2] **and Ali Tao**[2]

[1]*Bozhou Vocational and Technical College, Bozhou 236800, China*
[2]*College of Pharmacy, Anhui Xinhua University, Hefei 230088, China*

Correspondence should be addressed to Xuehua Feng; fengxuehua@axhu.edu.cn

Received 19 August 2021; Accepted 12 October 2021; Published 27 October 2021

Academic Editor: Xiaolong Ji

Copyright © 2021 Guangjiao Zhou et al. This is an open access article distributed under the Creative Commons Attribution License, which permits unrestricted use, distribution, and reproduction in any medium, provided the original work is properly cited.

Objective. To predict the target of the active ingredient of lotus leaf for lowering fat and losing weight. Explore its multicomponent, multitarget, multipath mechanism. *Methods*. Screen the main active ingredients of lotus leaves through the TCMSP database, and use the TCMSP database to predict the potential targets of the active ingredients. Obtain obesity-related targets from the human genome annotation (GeneCards) database. Use Venn software to take the intersection of the two to obtain the effect target of the lotus leaf lipid-lowering and weight-reducing effects. Use Cytoscape 3.6.0 software to construct an effective ingredient-target network. Use the STRING database to construct an intersection target protein interaction (PPI) network, visualize it with Cytoscape 3.6.0 software, and perform network topology analysis to obtain the core target. Use the DAVID database to perform gene ontology (GO) and metabolic pathway (KEGG) enrichment analysis for the above targets. Use AutoDockTools software for molecular docking to verify the binding strength. *Results*. A total of 15 main active ingredients such as quercetin, isorhamnetin, sitosterol, and kaempferol were obtained, which can act on 135 targets related to obesity. These targets are significantly enriched in multiple GO and KEGG entries such as hypoxia response, positive regulation of gene expression, response to toxic substances, aging, and positive regulation of RNA polymerase II promoter transcription. Molecular docking shows that flavonoids such as quercetin have better binding to the target protein Akt1. *Conclusion*. The lipid-lowering and weight-reducing effects of lotus leaf embody the characteristics of multicomponent, multitarget, and multipathway of traditional Chinese medicine, which provides a certain scientific basis for the screening and in-depth study of the effective ingredients of lotus leaf.

1. Introduction

The lotus leaf belongs to the leaf of the Nymphaeaceae plant lotus, which is a medicinal and food homologous plant published by the Ministry of Health [1]. The lotus leaf mainly contains lotus leaf essential oil, lotus leaf alkaloids, lotus leaf polysaccharides, and lotus leaf flavonoids. Lotus leaf flavone is its main active substance, which has the effects of antioxidation, stabilizing blood vessels, dredging blood vessels, and lowering blood pressure. At the same time, it is also a good medicine for weight loss, has the effect of lowering blood lipids, and is often used clinically for the treatment of obesity [2–5]. The fat-lowering and weight-reducing effects of lotus leaves have long been recorded in ancient Chinese medicine books. Due to the complex composition and variety of active ingredients, lotus leaves and their crude extracts have been used for overall functional research for a long time. They all show very good fat-lowering and weight-loss effects [6, 7].

Traditional Chinese medicine has the characteristics of multicomponent, multitarget, and synergistic effects between each component. Network pharmacology is based on the theory of systems biology, and it is a new technology to explain the drug's action and its mechanism [8–10].

Integrating computational virtual computing and network database methods to construct a "medicine-component-target" network, analyze the pathway mechanism and provide guidance for the prediction of the mechanism of traditional Chinese medicine and the multidirectional treatment of diseases [11]. In this study, the network pharmacology method was used to study the characteristics of the multicomponent, multitarget, and multipathway effects of the lotus leaf and to explore the material basis and mechanism of the lotus leaf's lipid-lowering and weight-reducing effects.

2. Analysis Method

2.1. Screening of Active Ingredients and Targets. Use the Computational Systems Biology Laboratory (TCMSP) to retrieve all the active ingredient data of lotus leaves. It is an important evaluation index for drugs to participate in the process of absorption, distribution, metabolism, and excretion. Taking oral bioavailability (OB) and drug-like properties (DL) as screening conditions, set oral bioavailability (OB) ≥30%, and drug-like properties (DL) ≥0.18 to obtain active compounds that meet the conditions. Obtain the corresponding target points of each active ingredient in TCMSP [12, 13].

2.2. Screening Obesity-Related Disease Targets and Lotus Leaf Weight Loss Targets. Search for obesity-related disease targets through the GeneCards database (https://www.genecards.org). Deduplicate, set the correlation score to be greater than 1, and screen out disease targets [14]. Draw a Venn diagram to obtain the intersection of the lipid-lowering and weight-reducing effects of the lotus leaf and the obesity-related targets, which is the pharmacological target of the lotus leaf's lipid-lowering and weight-reducing effects.

2.3. Lotus Leaf-Composition-Target-Disease Network Construction. The intersection of the active ingredients of the lotus leaf, obesity, obesity, and the active ingredients obtained from the above screening is taken as the node. Cytoscape 3.6.0 software was used to visually analyze the process of reducing fat and losing weight in lotus leaves. Construct a lotus leaf-component-target-obesity network [15, 16].

2.4. Construction of the Protein Interaction (PPI) Network. Enter the lotus leaf lipid-lowering and weight-loss targets in the STRING database (https://string-db.org/). The minimum interaction threshold is set to "highest confidence" (>0.4) to obtain the PPI network and obtain protein interaction information. Use Cytoscape 3.6.0 software to draw the PPI network diagram, and screen out the core targets according to the node degree value [17].

2.5. Target Enrichment Analysis and Visualization. Enter the intersection target of obesity and lotus leaf active ingredients in the DAVID database, and perform GO enrichment analysis and KEGG pathway enrichment analysis, respectively. According to the *P* value, the top 10 GO items are selected for analysis. Carry out KEGG enrichment analysis on the signal pathway in which the target participates. According to the *P* value, list the top 10 items for analysis, and draw the core signal pathway diagram [18].

2.6. Molecular Docking. Enter the main active ingredients selected under 1.1 into the PubChem (https://pubchem.ncbi.nlm.nih.gov/) database to download the structure of small molecule ligands. Enter the core target protein screened under item 1.2 into the RCSB PDB (http://www.rcsb.org/) database, and download the 3D structure of the target protein. Prepare ligand files and receptor files, and use AutoDockTools software for molecular docking [19].

3. Results and Analysis

3.1. The Main Active Ingredients of Lotus Leaf. A total of 93 compounds in lotus leaves were retrieved through the TCMSP database, and 15 active ingredients were screened based on oral bioavailability (OB) ≥30% and drug-like activity (DL) ≥0.18. The results are given in Table 1.

3.2. Drug-Disease Intersection Target Acquisition. Through the TSMSP database, 189 target proteins of 15 active ingredients in the lotus leaf were retrieved, and the target proteins and gene information were corrected through the STRING database [20]. The GeneCards (https://www.genecards.org) database was searched with "Obesity" as the keyword, and 9,510 obesity-related target genes were obtained. Take 2569 genes with a correlation score greater than 1 and draw a Venn diagram of the targets of the active ingredients in the lotus leaf and the targets of obesity-related diseases. The results are shown in Figure 1. There are 135 intersection targets between component targets and disease targets. The results showed that the lipid-lowering and weight-reducing effects of lotus leaves are related to the 15 active ingredients in lotus leaves and the above 135 targets.

3.3. Lotus Leaf-Components-Target-Disease Network Construction. The lotus leaf-components-target-obesity network was constructed by Cytoscape 3.6.0 software. The results are shown in Figure 2.

It can be seen from Figure 2 that the active ingredients and most targets have more interactions. This fully shows that the lotus leaf has the effect of reducing fat and losing weight through multicomponent, multitarget, and multichannel synergistic action. Among the active ingredients, the top 5 active ingredients ranked by the degree value are quercetin, kaempferol, isorhamnetin, O-nornopine, and papaverine. It shows that these ingredients are the main active ingredients of the lotus leaf's lipid-lowering and weight-loss effect [21].

3.4. PPI Network Construction and Topology Analysis. Import the obtained 135 intersection targets into the STRING database to obtain the PPI relationship. The results

Table 1: Basic information of the main active ingredients in lotus leaves.

Number	Id	Compound	OB	DL
1	MOL000098	Quercetin	46.43	0.28
2	MOL000354	Isorhamnetin	49.6	0.31
3	MOL000359	Sitosterol	36.91	0.75
4	MOL000422	Kaempferol	41.88	0.24
5	MOL006405	(1S)-1-(4-Hydroxybenzyl)-2-methyl-3,4-dihydro-1H-isoquinoline-6,7-diol	67.14	0.23
6	MOL003578	Cycloartenol	38.69	0.78
7	MOL007206	Armepavine	69.31	0.29
8	MOL007207	Machiline	79.64	0.24
9	MOL007210	o-Nornuciferine	33.52	0.36
10	MOL007213	Nuciferin	34.43	0.4
11	MOL007214	(+)-Leucocyanidin	37.61	0.27
12	MOL007217	Leucodelphinidin	30.02	0.31
13	MOL007218	Remerin	40.75	0.52
14	MOL000073	Ent-epicatechin	48.96	0.24
15	MOL000096	(−)-Catechin	49.68	0.24

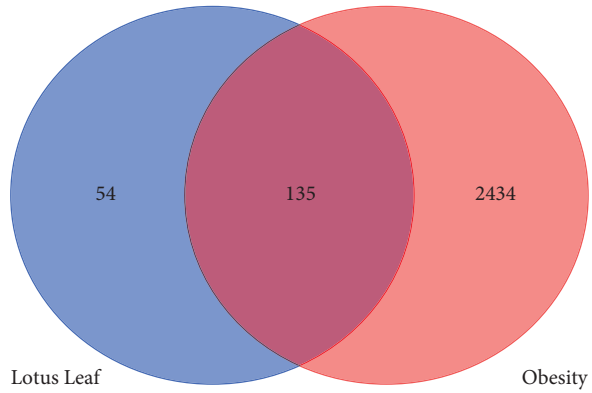

Figure 1: Venn diagram of the common target of lotus leaf and obesity.

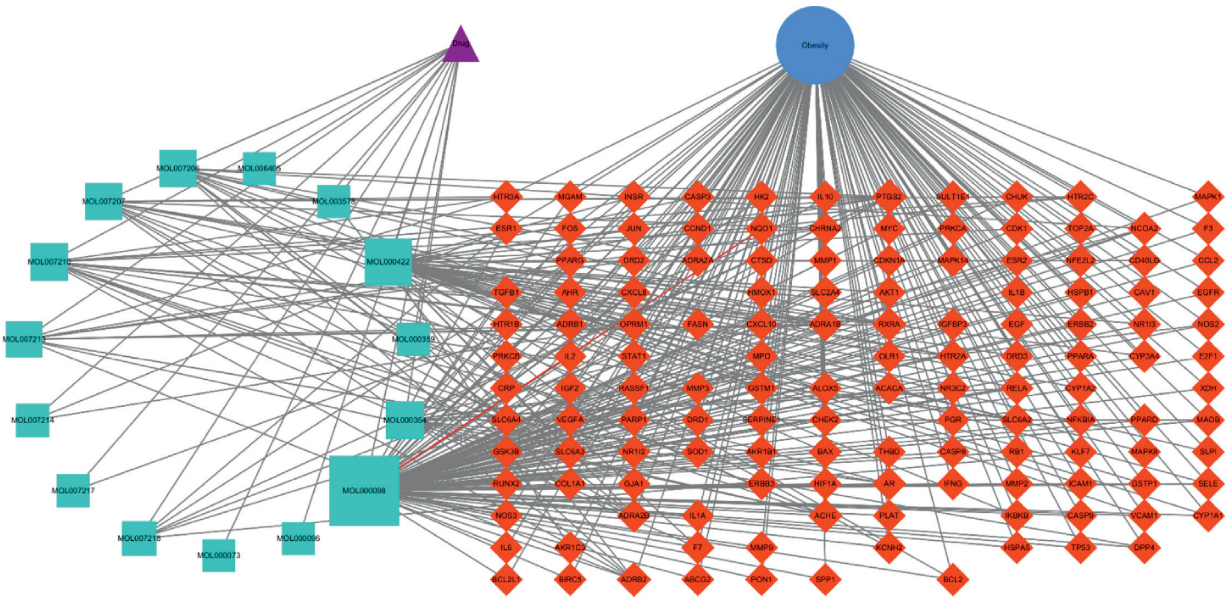

Figure 2: "Lotus leaf-components-target-obesity" interaction network.

are shown in Figure 3. Figure 3 shows that the network has a total of 135 nodes and 2348 edges. According to the degree value, the top 10 key target proteins are screened out. The results are given in Table 2.

The top 10 targets in terms of the degree value are protein kinase B1 (Akt1), interleukin 6 (IL6), tumor necrosis protein p53 (TP53), caspase 3 (CASP3), JUN protein (JUN), myeloma virus oncogene homolog (MYC), epidermal

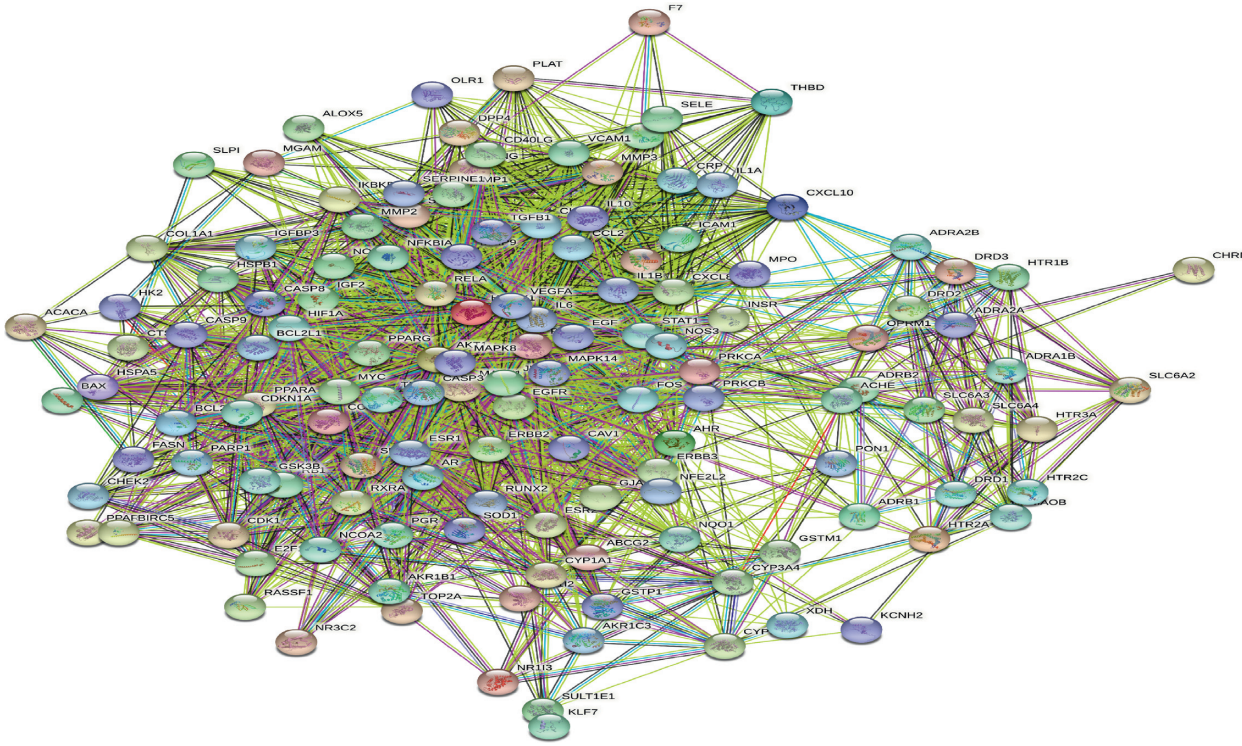

Figure 3: PPI network diagram of the intersection target of lotus leaf and obesity.

Table 2: Key targets of the lotus leaf weight loss PPI network.

Number	Target	Degree
1	Akt1	103
2	IL6	92
3	TP53	89
4	VEGFA	87
5	CASP3	83
6	JUN	78
7	MYC	76
8	EGFR	74
9	EGF	74
10	MAPK8	74

growth factor receptor (EGFR), epidermal growth factor (EGF), and mitogen activated protein kinase 8 (MAPK8). These targets may be the key targets for the lotus leaf to lower fat and lose weight.

3.5. GO Enrichment Analysis Results. A total of 622 GO entries were screened in the DAVID database ($P < 0.05$). GO analysis consists of three parts: biological process (BP), cellular component (CC), and molecular function (MF). Among them, there are 479 BP entries, 44 CC entries, and 99 MF entries [22]. According to the size of the P value, the top 10 GO items are listed, respectively, as shown in Figure 4.

It can be seen from Figure 2 that biological process notes mainly include response to hypoxia, positive regulation of gene expression, response to toxic substance, aging, and positive regulation of transcription from RNA polymerase II promoter. The annotation of cell components indicates that the relevant mechanism mainly occurs in the extracellular space, cytosol, plasma membrane, mitochondrion, and extracellular matrix. Molecular functions mainly include enzyme binding, protein binding, identical protein binding, transcription factor binding, and steroid hormone receptor activity.

3.6. KEGG Enrichment Analysis. 112 KEGG-enriched signal pathways were screened by the DAVID database ($P < 0.05$) [23]. Select the first 10 KEGG signal pathways. Table 3 provides the details of the pathways.

Analysis shows that the targets are significantly enriched in the hepatitis B signaling pathway, hypoxia-inducible factor-1 (HIF-1) signaling pathway, tumor necrosis factor (TNF) signaling pathway, Chagas disease signaling pathway, and multiple signaling pathways related to cancer. The HIF-1 signaling pathway is shown in Figure 5.

3.7. Molecular Docking. Search the three-dimensional structure of the interaction between quercetin (MOL000098), the active ingredient of lotus leaf, and the target Akt1 through the PDB database, download the MOL structural formula of the compound, and import them into the AutoDockTools software, respectively [24]. The binding energy is −6.2. This shows that the receptor and the ligand can bind spontaneously and the result of the binding of quercetin to the target Akt1 target protein (Figure 6).

4. Discussion

This study uses the method of network pharmacology to explore the mechanism of the effect of lotus leaf in reducing fat and reducing weight. From the "lotus leaf-components-

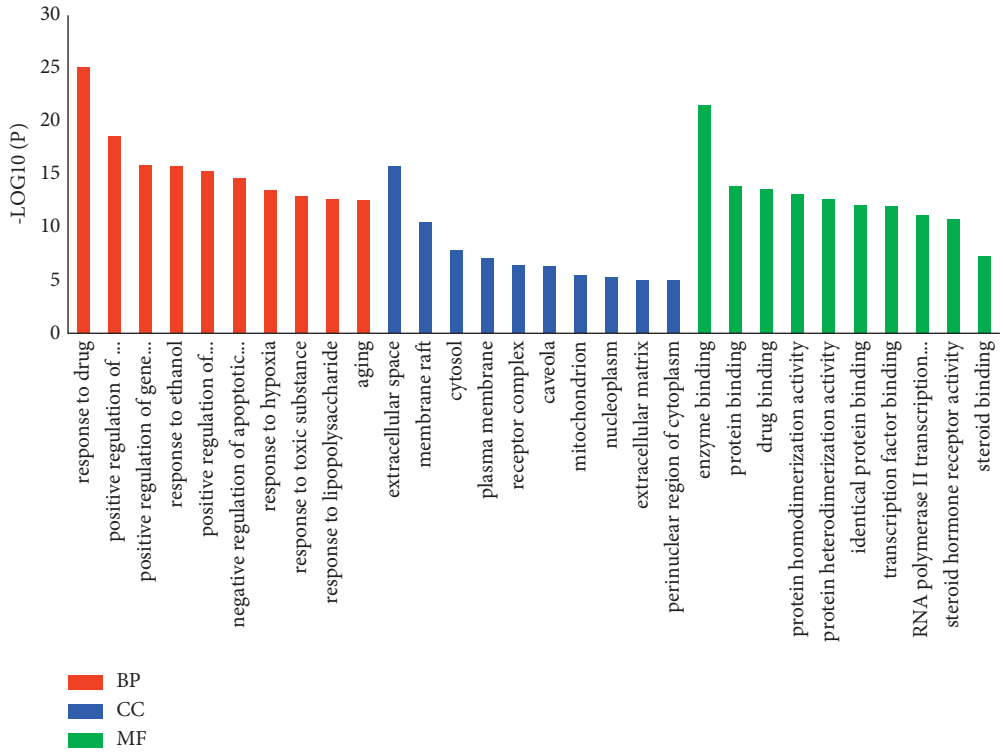

Figure 4: GO enrichment analysis diagram of the lotus leaf's weight-reducing effect.

Table 3: KEGG channel details.

Number	Pathway	*P* value
hsa05200	Pathways in cancer	2.20*E*−24
hsa05161	Hepatitis B	1.16*E*−20
hsa04668	TNF signaling pathway	1.08*E*−16
hsa05219	Bladder cancer	1.21*E*−16
hsa05212	Pancreatic cancer	6.35*E*−16
hsa05142	Chagas disease (American trypanosomiasis)	1.05*E*−15
hsa04066	HIF-1 signaling pathway	3.19*E*−15
hsa05145	Toxoplasmosis	4.41*E*−14
hsa05215	Prostate cancer	1.54*E*−13
hsa05210	Colorectal cancer	2.55*E*−12

targets-obesity" network diagram, it can be seen that compounds such as quercetin, kaempferol, isorhamnetin, O-nornopine, and papaverine are important nodes in the network. It is speculated that these compounds may be the material basis of lotus leaf's lipid-lowering and weight-reducing effects. The PPI network of the intersection target of lotus leaf and obesity shows that protein kinase B1 (Akt1), interleukin 6 (IL6), tumor necrosis protein p53 (TP 53), caspase 3 (CASP3), JUN protein (JUN), myeloma virus oncogene homolog (MYC), epidermal growth factor receptor (EGFR), epidermal growth factor (EGF), and mitogen-activated protein kinase 8 (MAPK8) interact with multiple compounds and have high degrees and play a key role in the network diagram. It is suggested that it may be the key target of lotus leaf's lipid-lowering and weight-reducing effects. The GO function is significantly enriched in biological processes such as the positive regulation of gene expression and the positive regulation of RNA polymerase II promoter transcription. KEGG pathway enrichment analysis results show that lotus leaf can play a weight loss effect through the hypoxia-inducible factor-1 (HIF-1) signaling pathway, tumor necrosis factor (TNF) signaling pathway, and multiple signaling pathways related to cancer. The results of molecular docking show that flavonoids such as quercetin have good binding to the target protein Akt1, which provides a strong basis for network pharmacology to predict the reliability of the target. On the basis of network pharmacology, this study discussed the active ingredients of lotus leaf and its multitarget and multipathway characteristics in the process of reducing fat and losing weight. Preliminary explanation of the mechanism of the lotus leaf weight loss effect is provided for the further in vivo and in vitro experimental verification of the lotus leaf weight loss activity and the screening and evaluation of traditional Chinese medicine for weight loss.

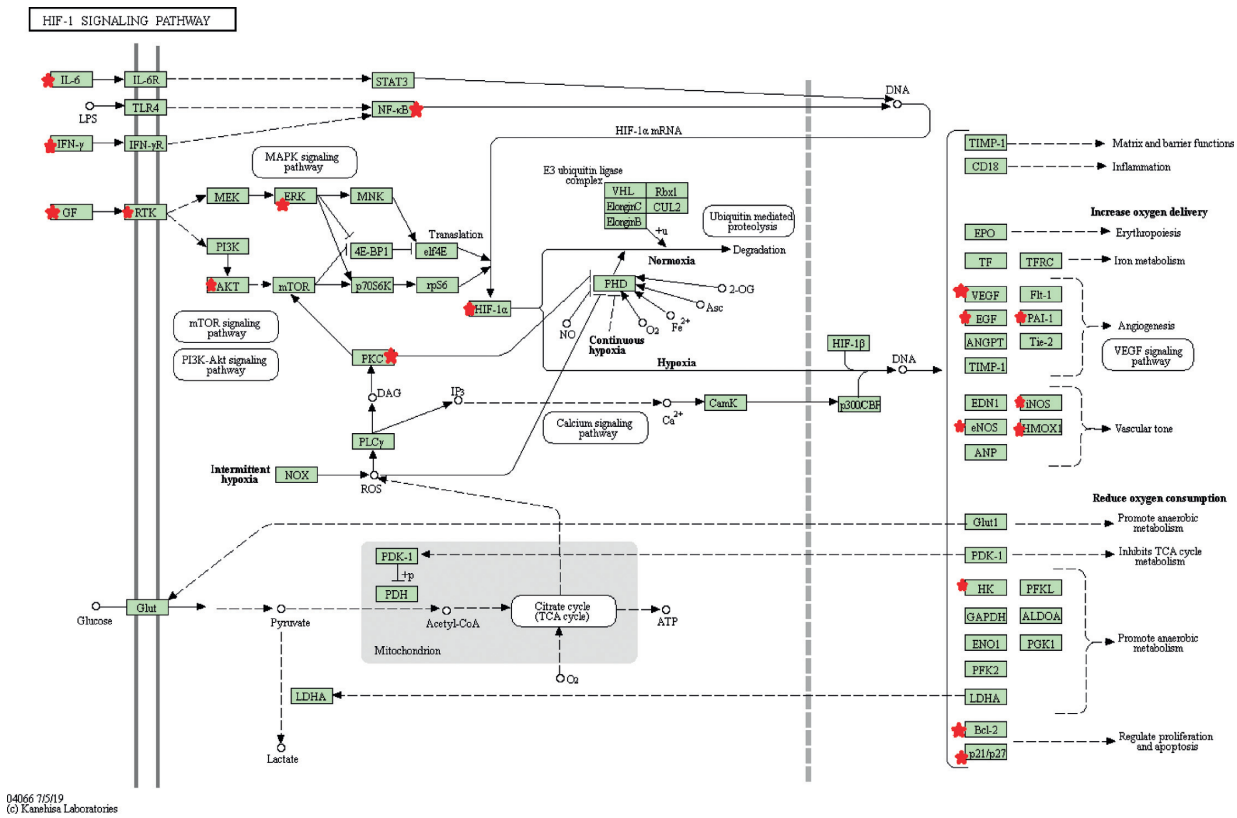

Figure 5: HIF-1 signal pathway diagram of the lotus leaf weight loss effect.

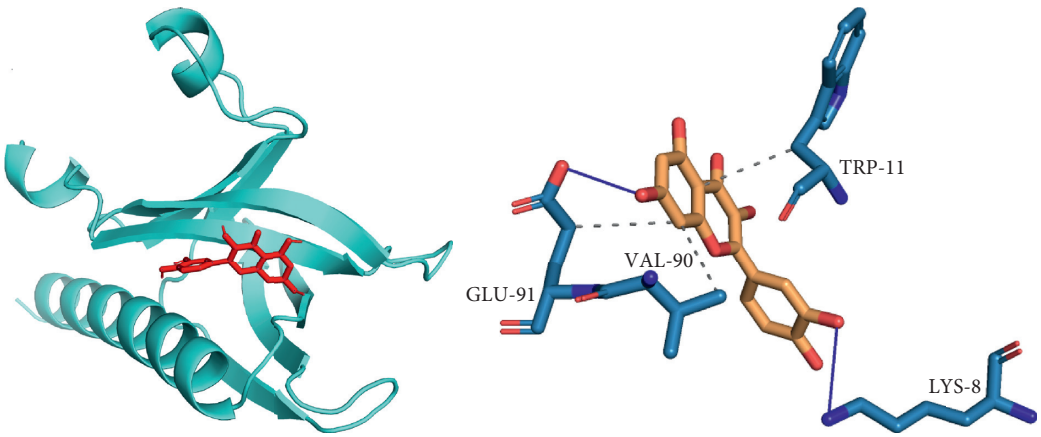

Figure 6: Docking analysis diagram of quercetin and Akt1.

Data Availability

The data used to support the findings of this study are available from the corresponding author upon request.

Conflicts of Interest

The authors declare that there are no conflicts of interest.

Acknowledgments

This research was funded by the Modern Chinese Medicine Technical Innovation and Social Service Team of Bozhou Vocational and Technical College (yptd001), the Natural Science Research Foundation of the Department of Education of Anhui Province (KJ2020A0789), Anhui Provincial-Level Quality Engineering Project (2020jyxm0790, 2020zyrc077, and gxbjZD2021089), and school-level grassroots teaching and research office demonstration project of Anhui Xinhua University (2019jyssfx02).

References

[1] Y. Tan and F. Deng, "Research progress in lotus leaf components and biological functions," *Food Research and Development*, vol. 41, no. 10, pp. 193–197, 2020.

[2] Y. Fan and L. Cao, "Study on the extraction process of lotus leaf total flavonoids and its antioxidant activity," *Anhui Chemical Industry*, vol. 47, no. 2, pp. 55–58, 2021.

[3] Y. Chen, L. Tang, J. Liang, S. Zhang, B. Chen, and J. Chen, "Nuciferine promotes the proliferation of human aortic endothelial cells by up-regulating the SDF-1/CXCR4 signaling pathway," *Chinese Journal of Arteriosclerosis*, vol. 28, no. 11, pp. 981–985, 2020.

[4] G. Zhou, X.-W. Li, J.-C. Li, and X.-H. Feng, "Study on preparation technology and physical fingerprint of chuilian jianpi granules based on QbD," *Complexity*, vol. 2021, Article ID 9992202, 9 pages, 2021.

[5] F. Xuehua, G. Zhou, and T. Ali, "Establishment of the quantitative analysis of multiindex in Euphorbia lathyris by the single marker method for Euphorbia lathyris based on the quality by design concept," *Journal of Analytical Methods in Chemistry*, vol. 2021, Article ID 4311934, 8 pages, 2021.

[6] C. Wang and Y. Yang, "Research progress on the chemical constituents and pharmacological activities of lotus leaves," *Modern Chinese Medicine Research and Practice*, vol. 34, no. 4, pp. 74–81, 2020.

[7] T. Li, Y. Xiao, Z. Chen et al., "Research progress in lipid-lowering effects and active ingredients of Chinese medicine for food and medicine," *Strait Pharmacy*, vol. 32, no. 9, pp. 42–46, 2020.

[8] J. Tang, S. Zheng, and X. Cao, "Research on the mechanism of action of "dandelion-prunella" based on network pharmacology in the treatment of breast cancer," *Evaluation and Analysis of Drug Use in Chinese Hospitals*, vol. 20, no. 1, pp. 44–49, 2020.

[9] X. Ji, C. Hou, Y. Gao, Y. Xue, Y. Yan, and X. Guo, "Metagenomic analysis of gut microbiota modulatory effects of jujube (Ziziphus jujuba Mill.) polysaccharides in a colorectal cancer mouse model," *Food & Function*, vol. 11, no. 1, pp. 163–173, 2020.

[10] X. Ji, B. Peng, H. Ding, B. Cui, H. Nie, and Y. Yan, "Purification, structure and biological activity of pumpkin (Cucurbita moschata) polysaccharides: a review," *Food Reviews International*, Article ID 1904973, 2021.

[11] Y. Shang, C. Li, and W. Luqiu, "A preliminary study on the blood-enriching mechanism of jujube based on network pharmacology," *Chinese Food and Nutrition*, vol. 27, no. 5, pp. 58–62, 2021.

[12] J. Yuan, X. Li, C. Chen, X. Song, and S. Wang, "Prediction of the effective components and potential targets of Ginkgo biloba in the treatment of cardiovascular and cerebrovascular diseases based on network pharmacology methods," *Chinese Journal of Experimental Formulas*, vol. 20, no. 11, pp. 208–212, 2014.

[13] J. An, W. Sun, and Y. Wang, "Based on network pharmacology to analyze the mechanism of action of Panax notoginseng in the treatment of hepatocellular carcinoma," *Journal of Chinese Medicine*, vol. 35, no. 4, pp. 848–852, 2020.

[14] X. Huang, M. Zou, and Y. Chen, "Based on network pharmacology and molecular docking analysis of the mechanism of action of Astragalus in the treatment of ulcerative colitis," *Chinese Medicine New Drugs and Clinical Pharmacology*, vol. 32, no. 6, pp. 815–824, 2021.

[15] J. Liao, Z. Qin, Q. Yang, R. Li, and W. Xu, "Study on the mechanism of action of spatholobi in the treatment of hepatocellular carcinoma based on network pharmacology," *Guangxi Medicine*, vol. 42, no. 14, pp. 1840–1845, 2020.

[16] Y. Wang, W. Xue, and P. Liu, "Discussion on the mechanism of action of astragalus on pancreatic cancer based on network pharmacology," *Journal of Precision Medicine*, vol. 34, no. 6, pp. 522–527, 2019.

[17] Y. Xia, T. Liu, and F. Gong, "Based on network pharmacology to explore the mechanism of blood pressure reduction of mulberry branch," *Journal of Jiangxi University of Traditional Chinese Medicine*, vol. 33, no. 3, pp. 77–84, 2021.

[18] H. Xu, S. Wang, and H. Yang, "Based on network pharmacology, research on the mechanism of compound donkey-hide gelatin in adjuvant treatment of tumors," *Chinese Journal of Chinese Materia Medica*, vol. 39, no. 16, pp. 3148–3151, 2014.

[19] J. Yao, Y. Yuan, and Q. Wang, "Research on the mechanism of Scutellaria baicalensis-Coptis in the treatment of ulcerative colitis based on network pharmacology," *Journal of Clinical Drug Therapy*, vol. 19, no. 7, pp. 48–54, 2021.

[20] Y. Liu and L. Liu, "Based on network pharmacology and molecular docking technology to explore the mechanism of the effect of active ingredients of Shenmai injection on cytochrome P450," *China Pharmaceuticals*, vol. 30, no. 13, pp. 27–31, 2021.

[21] Y. Da, "Discussion on the mechanism of agarwood in the treatment of abdominal pain based on network pharmacology," *Bachu Medicine*, vol. 4, no. 2, pp. 78–84, 2021.

[22] Q. Yang and Y. Mao, "Discussion on the mechanism of Aconite-Asarum on hypertension based on network pharmacology," *Hunan Journal of Traditional Chinese Medicine*, vol. 37, no. 6, pp. 149–155, 2021.

[23] H. Jin, C. Hui, and H. Zhang, "Research on the anti-tumor active ingredients and mechanism of Jue Chuang based on network pharmacology," *Chinese Journal of Modern Medicine*, vol. 23, no. 6, pp. 1–6, 2021.

[24] K.·Y. Yilimire·Wufuer and L. Guo, "etc. Study on the network pharmacological mechanism of the antitumor effect of snow chrysanthemum total flavonoids on colon cancer cells," *Journal of Xinjiang Medical University*, vol. 44, no. 6, pp. 670–678, 2021.

Hindawi
Evidence-Based Complementary and Alternative Medicine
Volume 2021, Article ID 7383062, 10 pages
https://doi.org/10.1155/2021/7383062

Research Article

Effects and Mechanism of Zishen Jiangtang Pill on Diabetic Osteoporosis Rats Based on Proteomic Analysis

Shufang Chu,[1] Deliang Liu,[1] Hengxia Zhao,[1] Mumin Shao,[2] Xuemei Liu,[1] Xin Qu,[1] Zengying Li,[1] Jinhua Li,[1] and Huilin Li[1]

[1]*Department of Endocrinology, Shenzhen TCM Hospital, The Fourth Clinical Medical College of Guangzhou University of Chinese Medicine, Shenzhen 518033, China*
[2]*Department of Pathology, Shenzhen TCM Hospital, The Fourth Clinical Medical College of Guangzhou University of Chinese Medicine, Shenzhen 518033, China*

Correspondence should be addressed to Huilin Li; sztcmlhl@163.com

Received 30 April 2021; Revised 5 July 2021; Accepted 6 August 2021; Published 25 September 2021

Academic Editor: Li Zhang

Copyright © 2021 Shufang Chu et al. This is an open access article distributed under the Creative Commons Attribution License, which permits unrestricted use, distribution, and reproduction in any medium, provided the original work is properly cited.

Context. Zishen Jiangtang Pill (ZJP) is a Chinese herbal compound, which has a positive therapeutic effect on diabetic osteoporosis (DOP) by regulating glucose metabolism and bone metabolism. However, its regulatory role and mechanism are still unclear. *Objective*. To explore the effect and mechanism of ZJP on DOP rats by proteomic analysis. *Materials and Methods*. After the establishment of diabetes model by Streptozocin (STZ, 60 mg/kg), 40 Wistar rats were equally divided into normal group, model group (diabetic rats), high-dose group (3.0 g/kg/d ZJP), and low-dose group (1.5 g/kg/d ZJP) and received treatment for 3 months. Histological changes in bone and pancreas tissues were observed by hematoxylin and eosin staining, electron microscopy, and immunofluorescence. Proteomic and bioinformatic analyses were performed to identify the differentially expressed proteins. The fingerprint and active ingredients of ZJP were identified via high-performance liquid chromatography (HPLC). *Results*. Compared with the model group, ZJP could rescue the weight, fasting blood glucose, and fasting insulin of rats in both high-dose and low-dose group. ZJP could also improve the microstructures of pancreatic islet cells, bone mass, and trabecular and marrow cavities in DOP rats. Bioinformatic analysis suggested that ZJP might influence DOP via multiple pathways, mainly including ribosomes, vitamin digestion and absorption, and fat digestion and absorption. The primary active ingredients, including notoginsenoside R1, ginsenoside Rg1, ginsenoside Re, icariin, and ginsenoside Rb1, were detected. *Conclusion*. ZJP could significantly improve the histomorphology and ultrastructure of bone and islets tissues and might serve as an effective alternative medicine for the treatment of DOP.

1. Background

DOP is a common diabetic complication [1, 2]. The main pathological changes associated with DOP are a decrease in bone mass per unit volume, a reduction in bone strength, and an increase in bone fragility [3, 4]. With the aging of the global population, the incidence of DM is increasing every year, which directly leads to an increase in the incidence of DOP [5, 6]. At present, the treatment of DOP is mainly based on antiosteoporosis drugs [7, 8]. Western medicine treatments generally include taking calcium, vitamin D, sex hormones, bisphosphonates, calcitonin, and/or fluoride or using monoclonal antibodies [9–11]. However, the therapeutic effects of such drugs are still controversial, and some patients cannot tolerate their side effects or afford their expensive prices. As such, there is an urgent need to identify the mechanism of osteoporosis in patients with diabetes in an effort to identify more cost-effective treatments.

Recently, a large number of experimental and clinical studies detailing the treatment of DOP have affirmed the efficacy of Traditional Chinese Medicine (TCM) [12–14]. Zishen Jiangtang Pill (ZJP) is a TCM compound developed by Shenzhen TCM Hospital. The components of ZJP have the functions of nourishing the breath feminine, nourishing

the kidneys, and strengthening the bones. Its use is in line with the theory of "kidney dominating bone" for the treatment of osteoporosis. A previous study has found that ZJP has a positive function with regard to hypoglycemic action, decreasing lipids, and improving insulin sensitivity and revealed that ZJP could play an antiosteoporosis role on multiple targets, as based on *in vitro* experiments [15]. However, the molecular mechanism by which ZJP works is still not fully understood.

Based on a previous study, we have known that ZJP has glycemic control effects with regulating effects on bone metabolism and hypothesized that ZJP can effectively treat DOP rats. In order to explore the effect and mechanism of ZJP on diabetic osteoporosis rats, we established a DOP rat model and treated these rats with different doses of ZJP and observed the bones and histomorphology of pancreatic tissue. By using gene ontology (GO) and Kyoto Encyclopedia of Genes and Genomes (KEGG) analysis, these results reveal that ZJP may affect DOP via multiple pathways.

2. Materials and Methods

2.1. Drugs, Reagents, and Antibodies. Zishen Jiangtang Pills (ZJP) were prepared by the Pharmacy Department of Shenzhen TCM Hospital. The main components were *Astragali Radix, Rehmanniae Radix Praeparata, Epimedii Folium, Notoginseng Radix et Rhizoma, Codonopsis Radix, Achyranthis Bidentatae Radix, Schisandrae Chinensis Fructus, Polygonati Rhizoma,* and *Drynariae Rhizoma* (Batch No. Guangdong Z20070085). The specific formula composition and preparation method are referred from chen et al [16].

The main reagents and antibodies used are as follows: STZ and carboxymethyl cellulose sodium (CMC) (No. S0130/C4888, Sigma, USA), insulin primary antibody (No. 3014s, CST, USA), fluorescent secondary antibody (No. 111-585-003, Jackson ImmunoResearch Laboratories, Inc., USA; and No. A23210, Abbkine, USA), glucagon primary antibody (No. ab10988, Abcam, UK), DAPI fluorescent seal tablets (No. 0100-20, Southern Biotech), chromatographically pure acetonitrile (Merck, USA), and the reference products including notoginsenoside R1, ginsenoside Rg1, ginsenoside Re, icariin, and ginsenoside Rb1 (China Food and Drug Testing Institute). ZJP is evenly mixed and suspended in CMC.

2.2. Animals. A total of 70 2-month-old Specific Pathogen-Free (SPF) male Wistar rats, weighing from 160 to 190 g, were purchased from the experimental animal center of Southern Medical University with a quality certificate No. 44002100006561. The animals were housed in the SPF room in Shenzhen Municipal Center for Disease Control and Prevention, with an ambient temperature of 18–22 ˚C, natural circadian rhythm illumination (12 h: 12 h), and environmental humidity of 40–70%. The rats were kept in microisolator cages and were given free access to food and water. All animal experiments were in accordance with the Animal Research Ethics Committee and approved by the Animal Protection and Use Committee of the Guangdong Experimental Animal Center (approval number: IACUC-G16003).

2.3. Plasma Measurements. Blood samples were collected from the animals' tail veins. The fasting blood glucose (FBG) levels and fasting plasma insulin (FINS) were determined by test assay kits abiding by the manufacturer's instructions (Roche Diagnostics Co., Ltd., Germany, and USBiological Co., Ltd., United States).

2.4. Bone Mineral Density (BMD) Detection. The BMD of lumbar vertebrae (L1–L4) was detected by using dual-energy X-ray absorptiometry (DEXA) scanning system (GE, United States) on the last day of the experiment. The measurement parameters are dual-energy voltage 41 kVp and 100 kVp, scanning window width 18 am, and scanning rate 4.8 s/am.

2.5. Establishment of a Rat Diabetes Model. Rats were adaptively fed for 2 weeks, and 10 rats were randomly selected as normal controls. The remaining 60 rats were used to establish the diabetes model. After fasting for 12 h, rats were injected intraperitoneally with 0.2% STZ (diluent 0.1 M citrate-sodium buffer, pH 4.5) at a dose of 60 mg/kg [17]. The blood glucose of the rats was measured using a blood glucose meter 72 h after administration. Rats with a fasting blood glucose >16.7 mmol/L were fed commonly for 2 weeks. Those rats that still had a fasting blood glucose >16.7 mmol/L were considered as successful models [18]. The normal control group was injected intraperitoneally with the same amount of 0.1 M citrate-sodium buffer (pH = 4.5). In the diabetes induction, 8 animals were dead and 12 animals were failed. The failed animal studies were performed under isoflurane anesthesia and every effort was made to minimize suffering. Finally, a total of four groups with 10 rats in each group were obtained. The rats of four groups then received treatment for 3 months. The normal group and model group were given 0.5% sodium carboxymethyl cellulose 10 mL/kg/day via intragastric administration, and the high-dose (3.0 g/kg/d ZJP) and low-dose (1.5 g/kg/d ZJP) groups were simultaneously given 0.5% sodium carboxymethyl cellulose 10 mL/kg/day via intragastric administration. At the end of the treatment, all of the rats were fasted for 12 h and then anesthetized using sodium pentobarbital (50 mg/kg) and sacrificed via abdominal aorta bleeding. The blood was obtained, and the pancreas and bone tissues were stored at -80 ˚C. After muscle and tendons were removed, the femoral bone was utilized for biochemical and histologic evaluation.

2.6. Hematoxylin and Eosin (H&E) Staining. Pancreatic tissues were sliced, fixed in 4% paraformaldehyde, rinsed with water for 24 h, dehydrated with an ethanol gradient, placed in anhydrous acetone, and embedded in polymethyl methacrylate [19]. H&E staining was performed as follows: xylene for 5 min, xylene for 3 min, 100% alcohol for 30 s, 100% alcohol for 30 s, 95% alcohol for 30 s, 90% alcohol for 30 s, hematoxylin staining for 10–15 min, 1% hydrochloric acid alcohol differentiated slice for 10 s, 1% eosin staining for

3 min, 90% alcohol for 30 s, 95% alcohol for 30 s (2x), 100% alcohol for 30 s (3x), carbonic acid xylene for 30 s, xylene for 30 s (3x), and a neutral gum seal.

2.7. Double-Label Pancreatic Immunofluorescence. The paraffin slices were baked at 60°C, dewaxed with xylene and ethanol, and repaired using citrate antigen repair solution. The slices were then incubated with insulin (1 : 400) and glucagon (1 : 1000) primary antibodies in the dark at 4°C overnight. The slices were then incubated with a fluorescent secondary antibody (1 : 100) at 37°C in the dark for 1 h, stained with DAPI, and sealed using a fluorescent sealing tablet. The positive islet beta cells appeared red, the positive islet alpha cells appeared green, and the nuclei appeared blue.

2.8. Pancreatic Transmission Electron Microscopy. Pancreatic tissues were fixed with 2.5% glutaraldehyde, dehydrated in ethanol, penetrated with propylene oxide, and embedded with a 1 : 1 propylene oxide and resin mixture for 2 h, pure resin for 2 h, and resin at 48 °C for 10 h. The samples were then sliced at 500–1000 nm, stained with toluidine blue, sliced at 70 nm, and stained with lead and uranium.

2.9. Femoral Electron Microscope Scanning. The fixed bone tissue sections were processed as follows: sections were stained with Weigert's iron lignin on a glass slide for 40 min and rinsed with water until it turned blue. These were then incubated in 1% hydrochloric acid ethanol and washed with water until it turned blue, dyed with Van Gieson picric acid-magenta solution for 3 min, dehydrated with 95% ethanol and anhydrous ethanol, quickly dipped in fresh anhydrous ethanol, and then blotted dry. After the above treatment, the sections were immersed in an acetonitrile solution, which was then replaced with 70%, 80%, 90%, 95%, and 100% acetonitrile, soaked for 15–20 min each time, and finally replaced with 100% acetonitrile and dried. The sections were then sprayed with carbon and gold and observed under an electron microscope.

2.10. Proteomic Analysis. The proteins were extracted from the rats' bone tissues in different groups. The extracted protein samples were subjected to reductive alkylation treatment to open the disulfide bonds for subsequent enzymatic hydrolysis of the proteins. Trypsin and 8-plex iTRAQ reagent (AB Sciex, Cat. No. 4381664) were used to label the protein. The mixed peptides were preisolated using high pH reverse phase chromatography, and liquid chromatography was performed coupled with tandem mass spectrometry (LC-MS/MS) analysis. The mass spectrometry data was assessed using Protein Pilot software (AB, Version 5.0) and aligned for identification; the database used was UniProtKB/Swiss-Prot. The identification criteria for the differentially expressed proteins had a fold difference of ≥1.5 or ≤0.667, and the number of unique peptides per protein ≥2 and <0.05 was considered to be a significant difference.

The OmicsBean (https://www.omicsbean.cn/) multifunctional bioinformatics analysis tool, integrated STRING (https://www.string-db.org) biological database, and Cytoscape software were used to perform enrichment analysis on the identified differentially expressed proteins based on GO biological process, cellular component, and molecular function. Additionally, KEGG (https://www.kegg.jp/kegg/pathway.html) biological pathway enrichment analysis was performed on the differentially expressed proteins.

2.11. HPLC Fingerprinting and Active Ingredient Detection. A reference solution that contained notoginsenoside R1, ginsenoside Rg1, ginsenoside Re, icariin, and ginsenoside Rb1 was mixed with methanol at a concentration of 0.1 mg/mL. The ZJP powder was dissolved in 100% methanol and filtered as test solution. The reference solution and the test solution were tested via HPLC, and the characteristic maps of both solutions were obtained. The chromatographic conditions were as follows: octadecyl silane-bonded silica gel was used as filler, and gradient elution was carried out at a detection wavelength of 203 nm. The column was an Agilent TC-C18 (250 mm × 4.6 mm, 5 μm) with water as mobile phase A and acetonitrile as mobile phase B (gradient elution: 0–12 min, 81% A, and 12–60 min, 81%–64% A; flow rate 1.0 mL/min; and a detection wavelength of 203 nm).

2.12. Statistical Analysis. The obtained data were statistically analyzed and processed using State 12.0 software, and the measured data were expressed as the mean ± standard deviation ($\overline{x}$ ± SD). One-way analysis of variance (ANOVA) was used to assess the differences between the groups, and the Bonferroni test was used for multiple comparisons between the groups. Wilcoxon rank-sum test was used for comparison between the group data which did not conform to a normal distribution or variance. Statistical significance was defined as $P < 0.05$.

3. Results

3.1. Body Weight, Fasting Blood Glucose, and Fasting Insulins. The body weight of the model group (238.7 ± 22.08 g) was significantly lower than that in the normal group (408.8 ± 21.06 g) ($P < 0.01$). Compared with the model group, the rats in the high-dose ZJP group (308.3 ± 19.35 g) and the low-dose ZJP group (305.9 ± 13.25 g) had gained significant weight ($P < 0.01$). The results are shown in Figure 1(a). In addition, as shown in Figure 1(b), both the high-dose (13.16 ± 2.15 mM) and low-dose groups (14.66 ± 1.22 mM) of ZJP could effectively reduce the fasting blood glucose of the model group (23.79 ± 5.54 mM) ($P < 0.01$), and there was no significant difference between the two groups. Also, ZJP could significantly improve the fasting insulin of model group (514.0 ± 180.7 pg/mL) ($P < 0.01$), while there was no significant difference between high-dose (2360 ± 718.2 pg/mL) and low-dose groups (2508 ± 925 pg/mL) (Figure 1(c)).

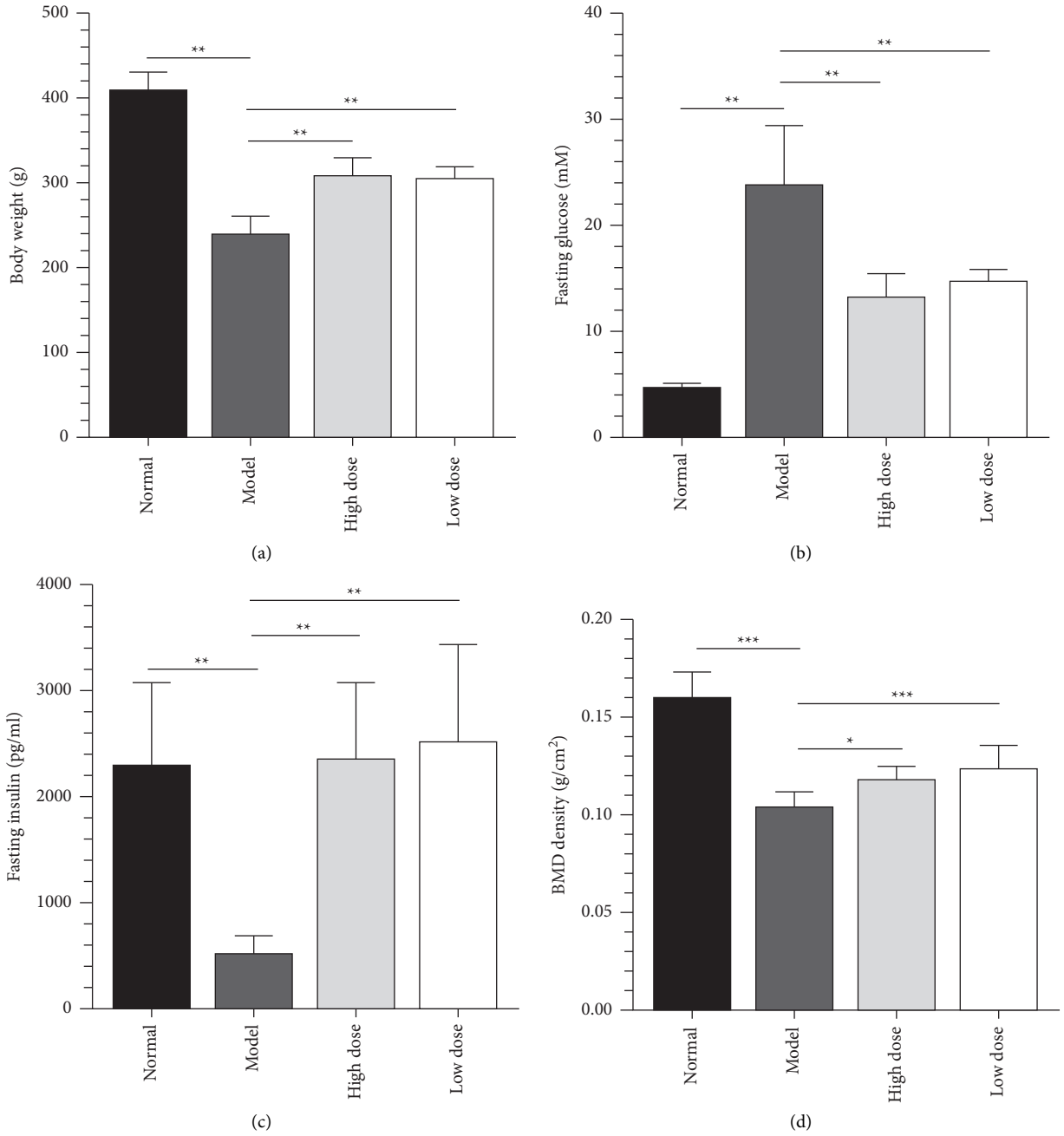

Figure 1: Body weight. (a) Fasting blood glucose and (b) and fasting insulin (c) of each group. (d) BMD.

3.2. ZJP Can Improve the BMD of Lumbar Vertebrae in DOP Model Rats. As shown in Figure 1(d), the BMD of the model group (0.11 ± 0.01 g/cm^2) was significantly lower than that in the normal group (0.16 ± 0.01 g/cm^2) ($P < 0.001$). Compared with the model group, the rats in the high-dose ZJP (0.12 ± 0.01 g/cm^2) and the low-dose ZJP groups (0.13 ± 0.01 g/cm^2) had proven the BMD of lumbar vertebrae in DOP model rats ($P < 0.001$ and $P < 0.05$, respectively.).

3.3. ZJP Can Improve the Status of Pancreatic Islet Cells in DOP Model Rats. We assessed the effect of ZJP on pancreatic islet cells by H&E staining, immunofluorescence, and transmission electron microscopy. The islet cells in the normal group were lightly stained, with a high cell density, uniform distribution, and regular morphology (Figures 2(a) and 2(e)). The mitochondria, endoplasmic reticulum, and Golgi were abundant in the cytoplasm of the normal group (Figure 2(i)). In the model group, the islets were significantly reduced, their shape was irregular, their cell density was reduced, and more cells presented with nuclear pyknosis. The peripheral acinar cells also demonstrated substantial atrophy and degeneration (Figures 2(b) and 2(f)). Moreover, the number of mitochondria was decreased, and they were swollen and deformed, the endoplasmic reticulum had expanded to different extents, and a degranulation

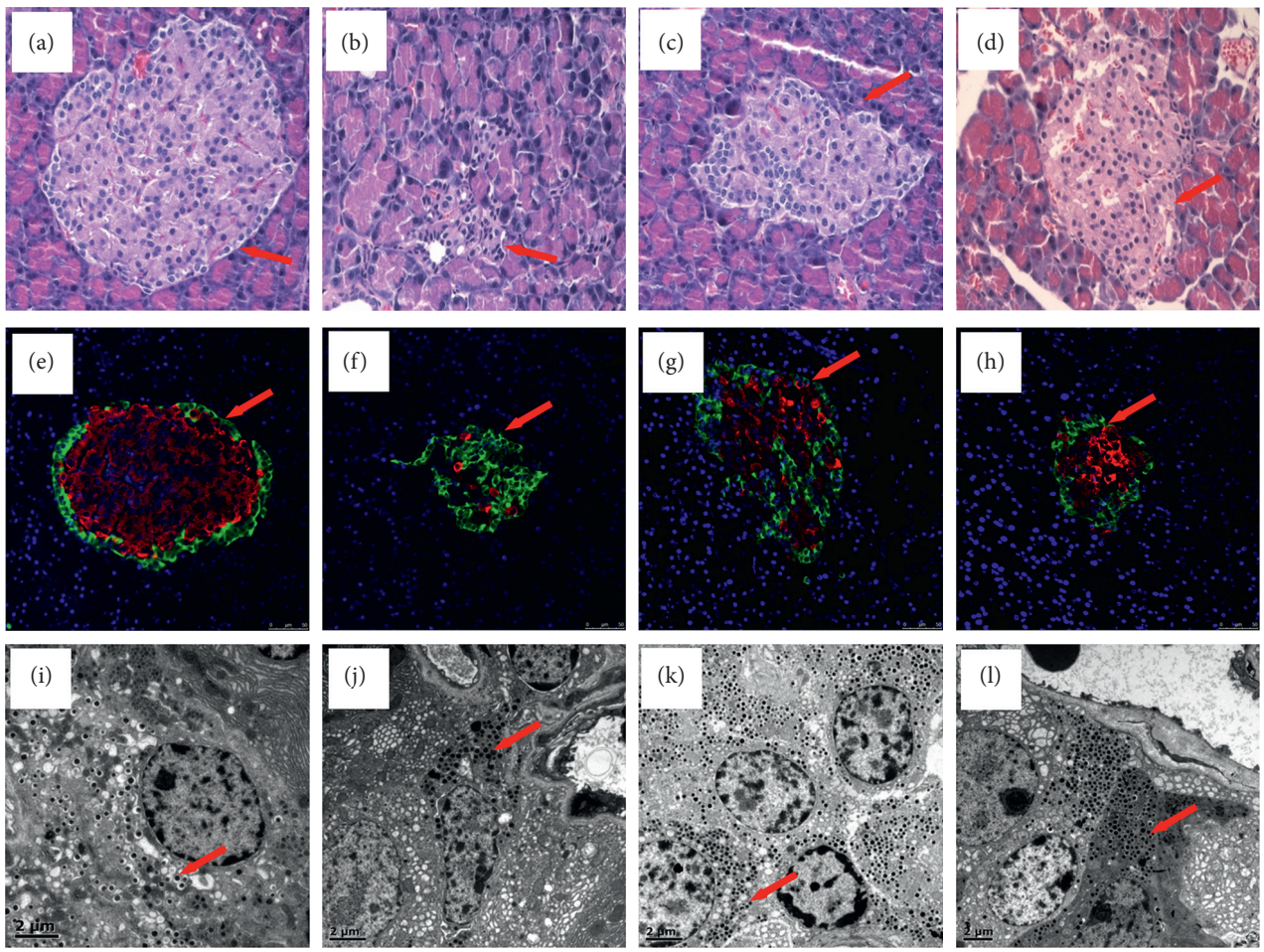

Figure 2: Pancreatic microstructure in each group. (a–d) H&E staining (×400); (e–h) insulin-glucagon double-label immunofluorescence (×400); (i–l) transmission electron microscopy (×5000). A, E, and I: normal group. B, F, and J: model group. C, G, and K: high-dose ZJP group. D, H, and L: low-dose ZJP group.

phenomenon could be seen (Figure 2(j)). The pancreatic islet structures in the high-dose and low-dose ZJP groups were significantly improved compared with the model group. In these treatment groups, the islet size was basically normal, the morphology was regular, the islet cells were arranged neatly, the density was acceptable, and the numbers of atrophied and degenerated islet cells were decreased (Figures 2(c), 2(d), 2(g), and 2(h)). Additionally, in these treatment groups, the endoplasmic reticulum was not significantly expanded (Figures 2(k) and 2(l)).

3.4. ZJP Can Improve the Histological Morphology of Bone Tissues in DOP Model Rats. In addition to the effects of bone mass reduction, DOP is also related to bone structure factors and the number of microinjuries in the bone [20, 21]. Therefore, we performed electron microscopy to assess for these changes in the bone microstructures. The bone density of the femurs in the normal group was thick and the trabecular bones were arranged neatly. The surface of the trabecular bone was regular and smooth, the gap between the trabeculae was small, and the collagen fibers were neatly arranged in the trabecular bone (Figure 3(a)). In the model group, the bone density appeared to be significantly thinner, the marrow cavity was larger, the trabecular bone connection was interrupted, and the reticular structure was destroyed (Figure 3(b)). The trabecular bone structures in the high-dose and low-dose ZJP groups were more organized compared with the model group. The bone marrow cavities were also smaller (Figures 3(c) and 3(d)).

3.5. GO and KEGG Analysis of ZJP Function in DOP Model Rats. In order to better clarify how ZJP exerts its anti-osteoporosis function, we carried out proteomic GO and KEGG analyses. We classified the altered proteins after low-dose ZJP treatment into GO classification due to the equal effect with high-dose ZJP treatment on DOP rats. Compared to the normal group, the results in the model group indicated that DOP mostly resulted in protein changes in biological process including anatomical structure development (13%), response to stress (13%), biosynthetic process (12%), and cellular nitrogen compound metabolic process (12%) (Figure 4(a)). The molecular functions of these proteins most

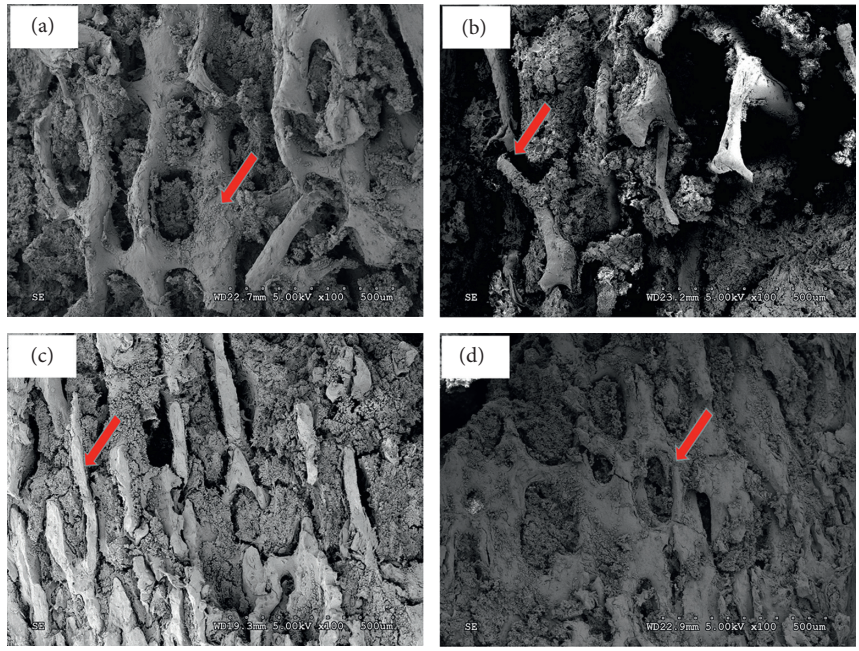

Figure 3: Scanning electron micrograph of a femur from each group (×100). (a) Normal group. (b) Model group. (c) High-dose ZJP group. (d) Low-dose ZJP group.

likely reflected ion binding (19%), RNA binding (17%), and enzyme binding (15%) (Figure 4(b)). As for the cellular component, the highest probability of existence included the extracellular region (17%), organelle (17%), and cytoplasm (16%) (Figure 4(c)). By comparing the low-dose ZJP group with the model group, we arrived at a similar conclusion with regard to these three categories (Figures 4(d)–4(f)).

We then performed pathway enrichment analysis on the differentially expressed proteins. Comparing the normal group with the model group, the pathways with the highest degree of enrichment involved the following aspects: fatty acid elongation, arginine and proline metabolism, fatty acid degradation, PPAR signaling pathway, fat digestion and absorption, adipocytokine signaling pathway, and DNA replication (Figure 5(a)). Meanwhile, comparing the model group with ZJP treatment groups, the most enriched pathways were ribosome, vitamin digestion and absorption, DNA replication, arginine and proline metabolism, and fat digestion and absorption (Figure 5(b)).

3.6. ZJP Fingerprint and Active Ingredients. We first determined the fingerprint map of ZJP via HPLC and identified its active ingredients (Figure 6). There were five major characteristic peaks in the map with relative retention time specifications, including notoginsenoside R1 (peak 1), ginsenoside Rg1 (peak 2), ginsenoside Re (peak 3), icariin (peak 4), and ginsenoside Rb1 (peak 5).

4. Discussion

DOP is a common complication of DM. With the aging of the global population, the incidence of both DM and DOP is becoming higher and is affecting people's quality of life. At present, the treatment for DOP includes three types: supplementation of calcium and vitamin D [22, 23], inhibition of bone resorption with drugs such as bisphosphonates [24–26], and promotion of bone formation with drugs such as PTH1-34 [27, 28]. However, the overall effect of these treatments is not particularly good, with a high rate of side effects and a high cost. Currently, numerous studies are focusing on the effects of TCM with regard to osteoporosis [29–31], but the concise role and mechanism underlying such treatments are still unclear. As such, it is important to understand the molecular mechanism and related pathogenesis of DOP, so as to help identify an effective therapy. This study found that ZJP can significantly improve the BMD of lumbar vertebrae in DOP model rats, the histomorphology, and ultrastructure of bone and pancreatic islet tissues. After further proteomic analysis of differentially expressed proteins, it is found that ZJP can exert its effects by affecting various aspects of glucose metabolism and bone metabolism. The influence of DOP, which involves multiple pathways, indicates that ZJP, a traditional Chinese medicine compound, plays a role through the characteristics of multiple components and multiple targets and may be used as an effective alternative drug for the treatment of DOP.

A previous study has demonstrated that ZJP can effectively improve glucose metabolism and abnormal bone metabolism and regulate blood and urinary metabolism in DOP rats [15]. ZJP has a clear hypoglycemic and lipid-lowering effect and can improve insulin sensitivity, promote resistance to oxidation, protect the vascular endothelium, and reduce the level of inflammatory factors [32, 33]. Based on the establishment of our DOP rat model, we found that ZJP could reduce the weight loss of rat caused by DOP and improve the fasting blood glucose and fasting insulin of these rats (Figure 1). The most important changes occurring

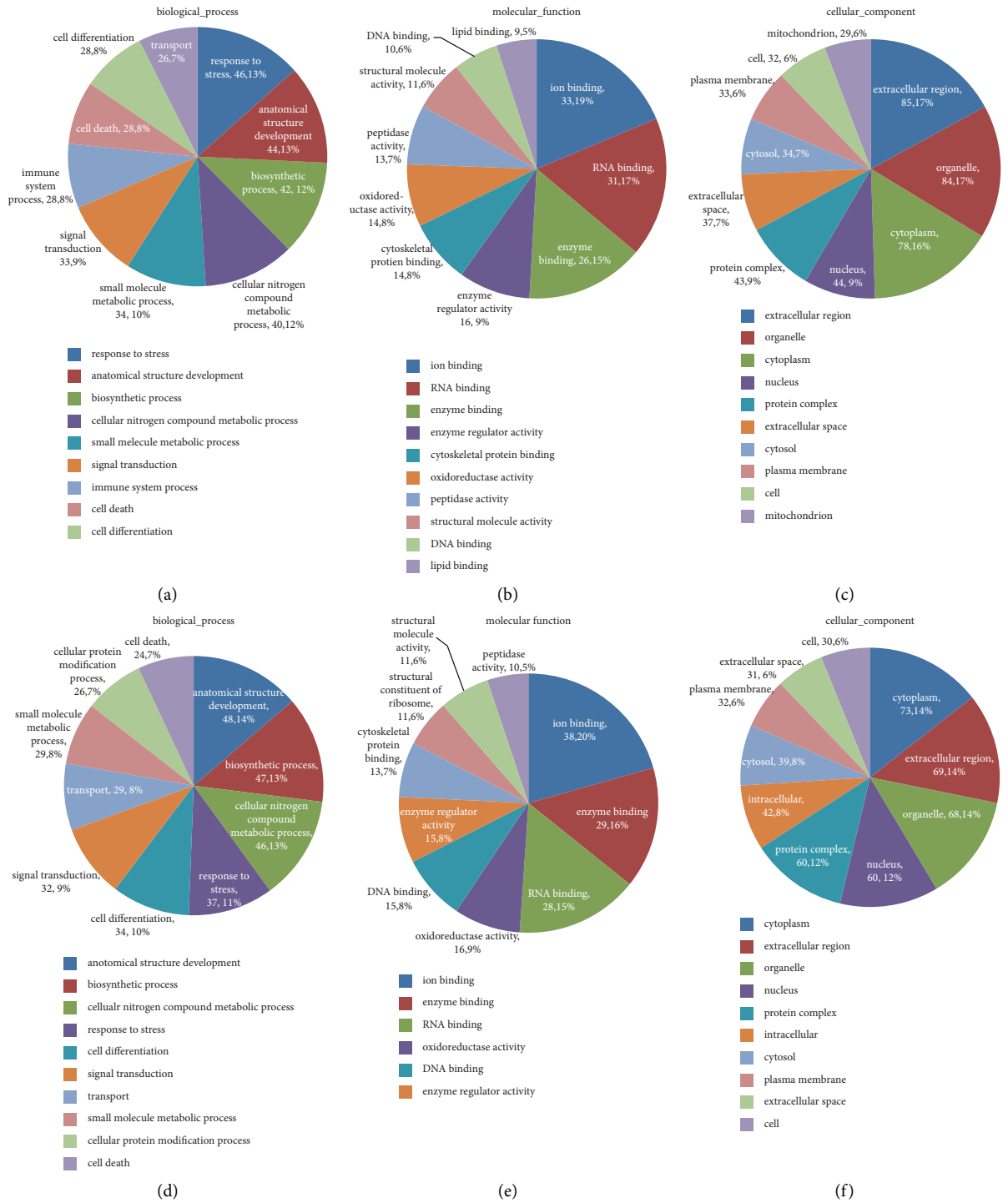

Figure 4: GO analysis results for the different groups of DOP rats. The normal group versus model group: (a) biological process, mainly differenced in response to stress, anatomical structure development, and biosynthetic process; (b) molecular function, mainly differenced in ion binding, RNA binding, and enzyme binding; (c) cellular component, mainly differenced in the extracellular region, organelle, and cytoplasm. The model group versus low-dose ZJP group: (d) biological process, mainly differenced in anatomical structure development, biosynthetic process, and cellular nitrogen compound metabolic process; (e) molecular function, mainly differenced in ion binding, enzyme binding, and RNA binding; (f) cellular component, mainly differenced in the cytoplasm, extracellular region, and organelle.

in patients with DOP involve alterations in blood glucose and the skeletal system. Therefore, microscopic analyses of islet cells and bone tissues were performed in the present study. The results indicated that ZJP conferred an obvious improvement to the histomorphology and ultrastructure of islets (Figure 2) and could improve bone formation, reduce bone resorption, increase bone density, and improve the bone microstructure (Figure 3). These pathology results

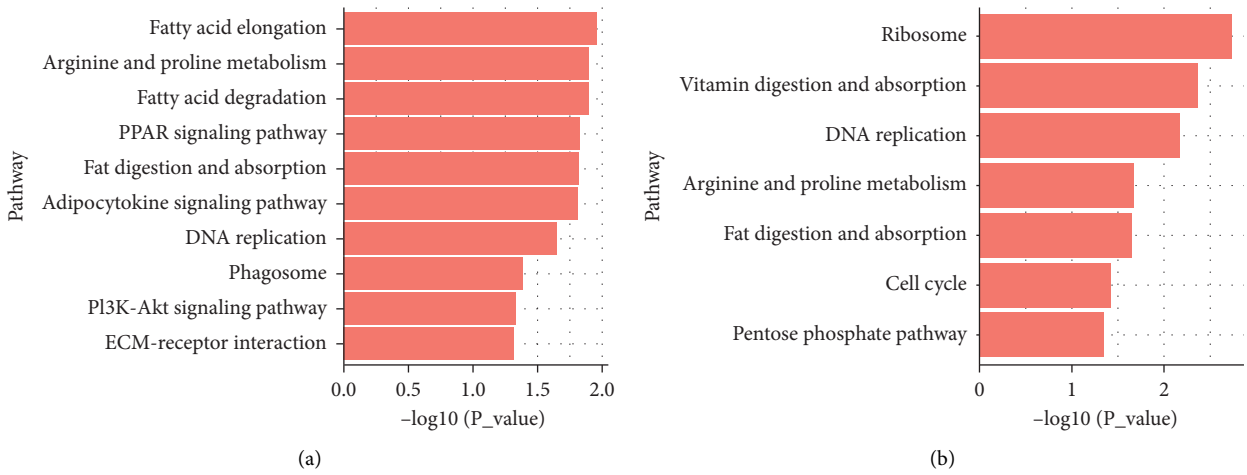

Figure 5: Pathway analysis of the differentially expressed proteins between the different groups. (a) Normal group versus model group, mainly in fatty acid elongation, arginine and proline metabolism, and fatty acid degradation pathway. (b) Model group versus low-dose ZJP group, mainly in ribosome, vitamin digestion and absorption, and DNA replication pathway.

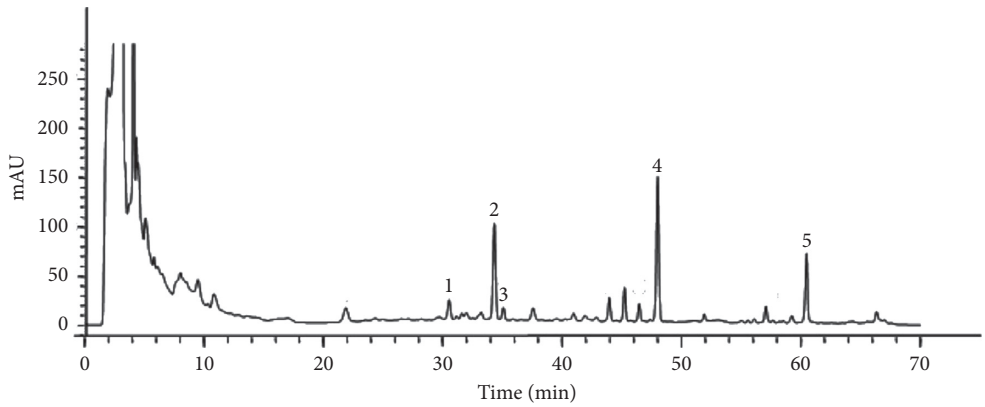

Peak 1: notoginsenoside R1
Peak 2: ginsenoside Rg1
Peak 3: ginsenoside Re
Peak 4: icariin
Peak 5: ginsenoside Rb1

Figure 6: HPLC fingerprint of ZJP. Peak 1: notoginsenoside R1; peak 2: ginsenoside Rg1; peak 3: ginsenoside Re; peak 4: icariin; peak 5: ginsenoside Rb1.

support our previous findings [15] that ZJP was shown to exert its influence by affecting aspects of glucose metabolism and bone metabolism.

To further investigate the potential mechanism of ZJP in the treatment of DOP, we performed proteomic GO and KEGG analyses on the identified differentially expressed proteins. The results revealed that ZJP most likely affected ion binding, RNA binding, and enzyme binding involved in several biological processes, including anatomical structure development, response to stress, biosynthetic processes, and cellular nitrogen compound metabolic processes. The roles of ZJP in these aspects are closely related to known factors related to the occurrence and development of DOP. Moreover, these roles are reflected in several aspects of DOP, such as bone structure changes and blood metabolism. The highest probabilities of existence with regard to the cellular component were the extracellular region, organelles, and cytoplasm, indicating that it is possible that ZJP might have some functions affecting the cellular microenvironment. The enrichment pathways identified mostly referred to the ribosome, vitamin digestion and absorption, DNA replication, arginine and proline metabolism, and fat digestion and absorption, indicating that ZJP is closely related to changes in body weight and calcium absorption as well as protein synthesis. However, to further characterize the protein signaling network associated with the treatment of DOP via ZJP, it will be necessary to further identify the specific target genes via additional methods, both *in vitro* and *in vivo*, in an effort to define the mechanism of action of ZJP with regard to the treatment of DOP.

ZJP is a Chinese herbal compound developed by Shenzhen TCM Hospital, and this study was the first to define the fingerprint map of ZJP via HPLC and ascertain the primary active ingredients, including notoginsenoside R1, ginsenosideRg1, ginsenoside Re, icariin, and ginsenoside Rb1. Thus, notoginsenoside R1, ginsenoside Rg1, ginsenoside Re, icariin, and ginsenoside Rb1 together were found to have both an antihypoglycemic action and an anti-osteoporosis effect in the previous study [34, 35]. Pharmacological studies have confirmed that epimedium extracts can inhibit the activity of osteoclasts via various means and promote the differentiation of osteoblasts and increased bone formation and bone density [36–38]. Ginsenoside Rg1 treatment of diabetic rats was associated with reduced oxidative stress and attenuated myocardial apoptosis [35]. Icariin could significantly regulate the nNOS and calponin in penile tissues of all rats [34]. Icariin attenuates titanium-particle inhibition of bone formation by activating the Wnt/β-catenin signaling pathway *in vivo* and *in vitro* [37]. These observations provided theoretical support for the prevention and treatment of DOP by ZJP.

5. Conclusions

Overall, this study identified the main active components of ZJP and determined that ZJP could significantly improve the histomorphology and ultrastructure of bone and islets tissues using a DOP rat model and might serve as an effective alternative medicine for the treatment of DOP. In the further study, we will focus on one compound as a representative ingredient and verify the predicted mechanisms.

Data Availability

All the data and materials of this manuscript are available.

Ethical Approval

This manuscript was in accordance with the Animal Research Ethics Committee and approved by the Animal Protection and Use Committee of the Guangdong Experimental Animal Center (approval number: IACUC-G16003).

Disclosure

This manuscript has been submitted as a preprint in the following link: https://www.researchsquare.com/article/rs-63628/v1.

Conflicts of Interest

The authors declare that they have no conflicts of interest related to this work.

Authors' Contributions

Chu SF and Li HL designed the study. Chu SF, Liu DL, Zhao HX, Shao MM, Chen JP, Liu XM, and Qu X performed the research. Liu DL, Li ZY, and Li JH analyzed data. Chu SF and Li HL wrote the paper. The manuscript was approved by all authors for publication.

Acknowledgments

The study was supported by the Shenzhen Municipal Science and Technology Bureau (JCYJ20140408153331810 and JCYJ20170817094838619) and Sanming Project of Medicine in Shenzhen (SZSM201512043).

References

[1] M. Lechleitner, K. Pils, R. Roller-Wirnsberger et al., "Diabetes and osteoporosis: pathophysiological interactions and clinical importance for geriatric patients," *Zeitschrift für Gerontologie und Geriatrie*, vol. 46, no. 5, pp. 390–397, 2013.

[2] C. Hamann, S. Kirschner, K.-P. Günther, and L. C. Hofbauer, "Bone, sweet bone--osteoporotic fractures in diabetes mellitus," *Nature Reviews Endocrinology*, vol. 8, no. 5, pp. 297–305, 2012.

[3] A. Montagnani, S. Gonnelli, M. Alessandri, and R. Nuti, "Osteoporosis and risk of fracture in patients with diabetes: an update," *Aging Clinical and Experimental Research*, vol. 23, no. 2, pp. 84–90, 2011.

[4] S. Kurra and E. Siris, "Diabetes and bone health: the relationship between diabetes and osteoporosis-associated fractures," *Diabetes/Metabolism Research and Reviews*, vol. 27, no. 5, pp. 430–435, 2011.

[5] A. Montagnani and S. Gonnelli, "Antidiabetic therapy effects on bone metabolism and fracture risk," *Diabetes, Obesity and Metabolism*, vol. 15, no. 9, pp. 784–791, 2013.

[6] P. Vestergaard, "Discrepancies in bone mineral density and fracture risk in patients with type 1 and type 2 diabetes--a meta-analysis," *Osteoporosis International*, vol. 18, no. 4, pp. 427–444, 2007.

[7] A. V. Schwartz, "Efficacy of osteoporosis therapies in diabetic patients," *Calcified Tissue International*, vol. 100, no. 2, pp. 165–173, 2017.

[8] T. Wang, L. Cai, Y. Wang et al., "The protective effects of silibinin in the treatment of streptozotocin-induced diabetic osteoporosis in rats," *Biomedicine & Pharmacotherapy*, vol. 89, pp. 681–688, 2017.

[9] B. Chang, Q. Quan, Y. Li, H. Qiu, J. Peng, and Y. Gu, "Treatment of osteoporosis, with a focus on 2 monoclonal antibodies," *Medical Science Monitor*, vol. 24, pp. 8758–8766, 2018.

[10] J. C. Gallagher, "Advances in osteoporosis from 1970 to 2018," *Menopause*, vol. 25, no. 12, pp. 1403–1417, 2018.

[11] T. Suzuki, Y. Nakamura, and H. Kato, "Vitamin D and calcium addition during denosumab therapy over a period of four years significantly improves lumbar bone mineral density in Japanese osteoporosis patients," *Nutrients*, vol. 10, 2018.

[12] C. Choi, H. Lee, H. Lim, S. Park, J. Lee, and S. Do, "Effect of Rubus coreanus extracts on diabetic osteoporosis by simultaneous regulation of osteoblasts and osteoclasts," *Menopause*, vol. 19, no. 9, pp. 1043–1051, 2012.

[13] W. Qi, Y. Zhang, Y. B. Yan et al., "The protective effect of cordymin, a peptide purified from the medicinal mushroom cordyceps sinensis, on diabetic osteopenia in alloxan-induced diabetic rats," *Evidence-based Complementary and Alternative Medicine*, vol. 2013, Article ID 985636, 2013.

[14] X.-J. Li, Z. Zhu, S.-L. Han, and Z.-L. Zhang, "Bergapten exerts inhibitory effects on diabetes-related osteoporosis via the regulation of the PI3K/AKT, JNK/MAPK and NF-kappaB

signaling pathways in osteoprotegerin knockout mice," *International Journal of Molecular Medicine*, vol. 38, no. 6, pp. 1661–1672, 2016.

[15] H. Li, S. Chu, H. Zhao et al., "Effect of zishen Jiangtang Pill, a Chinese herbal product, on rats with diabetic osteoporosis," *Evidence-based complementary and alternative medicine*, vol. 2018, Article ID 7201914, 2018.

[16] J. Chen, L. Zheng, Z. Hu et al., "Metabolomics reveals effect of zishen Jiangtang Pill, a Chinese herbal product on high-fat diet-induced type 2 diabetes mellitus in mice," *Frontiers in Pharmacology*, vol. 10, p. 256, 2019.

[17] G. Kizilay, O. Ersoy, A. Cerkezkayabekir, and Y. Topcu-Tarladacalisir, "Sitagliptin and fucoidan prevent apoptosis and reducing ER stress in diabetic rat testes," *Andrologia*, vol. 53, no. 3, Article ID e13858, 2021.

[18] S. Qi, J. He, H. Han et al., "Anthocyanin-rich extract from black rice (Oryza sativa L. Japonica) ameliorates diabetic osteoporosis in rats," *Food & Function*, vol. 10, no. 9, pp. 5350–5360, 2019.

[19] X. Ying, X. Chen, T. Wang, W. Zheng, L. Chen, and Y. Xu, "Possible osteoprotective effects of myricetin in STZ induced diabetic osteoporosis in rats," *European Journal of Pharmacology*, vol. 866, Article ID 172805, 2020.

[20] Y. H. An, J. Zhang, Q. Kang, and R. J. Friedman, "Mechanical properties of rat epiphyseal cancellous bones studied by indentation testing," *Journal of Materials Science: Materials in Medicine*, vol. 8, no. 8, pp. 493–495, 1997.

[21] L. M. Coe, R. Irwin, D. Lippner, and L. R. McCabe, "The bone marrow microenvironment contributes to type I diabetes induced osteoblast death," *Journal of Cellular Physiology*, vol. 226, no. 2, pp. 477–483, 2011.

[22] A. C. Ross, J. E. Manson, S. A. Abrams et al., "The 2011 report on dietary reference intakes for calcium and vitamin D from the Institute of Medicine: what clinicians need to know," *Journal of Clinical Endocrinology & Metabolism*, vol. 96, no. 1, pp. 53–58, 2011.

[23] K. Li, R. Kaaks, J. Linseisen, and S. Rohrmann, "Associations of dietary calcium intake and calcium supplementation with myocardial infarction and stroke risk and overall cardiovascular mortality in the Heidelberg cohort of the European Prospective Investigation into Cancer and Nutrition study (EPIC-Heidelberg)," *Heart*, vol. 98, no. 12, pp. 920–925, 2012.

[24] L. M. Coe, S. A. Tekalur, Y. Shu, M. J. Baumann, and L. R. McCabe, "Bisphosphonate treatment of type I diabetic mice prevents early bone loss but accentuates suppression of bone formation," *Journal of Cellular Physiology*, vol. 230, no. 8, pp. 1944–1953, 2015.

[25] Y. Takeuchi, "Innovation of bisphosphonates for improvement of adherence," *Clinical Calcium*, vol. 27, pp. 197–202, 2017.

[26] S. Davis, M. Martyn-St James, J. Sanderson et al., "A systematic review and economic evaluation of bisphosphonates for the prevention of fragility fractures," *Health Technology Assessment*, vol. 20, no. 78, pp. 1–406, 2016.

[27] K. Suzuki, N. Miyakoshi, T. Tsuchida, Y. Kasukawa, K. Sato, and E. Itoi, "Effects of combined treatment of insulin and human parathyroid hormone(1-34) on cancellous bone mass and structure in streptozotocin-induced diabetic rats," *Bone*, vol. 33, no. 1, pp. 108–114, 2003.

[28] T. Tsuchida, K. Sato, N. Miyakoshi et al., "Histomorphometric evaluation of the recovering effect of human parathyroid hormone (1–34) on bone structure and turnover in streptozotocin-induced diabetic rats," *Calcified Tissue International*, vol. 66, no. 3, pp. 229–233, 2000.

[29] D. Ju, M. Liu, H. Zhao, and J. Wang, "Mechanisms of "kidney governing bones" theory in traditional Chinese medicine," *Frontiers of Medicine*, vol. 8, no. 3, pp. 389–393, 2014.

[30] Y. Li, S.-S. Lü, G.-Y. Tang et al., "Effect of Morinda officinalis capsule on osteoporosis in ovariectomized rats," *Chinese Journal of Natural Medicines*, vol. 12, no. 3, pp. 204–212, 2014.

[31] N. Lai, Z. Zhang, B. Wang et al., "Regulatory effect of traditional Chinese medicinal formula Zuo-Gui-Wan on the Th17/Treg paradigm in mice with bone loss induced by estrogen deficiency," *Journal of Ethnopharmacology*, vol. 166, pp. 228–239, 2015.

[32] X. Yongping, G. Bin, and L. Yingrong, "Effect of zishen Jiangtang Pill on insulin sensitivity in high-fat mouse model and its mechanism," *Chinese Medicine Guide*, vol. 10, pp. 7–9, 2012.

[33] G. Yunshan, L. Huilin, and Z. Hengxia, "Effects of zishen Jiangtang Pill on serum adiponectin and vascular endothelial function in patients with diabetic macroangiopathy," *China Medical Herald*, vol. 5, pp. 18–20, 2008.

[34] A. W. Shindel, Z.-C. Xin, G. Lin et al., "Erectogenic and neurotrophic effects of icariin, a purified extract of horny goat weed (Epimedium spp.) in vitro and in vivo," *The Journal of Sexual Medicine*, vol. 7, no. 4, pp. 1518–1528, 2010.

[35] H.-t. Yu, J. Zhen, B. Pang, J.-n. Gu, and S.-s. Wu, "Ginsenoside Rg1 ameliorates oxidative stress and myocardial apoptosis in streptozotocin-induced diabetic rats," *Journal of Zhejiang University - Science B*, vol. 16, no. 5, pp. 344–354, 2015.

[36] S. Liu, H. Dong, H. Dai, D. Liu, and Z. Wang, "MicroRNA-216b regulated proliferation and invasion of non-small cell lung cancer by targeting SOX9," *Oncology letters*, vol. 15, pp. 10077–10083, 2018.

[37] J. Wang, Y. Tao, Z. Ping et al., "Icariin attenuates titanium-particle inhibition of bone formation by activating the Wnt/beta-catenin signaling pathway in vivo and in vitro," *Scientific Reports*, vol. 6, no. 1, Article ID 23827, 2016.

[38] J. An, H. Yang, Q. Zhang et al., "Natural products for treatment of osteoporosis: the effects and mechanisms on promoting osteoblast-mediated bone formation," *Life Sciences*, vol. 147, pp. 46–58, 2016.

Hindawi
Evidence-Based Complementary and Alternative Medicine
Volume 2021, Article ID 2073296, 13 pages
https://doi.org/10.1155/2021/2073296

Research Article

Zanthoxylum bungeanum Seed Oil Attenuates LPS-Induced BEAS-2B Cell Activation and Inflammation by Inhibiting the TLR4/MyD88/NF-κB Signaling Pathway

Jing Hou, Jun Wang, Jingyi Meng, Xiaoting Zhang, Yuanjing Niu, Jianping Gao, Yun'e Bai, and Jiangtao Zhou

School of Pharmaceutical Science, Shanxi Medical University, Taiyuan, Shanxi Province, China

Correspondence should be addressed to Jiangtao Zhou; zjt881206@sxmu.edu.cn

Received 24 May 2021; Revised 13 July 2021; Accepted 8 September 2021; Published 24 September 2021

Academic Editor: Jianping Chen

Copyright © 2021 Jing Hou et al. This is an open access article distributed under the Creative Commons Attribution License, which permits unrestricted use, distribution, and reproduction in any medium, provided the original work is properly cited.

Background. *Zanthoxylum bungeanum* seed oil (ZBSO) is a natural essential oil derived from the seeds of the Chinese medicinal plant *Zanthoxylum bungeanum*, which has been investigated for antitumor and anti-inflammatory effects. However, little is known regarding the effects of ZBSO in chronic obstructive pulmonary disease (COPD). *Methods*. In this study, lung epithelial cells (BEAS-2B) were induced by lipopolysaccharide (LPS) to establish an *in vitro* model of COPD, and cytotoxicity was detected by a cell counting kit 8 (CCK-8) assay. Griess test, enzyme-linked immunosorbent assay (ELISA), reverse transcriptase quantitative polymerase chain reaction (RT-qPCR), western blot, immunofluorescence, and molecular docking analyses were used to investigate the effects of ZBSO and its potential mechanisms. *Results*. The results showed that LPS promoted the expression of nitric oxide (NO), reactive oxygen species (ROS), malondialdehyde (MDA), tumor necrosis factor-α (TNF-α), interleukin-6 (IL-6), monocyte chemoattractant protein-1 (MCP-1), matrix metalloproteinase-2 (MMP-2), MMP-9, cyclooxygenase-2 (COX-2), and prostaglandin E_2 (PGE2), suggesting that LPS can induce inflammation and oxidative stress in BEAS-2B cells. ZBSO inhibits the LPS-induced expression of inflammatory mediators and proinflammatory cytokines in BEAS-2B cells. The molecular docking results indicated that active components in ZBSO could successfully dock with toll-like receptor 4 (TLR4), myeloid differentiation factor 88 (MyD88), and p65. Immunofluorescence and western blot analyses further demonstrated that ZBSO repressed protein expression associated with the TLR4/MyD88/nuclear factor-κB (NF-κB) signaling pathway. *Conclusions*. ZBSO reduced the inflammatory response and oxidative stress induced by LPS by inhibiting the TLR4/MyD88/NF-κB signaling pathway, thereby suppressing COPD. ZBSO may represent a promising therapeutic candidate for COPD treatment.

1. Introduction

According to data from the Global Initiative for Chronic Obstructive Lung Disease (GOLD), chronic obstructive pulmonary disease (COPD) is a common, preventable, and treatable respiratory disease [1]. Because of the aging of the population, increased air pollution, smoking, and other factors, the incidence of COPD has increased, becoming the fourth leading cause of death worldwide [2]. COPD symptoms include airflow obstruction and difficulty breathing, including emphysema, chronic bronchitis, and asthma [3]. The primary cause of COPD development is tobacco smoke, but factors including environmental exposure and genetic risk may worsen the COPD course [4]. Airway inflammation is the primary pathological feature of COPD and has been implicated in the pathogenesis and progression of COPD; therefore, anti-inflammatory therapy is the typical treatment strategy for COPD [5]. Glucocorticoids, which have significant anti-inflammatory effects, have been increasingly used to treat COPD in recent years

[6]. However, glucocorticoids are associated with numerous and serious side effects, warranting a search for safe alternative therapeutic agents [7].

Inflammation is the initial response of the body's innate immune system to external infections and stimuli. Pathogens, chemical immune responses, damaged cells, irritants, etc. can all induce inflammation. However, excessive inflammation can lead to disorders of the body, excessive production of oxygen free radicals, and ultimately destruction of homeostasis, which often leads to diseases such as fever, COPD, arthritis, and even cancer [8]. The toll-like receptor 4 (TLR4)/myeloid differentiation factor 88 (MyD88)/nuclear factor-κB (NF-κB) signaling pathway is involved in the development of the COPD airway inflammation [9]. Lipopolysaccharide (LPS) is an outer cell wall component found in Gram-negative bacteria that is well known to induce an inflammatory process mediated by the transmembrane receptor TLR4 [10]. When TLR4 recognizes LPS, a cascade of reactions occurs, including the TLR4-mediated activation of downstream NF-κB signaling pathway via MyD88 [11, 12]. NF-κB is a key regulator of inflammatory dysregulation and is necessary for the transcription of inflammatory cytokines, such as interleukin (IL)-6, IL-1β, and tumor necrosis factor-α (TNF-α) [13]. The activation of NF-κB by TLR4 is thought to play a key role in COPD pathogenesis [14].

Medicinal plants have been used for thousands of years in Asia and have traditionally played an important role in primary health care. A large number of plant extracts and bioactive compounds derived from medicinal plants have been shown to be effective in the treatment of COPD [15, 16], such as betulin [17] and Liu-Jun-Zi-Tang [18]. Therefore, effective drugs for COPD treatment may be derived from traditional Chinese medicine. *Zanthoxylum bungeanum* is a common food additive and herbal medicine used in China and is widely distributed across Asian countries [19]. In 2002, the Chinese Ministry of Health officially approved *Zanthoxylum bungeanum* Maxim. (ZBM) as a dietary, medicinal herb for improved public health [20]. *Zanthoxylum bungeanum* seeds, a byproduct of *Zanthoxylum bungeanum*, are produced at a rate of approximately 1 million tons each year and are often viewed as a byproduct or waste fuel. To date, studies have revealed the pharmacodynamic properties of *Zanthoxylum bungeanum* seed oil (ZBSO) in inflammatory diseases, such as asthma and burn [21, 22] and antitumor effects [20, 23, 24]. However, the effects of ZBSO and mechanisms through which ZBSO acts on airway inflammation, a common symptom of COPD, remain unclear.

Based on the relationship between COPD pathogenesis and the TLR4 signaling pathway, the anti-COPD effects of ZBSO may be associated with the inhibition of TLR4/MyD88/NF-κB signaling pathway activation and the prevention of excessive oxidative stress generation. This paper will provide a basis for further understanding the potential mechanism through which ZBSO mediates the treatment of COPD.

2. Materials and Methods

2.1. Reagents and Chemicals. LPS was obtained from Solarbio (055: B5, Beijing, China). The antibodies against MyD88 (23230-1-AP), NF-κB p65 (10745-1-AP), and phospho-NF-κB p65 were obtained from Proteintech (Hubei, China). The antibodies against TRL4 (GB11519) and β-actin were gained from Servicebio (Hubei, China). All secondary antibodies used for western blot were purchased from ImmunoWay (Plano, TX). Cy3-conjugated goat anti-rabbit IgG (H + L) used in immunofluorescence experiments was obtained from Servicebio (Hubei, China).

2.2. Preparation of ZBSO. *Zanthoxylum bungeanum* seeds were purchased from Yuncheng City, Shanxi Province, and identified as *ZBM* by Professor Yun'e Bai (School of Pharmaceutical Science, Shanxi Medical University) in August 2018. The samples were stored in the Herbarium of Traditional Chinese Medicine, School of Pharmacy, Shanxi Medical University. The extraction and separation methods used to obtain ZBSO were based on previous research performed in our laboratory [25, 26]. In short, the *Zanthoxylum bungeanum* seeds (100 g) were pulverized and extracted twice, using 800 mL and 600 mL 95% ethanol (Sanwei, Henan, China). The filtrates were combined and concentrated under reduced pressure, and the ZBSO content was calculated. After filtering through a 0.22 μm filter membrane, the extract was stored in the dark at −20°C. This extract was used in all experiments described in this study. The final concentration of dimethyl sulfoxide (DMSO) does not exceed 0.05%.

2.3. Cell Culture and Treatment. The human lung epithelial cell line BEAS-2B (EK-Bioscience, Shanghai) was maintained in Dulbecco's modified Eagle's medium (DMEM) supplemented with 10% fetal bovine serum (FBS) and 1% penicillin/streptomycin in a 95% air and 5% CO_2 environment at 37°C. In all experiments, ZBSO (0.025%, 0.05%, and 0.1%) or indomethacin (the positive control drug) were administered prophylactically for 4 h, followed by continued exposure to 100 ng/mL LPS for 24 h.

2.4. Cell Viability Assay. ZBSO (0.025%, 0.05%, and 0.1% *v/v*) was applied to cells plated in a 96-well plate at a cell density of 5×10^4 cells/well. After 24 h, CCK-8 was added to each well and incubated for 2 h at 37°C. Absorbance (optical density (OD) values) was measured at 450 nm.

2.5. Griess Reagent Assay. BEAS-2B cells were cultured overnight in 96-well plates at a density of 5×10^4 cells/well. The cells were treated with indomethacin (5 μM) or ZBSO (0.025%, 0.05%, and 0.1% *v/v*) for 4 h, followed by incubation with 100 ng/mL LPS for 24 h. The supernatant was collected, and nitrite levels were measured using the Griess method, according to the manufacturer's instructions (Elabscience, Wuhan, China).

2.6. Dichlorodihydrofluorescein Diacetate (DCFH-DA) Assay. BEAS-2B cells (10^6 cells per 1 mL medium) were treated for 4 h with ZBSO (0.025%, 0.05%, and 0.1% *v/v*), followed by incubation with or without 1 μg/mL LPS for 24 h.

Dichlorodihydrofluorescein diacetate (DCFH-DA) staining was used to measure total intracellular reactive oxygen species (ROS) levels according to the manufacturer's protocol (Elabscience, Wuhan, China). In brief, the cell culture medium was removed, DCFH-DA was added at a final concentration of 10 μM, and the cells were incubated at 37°C in the dark for 1 h. Cells were washed with phosphate-buffered saline (PBS) 3 times to completely remove excess DCFH-DA, and ROS production was observed by inverted fluorescence microscopy (magnification × 20; Leica, Germany) and quantified using ImageJ software version 1.46 (National Institutes of Health, Bethesda, MD, USA). The experiments were repeated in triplicate.

2.7. Analysis of Antioxidative Enzymatic Activities. BEAS-2B cells were stimulated with ZBSO (0, 0.025%, 0.05%, and 0.1% *v/v*) for 4 h. The positive control group (indomethacin 5 μM) and ZBSO-treated groups were then exposed to LPS (100 ng/mL) for 24 h. The cellular activities of superoxide dismutase (SOD), glutathione peroxidase (GSH), and malondialdehyde (MDA) were determined using a commercial kit, according to the manufacturer's instructions (Elabscience, Wuhan, China).

2.8. Real-Time Polymerase Chain Reaction (RT-PCR). The total RNA in BEAS-2B cells was extracted using a TransGen (Beijing, China) TransZol Kit and quantified using Eppendorf Bioluminometer D30. A total of 1 μg RNA was used to synthesize the corresponding cDNA using a one-step gDNA Removal and cDNA Synthesis SuperMix Kit (TransGen, Beijing, China). SYBR Green-based real-time PCR experiments were performed to detect the total mRNA transcripts on a LightCycler 96 Real-Time PCR System (Roche, Mannheim, Germany) platform. Table 1 shows the primer sequences. Gene expression was calculated as previously described, using the $2^{-\Delta\Delta Ct}$ method.

2.9. ELISA Assay for COX-2 and PGE2. The culture medium was collected, and the levels of cyclooxygenase 2 (COX-2) and prostaglandin E_2 (PGE2) were determined under different conditions using an ELISA, according to the manufacturer's protocol. The absorbance at 450 nm and 570 nm were measured with a microplate analyzer (SpectraMax®190, USA). The absolute value was obtained using a standardized 4-parameter logistic curve.

2.10. Molecular Docking. The oral bioavailability (OB) of ZBSO was evaluated by the OBioavail 1.1 model in the traditional Chinese medicine systems pharmacology (TCMSP) database (http://ibts.hkbu.edu.hk/LSPtcmsp.php). Drug-likeness (DL) was analyzed using a model from the TCMSP database, which was constructed according to the molecular descriptors and Tanimoto coefficient [25]. Active ingredients were screened using OB ≥ 30% and DL ≥ 0.18 as cutoff parameters [27]. The Tripos Mol2 type files for selected active ingredients were searched using the TCMSP database. Active ingredients were imported into Discovery Studio 3.5 software for hydrogenation optimization and saved in .pdb format as a ligand for backup. The three-dimensional structure of the target protein (Table 2) was obtained from the Protein Database (PDB) (https://www.rcsb.org/pdb/home/home.do), and AutoDock Tools software was used to remove water, hydrogenate the protein, add atomic charges, and set the atom type, which was then saved in .pdbqt format for use as a recipient. AutoDock 1.5.6 software was used to conduct molecular docking between the compounds and protein receptors, and the docking results were analyzed. Binding energy≤−5.0 kJ/mol was used as the screening criteria.

2.11. NF-κB P65 Immunofluorescence Assay. The cells were pretreated with ZBSO (0.025%, 0.05%, and 0.1% *v/v*) and positive control for 4 h and then stimulated with LPS (100 ng/mL) for 24 h. Untreated cells served as a control. Subsequently, the cells were immobilized in 4% paraformaldehyde (Beyotime, Beijing) and permeated in PBS containing 0.1% Triton X-100. The cells were sealed with 5% goat serum for 1 h at room temperature, followed by incubation with primary anti-NF-κB p65 antibody at 4°C overnight. Cells were washed 3 times and labeled with Cy3 at room temperature for 1 h. Finally, Hoechst 33258 (1 μg/mL) was added and incubated in the dark at 37°C for 30 min. Images were taken using a fluorescence microscope (Olympus X81, Tokyo, Japan) with excitation/emission wavelengths of 490 nm/540 nm for Cy3 and 360 nm/450 nm for Hoechst 33258. All morphometric measurements were determined by at least three independent individuals in a blinded manner.

2.12. Western Blot Analyses. The collected BEAS-2B cells were washed 3 times with precooled PBS, followed by the addition of 150 μL radioimmunoprecipitation assay (RIPA) lysis buffer (lysis buffer: phenylmethylsulfonyl fluoride [PMSF]: protein phosphatase inhibitor = 100 : 1 : 1). After incubation in an ultrasonic cell crusher ice bath for 6 min, samples were centrifuged (12000 × g) at 4°C for 10 min to collect the supernatant. The extracted proteins were quantified by using a bicinchoninic acid (BCA) protein assay kit (Thermo, Waltham, MA, USA). The protein concentrations were adjusted using lysis buffer. Protein loading buffer was added (total protein: loading buffer = 4 : 1) and heated for 5 min at 100°C, and then the samples were cooled to room temperature and stored at −20°C. Equal amounts of sample protein were separated by electrophoresis (8% SDS-PAGE) and transferred to polyvinylidene difluoride (PVDF) membranes. The membranes were blocked with 5% milk for 1 h at room temperature and incubated with primary antibodies against TLR4 (1 : 1000), MyD88 (1 : 4000), p65 (1 : 3000), p-p65 (1 : 2000), histone 3 (1 : 1000) and β-actin (1 : 2000) at 4°C overnight. After washing adequately with Tris-buffered saline containing Tween 20 (TBST) three times, the membranes were incubated with secondary antibodies (Goat anti-Rabbit IgG-HRP) at room temperature for 1 h. The membranes were washed three times and exposed to a gel imager using an enhanced chemiluminescence (ECL) kit.

Table 1: Primers used in this study.

Gene primer name	Primer sequence (5′-3′)
TNF-α F	CGAGTGACAAGCCTGTAGCC
TNF-α R	TGAAGAGGACCTGGGAGTAGAT
IL-6 F	GGAGACTTGCCTGGTGAA
IL-6 R	GCATTTGTGGTTGGGTCA
IL-10 F	GTCCTCCTGACTGGGGTGAG
IL-10 R	GCCTTGATGTCTGGGTCTTG
MCP-1 F	CCTTCTGTGCCTGCTGCTCA
MCP-1 R	CACTTGCTGCTGGTGATTCTTC
MMP-2 F	TGGATGATGCCTTTGCTCG
MMP-2 R	GAGTCTCCCCCAACACCAGT
MMP-9 F	CAACATCACCTATTGGATCC
MMP-9 R	GGGTGTAGAGTCTCTCGCT
GAPDH F	CTGACTTCAACAGCGACACC
GAPDH R	TGCTGTAGCCAAATTCGTTGT

Table 2: The relevant targets of TLR4/MYD88/NF-κB pathway.

Targets	PDB number
TLR4	2z64
MyD88	3mop
P65	1K3Z

The bands were visualized with a Bio-Rad ChemiDoc XRS. The density of the western blot bands was quantified using Quantity One software (Bio-Rad, CA, USA).

2.13. Statistical Analysis. The data are expressed as the mean ± standard deviation (SD) of three independent experiments. Statistical analyses were performed using one-way analysis of variance followed by a least significant difference (LSD) test for multiple comparisons using SPSS 26.0 software (IBM, New York, USA) and GraphPad Prism 8.3 (GraphPad Software, Inc., La Jolla, CA, USA). Student's t-test was used to evaluate comparisons between two groups. A p value of <0.05 was considered significant.

3. Results

3.1. ZBSO Exhibits Little Cytotoxicity in BEAS-2B Cells. The extraction method used to obtain ZBSO was based on previous research. The oil yield for ZBSO was 23.2%, which was equivalent to 0.8898 g of crude drug per mL, and the main components were unsaturated fatty acids (19.82%–28.08%) [28]. To investigate the cytotoxicity of ZBSO in human lung epithelial cells, BEAS-2B cells were treated with various doses of ZBSO, ranging from 0.01% to 0.1%, for 24 h. The results, shown in Figure 1(a), revealed that ZBSO concentrations below 0.1% have no inhibitory effects on BEAS-2B cell growth. Therefore, to avoid affecting cell growth and ensure the effectiveness of the drug, the final tested concentrations used for ZBSO in the present study were 0.025%, 0.05%, and 0.1% *v/v*. The effects of low, medium, and high ZBSO doses were examined on LPS-induced changes in nitrite levels in BEAS-2B cells, which revealed that ZBSO could significantly inhibit NO generation (Figure 1(b)), inhibiting the inflammatory response.

3.2. ZBSO Protects BEAS-2B Cells against LPS-Induced Oxidative Stress. To elucidate the effects of ZBSO on LPS-induced oxidative stress in BEAS-2B cells, we examined the intracellular levels of ROS, SOD, GSH, and MDA. As shown in Figure 2, the levels of ROS and MDA in the LPS group significantly increased compared with those of the control group ($p < 0.05$). However, compared with the LPS-treated group, ZBSO and indomethacin treatment significantly alleviated oxidative stress, as indicated by reduced intracellular ROS and MDA levels ($p < 0.01 - 0.05$). The levels of SOD and GSH in the LPS group significantly decreased compared with those in the control group ($p < 0.05$), whereas the levels of SOD and GSH in the ZBSO and indomethacin treatment groups significantly increased ($p < 0.05$).

3.3. ZBSO Suppresses the Release of Proinflammatory Cytokines in LPS-Stimulated BEAS-2B Cells. The effects of ZBSO on the LPS-induced expression of TNF-α, IL-6, IL-10, and MCP-1 were investigated by RT-qPCR. As shown in Figure 3, the expression of TNF-α, IL-6, and MCP-1 genes in cells significantly increased after LPS stimulation ($p < 0.05$). IL-10 inhibits the inflammatory response by preventing the production of cytokines and chemokines at the transcriptional level and regulating mRNA degradation to regulate posttranscriptional expression [29]. Treatment with increasing ZBSO concentrations resulted in a significant and concentration-dependent increase in IL-10 expression levels ($p < 0.01$), with 0.1% ZBSO treatment showing the maximal effect.

3.4. ZBSO Protects BEAS-2B Cells against LPS-Induced Expression of COX-2 and PGE2. COX-2 is the rate-limiting enzyme that catalyzes the production of prostaglandins from arachidonic acid, accelerating the production of PGE2. COX-2 expression is rapidly upregulated following stimulation, which can induce acute inflammation [30]. The effects of ZBSO on COX-2 and PGE2 induction following LPS treatment were measured by ELISA. As shown in Figures 4(a) and 4(b), ZBSO significantly reduced the protein expression of COX-2 in a dose-dependent manner. Consistently, exposure to LPS alone significantly increased the production of PGE2, and treatment with various concentrations of ZBSO significantly reduced PGE2 expression.

3.5. ZBSO Inhibits the Expression of MMP-2 and MMP-9 Induced by LPS. The overexpression of MMP-2 and MMP-9 is positively correlated with certain inflammatory mediators released during the initial stages of inflammation. The degradation of the extracellular matrix and basement membrane proteins can further aggravate the infiltration range of inflammatory cells, aggravating the inflammatory response [31]. Next, we evaluated the effects of ZBSO on the expression of MMP-2 and MMP-9. The results of RT-qPCR analysis (Figures 3(e) and 3(f)) showed that exposure to LPS alone increased the mRNA levels of MMP-2 and MMP-9 by 3.0- and 8.19-fold, respectively, relative to untreated cells.

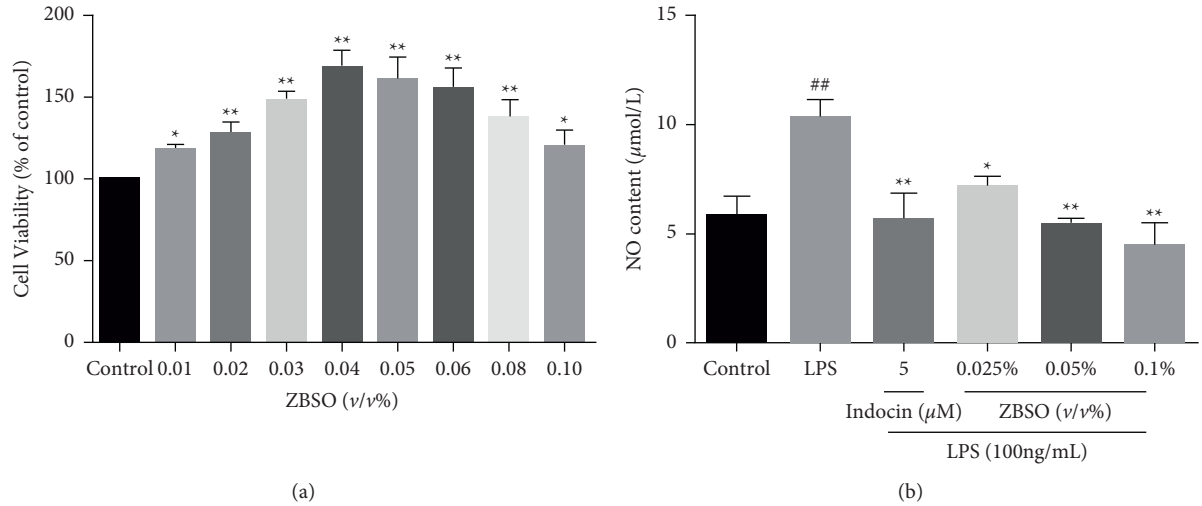

Figure 1: BEAS-2B cells were treated with different concentrations of ZBSO (0.01%–0.1% *v/v*) for 24 hours. CCK-8 assay was used to detect cell viability. (a) The level of NO in the medium was determined by the Griess method. (b) Each point represents the mean ± SD of three experiments; $^{\#}p < 0.05$ and $^{\#\#}p < 0.01$ versus the control group; $^{*}p < 0.05$ and $^{**}p < 0.01$ versus the LPS group.

However, the levels of MMP-2 mRNA in the groups treated with 0.025%, 0.05%, and 0.1% (*v/v*) ZBSO were only 3.0-, 2.2-, and 0.63-fold those of untreated cells, respectively, whereas the levels of MMP-9 mRNA were reduced to 4.7-, 4.6-, and 3.8-fold those of untreated cells. The effects observed in the high-dose ZBSO treatment group were relatively better than those observed following treatment with the positive control.

3.6. Molecular Docking. Molecular docking experiments were conducted to further explore the anti-COPD mechanisms of ZBSO treatment. By screening the ingredients in ZBSO, combined with a review of the literature, seven active ingredients were identified, including α-linolenic acid [32], quercetin, isoimperatorin, eucalyptol, ent-epicatechin, β-sitosterol, and andrographolide. The basic information for these components is shown in Table 3. Molecular docking was performed to examine interactions between these components and key proteins in the TLR4/MyD88/NF-κB signaling pathway, as shown in Figure 5. If the binding energy is less than 0, the ligand and the receptor can bind freely, with lower binding energy indicating a greater affinity between the receptor and the ligand and a higher interaction probability between the two components. As shown in Table 4, the binding energies determined for α-linolenic acid, quercetin, isoimperatorin, eucalyptol, ent-epicatechin, β-sitosterol, andrographolide, and indomethacin with anti-COPD target proteins were all lower than 0, indicating that the main active ingredients in ZBSO present good binding activity with TLR4, MyD88, and p65 receptor proteins. The binding effects were better than or equal to those observed for indomethacin.

3.7. ZBSO Suppresses LPS-Induced NF-κB Nuclear Translocation in BEAS-2B Cells. NF-κB is a nucleoprotein factor that regulates the expression of a wide range of genes and serves in a pivotal role for LPS-induced inflammatory processes [33]. LPS induces the translocation of NF-κB/p65 from the cytoplasm to the nucleus, and the nuclear translocation of NF-κB is associated with the release of large quantities of inflammatory mediators, such as TNF-α, IL-6, IL-10, NO, COX-2, and PGE2. The expression of p65 and its phosphorylated proteins in the nucleus and cytoplasm were analyzed by western blot. The nuclear translocation of p65 was also observed by immunofluorescence. As presented in Figure 6(b), the phosphorylated p65 contents of BEAS-2B cells significantly increased after LPS stimulation, whereas excessive phosphorylation was significantly inhibited by ZBSO treatment in a concentration-dependent manner. As shown in Figures 6(c) and 6(d), LPS stimulation caused p65 to shift to the nucleus and ZBSO treatment effectively blocked the nuclear accumulation of p65 induced by LPS. In addition, immunofluorescence analysis showed that ZBSO inhibited NF-κB/p65 transport into the nucleus (Figure 6(a)).

3.8. ZBSO Reduces LPS-Induced Expression of TLR4 and MyD88. As a component of the upstream pathway for NF-κB, TLR4 binds MyD88. The MyD88-dependent TLR4 pathway promotes the production of inflammatory factors, activating the NF-κB signaling pathway and leading to the expression of a variety of inflammatory factors [34]. Western blot analysis was performed to evaluate the expression of TLR4 and MyD88. As shown in Figure 7, compared with the normal control group, TLR4 and MyD88 protein expression in BEAS-2B cells increased significantly after LPS stimulation ($p < 0.05$). At low concentrations, ZBSO treatment (0.025%, *v/v*) did not significantly decrease TLR4 and MyD88 protein expression levels, whereas ZBSO treatments at 0.05% and 0.1% resulted in the significantly reduced expression of these two proteins ($p < 0.01 - 0.05$), to levels similar to those observed following treatment by the positive control drug.

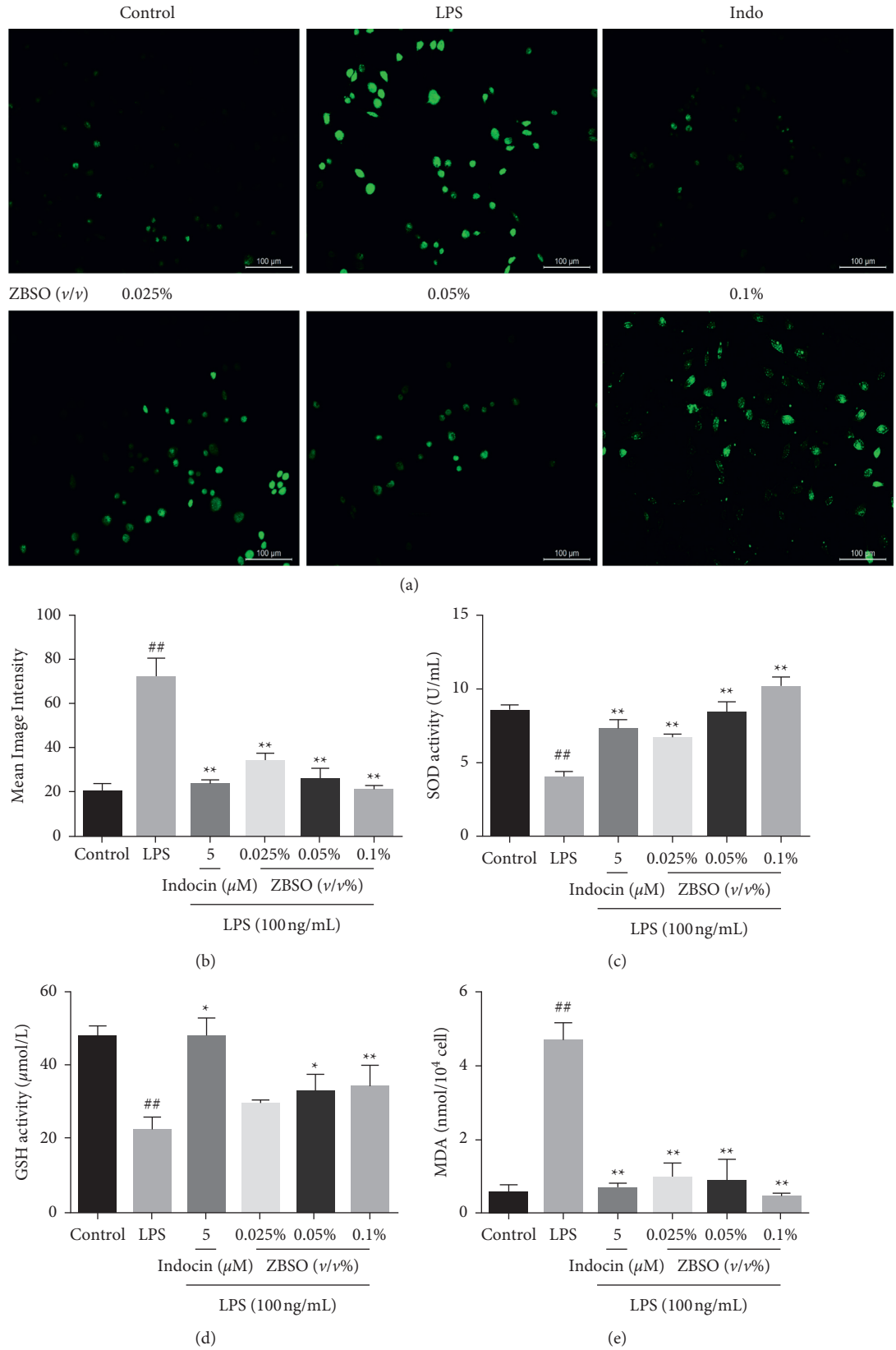

Figure 2: ZBSO protects BEAS-2B cells from LPS-induced oxidative stress. DCFH-DA staining (a, b) was used to detect intracellular reactive oxygen species (ROS), and the levels of the antioxidants SOD (c), GSH (d), and MDA (e) were detected using a commercial kit. The experiment was repeated three times. The results are expressed as the mean ± SD; $^{\#}p < 0.05$ and $^{\#\#}p < 0.01$ versus the control group; $^{*}p < 0.05$ and $^{**}p < 0.01$ versus the LPS group.

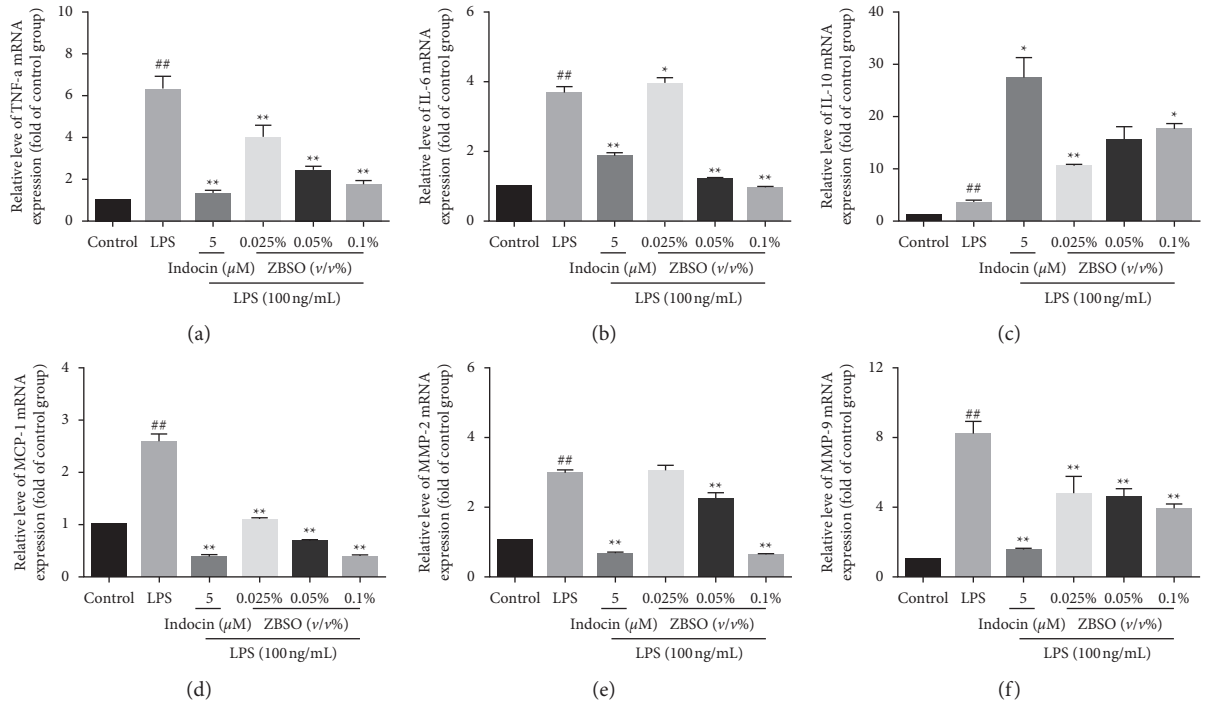

Figure 3: ZBSO inhibited the mRNA expression of LPS-stimulated proinflammatory factors. BEAS-2B cells were pretreated with ZBSO (0.025%, 0.05%, or 0.1% *v/v*) for 4 h and then treated with LPS (100 ng/mL) for 24 h. The results showed that ZBSO significantly inhibited LPS induction of TNF-α (a), IL-6 (b), IL-10 (c), MCP-1 (d), MMP-2 (e), and MMP-9 (f) expression. The experiment was repeated three times. The results are expressed as the mean ± SD; $^{\#}p < 0.05$ and $^{\#\#}p < 0.01$ versus the control group; $^{*}p < 0.05$ and $^{**}p < 0.01$ versus the LPS group.

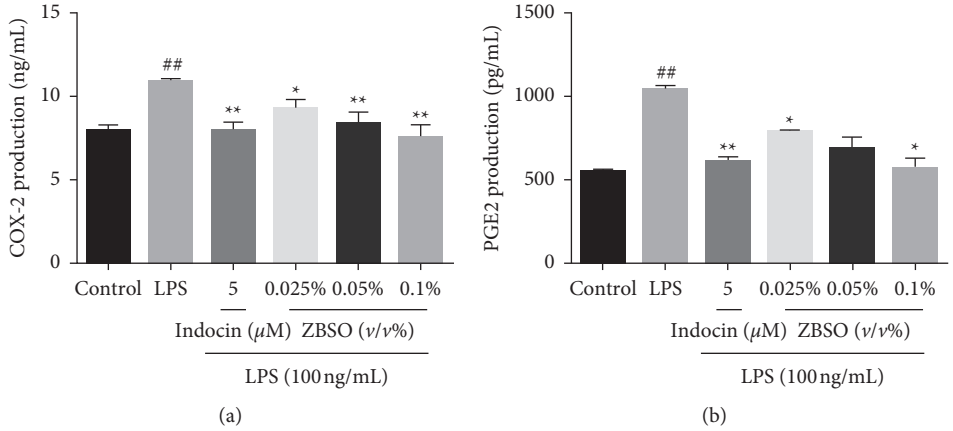

Figure 4: The effects of ZBSO on COX-2 and PGE2 expression in the supernatant of BEAS-2B cells. The secretion of (a) COX-2 and (b) PGE2. Data are expressed as the mean ± SD ($n = 3$); $^{\#}p < 0.05$ and $^{\#\#}p < 0.01$ versus the control group; $^{*}p < 0.05$ and $^{**}p < 0.01$ versus the LPS group.

Table 3: Basic information of some compounds in ZBSO.

MOL id	Chemical compound	OB (%)	DL (%)
MOL000432	α-Linolenic acid	45.01	0.15
MOL000098	Quercetin	46.43	0.28
MOL001942	Isoimperatorin	45.46	0.23
MOL000073	Ent-epicatechin	48.96	0.24
MOL000359	Beta-sitosterol	36.91	0.75
MOL002395	Andrographolide	56.3	0.31

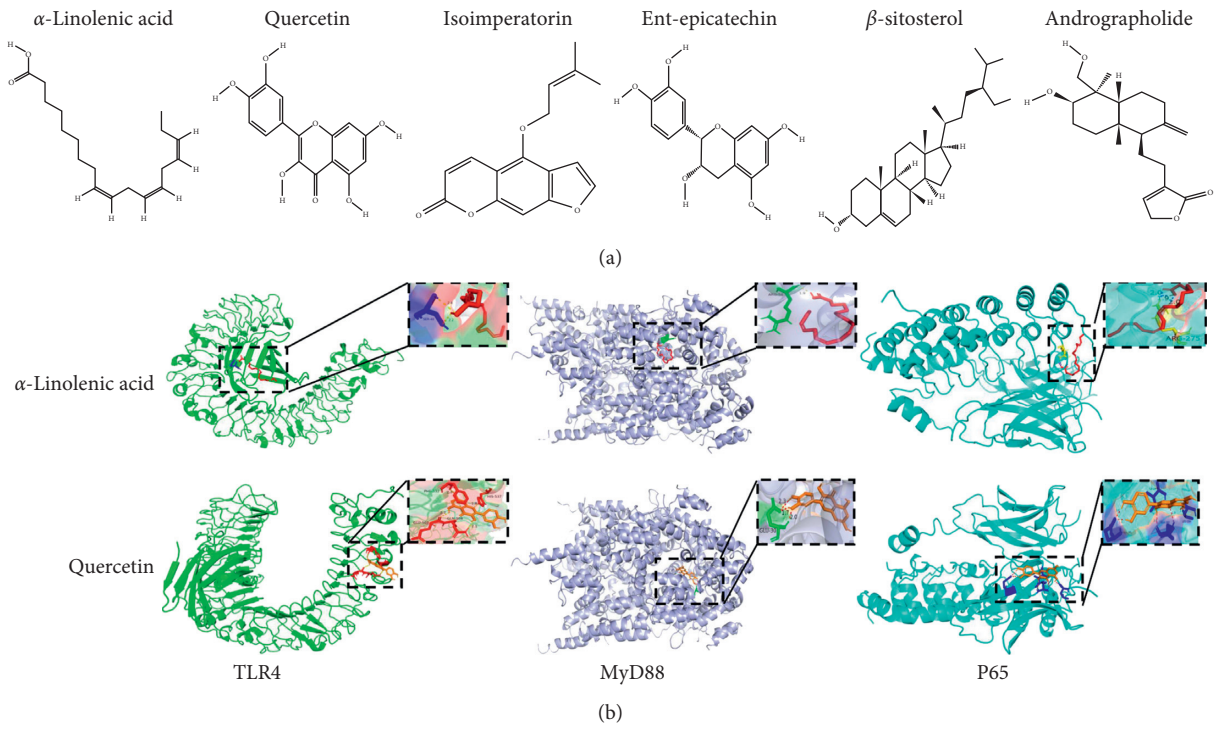

Figure 5: Docking results for the active components in ZBSO with key protein molecules in the TLR4/MyD88/NF-κB signaling pathway. (a) The structures of active components in ZBSO were obtained by screening. (b) α-Linolenic acid, quercetin, and TLR4, MyD88, or NF-κB p65 proteins in molecular docking mode.

Table 4: Molecular docking results of major active components of ZBSO and indomethacin with related targets of TLR4/MyD88/NF-κB pathway.

Ligands	Binding energy (kJ/mol^{-1})		
	TLR4	MyD88	P65
α-Linolenic acid	−22.468	−14.309	−18.702
Quercetin	−27.447	−17.824	−26.903
Isoimperatorin	−26.317	−26.652	−25.313
Ent-epicatechin	−25.732	−19.372	−25.899
Beta-sitosterol	−16.903	−17.573	−23.389
Andrographolide	−27.747	−25.313	−25.230
Indomethacin	−25.713	−24.054	−28.451

4. Discussion

COPD is a global public health issue [35]. Current treatments include surgery and certain medications, including bronchodilators, anti-inflammatory agents, antioxidants, protease inhibitors, and antibiotics. However, the COPD prognosis is poor and no specific cure for COPD currently exists [36]. Exposure to LPS causes persistent inflammation and oxidative stress [5, 37]. In this study, to further explore the effects of ZBSO on COPD and its underlying mechanisms, LPS-treated lung epithelial cells were used to simulate the COPD microenvironment *in vitro*.

Natural medicines or traditional Chinese medicines exhibit unique and diverse chemical and biological activities, representing an important resource for new lead compounds, especially for the treatment of critical diseases. *Zanthoxylum bungeanum* belongs to the rue family and is widely used as both a spice and traditional Chinese medicine due to its unique flavor and medicinal properties. ZBSO is rich in unsaturated fatty acids [38], particularly α-linolenic acid, which has been reported to have anti-inflammatory and antithrombotic properties and is beneficial for the treatment of asthma and thrombosis [39]. Wang et al. [40] obtained obtucarbamate A, ent-epicatechin, quercetin, 9,19-cyclolanost-24-en-3-one, suberic acid, stearic acid, β-sitosterol, daucosterol, isoimperatorin, and isopimpinellin from ZBSO by extraction and isolation. The results of these component analyses are useful for understanding the biological activities of ZBSO. In recent years, molecular docking has become an important technology in the field of computer-aided drug research. Molecular docking is a drug design method that directly analyzes the characteristics of the receptor and the interaction between the receptor and the drug molecule and can

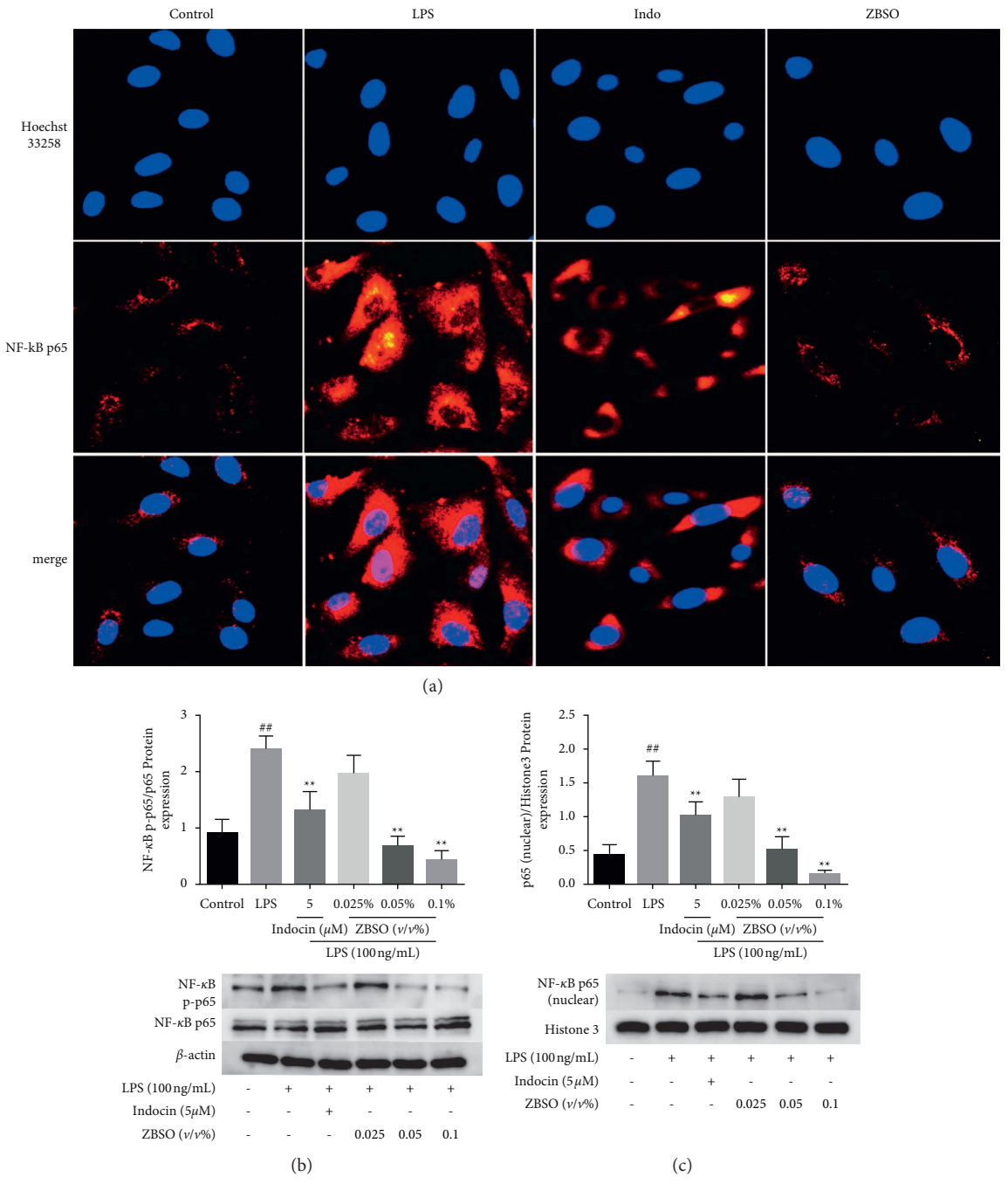

Figure 6: Continued.

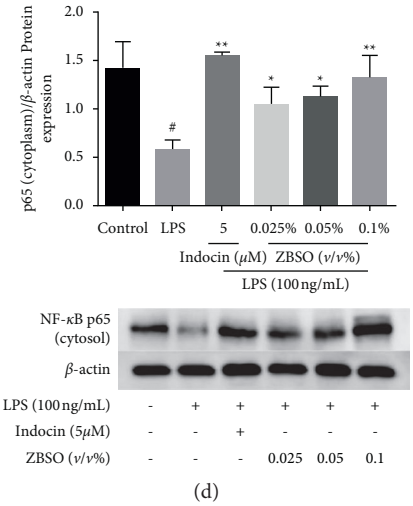

(d)

Figure 6: ZBSO inhibition of LPS-induced p65 nuclear translocation. (a) Typical immunofluorescence images of NF-κB p65 (red) and Hoechst 33258 (blue) induced by LPS (20 × magnification). Western blot analysis of NF-κB p65 total protein, NF-κB p65 phosphorylation (b), and NF-κB p65 in the nucleus (c) and cytoplasm (d). The values are expressed as the mean ± SD ($n = 3$) of three independent experiments. $^{\#}p < 0.05$ and $^{\#\#}p < 0.01$ versus the control group; $^{*}p < 0.05$ and $^{**}p < 0.01$ versus the LPS group.

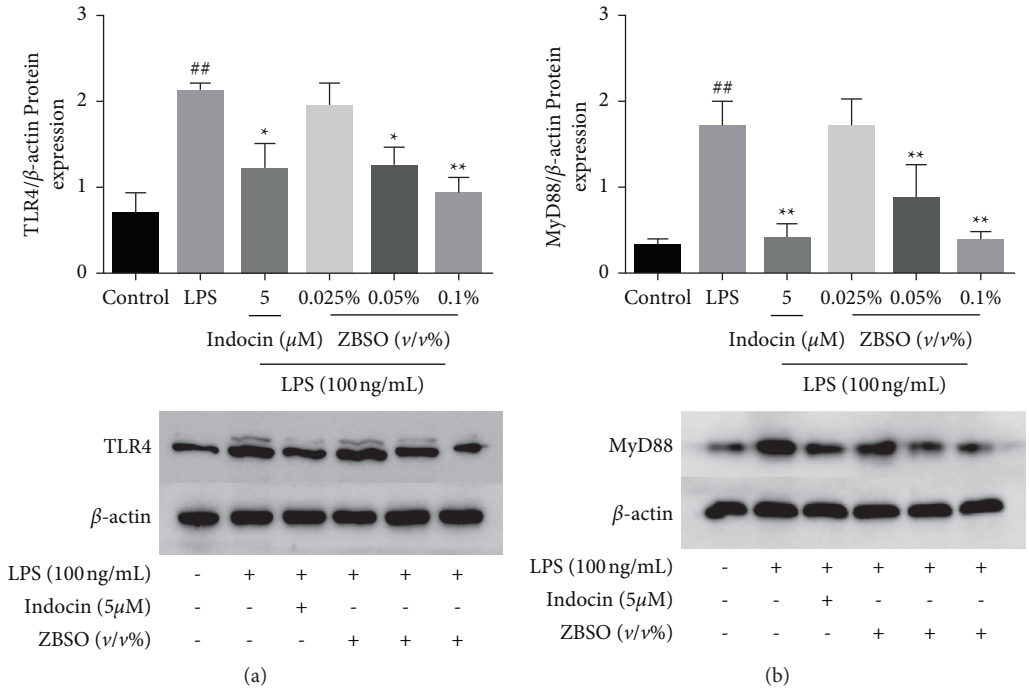

(a) (b)

Figure 7: Effects of different doses of ZBSO (0.025%, 0.05%, or 0.1% *v/v*) and indomethacin on TLR4 and MyD88 protein levels in LPS-induced BEAS-2B cells. Western blot analysis of (a) TLR4 and (b) MyD88 expression levels. The values are expressed as the mean ± SD ($n = 3$) of three independent experiments. $^{\#}p < 0.05$ and $^{\#\#}p < 0.01$ versus the control group; $^{*}p < 0.05$ and $^{**}p < 0.01$ versus the LPS group.

be used to predict binding patterns and affinities [41]. The known components were screened through the TCMSP database, and the active compounds were obtained in combination with a review of the existing literature. The molecular docking technology was used to score the docking of the identified active compounds with the target protein, and the binding energies were all stronger than −5 kJ/mol, indicating that the active components may have high affinities for these proteins. Therefore, the components in ZBSO may act on the TLR4/MyD88/NF-κB signaling pathway. However, because of the limitations of molecular docking, the flexibility of the protein and

changes in the acid-base balance of the environment are generally not considered. Therefore, we used western blot analysis to verify the biological results.

TNF-α, IL-6, and MCP-1 are proinflammatory cytokines, which are closely related to pulmonary inflammation caused by COPD [42]. When stimulated, COX-2 expression is rapidly upregulated, which can induce acute inflammatory response in humans and animals. MMP-2 and MMP-9 are considered to be important collagenases in inflammatory diseases, and the synthesis and secretion of MMP-2 and MMP-9 are highly related to TNF-α [43]. IL-10 expression can reduce lung neutrophil infiltration and inhibit the expression of TNF-α, IL-6, and MCP-1. NO is a bioactive inflammatory inducer in the body, directly triggering the occurrence of the inflammatory process [44]. COX-2 is an inducible enzyme that is expressed at low levels in normal tissues, whereas expression increases when cells are stimulated by inflammation. PGE2 is a bioactive lipid that induces a range of biomolecules associated with inflammation. When the expression of COX-2 increases, PGE2 is released as the major COX product secreted by lung epithelial cells [45]. The results of this study demonstrated that ZBSO significantly inhibited the expression of inflammatory mediators in LPS-induced BEAS-2B cells, consistent with the results reported by Wang et al. for ZBSO in ovalbumin-induced pneumonia in an asthmatic mouse model [22]. TLR4 mediates the pathogen-induced activation of NF-κB in endothelial cells through the homologous structure of intracellular IL-1 receptor, which subsequently initiates the downstream MyD88 signaling pathway, resulting in the secretion of immune-inflammatory cytokines and the development of COPD [46]. LPS could activate the TLR4/MyD88/NF-κB signaling pathway in BEAS-2B cells and promote the expression of TLR4, MyD88, p65, and p-p65. In this study, immunofluorescence and western blot analyses were used to observe the expression levels of TLR4, MyD88, and p65, which were enhanced after LPS stimulation in BEAS-2B cells compared with those in the normal control group. ZBSO treatment significantly suppressed the expression levels of TLR4, MyD88, and p65 and prevented the nuclear translocation of p65. In addition, ZBSO treatment significantly blocked LPS-mediated oxidative stress and altered the levels of the oxidative stress markers ROS, MDA, GSH, and SOD.

5. Conclusions

In summary, the present work well illuminated that ZBSO exerted the anti-COPD effects, at least in part, by downregulating TLR4/MyD88/NF-κB-mediated inflammatory responses; we believe that ZBSO has a beneficial effect on the treatment of COPD and may be a potential drug for the treatment of inflammatory diseases. Nevertheless, the composition of ZBSO is complex and diverse; meanwhile, the pathogenesis of COPD involves various signaling molecules. Therefore, in our future endeavor, more in-depth investigations on the anti-COPD effect of ZBSO, including seeking main active ingredients of ZBSO and their corresponding targeting molecules, would be performed. On the other hand, *in vivo* animal models would be employed in the future studies to depict a more comprehensive picture. These enlightenments in the future should broaden our understanding of the anti-COPD mechanism and potential of ZBSO.

Abbreviations

ZBSO: *Zanthoxylum bungeanum* seed oil
COPD: Chronic obstructive pulmonary disease
LPS: Lipopolysaccharide
TLR4: Toll-like receptor 4
MyD88: Myeloid differentiation factor 88
ZBM: *Zanthoxylum bungeanum* Maxim.
DMEM: Dulbecco's modified Eagle's medium
DCFH-DA: Dichlorodihydrofluorescein diacetate
OD: Optical density
PGE2: Prostaglandin E2
SOD: Superoxide dismutase
GSH: Glutathione peroxidase
MDA: Malondialdehyde
OB: Oral bioavailability
DL: Drug-likeness.

Data Availability

There are no basic data to support our results.

Conflicts of Interest

The authors declare that no conflicts of interest exist.

Authors' Contributions

Jing Hou and Jun Wang contributed equally to this work.

Acknowledgments

This research was funded by the National Key R&D Program of China (2019YFC171 0800), National Natural Science Foundation of China (81904031), Plan of Shanxi Province Science and Technology Research (201901D211325), Shanxi Higher Education Innovation Project (2019L0448), Science Research Start-up Fund for Doctor of Shanxi Province (SD1801), and Science Research Start-up Fund for Doctor of Shanxi Medical University (XD1802).

Supplementary Materials

Figures S1–S4: *Zanthoxylum bungeanum* Maxim., *Zanthoxylum bungeanum* seed, *Zanthoxylum bungeanum* seed sample specimen, and *Zanthoxylum bungeanum* seed oil used in this study. (*Supplementary Materials*)

References

[1] H. A. H. Albitar and V. N. Iyer, "Adherence to global initiative for chronic obstructive lung disease guidelines in the real world: current understanding, barriers, and solutions," *Current Opinion in Pulmonary Medicine*, vol. 26, no. 2, pp. 149–154, 2020.

[2] S. Mirza, R. D. Clay, M. A. Koslow, and P. D. Scanlon, "COPD guidelines: a review of the 2018 GOLD report," *Mayo Clinic Proceedings*, vol. 93, no. 10, pp. 1488–1502, 2018.

[3] B. Zhu, Y. Wang, J. Ming, W. Chen, and L. Zhang, "Disease burden of COPD in China: a systematic review," *International Journal of Chronic Obstructive Pulmonary Disease*, vol. 13, pp. 1353–1364, 2018.

[4] S. C. Lareau, B. Fahy, P. Meek, and A. Wang, "Chronic obstructive pulmonary disease (COPD)," *American Journal of Respiratory Critical Care Medicine*, vol. 199, no. 1, 2019.

[5] C. Brightling and N. Greening, "Airway inflammation in COPD: progress to precision medicine," *Europen Respiratory Journal*, vol. 54, no. 2, 2019.

[6] S. S. Sohal, M. S. Eapen, C. Ward, and E. H. Walters, "Airway inflammation and inhaled corticosteroids in COPD," *Europen Respiratory Journal*, vol. 49, no. 6, 2017.

[7] P. J. Barnes, "Glucocorticosteroids," *Handbook of Experimental Pharmacology*, vol. 237, pp. 93–115, 2017.

[8] Q. Chu, X. Yu, R. Jia et al., "Flavonoids from apios americana medikus leaves protect RAW264.7 cells against inflammation via inhibition of MAPKs, Akt-mTOR pathways, and Nfr2 activation," *Oxidative Medicine Cellular Longevity*, vol. 2019, Article ID 1563024, 14 pages, 2019.

[9] L. Zuo, K. Lucas, C. A. Fortuna, C. C. Chuang, and T. M. Best, "Molecular regulation of toll-like receptors in asthma and COPD," *Frontiers in Physiology*, vol. 6, p. 312, 2015.

[10] Z. Tianzhu and W. Shumin, "Esculin inhibits the inflammation of LPS-induced acute lung injury in mice via regulation of TLR/NF-κB pathways," *Inflammation*, vol. 38, no. 4, pp. 1529–1536, 2015.

[11] Q. Jiang, M. Yi, Q. Guo et al., "Protective effects of polydatin on lipopolysaccharide-induced acute lung injury through TLR4-MyD88-NF-κB pathway," *International Immunopharmacology*, vol. 29, no. 2, pp. 370–376, 2015.

[12] J. He, S. Han, X. X. Li et al., "Diethyl blechnic exhibits anti-inflammatory and antioxidative activity via the TLR4/MyD88 signaling pathway in LPS-stimulated RAW264.7 cells," *Molecules*, vol. 24, no. 24, 2019.

[13] X. Chang, H. He, L. Zhu et al., "Protective effect of apigenin on Freund's complete adjuvant-induced arthritis in rats via inhibiting P2X7/NF-κB pathway," *Chemical Biological Interactions*, vol. 236, pp. 41–46, 2015.

[14] P. M. Hansbro, T. J. Haw, M. R. Starkey, and K. Miyake, "Toll-like receptors in COPD," *European Respiratory Journal*, vol. 49, no. 5, 2017.

[15] K. K. Auyeung, Q. B. Han, and J. K. Ko, "Astragalus membranaceus: a review of its protection against inflammation and gastrointestinal cancers," *American Journal of Chinese Medicine*, vol. 44, no. 1, pp. 1–22, 2016.

[16] R. Yang, B. C. Yuan, Y. S. Ma, S. Zhou, and Y. Liu, "The anti-inflammatory activity of licorice, a widely used Chinese herb," *Pharmaceutical Biology*, vol. 55, no. 1, pp. 5–18, 2017.

[17] M. Chunhua, H. Long, W. Zhu et al., "Betulin inhibited cigarette smoke-induced COPD in mice," *Biomedicine and Pharmacotherapy*, vol. 85, pp. 679–686, 2017.

[18] R. Zhou, F. Luo, H. Lei et al., "Liujunzi Tang, a famous traditional Chinese medicine, ameliorates cigarette smoke-induced mouse model of COPD," *Journl of Ethnopharmacology*, vol. 193, pp. 643–651, 2016.

[19] M. Zhang, J. Wang, L. Zhu et al., "*Zanthoxylum bungeanum* Maxim. (rutaceae): a systematic review of its traditional uses, botany, phytochemistry, pharmacology, pharmacokinetics, and toxicology," *International Journal of Molecular Science*, vol. 18, no. 10, 2017.

[20] W. Pang, S. Liu, F. He et al., "Anticancer activities of *Zanthoxylum bungeanum* seed oil on malignant melanoma," *Journal of Ethnopharmacology*, vol. 229, pp. 180–189, 2019.

[21] X. Q. Li, R. Kang, J. C. Huo, Y. H. Xie, S. W. Wang, and W. Cao, "Wound-healing activity of *Zanthoxylum bungeanum* maxim seed oil on experimentally burned rats," *Pharmacognosy Magazine*, vol. 13, no. 51, pp. 363–371, 2017.

[22] J. Q. Wang, X. W. Li, M. Liu, S. C. Wang, and Z. F. Cao, "Inhibitory effect of *Zanthoxylum bungeanum* seed oil on ovalbumin-induced lung inflammation in a murine model of asthma," *Molecular Medicine Reports*, vol. 13, no. 5, pp. 4289–4302, 2016.

[23] K. Li, R. Zhou, W. Wang Jia et al., "*Zanthoxylum bungeanum* essential oil induces apoptosis of HaCaT human keratinocytes," *Journal of Ethnopharmacology*, vol. 186, pp. 351–361, 2016.

[24] Y. Bai, J. Hou, X. T. Zhang, J. P. Gao, and J. T. Zhou, "*Zanthoxylum bungeanum* seed oil elicits autophagy and apoptosis in human laryngeal tumor cells via PI3K/AKT/mTOR signaling pathway," *Anticancer Agents Medicinal Chemistry*, 2021.

[25] Y. Bai, S. Wang, and X. Bai, "Determination of fatty acids in zanthoxyli semen based on solidification of floating organic drop liquid phase microextraction with gas chromatography," *Chromatographia*, vol. 80, no. 12, pp. 1813–1818, 2017.

[26] T. Pei, C. Zheng, C. Huang et al., "Systematic understanding the mechanisms of vitiligo pathogenesis and its treatment by Qubaibabuqi formula," *Journal of Ethnopharmacology*, vol. 190, pp. 272–287, 2016.

[27] B. Pan, X. Shi, T. Ding, and L. Liu, "Unraveling the action mechanism of polygonum cuspidatum by a network pharmacology approach," *American Journal of Translational Research*, vol. 11, no. 11, pp. 6790–6811, 2019.

[28] S. P. Wang, H. H. Sun, S. S. Zhang, J. P. Gao, and Y. Bai, "Quality evaluation of pepper herbs from different producing areas," *Journal of Shanxi Medical University*, vol. 048, pp. 445–450, 2017.

[29] R. Sabat, G. Grütz, K. Warszawska et al., "Biology of interleukin-10," *Cytokine Growth Factor Reviews*, vol. 21, no. 5, pp. 331–344, 2010.

[30] K. Shimizu, R. Okita, S. Saisho, A. I. Maeda, Y. Nojima, and M. Nakata, "Impact of COX2 Inhibitor for regulation of PD-L1 expression in non-small cell lung cancer," *Anticancer Research*, vol. 38, no. 8, pp. 4637–4644, 2018.

[31] M. J. Hannocks, X. Zhang, H. Gerwien et al., "The gelatinases, MMP-2 and MMP-9, as fine tuners of neuroinflammatory processes," *Matrix Biology*, vol. 75-76, pp. 102–113, 2019.

[32] S. C. Lemoine, E. P. Brigham, H. Woo et al., "Omega-3 fatty acid intake and prevalent respiratory symptoms among U.S. adults with COPD," *BMC Pulmonary Medicine*, vol. 19, no. 1, p. 97, 2019.

[33] T. Muhammad, M. Ikram, R. Ullah, S. U. Rehman, and M. O. Kim, "Hesperetin, a citrus flavonoid, attenuates LPS-induced neuroinflammation, apoptosis and memory impairments by modulating TLR4/NF-κB signaling," *Nutrients*, vol. 11, 3 pages, 2019.

[34] X. Tian, C. Liu, Z. Shu, and G. Chen, "Review: therapeutic targeting of HMGB1 in stroke," *Current Drug Delivery*, vol. 14, no. 6, pp. 785–790, 2017.

[35] K. F. Rabe, S. Hurd, A. Anzueto et al., "Global strategy for the diagnosis, management, and prevention of chronic obstructive pulmonary disease: GOLD executive summary," *American Journal of Respiratory and Critical Care Medicine*, vol. 176, no. 6, pp. 532–555, 2007.

[36] F. Lu, H. Yang, S. D. Lin et al., "Cyclic peptide extracts derived from pseudostellaria heterophylla ameliorates COPD via regulation of the TLR4/MyD88 pathway proteins," *Frontiers in Pharmacology*, vol. 11, p. 850, 2020.

[37] P. J. Barnes, "Inflammatory endotypes in COPD," *Allergy*, vol. 74, no. 7, pp. 1249–1256, 2019.

[38] W. Tang, Q. Xie, J. Guan, S. Jin, and Y. Zhao, "Phytochemical profiles and biological activity evaluation of *Zanthoxylum bungeanum* maxim seed against asthma in murine models," *Journal of Ethnopharmacology*, vol. 152, no. 3, pp. 444–450, 2014.

[39] Q. Yang, W. Cao, X. Zhou, W. Cao, Y. Xie, and S. Wang, "Anti-thrombotic effects of α-linolenic acid isolated from *Zanthoxylum bungeanum* maxim seeds," *BMC Complementary and Alternative Medicine*, vol. 14, p. 348, 2014.

[40] W. Z. Wang and Y. Q. Zhao, "Chemical constituents of *Zanthoxylum bungeanum* maxim seeds," *Journal of Shenyang Pharmaceutical University*, pp. 91-92, 2006.

[41] L. Pinzi and G. Rastelli, "Molecular docking: shifting paradigms in drug discovery," *Internationa Journal of Molecular Science*, vol. 20, no. 18, 2019.

[42] G. Pelaia, A. Vatrella, L. Gallelli et al., "Biological targets for therapeutic interventions in COPD: clinical potential," *International Journal of Chronic Obstructive Pulmonary Disease*, vol. 1, no. 3, pp. 321–334, 2006.

[43] Y. Zhang, Y. Li, Z. Ye, and H. Ma, "Expression of matrix metalloproteinase-2, matrix metalloproteinase-9, tissue inhibitor of metalloproteinase-1, and changes in alveolar septa in patients with chronic obstructive pulmonary disease," *Medical Science Monitor*, vol. 26, Article ID e925278, 2020.

[44] D. T. Ha, P. T. Long, T. T. Hien et al., "Anti-inflammatory effect of oligostilbenoids from Vitis heyneana in LPS-stimulated RAW 264.7 macrophages via suppressing the NF-κB activation," *Chemistry Central Journal*, vol. 12, no. 1, p. 14, 2018.

[45] P. D. N'Guessan, B. Temmesfeld-Wollbrück, J. Zahlten et al., "Moraxella catarrhalis induces ERK- and NF-kappaB-dependent COX-2 and prostaglandin E2 in lung epithelium," *European Respiratory Journal*, vol. 30, no. 3, pp. 443–451, 2007.

[46] P. J. Barnes, "Frontrunners in novel pharmacotherapy of COPD," *Current Opinion in Pharmacology*, vol. 8, no. 3, pp. 300–307, 2008.

Hindawi
Evidence-Based Complementary and Alternative Medicine
Volume 2021, Article ID 5547424, 12 pages
https://doi.org/10.1155/2021/5547424

Research Article

Essential Oil-Rich Chinese Formula Luofushan-Baicao Oil Inhibits the Infection of Influenza A Virus through the Regulation of NF-κB P65 and IRF3 Activation

Xin Mao,[1] **Shuyin Gu**,[1] **Huiting Sang**,[1] **Yilu Ye**,[1] **Jingyan Li**,[1] **Yunxia Teng**,[2] **Feiyu Zhang**,[2] **Qinhai Ma**,[3] **Ping Jiang**,[1] **Zifeng Yang**,[3] **Weizhong Huang**,[2] **and Shuwen Liu**[1]

[1]*Guangdong Provincial Key Laboratory of New Drug Screening, School of Pharmaceutical Sciences, Southern Medical University, Guangzhou 510515, China*
[2]*Guangdong Provincial Key Laboratory of Gynecological Chinese Medicine, Huizhou 516113, China*
[3]*State Key Laboratory of Respiratory Disease, National Clinical Research Center for Respiratory Disease, Guangzhou Institute of Respiratory Health, The First Affiliated Hospital of Guangzhou Medical University, Guangzhou 510230, China*

Correspondence should be addressed to Weizhong Huang; 18933237516@163.com and Shuwen Liu; liusw@smu.edu.cn

Received 30 April 2021; Revised 30 June 2021; Accepted 27 July 2021; Published 30 August 2021

Academic Editor: Miranda Li Xu

Copyright © 2021 Xin Mao et al. This is an open access article distributed under the Creative Commons Attribution License, which permits unrestricted use, distribution, and reproduction in any medium, provided the original work is properly cited.

Background. Luofushan-Baicao Oil (LBO) is an essential oil-rich traditional Chinese medicine (TCM) formula that is commonly used to treat cold, cough, headache, sore throat, swelling, and pain. However, the anti-influenza activities of LBO and the underlying mechanism remain to be investigated. *Methods*. The *in vitro* anti-influenza activity of LBO was tested with methyl thiazolyl tetrazolium (MTT) and plaque assays. The effects of LBO on the expressions of viral nucleoprotein and cytokines were evaluated. In the polyinosinic-polycytidylic acid- (Poly I: C-) induced inflammation model, the influences of LBO on the expression of cytokines and the activation of NF-κB P65 (P65) and interferon regulatory factor 3 (IRF3) were tested. After influenza A virus (IVA) infection, mice were administered with LBO for 5 days. The lung index, histopathologic change, the expression of viral protein, P65, and IRF3 in the lung tissue were measured. The levels of proinflammatory cytokines in serum were examined. *Results*. *In vitro*, LBO could significantly inhibit the infection of IVA, decrease the formation of plaques, and reduce the expression of viral nucleoprotein and cytokines. LBO could also effectively downregulate the expression of interleukin-1β (IL-1β), interleukin-6 (IL-6), and interferon-β and the activation of P65 and IRF3 in Poly I:C-treated cells. In the IVA-infected mice model, inhalation of LBO with atomizer could decrease the lung index, alleviate the pathological injury in the lung tissue, and reduce the serum levels of IL-1β and IL-6. LBO could significantly downregulate the expression of viral protein (nucleoprotein, PB2, and matrix 2 ion channel) and the phosphorylation of P65 and IRF3 in the lungs of mice. *Conclusion*. The therapeutic effects of LBO on treating influenza might result from the regulation of the immune response of IVA infection. LBO can be developed as an alternative therapeutic agent for influenza prevention.

1. Introduction

The influenza virus is one of the most common respiratory pathogens, which is a substantial threat to the world [1]. Influenza virus infections could affect the upper and lower respiratory tract, inducing cough, fever, sore throat, rhinorrhea, and pneumonia [2]. Influenza virus can induce seasonal epidemics and worldwide pandemics. There have been three influenza pandemics in the past hundred years (1957, 1968, and 2009). First reported in Mexico and the United States, the 2009 H1N1 pandemic caused significant morbidity and mortality; about half a million people were dead from it [3, 4]. Children, old people, pregnant women, and people with chronic illness are considered to be high-risk groups that can be easily infected by the influenza virus [5]. With the outbreak of the worldwide pandemic induced

by coronavirus (SARS-CoV-2) at the end of 2019, evidence shows that the influenza A virus (IVA) could aggravate SARS-CoV-2 infection. Hence, the prevention of influenza infection is of great significance [6]. Neuraminidase inhibitor, oseltamivir, is the most commonly used antiviral drug in treating influenza. However, with the widespread oseltamivir-resistance gene, the limitation of oseltamivir is getting more serious [7, 8].

Influenza virus can be recognized by many pattern recognition receptors (PRRs), such as retinoic acid-inducible gene I (RIG-I) and Toll-like receptors (TLRs). Expressed in airway epithelial cells, TLR3 is able to detect the dsRNA intermediate by influenza virus [9, 10]. The activation of PRRs initiates innate immune responses, resulting in the releasing of interferons (IFNs), interleukins (ILs), and chemokines, leading to clearance of viruses and infected cells. However, the excessive activation of innate immune also results in lung injury [11]. In recent years, the attenuating of proinflammatory responses and limiting influenza-induced tissue damage has been considered as an alternative strategy for treating influenza virus infection [12, 13].

Luofushan-Baicao Oil (LBO) is a unique essential oil-rich traditional Chinese herbal (TCM) formula composed of seventy-nine kinds of herbs and related extractions: methyl salicylate, peppermint oil, camphor oil, turpentine oil, eucalyptus oil, camphor, menthol, cinnamon oil, *Ocimum gratissimum* oil, borneol, star anise oil, and Baicaojing extraction (tea seed oil extraction of the rest of sixty-eight herbs). LBO originated from Ge-Hong, a famous pharmacist in Jin Dynasty. In the Taoism prescription in Ming Dynasty, the formula of LBO was described. The preparation skill of LBO had been listed in the Chinese intangible cultural heritage in recent years.

According to the theory of TCM, influenza and other epidemics belong to the category of "plague (Wenyi)." The "fragrant repelling foulness (Fangxiang Pihui)" is considered to be a therapeutic strategy against epidemic since the Ming Dynasty. In TCM, many fragrant herbs can be used for the prevention and treatment of epidemics through burning, smelling, sneezing, and bathing [14]. LBO is commonly used to treat cold, cough, headache, sore throat, swelling, and pain. However, due to the complex composition, the bioactivity investigation and mechanism study of LBO is very limited. In this research, we evaluate *in vitro* and *in vivo* anti-influenza effects of LBO and investigate the underlying mechanisms.

2. Material and Methods

2.1. Preparation of LBO. LBO (Lot No. 20E201) was provided by Guangdong Luofushan Sinopharm Co., Ltd. (Huizhou, China). LBO is composed of methyl salicylate, peppermint oil, camphor oil, turpentine oil, eucalyptus oil, camphor, menthol, cinnamon oil, *Ocimum gratissimum* oil, borneol, star anise oil, and Baicaojing extraction (the rest of sixty-eight herbs, listed in Table S1, were extracted with 5-fold tea seed oil for 15 days in room temperature, and the solution was filtered to get baicaojing extraction). Methyl salicylate 250 g, peppermint oil 250 g, camphor oil 150 g, turpentine oil 95 g, eucalyptus oil 40 g, camphor 30 g, menthol 27.5 g, cinnamon oil 20 g, *Ocimum gratissimum* oil 15 g, borneol 2.5 g, and star anise oil 2g were mixed with the baicaojing extraction, with extra tea seed oil added to get 1 liter of LBO (relative density 0.96 mg/mL).

2.2. Drugs and Reagents. Reference substance: methyl salicylate, camphor, trans-anethole, eugenol, cinnamaldehyde, eucalyptol, borneol, menthol, nitidine chloride, ligustilide, ginsenoside rb1, hesperidin, and kinsenoside were purchased from National Institutes for Food and Drug Control (Beijing, China).

Ribavirin was purchased from Aladdin (Shanghai, China). Polyinosinic-polycytidylic acid (Poly I: C), methyl thiazolyl tetrazolium (MTT), and 2′-(4-methylumbelliferyl)-α-D-N-acetylneuraminic acid sodium salt hydrate (MU-NANA) were purchased from Sigma-Aldrich (Missouri, USA). Lipo3000 was purchased from Invitrogen (Massachusetts, USA). Mouse interleukin-6 (IL-6) enzyme linked immunosorbent assay (ELISA) kit and mouse interleukin-1β (IL-1β) ELISA kit were purchased from Shanghai Enzyme-linked Biotechnology (Shanghai, China). TRIzol reagent was purchased from Invitrogen (Massachusetts, USA). PrimeScript RT-PCR Kit was purchased from Takara (Beijing, China). RIPA lysis buffer was purchased from Beyotime (Shanghai, China).

Anti-NF-κB p65 (phospho S536) antibody (ab86299) was provided by Abcam (Cambridge, UK). Anti-NF-κB p65 antibody (#8242), anti-phospho-IRF-3 (Ser396) antibody (#29047), and anti-IRF-3 antibody (#4302) were provided by Cell Signaling Technology Inc. (Massachusetts, USA). IVA NP (nucleoprotein) antibody (GTX125989), IVA PB2 protein antibody (GTX125926), and IVA M2 (matrix protein) antibody (GTX125951) were provided by Gene Tex (California, USA). Anti-GAPDH antibody 60004-1-Ig was provided by Proteintech (Wuhan, China).

2.3. Viruses. Influenza virus A/FM/1/47 (H1N1) and influenza virus A/WSN/1933 (H1N1) were donated by Prof. Zifeng Yang in the State Key Laboratory of Respiratory Diseases, Guangzhou Medical University (Guangzhou, China). *In vivo* influenza virus experiment was performed in BSL2 barrier animal facility in Guangzhou Medical University. *In vitro* influenza virus experiment was performed in BSL2 laboratory in Southern Medical University.

2.4. GC-MS and LC-MS Analysis of LBO. The compositions of LBO were analyzed using GC-MS and LC-MS methods. GC-MS analysis was performed on an Agilent 7890B GC system coupled to an Agilent 7000D triple quadrupole MS (QQQ-MS) (Agilent Technologies, California, USA) and HP-INNOWAX column (30 m × 0.32 mm × 0.25 μm, Agilent Technologies, California, USA). The column temperature was programmed as follows: the initial temperature was 50°C and increased to 90°C at 10°C/min, then raised to 150°C at 15°C/min and held for 5 min, and finally increased to

240°C at 20°C/min and held for 5 min. Mass scanning was examined in ionization mode of EI at 45–500 amu.

LC-MS analysis was performed on Vanquish UHPLC system coupled to Orbitrap Fusion Tribrid mass spectrometer (Thermo Fisher Scientific, Massachusetts, USA) and Hypersil Gold column (100 mm × 2.1 mm × 1.9 μm, Thermo Fisher Scientific, Massachusetts, USA). The elution was performed with mobile phase composed of 0.1% formic acid in water (solvent A) and acetonitrile (solvent B) using the following gradient program at the flow rate of 0.3 mL/min: 0–7 min, linear gradient 22–40% (B); 7–12 min, linear gradient 40–70% (B); 12–22 min, linear gradient 70–50% (B); 22–23 min, linear gradient 50–22% (B); 23–28 min, and isocratic gradient 22–22% (B). The column temperature was 35°C and the injection volume was 2 μL. Mass scanning was examined in ionization mode of ESI at scan range (m/z) of 120–1200.

2.5. Cytotoxicity Assay. Madin–Darby Canine Kidney (MDCK) cells were cultured in Dulbecco's modified Eagle's medium with 10% fetal bovine serum, 100 units/mL penicillin, and 100 μg/mL streptomycin. The MDCK cells are recommended by ATCC to using as the host cells of influenza [15]. MDCK cells were plated in 96-well plates and cultured overnight at 37°C in 5% CO_2. The LBO were mixed with tween 20 and diluted with DMEM. The medium was removed and the cells were then incubated with various concentrations of LBO (800–50 μg/mL) for 48 h. MTT was added to each well and further incubated for 4 h. The medium was subsequently removed, and formazan crystals were solubilized with dimethyl sulfoxide (DMSO). The absorbance was tested at 490 nm.

2.6. Antiviral Assay. MDCK cells were infected with influenza virus A/WSN/1933 (H1N1) at 37°C for 2 h. The medium was replaced with various concentrations of LBO (12.5–100 μg/mL) at 37°C in 5% CO_2 for 2 days. MTT was added to each well and further incubated for 4 h. The medium was subsequently removed, and formazan crystals were solubilized with DMSO and tested at 490 nm.

MDCK cells were infected with influenza virus A/WSN/1933 (H1N1) at 37 °C for 2 h. The medium was replaced with LBO (50 μg/mL, 100 μg/mL) at 37°C in 5% CO_2 for 24 h. MDCK cells were harvested for RT-PCR analysis.

2.7. Plaque Reduction Assay. Confluent monolayers of MDCK cells were infected with influenza virus A/WSN/1933 (H1N1) at 37°C for 2 h. After incubation, the cell monolayer was covered with the overlay medium containing LBO (50 μg/mL and 100 μg/mL) and further cultured at 37°C in 5% CO_2 for 72 h. Subsequently, the overlay medium was removed, and the cell monolayer was fixed with 4% paraformaldehyde and stained with 1% crystal violet, and the plaques were visualized with ImmunoSpot S6 (CTL, Ohio, USA).

2.8. Immunofluorescence Staining. MDCK cells were infected with influenza virus A/WSN/1933 (H1N1) at 37°C for 2 h. After incubation, the medium was replaced with LBO (50 μg/mL and 100 μg/mL) and incubation at 37°C in 5% CO_2 for another 24 h; the cells were fixed with 4% paraformaldehyde for 30 min and then permeabilized with 0.1% Triton X-100 for 5 min. After blocking with 3% BSA for 1 h, the cells were incubated with anti-IVA NP antibody overnight at 4 °C. The cells were incubated with FITC-labeled secondary antibody for 1 h and further stained with 4′′,6-diamidino-2-phenylindole (DAPI). The fluorescence was visualized using Axio Observer (Zeiss, Oberkochen, Germany).

2.9. NA Inhibition Assay. First, 60 μl of influenza virus A/WSN/1933 (H1N1) was incubated with 10 μl of LBO (200–3.12 μg/mL) and zanamivir at 37°C for 10 min in black 96-well microplate. Next, 30 μl of MU-NANA (80 μM) was added and incubated at 37°C for 30 min. Fluorescence was measured at Ex = 355 nm and Em = 460 nm.

2.10. Hemagglutination Inhibition Assay. 50 μL of hemagglutinin (HA) was mixed with an equal volume of LBO (200–3.12 μg/mL) or HA antibody and incubated for 30 min at 4°C. Afterward, 50 μL of 1% chicken RBCs was added to each well and incubated at 37°C for 40 min to test the agglutination.

2.11. Time-of-Addition Assay. MDCK cells were infected with the influenza virus A/WSN/1933 (H1N1) for 1 h. After removing unabsorbed virus, the cells were treated with LBO (100 μg/mL) at indicated time intervals (0–2, 2–5, 5–8, 8–10, and 0–10 h), which covered one cycle of influenza virus replication. At 10 h p.i., the expression level of viral NP protein was determined by western blotting.

2.12. Poly I:C Treatment. The Poly I:C is a synthetic analog of viral double-stranded RNA. A549 cell line is human lung cells. The Poly I:C-treated A549 cells were employed to investigate the anti-influenza mechanism of LBO, specifically, the influence of LBO on the host immunity during the virus infection [11]. A549 cells were plated in 6-well plates (4×10^5 cells/well) and incubated overnight. The medium was replaced with various concentrations of LBO (50 μg/mL and 100 μg/mL); cells were then transfected with Poly I:C (Lipo3000 regent treated) at 37°C in 5% CO_2 for 24 h. A549 cells were harvested for RT-PCR and western blot analysis.

2.13. Animals and Treatment. Female BALB/c mice (16–18 g) were purchased from Guangdong Medical Laboratory Animal Center (Guangzhou, China). The animal experiments were performed to the Guidelines of Guangdong Regulation for the Administration of Laboratory Animals. This animal study was approved by the Ethics Committee of Guangzhou Medical University (2019–645). The mice were intranasally inoculated with 35 μL of influenza virus A/FM/1/47 (H1N1).

After the infection, mice were treated with LBO (100 μg/mL and 400 μg/mL) with YLS-8B animal atomization device platform (Yiyan, Jinan, China). According to the instructions, 80% of aerosol diameter was 1–5 μm. The mice were treated in the container (285 × 240 × 160 mm), the device speed was set as 1.5 μL/s, each treatment lasted for 30 min, and LBO was administered twice a day for 5 days. The control animals were treated with the solvent. Ribavirin was used as a positive control.

Five days after virus infection, mice were weighed and sacrificed. The lung tissues were removed and weighed. The lung index was calculated (lung index = lung weight/body weight × 100%). Lung tissue was harvested for histopathologic examination and western blotting analysis.

2.14. RT-PCR. MDCK cells and A549 cells were scraped from the plate, and the total RNA of the cells were extracted with TRIzol reagent. The quality of the extracted RNA was determined by optical density measurement at 260 nm on a spectrophotometer (Thermo Fisher Scientific, Massachusetts, USA). Retrotranscription was performed using 2 μg of RNA. The mRNA levels of the target genes were determined by PrimeScript RT-PCR Kit using LightCycler 480 (Roche, Basel, Switzerland). Primer sequences are given in Table S2; the expression of target genes was tested by $2^{-\Delta\Delta Ct}$ method.

2.15. Immunoblotting. The protein of A549 and lung tissue were extracted with RIPA lysis buffer. Equal amounts of protein were separated using SDS-PAGE and transferred onto PVDF membranes. Membranes were blocked and incubated overnight at 4°C with primary antibodies (p-P65, P65, p-IRF3, IRF3, NP, M2, and PB2 GAPDH) and secondary HRP conjugated antibody. Western blot bands were examined by FluorChem E (Protein Simple, California, USA).

2.16. Enzyme-Linked Immunosorbent Assay (ELISA). The levels of IL-1β and IL-6 were determined by ELISA kit (Meilian, Shanghai, China) according to the manufacturer's instructions. The absorbance of each well was tested at 450 nm.

2.17. Histopathological Analysis. The lung tissues were harvested on the 6th day after infection and fixed with 4% paraformaldehyde for 24 h and embedded in paraffin. Embedded lung tissues were cut into 5 μm thick sections. The sections were stained with hematoxylin and eosin (H&E). The sections were captured by Axio Observer (Zeiss, Oberkochen, Germany).

2.18. Statistical Analyses. The data were expressed as means ± SEM and performed using GraphPad Prism v.6 (GraphPad Software). Statistical comparisons of the data were analyzed with one-way ANOVA followed by Dunnett's post hoc test. A value of $p < 0.05$ was considered to be significant.

3. Results

3.1. GC-MS and LC-MS Analysis of LBO. The GC-MS and LC-MS analysis of LBO is shown in Figure 1. Thirteen reference substances were used to identify the compositions in LBO. Seven components (eucalyptol, camphor, menthol, methyl salicylate, trans-anethole, cinnamaldehyde, and eugenol) were identified based on the retention times and product ion by GC-MS (Figures 1(a) and S1(a)). Ligustilide was identified based on the retention times and product ion by LC-MS (Figures 1(b) and S1(b)).

3.2. The In Vitro Anti-Influenza Activity of LBO. To investigate the antivirus activity of LBO, we evaluated the influence of LBO on the cell viability of MDCK. At a concentration of 100 μg/mL or less, LBO exerted no significant cytotoxicity in MDCK cells (Figure 2(a)). In MTT assay, LBO (25–100 μg/mL) could inhibit the reduction of cell viability induced by the influenza virus in a dose-dependent manner (Figure 2(b)). The infection of influenza virus A/WSN/1933 (H1N1) could induce plaque formation in the MDCK infection model. LBO (50 μg/mL and 100 μg/mL) could effectively decrease the plaque number (Figure 2(c)).

3.3. The Influence of LBO on the NP Expression in MDCK Cells. The expression and location of NP were used to confirm the influence of LBO on virus replication and nuclear export of viral ribonucleoprotein (vRNP). As shown in Figure 3, with the infection of influenza virus A/WSN/1933 (H1N1), a strong immunofluorescence signal, as well as the export of vRNP, could be observed in MDCK cells. LBO (50 μg/mL and 100 μg/mL) could remarkably downregulate the NP expression, while the vRNP export could not be alleviated by the treatment of LBO.

3.4. The Influence of LBO on the Replication Cycle of Influenza Virus. The neuraminidase inhibition test, hemagglutination inhibition test, and viral replication test were performed to investigate the effects of LBO on the influenza virus. As shown in Figure S2, LBO could not inhibit the neuraminidase and hemagglutination activity. During the whole replication cycle of influenza virus A/WSN/1933 (H1N1), LBO could not downregulate the expression of NP protein. These results indicated that LBO may not directly interact with IVA.

3.5. The Influence of LBO on the mRNA Expressions of IL-1β, IL-6, and IFN-β in Virus-Infected MDCK Cells and Poly I:C-Treated A549 Cells. The expressions of IL-1β, IL-6, and IFN-β were tested to evaluate the influence of LBO on the cytokine. With the stimulation of the influenza virus A/WSN/1933 (H1N1) as well as the Poly I:C, the mRNA expressions of IL-1β, IL-6, and IFN-β in MDCK cells and A549 cells could be strongly upregulated. With the treatment of LBO, the expression of IL-1β, IL-6, and IFN-β could be remarkably inhibited (Figures 4 and 5).

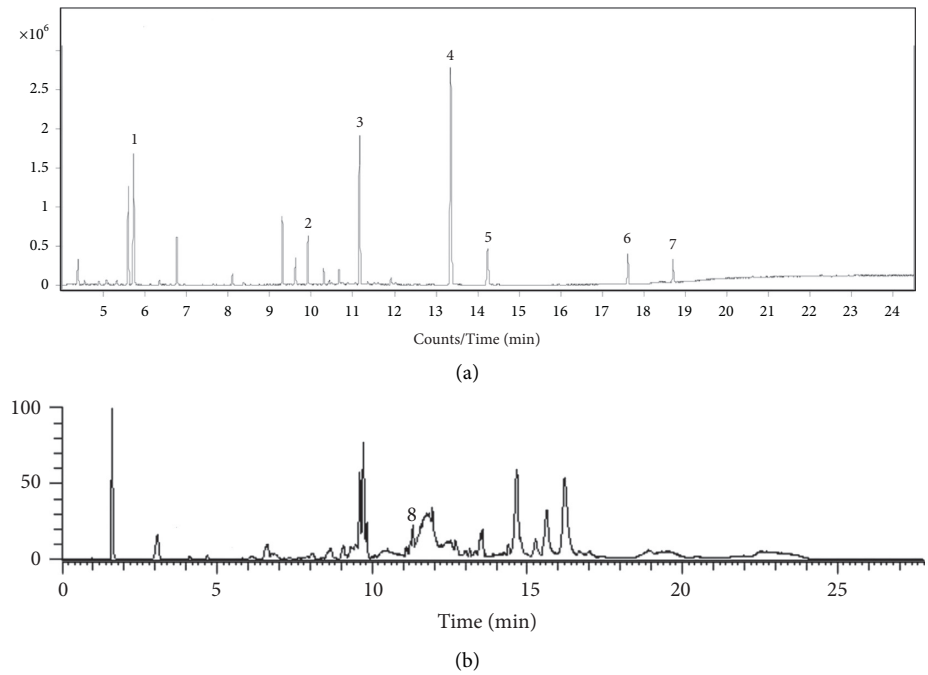

Figure 1: GC-MS and LC-MS analysis of LBO. (a) The GC-MS chromatogram of volatile part of LBO, (1) eucalyptol, (2) camphor, (3) menthol, (4) methyl salicylate, (5) trans-anethole, (6) cinnamaldehyde, and (7) eugenol. (b) The LC-MS chromatogram of nonvolatile part of LBO, (8) ligustilide.

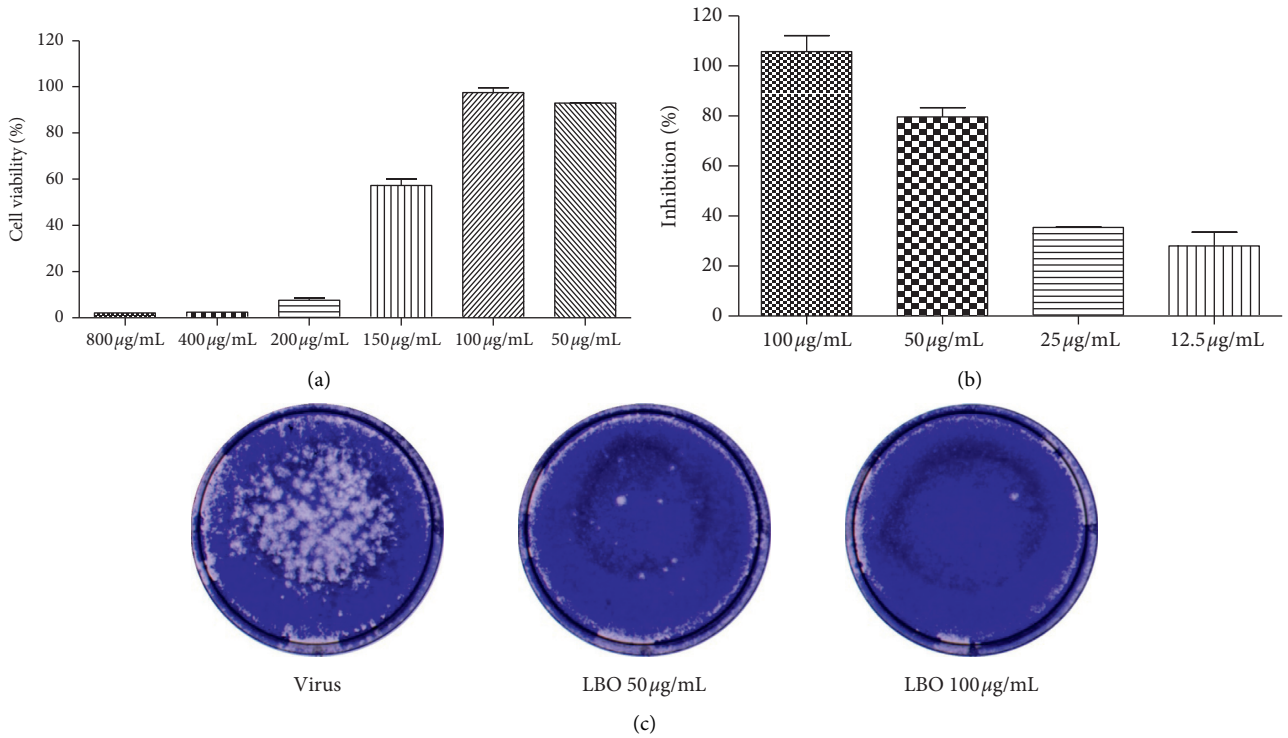

Figure 2: Anti-influenza activity of LBO. (a) The cytotoxicity of LBO in MDCK cells. (b) The anti-influenza activity of LBO. (c) The plaque reduction of LBO against influenza viruses.

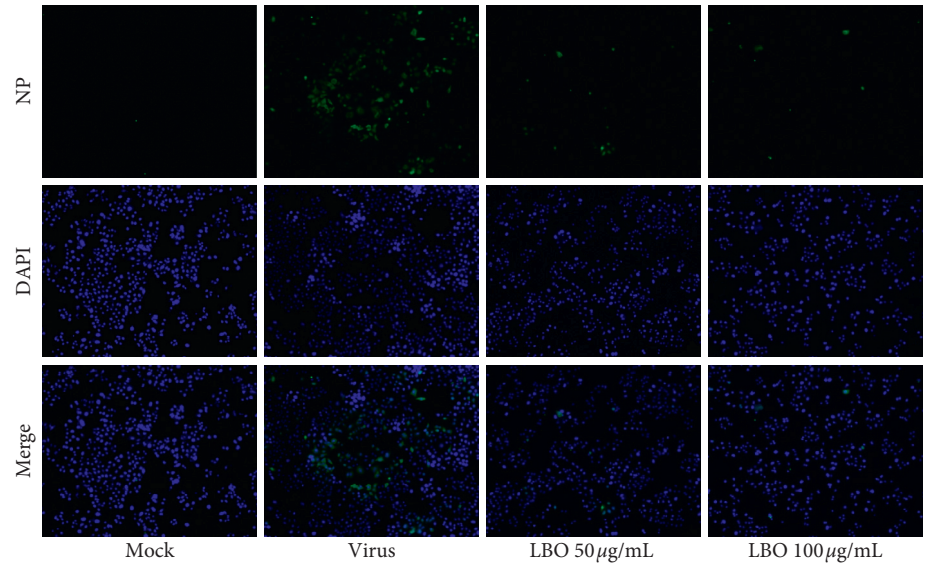

Figure 3: The influence of LBO on the NP expression in MDCK cells. The influenza A virus NP was stained with FITC-labeled antibody (green). The cell nuclei were stained with DAPI (blue). Samples were captured with a fluorescent microscope (magnification: 200×).

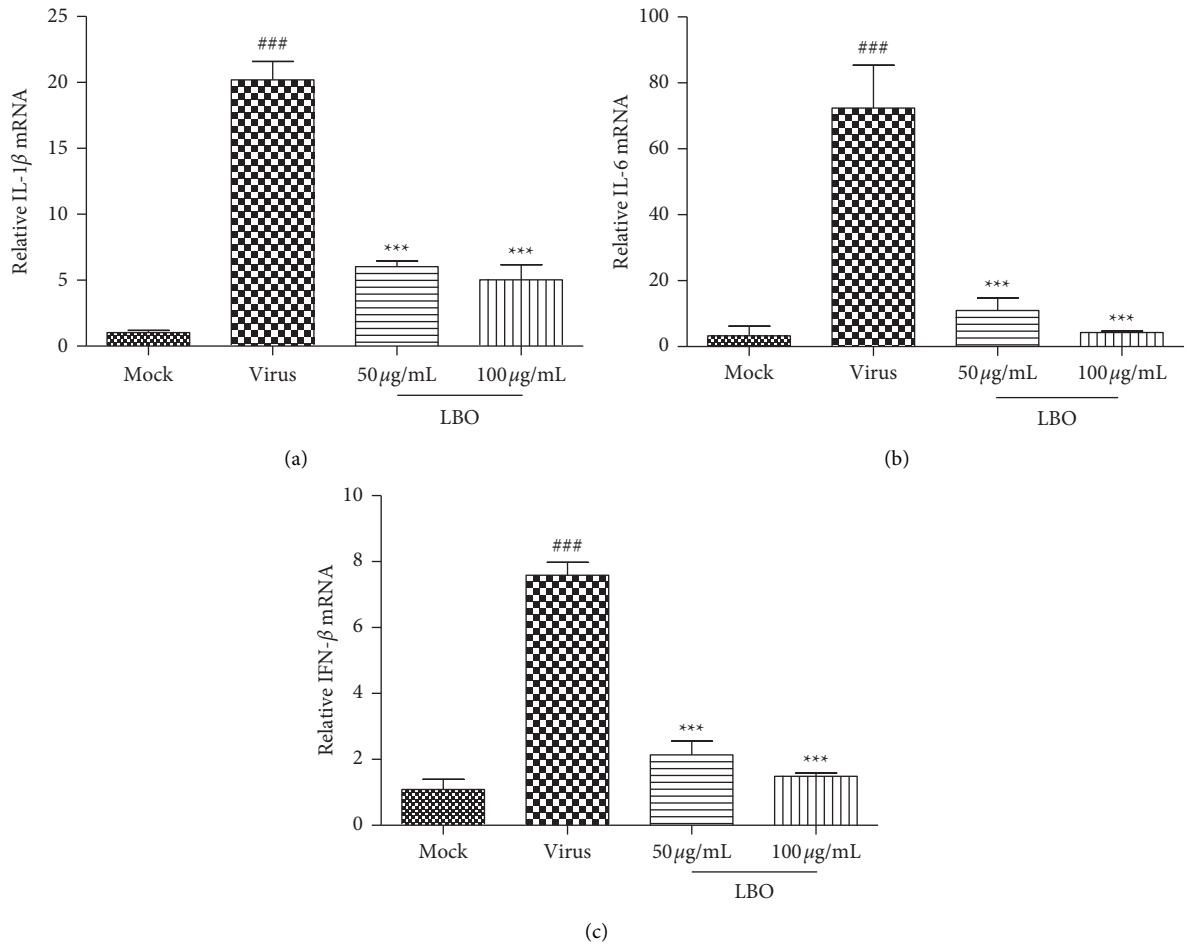

Figure 4: The influence of LBO on the mRNA expressions of IL-1β, IL-6, and IFN-β in IVA-infected MDCK cells. (a) The influence of LBO on the mRNA expressions of IL-1β. (b) The influence of LBO on the mRNA expressions of IL-6. (c) The influence of LBO on the mRNA expressions of IFN-β. Compared with mock group: $^{###}p < 0.001$; compared with virus group: $^{***}p < 0.001$.

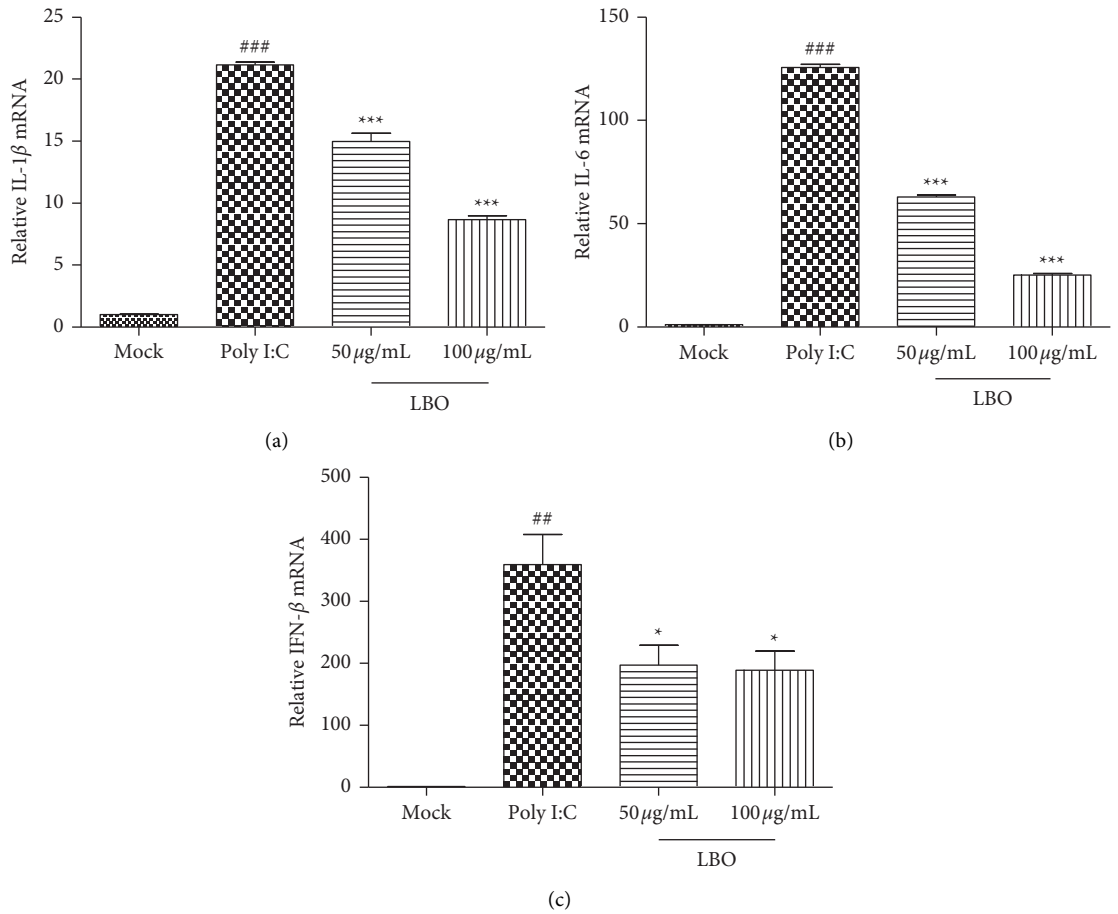

Figure 5: The influence of LBO on the mRNA expressions of IL-1β, IL-6, and IFN-β in Poly I:C-stimulated A549 cells. (a) The influence of LBO on the mRNA expressions of IL-1β. (b) The influence of LBO on the mRNA expressions of IL-6. (c) The influence of LBO on the mRNA expressions of IFN-β. Compared with mock group: $^{###}p < 0.001$, $^{##}p < 0.01$; compared with virus group: $^{***}p < 0.001$, $^{*}p < 0.05$.

3.6. The Influence of LBO on the Levels of NF-κB P65 and Interferon Regulatory Factor 3 in Poly I:C-Treated A549 Cells. To investigate the underlying mechanisms of the inhibition of LBO on cytokine expression, we tested the phosphorylation and expression levels of NF-κB P65 (P65) and interferon regulatory factor 3 (IRF3) in Poly I:C-treated A549 cells (Figure 6). With the stimulation of Poly I:C, the phosphorylation of P65 and IRF3 was strongly increased. LBO treatment could significantly alleviate the activation of P65 and IRF3 in A549 cells.

3.7. The Anti-Influenza Activity of LBO in Mice. Five days after virus infection, the histopathologic changes in the lung tissues were determined, and the lung index was calculated. With the infection of influenza virus A/FM/1/47 (H1N1), severe alveolar thickening and inflammatory cell infiltration could be observed in the lung tissues; the lung index was significantly increased from 0.7896% to 1.2952%. Inhalation of LBO (100 μg/mL and 400 μg/mL) with atomizer could significantly alleviate the pulmonary inflammation and the lung index; the inhibition rates were 29.23% and 33.03% (Table 1 and Figure 7).

3.8. The Influence of LBO on the Serum Levels of IL-1β and IL-6 in Mice. We further evaluate the effects of LBO on the expression of proinflammatory cytokines in mice serum. The concentrations of IL-1β and IL-6 in serum were tested with ELISA. The influenza virus A/FM/1/47 (H1N1) infection could substantially upregulate the serum levels of IL-1β and IL-6. The treatment of LBO could significantly reduce the expression of IL-1β and IL-6 in mice (Figure 8).

3.9. The Influence of LBO on the Virus Proteins, P65 and IRF3, in Mice. Nucleoprotein (NP), PB2, and matrix 2 ion channel (M2) are the three important proteins of IVA. We tested the expression of NP, PB2, and M2 to evaluate the virus clearance effect of LBO in the lung tissue. With the application of LBO, the expression of NP, PB2, and M2 could be significantly reduced (Figure 9). To further understand the underlying mechanisms of the treatment of LBO on the pneumonia mice, the activation of P65 and IRF3 was examined. After being infected by the influenza virus A/FM/1/47 (H1N1), the P65 and IRF3 in lung tissue were remarkably activated. Inhalation of LBO for five days could strongly inhibit the activation of P65 and IRF3 in mice (Figure 10).

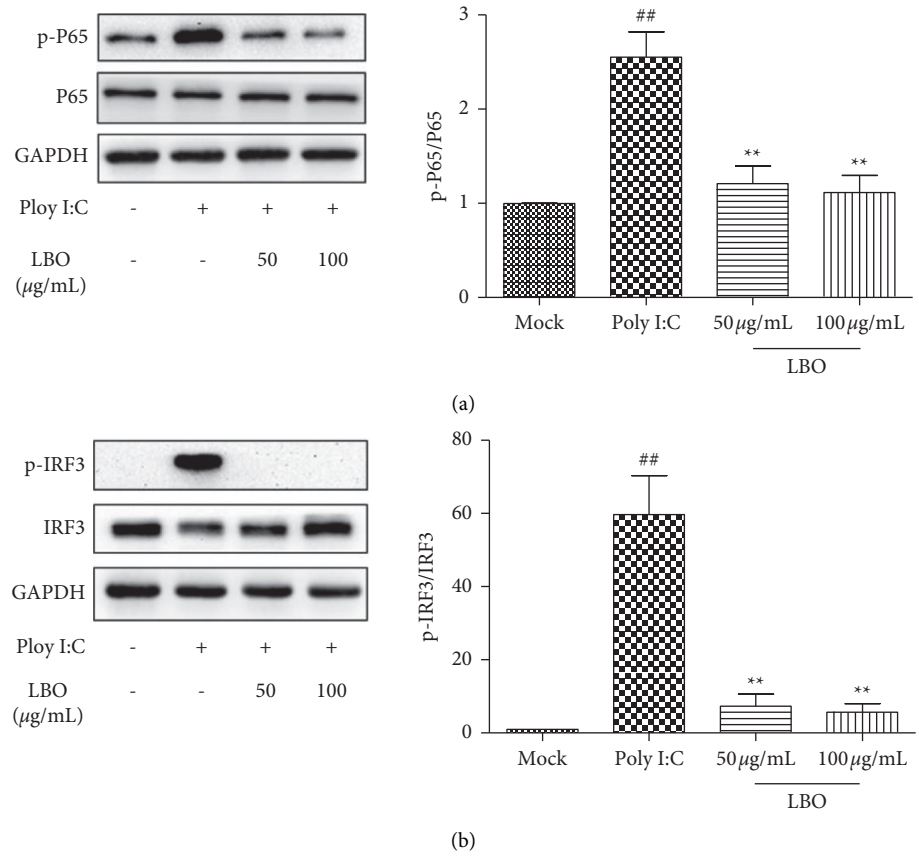

Figure 6: The influence of LBO on the levels of P65 and IRF3 in Poly I:C-stimulated A549 cells. (a) The influence of LBO on the expression of P65. (b) The influence of LBO on the expression of IRF3. Compared with mock group: $^{\#\#}p < 0.01$; compared with virus group: $^{**}p < 0.01$.

Table 1: The influence of LBO on the lung index in influenza-infected mice.

Group	Dose	Lung index (%)	Inhibition rate (%)
Control	—	0.7896	—
Virus	—	$1.2952^{\#\#\#}$	—
Ribavirin	75 mg/kg	0.9085^{**}	76.49
LBO	100 μg/mL	1.1474^{**}	29.23
LBO	400 μg/mL	1.1282^{**}	33.03

Compared with control group$^{\#\#\#}p < 0.001$; compared with virus group $^{**}p < 0.01$. Ribavirin was used as a positive control.

4. Discussion

According to the TCM theory of "fragrant repelling foulness "(Fangxiang Pihui)," burning, smelling, sneezing, and bathing the fragrant herbs could be used for the prevention and treatment of epidemic [14]. Many modern medical investigations support this ancient theory. According to the team of Zhang Q, the inhalation of the sachet (putting fragrant herbs into the small pocket) may prevent influenza through the enhancement of innate immune responses in mice [16]. Li Y proved that inhalation of Bing-Xiang-San, a fragrant Chinese formula, with an atomizer could inhibit the IVA infection in mice model [17]. Fragrant herbs are commonly rich in essential oil; many investigations indicated that essential oil could inhibit the infection of influenza both *in vitro* and *in vivo* [15, 18, 19].

The prescription of LBO is complex, but the content of essential oil and related components is more than ninety percent (882 g/L or 91.87%). Thirteen reference compounds were used to identify the composition of LBO. With the GC-MS method and LC-MS method, eight compounds (eucalyptol, camphor, menthol, methyl salicylate, trans-anethole, cinnamaldehyde, eugenol, and ligustilide) were identified. The bioactive compounds in LBO are uncertain; however, according to other researches, cinnamon oil, eugenol, and eucalyptol have anti-influenza effect. Inhalation and nasal inoculation of cinnamaldehyde, the main component of cinnamon oil, could significantly increase the survival rates of IVA mice [20]. Eugenol, the major component *Ocimum gratissimum* oil, exerted anti-influenza activity in both liquid and vapor phases via inhibition of ERK, p38, and IKK signal pathways [19, 21]. Eucalyptol from eucalyptus oil was able to

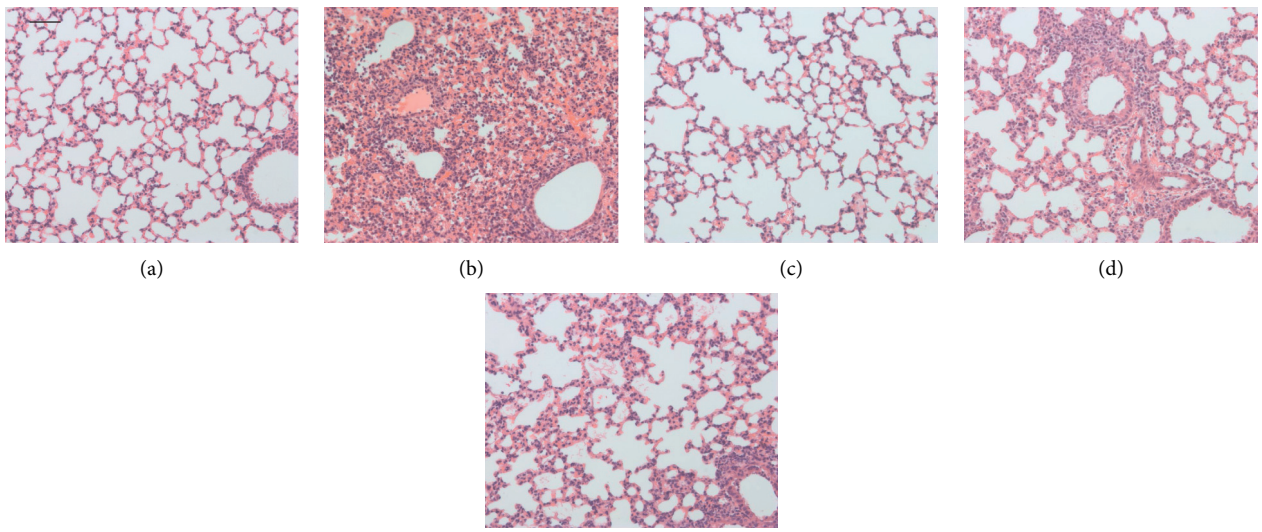

FIGURE 7: The influence of LBO on the pathological changes in the lung tissue in IVA-infected mice. (a) Control group, (b) virus group, (c) ribavirin 75 mg/kg group, (d) LBO 100 μg/mL group, and (e) LBO 400 μg/mL group; ribavirin was used as a positive control (magnification: 200×, scale bar = 100 μm).

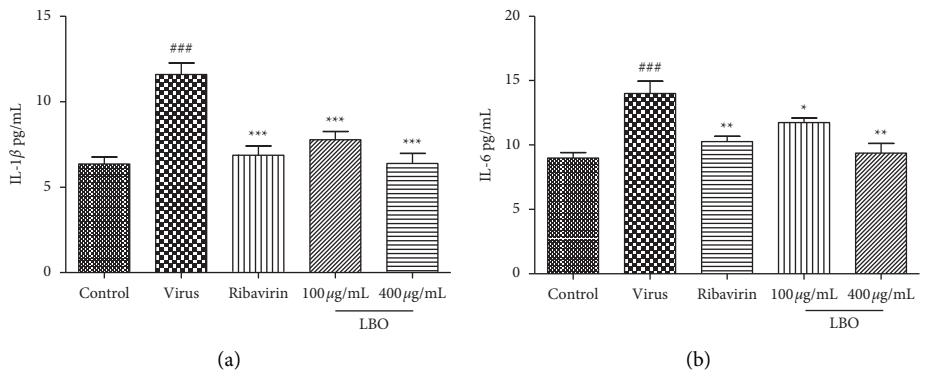

FIGURE 8: The influence of LBO on the serum levels of IL-1β and IL-6 in IVA-infected mice. (a) The influence of LBO on the levels of IL-1β. (b) The influence of LBO on the levels of IL-6. Compared with control group: $^{###}p < 0.001$; compared with virus group: $^{***}p < 0.001$, , $^{**}p < 0.01$, $^{*}p < 0.05$. Ribavirin was used as a positive control.

protect against IVA infection in mice through the attenuation of pulmonary inflammatory responses [22]. Moreover, trans-anethole from star anise oil could reduce LPS-induced acute lung injury by resolution of pulmonary inflammation [23].

In this research, we demonstrated that LBO significantly inhibits the infection of IVA, decreases the formation of plaques, and reduces the expression of viral nucleoprotein. To explore the mechanism of anti-influenza effects, we examined the neuraminidase inhibition and hemagglutination inhibition as well as viral replication inhibition effects of LBO. However, the present results indicate that LBO could not affect the IVA directly. Many investigations about the anti-influenza effects of herbal formulas found that apart from the direct antivirus effects these herbal formulas could regulate the immune response caused by the viral infection [24, 25]. Hence, we hypothesized that the anti-influenza effects of LBO may result from the regulation of host immunity.

After the infection of airway epithelial cells, the influenza virus can be recognized by TLR3 and result in the activation of NF-κB and IRF3 [9, 11]. The activation of NF-κB leads to the gene transcription of proinflammatory cytokines. The high levels of IL-1β and IL-6, typical cytokines that contribute to the cytokine storm phenomenon, are proved to be correlated directly with tissue injury [26]. Many findings proved that NF-κB pathway is a prerequisite for IVA infection, and the inactivation of NF-κB pathway can protect the mice from infection [27, 28]. Our research found that LBO could reduce the expression of IL-1β and IL-6 through the suppression of P65 phosphorylation.

The activation of IRF3 leads to the expression of type I IFNs, IFN-α, and IFN-β, which contribute to the restriction of viral replication [29]. However, excessive type I IFNs in

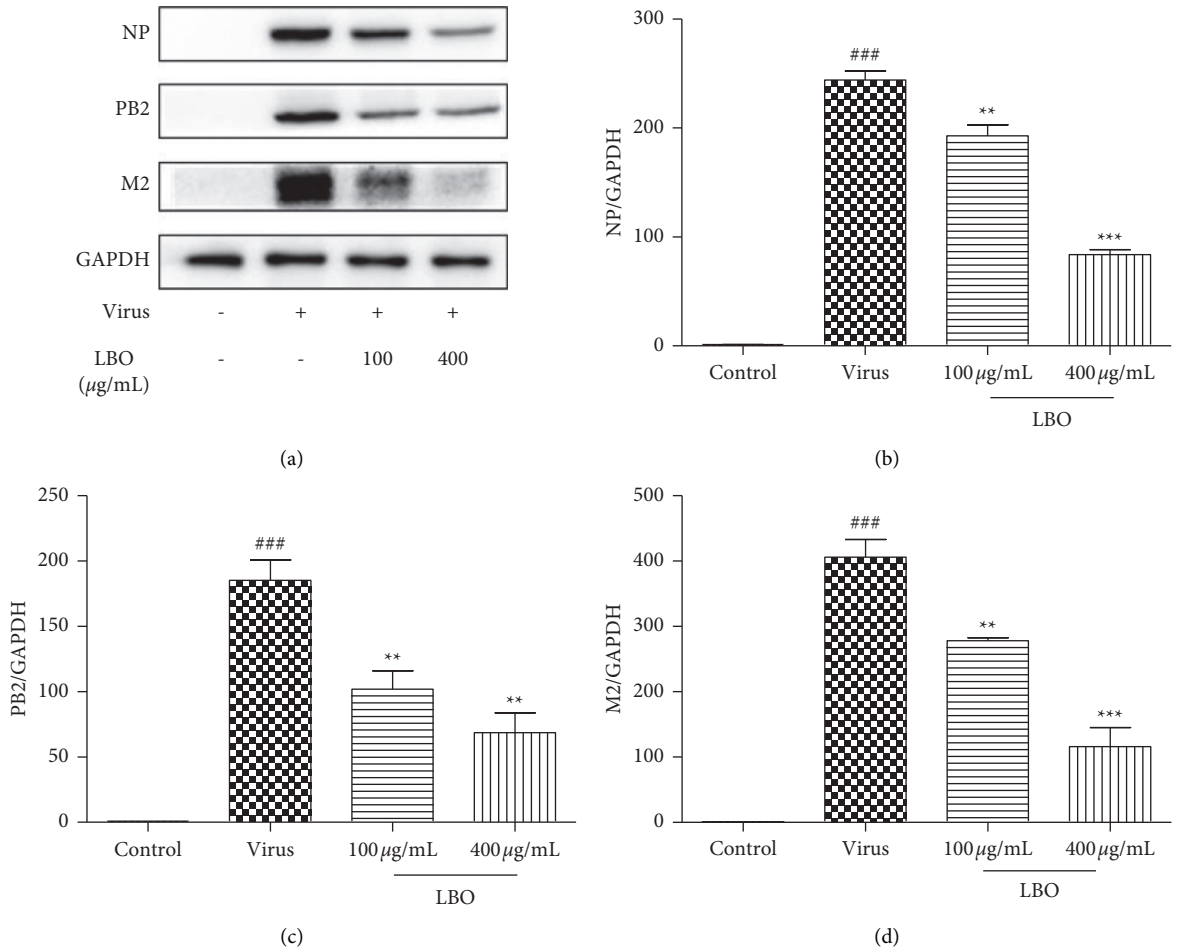

Figure 9: The influence of LBO on the levels of NP, PB2, and M2 in the lung tissue of IVA-infected mice. (a) Western blot result of NP, PB2, and M2. (b) Quantitative analysis of NP. (c) Quantitative analysis of PB2. (d) Quantitative analysis of M2. Compared with control group: $^{###}p < 0.001$; compared with virus group: $^{***}p < 0.001$, $^{**}p < 0.01$.

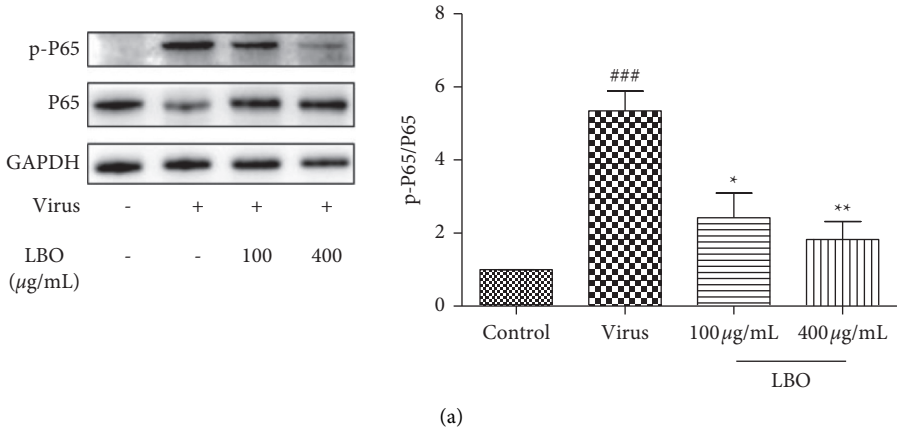

Figure 10: Continued.

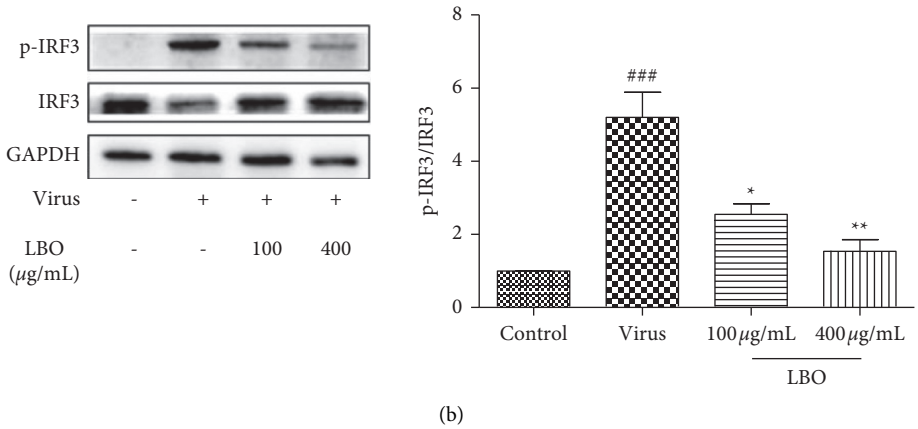

Figure 10: The influence of LBO on the levels of P65 and IRF3 in the lung tissue of IVA-infected mice. (a) The influence of LBO on the expression of P65. (b) The influence of LBO on the expression of IRF3. Compared with mock group: $^{###}p < 0.001$; compared with virus group: $^{***}p < 0.001$, $^{*}p < 0.05$.

response to acute influenza infection contribute to immune cell-mediated tissue damage [30, 31]. Interestingly, when it comes to the activation of IRF3 and transcription of IFN-β, host cells show different responses to different subtypes of IVA [32]. In this research, we found that influenza virus A/FM/1/47 (H1N1) infection and Poly I:C contribute to the activation of IRF3. Treatment with LBO blocked the activation of IRF3 and inhibited the expression of IFN-β.

The different concentrations of LBO were used in cell culture and animal study. The concentrations of LBO in the cell culture study were designed according to the cytotoxicity of LBO. The concentrations of LBO in the animal study were designed according to the results of cell culture study and our *in vivo* pre-experiment. Moreover, LBO exert more anti-inflammatory effects in MDCK cells compared to Poly I:C-stimulated A549 cells (Figures 4 and 5). The different anti-inflammatory effects of LBO in two models may result from the different systems.

The LBO is an essential oil-rich formula, the anti-influenza effects of which are considered to be contributed by the volatile components according to the TCM theory and modern researches [19, 33]. Oral administration of LBO is excluded considering about the traditional application and the great amount of volatile components. The administration of LBO was designed according to its clinical use, the inhalation of which could be used for the treatment of cough and sore throat. Inhalation with atomizer is employed by many researchers to investigate the essential oil related product [17, 20]. With the animal atomization device platform, we could control the dosage through the control of LBO concentration, device speed, and the treatment time.

In conclusion, the present study demonstrated that LBO could effectively prevent IVA infection both *in vitro* and *in vivo*. The anti-influenza effects of LBO may be attributed to the reduction of proinflammatory cytokines and the blocking of P65 and IRF3 activation. These findings suggest that LBO can be developed as an alternative therapeutic agent for influenza prevention.

Data Availability

All data generated or analyzed during this study are included in this published article.

Conflicts of Interest

The authors declare that they have no conflicts of interest.

Acknowledgments

This work was supported by the National Natural Science Foundation of China (82003815), PhD Start-up Fund of Natural Science Foundation of Guangdong Province (2017A030310602), and Medical Scientific Research Foundation of Guangdong Province (201610279833553).

Supplementary Materials

Table S1: the compositions of LBO. Table S2: the primer sequences. Figure S1: GC-MS and LC-MS chromatogram of reference substances. Figure S2: the influences of LBO on the influenza virus. (*Supplementary Materials*)

References

[1] P. Palese, "Influenza: old and new threats," *Nature Medicine*, vol. 10, no. 12, pp. S82–S87, 2004.

[2] R. Eccles, "Understanding the symptoms of the common cold and influenza," *The Lancet Infectious Diseases*, vol. 5, no. 11, pp. 718–725, 2005.

[3] P. R. Saunders-Hastings and D. Krewski, "Reviewing the history of pandemic influenza: understanding patterns of emergence and transmission," *Pathogens*, vol. 5, no. 4, Article ID 66, 2016.

[4] C. Fraser, C. A. Donnelly, S. Cauchemez et al., "Pandemic potential of a strain of influenza A (H1N1): early findings," *Science*, vol. 324, no. 5934, pp. 1557–1561, 2009.

[5] M. D. Van Kerkhove, K. A. Vandemaele, V. Shinde et al., "Risk factors for severe outcomes following 2009 influenza A

(H1N1) infection: a global pooled analysis," *PLoS Medicine*, vol. 8, no. 7, Article ID e1001053, 2011.

[6] L. Bai, Y. Zhao, J. Dong et al., "Coinfection with influenza a virus enhances SARS-CoV-2 infectivity," *Cell Research*, vol. 31, 2021.

[7] T. M. Uyeki, H. H. Bernstein, J. S. Bradley et al., "Clinical practice Guidelines by the infectious diseases society of America: 2018 update on diagnosis, treatment, chemoprophylaxis, and institutional outbreak management of seasonal influenzaa," *Clinical Infectious Diseases*, vol. 68, no. 6, pp. 895–902, 2019.

[8] N. J. Dharan, L. V. Gubareva, J. J. Meyer et al., "Infections with oseltamivir-resistant influenza A(H1N1) virus in the United States," *Journal of the American Medical Association*, vol. 301, no. 10, pp. 1034–1041, 2009.

[9] R. Le Goffic, J. Pothlichet, D. Vitour et al., "Cutting Edge: influenza A virus activates TLR3-dependent inflammatory and RIG-I-dependent antiviral responses in human lung epithelial cells," *The Journal of Immunology*, vol. 178, no. 6, pp. 3368–3372, 2007.

[10] A. Iwasaki and P. S. Pillai, "Innate immunity to influenza virus infection," *Nature Reviews Immunology*, vol. 14, no. 5, pp. 315–328, 2014.

[11] M. Matsumoto and T. Seya, "TLR3: interferon induction by double-stranded RNA including poly(I:C)☆," *Advanced Drug Delivery Reviews*, vol. 60, no. 7, pp. 805–812, 2008.

[12] I. Ramos and A. Fernandez-Sesma, "Modulating the innate immune response to influenza A virus: potential therapeutic use of anti-inflammatory drugs," *Frontiers in Immunology*, vol. 6, Article ID 361, 2015.

[13] L. M. Alleva, C. Cai, and I. A. Clark, "Using complementary and alternative medicines to target the host response during severe influenza," *Evidence-based Complementary and Alternative Medicine*, vol. 7, no. 4, pp. 501–510, 2010.

[14] L. Z. Sun and J. Liang, "[Modern enlightenment on aromatic drugs in the prevention and treatment of epidemic diseases in Ming and Qing dynasties]," *Zhonghua Zhongyiyao Zazhi*, vol. 30, no. 12, pp. 4007–4009, 2015.

[15] S. Wu, K. B. Patel, L. J. Booth et al., "Protective essential oil attenuates influenza virus infection: an *in vitro* study in MDCK cells," *BMC Complementary and Alternative Medicine*, vol. 10, Article ID 69, 2010.

[16] H. Wang, Q. Zhang, M. Ma et al., "Effect of the Miaoyao Fanggan sachet-derived isorhamnetin on TLR2/4 and NKp46 expression in mice," *Journal of Ethnopharmacology*, vol. 144, no. 1, pp. 138–144, 2012.

[17] Y. Li, Y. Lai, X. Li et al., "Therapeutic effect of Bingxiangsan essential oil on viral pneumonia induced by influenza virus," *Guangzhou University of Chinese Medicine*, vol. 27, no. 5, pp. 618–621, 2016.

[18] Q.-F. Wu, W. Wang, X.-Y. Dai et al., "Chemical compositions and anti-influenza activities of essential oils from *Mosla dianthera*," *Journal of Ethnopharmacology*, vol. 139, no. 2, pp. 668–671, 2012.

[19] S. Vimalanathan and J. Hudson, "Anti-influenza virus activity of essential oils and vapors," *American Journal of Essential Oils and Natural Products*, vol. 2, no. 1, pp. 47–53, 2014.

[20] K. Hayashi, N. Imanishi, Y. Kashiwayama et al., "Inhibitory effect of cinnamaldehyde, derived from *Cinnamomi cortex*, on the growth of influenza A/PR/8 virus *in vitro* and *in vivo*," *Antiviral Research*, vol. 74, no. 1, pp. 1–8, 2007.

[21] J. P. Dai, X. F. Zhao, J. Zeng et al., "Drug screening for autophagy inhibitors based on the dissociation of Beclin1-Bcl2 complex using BiFC technique and mechanism of eugenol on anti-influenza A virus activity," *PloS One*, vol. 8, no. 4, Article ID e61026, 2013.

[22] Y. Li, Y. Lai, Y. Wang, N. Liu, F. Zhang, and P. Xu, "1, 8-cineol protect against influenza-virus-induced pneumonia in mice," *Inflammation*, vol. 39, no. 4, pp. 1582–1593, 2016.

[23] S. Zhang, X. Chen, I. Devshilt et al., "Fennel main constituent, trans-anethole treatment against LPS-induced acute lung injury by regulation of Th17/Treg function," *Molecular Medicine Reports*, vol. 18, no. 2, pp. 1369–1376, 2018.

[24] Y. Ding, L. Zeng, R. Li et al., "The Chinese prescription lianhuaqingwen capsule exerts anti-influenza activity through the inhibition of viral propagation and impacts immune function," *BMC Complementary and Alternative Medicine*, vol. 17, no. 1, p. 130, 2017.

[25] H. Chen, C. Jie, L.-P. Tang et al., "New insights into the effects and mechanism of a classic traditional Chinese medicinal formula on influenza prevention," *Phytomedicine*, vol. 27, pp. 52–62, 2017.

[26] Q. Liu, Y.-H. Zhou, and Z.-Q. Yang, "The cytokine storm of severe influenza and development of immunomodulatory therapy," *Cellular and Molecular Immunology*, vol. 13, no. 1, pp. 3–10, 2016.

[27] E. Haasbach, S. J. Reiling, C. Ehrhardt et al., "The NF-kappaB inhibitor SC75741 protects mice against highly pathogenic avian influenza A virus," *Antiviral Research*, vol. 99, no. 3, pp. 336–344, 2013.

[28] F. Nimmerjahn, D. Dudziak, U. Dirmeier et al., "Active NF-κB signalling is a prerequisite for influenza virus infection," *Journal of General Virology*, vol. 85, no. 8, pp. 2347–2356, 2004.

[29] B. Hatesuer, H. T. T. Hoang, P. Riese et al., "Deletion of Irf3 and Irf7 genes in mice results in altered interferon pathway activation and granulocyte-dominated inflammatory responses to influenza A infection," *Journal of Innate Immunity*, vol. 9, no. 2, pp. 145–161, 2017.

[30] R.-L. Kuo, C. Zhao, M. Malur, and R. M. Krug, "Influenza A virus strains that circulate in humans differ in the ability of their NS1 proteins to block the activation of IRF3 and interferon-β transcription," *Virology*, vol. 408, no. 2, pp. 146–158, 2010.

[31] F. McNab, K. Mayer-Barber, A. Sher, A. Wack, and A. O'Garra, "Type I interferons in infectious disease," *Nature Reviews Immunology*, vol. 15, no. 2, pp. 87–103, 2015.

[32] S. Davidson, S. Crotta, T. M. McCabe et al., "Pathogenic potential of interferon $\alpha\beta$ in acute influenza infection," *Nature Communications*, vol. 5, Article ID 3864, 2014.

[33] W. N. Setzer, "Essential oils as complementary and alternative medicines for the treatment of influenza," *American Journal of Essential Oils and Natural Products*, vol. 4, no. 4, pp. 16–22, 2016.

Hindawi
Evidence-Based Complementary and Alternative Medicine
Volume 2021, Article ID 1696575, 8 pages
https://doi.org/10.1155/2021/1696575

Research Article

The Meridian Tropism and Classification of Red Yeast Rice Investigated by Monitoring Dermal Electrical Potential

Meng-Tian Wang,[1] Qiao-Juan He,[2] Jing-Ke Guo,[3] Shu-Tao Liu,[1] Li Ni,[4] Ping-Fan Rao,[2] Tian-Bao Chen,[5] Sheng-Bin Wu,[3] Shuai-Jun Zhao,[3] Jia-Hui Qiao,[3] Peng-Wei Zhang,[6] and Yu-Bo Li[7]

[1]*Institute of Biotechnology, Fuzhou University, Fuzhou 350002, Fujian, China*
[2]*School of Food Science and Biotechnology, Zhejiang Gongshang University, Hangzhou 310035, Zhejiang, China*
[3]*Department of Food and Biological Engineering, Zhicheng College, Fuzhou University, Fuzhou 350002, Fujian, China*
[4]*Institute of Food Science and Technology, Fuzhou University, Fuzhou 350108, Fujian, China*
[5]*Natural Drug Discovery Group, School of Pharmacy, Queen's University Belfast, Belfast BT9 7BL, Northern Ireland, UK*
[6]*Center for Preventive Treatment and Health Management, The Affiliated Hospital of Hangzhou Normal University, Hangzhou 310015, Zhejiang, China*
[7]*College of Information Science and Electronic Engineering, Zhejiang University, Hangzhou 310027, Zhejiang, China*

Correspondence should be addressed to Jing-Ke Guo; 2010021@qq.com and Shu-Tao Liu; stliu@fzu.edu.cn

Received 21 May 2021; Revised 20 July 2021; Accepted 14 August 2021; Published 21 August 2021

Academic Editor: Li Zhang

Copyright © 2021 Meng-Tian Wang et al. This is an open access article distributed under the Creative Commons Attribution License, which permits unrestricted use, distribution, and reproduction in any medium, provided the original work is properly cited.

Red yeast rice is a traditional Chinese medicine and food that has been purported to color food, ferment, and lower cholesterol. In order to study the antioxidative capacity of red yeast rice and the effects on electrical potential difference (EPD) of 12 acupuncture meridians, the pH value, oxidation reduction potential (ORP), ABTS, FRAP, T-SOD, and particle size distribution of red yeast rice were analyzed. 20 volunteers were recruited and randomly divided into two groups, the red yeast rice group (10 g red yeast rice and 40 g water) and control CK group (50 g water). The left 12 acupuncture meridians' EPD was real-time monitored. Samples were taken at the 10th minutes. The whole procedure continued for 70 minutes. It is shown that the pH value of the red yeast rice was 4.22, the ORP was 359.63 mV, the ABTS was 0.48 mmol Trolox, the FRAP was 0.08 mmol $FeSO_4$, the T-SOD was 4.71 U, and the average particle size was 108 nm (7.1%) and 398.1 nm (92.9%). The results of 12 acupuncture meridians' EPD showed that the red yeast rice can significantly affect the EPD of stomach, heart, small intestine, and liver meridians.

1. Introduction

As traditional Chinese medicinal material with dual functions of medicine and food, red yeast rice has been widely applied in food coloring, fermentation, cholesterol reduction, and other aspects [1]. In addition, the red yeast rice contains many bioactive substances, including multiple ketone isoflavones, plant sterols, and unsaturated fatty acids and [2]. The effect of red yeast rice cholesterol mainly comes from the monacolin K composition. It has a same kind of structure of the compound with lovastatin and contains anti-inflammatory and antioxidant activity of the material, such as sterol, dimer acid, and tannin [3].

Acupuncture meridians can be used as a reference index to observe the physiological effects of acupoint intervention and functional substances that can be used as medication and food [4, 5]. In traditional Chinese theories, meridian tropism refers to the selective therapeutic effects of a medication and food on a certain part of the body. A medication and food may elicit evident or specific therapeutic action on the pathological changes in one or several acupuncture meridians. Meridian tropism theory is most important because it has guided clinical practice for thousands of years in Eastern Asia [6]. In recent years, the explanation of meridian tropism theory by modern scientific techniques would facilitate the understanding and application of traditional Chinese medicine. The urinary

excretion rate, loss in weight of rats, and the electrolyte levels in the plasma were measured in order to study the meridian tropism for Tinglizi (*Semen Lepidii Apetali*), Yiyiren (*Semen Coicis*), and Cheqianzi (*Semen Plantaginis*) [7]. The relationship between the modified Wuzi Yanzong prescription and meridian tropism was studied according to the tissue distributions of the metabolites, mainly flavanoid compounds in rats [8]. The distribution of tryptanthrin in rat tissues, following oral administration at a dose of 100 mg/kg, was studied in order to characterize the relationship with meridian tropism of indigo naturalis [9]. The dermal acupuncture meridian electrical potential difference (EPD) also can be real-time monitored to observe and compare various medications' and foods' meridian tropism, for volunteers' acupoint antioxidant intervention [10, 11] and taking medicine and food functional materials, such as *Cordyceps militaris* [12], *Inonotus obliquus* (Fr.) Pilat [13], *Dendrobium officinale* Kimura et Migo [14], herbal drink [15], tea [16, 17], and so on.

Therefore, in order to study the antioxidative capacity of red yeast rice and the effects on EPD of 12 acupuncture meridians (the meridian tropism of red yeast rice), the pH value, oxidation reduction potential (ORP), ABTS, FRAP, T-SOD, and particle size distribution of red yeast rice were analyzed and the left 12 acupuncture meridians EPD were real-time monitored. This study mainly conducted physical and chemical analysis of red yeast rice in vitro and found that the EPD of 12 acupuncture meridians changed differently after volunteers took red yeast rice to provide a new idea for the application and development of red yeast rice.

2. Materials and Methods

2.1. Materials. Red yeast rice (Fujian screen red Bio Technology Co., Ltd., China); the total antioxidant capacity detection kit (ABTS method) (Shanghai beyotime Biotechnology Co., Ltd., China, Batch No. 092518190324); the total antioxidant capacity detection kit (FRAP method) (Shanghai beyotime Biotechnology Co., Ltd., China, Batch No. 1113118190524); and superoxide dismutase (T-SOD) assay kits (Nanjing Jiancheng Bioengineering Institute, China, Batch No. 20190511) were used.

A CS-700 Y crusher (Wuyi Haina Electric Appliance Co., Ltd., China); pH meter (American EUTECH company, US); ORP (Oxidation Reduction Potential) Analyzers (ORP electrode InLab Redox, Mettler Toledo Instrument Shanghai Co., Ltd., China); CF 15 RX II high-speed centrifuge (HITACHI, Japan); Zetasizer Nano laser particle size analyzer (Malvern Instrument Co., Ltd., UK); NH-4 digital display electronic constant temperature water bath (Jiangsu Guohua Electric Appliance Co., Ltd., China); KQ 5200E type ultrasonic cleaner (Kunshan Ultrasonic Instrument Co., Ltd., China); UV-1700 UV spectrophotometer (Tsujima Corporation, Japan); FlexStation 3 Microplate Reader (Molecular Devices, Inc., US); Ag/AgCl disposable electrocardiogram (ECG) electrode (Shanghai Junkang Medical Equipment Co., Ltd., China); and RM 6240C Multi-channel Physiological Signal Acquisition and Processing System (Chengdu Instrument Factory, China) were used.

2.2. Human Subjects. This study was performed with central enrollment and allocation by the SIBS.CAS-Zhejiang Gongshang University Joint Centre for Food and Nutrition Research (research center). 20 healthy volunteers who met the inclusion criteria were recruited and screened as experimental subjects from October 2018 to July 2019. All volunteers signed the informed consent voluntarily under the condition that they could fully accept the experimental scheme. This experiment was approved by the Ethics Committee of the SIBS.CAS-Zhejiang Gongshang University Joint Centre for Food and Nutrition Research (31500685-3).

(i) Inclusion criteria: (1) age: >18 years, regardless of gender; (2) voluntarily signing the informed consent; (3) not taking breakfast before the test; and (4) keeping regular diet and rest.

(ii) Exclusion criteria: (1) having kidney, liver, and cardiovascular disease or other serious diseases; (2) having bad habits, such as smoking, drinking, and drug abuse; (3) long-term drug treatment; (4) taking breakfast before the test; and (5) pregnant women and those with hyperactivity of fire due to yin deficiency.

2.3. Randomization. A computer-generated random number was assigned to each participant. Volunteers were randomly divided into two groups: the red yeast rice group (10 g red yeast rice and 40 g water) and the control CK group (50 g water), with the ratio of 1 : 1. The investigator had no clinical involvement in the trial.

2.4. Treatment Protocol. After the recruitment of volunteers was completed, it was uniformly stipulated that they should complete the monitoring in the morning from 8 : 30 am to 10 : 30 am. The changes of EPD were observed before and after the volunteers took the sample. This was repeated three times, with each time interval of more than 7 days. The volunteers were conscious, placed in a supine position, and asked to breathe calmly. The acupoints were localized according to World Health Organization standard acupoint locations in the Western Pacific Region [18]. The Source-Sea (Yuan-He) acupoint pairs of the 12 meridians on the left were selected as the measurement points of the meridian EPD, with the Sea acupoints (proximal) as the positive pole and the Source acupoints (distal) as the negative pole, respectively (Table 1) [10]. The hair on the selected detection acupoints was trimmed. After previously disinfected with medical alcohol, the acupoints were connected to a digital potentiometer via Ag/AgCl disposable ECG electrodes and the EPD of 12 meridians of volunteers was monitored in real time. When monitoring to 10 minutes, the prepared red yeast rice or water should be taken, and it should be taken within 5 min. A total of 70 min was monitored before and after the administration.

2.5. Sample Preparation. Weighing about 18 g of red yeast rice and grinding it several times with a grinder, the red yeast

Table 1: Acupuncture point selection of acupuncture meridians.

Meridian	Sea (He) acupoints	Source (Yuan) acupoints
Lung meridian	Chize LU5	Taiyuan LU9
Large intestine meridian	Quchi LI11	Hegu LI14
Stomach meridian	Zusanli ST36	Chongyang ST42
Spleen meridian	Yinlingquan SP9	Taibai SP3
Heart meridian	Shaohai HT3	Shenmen HT7
Small intestine meridian	Xiaohai SI8	Wangu SI4
Bladder meridian	Weizhong BL40	Jinggu BL64
Kidney meridian	Yingu KI10	Taixi KI3
Pericardium meridian	Quze PC3	Daling PC7
Triple energizer meridian	Tianjing TE10	Yangchi TE4
Gallbladder meridian	Yanglingquan GB34	Qiuxu GB40
Liver meridian	Ququan LR8	Taichong LR3

rice powder was obtained. After 60 mesh sieves, 10 g of it was accurately weighed and dissolved in 40 g of distilled water. The mixture was ultrasonized for 20 min and extracted by using a water bath thermostatic agitator for 1 hour at 37°C and 700 r/min and centrifuged at 25°C for 5000 r/min for 15 min; the supernatant was taken as the sample to be tested and stored in a refrigerator at −20°C for later use.

2.6. Determination of pH Value. The sample should be calibrated with a standard solution before testing. After calibration, the electrode is completely passed over the sample to be tested. When the data are stable, the reading is recorded, and the measurement is repeated three times to take the average value.

2.7. Determination of REDOX Potential (ORP). An appropriate amount of the sample was placed in a beaker for determination. The sample was immersed in the electrode, and the determination was repeated three times to take the average value and the determination time should not exceed 3 min.

2.8. Antioxidant Activity Determination. The total antioxidant capacity (ABTS and FRAP) and SOD activity of samples were analyzed with colorimetric assay kits (Shanghai beyotime Biotechnology Co., Ltd., China, and Nanjing Jiancheng Bioengineering Institute, China).

2.9. Particle Size Distribution Determination. Red yeast rice solution was detected using a Zetasizer Nano particle size tester. 1 mL sample was taken and placed in the detection dish. The relevant parameters of the instrument were set as temperature 25°C, scattering angle 173°, and preheating time 2 min, and each cycle was scanned 3 times.

2.10. Statistical Analysis. The study design called for at least 20 healthy subjects. Sample size estimations were not performed. Because of the complex design of this pilot study, sample size was chosen on the basis of practical considerations. Therefore, this study was not designed to have sufficient power, and the results of statistical testing have to be interpreted as descriptive, explorative, and hypothesis generating rather than as confirmatory. Data are reported as means ± standard deviation. The statistical analysis was performed with IBM SPSS Statistics 22. Results in patients and healthy subjects were compared using the two-sample t-test.

3. Results

3.1. Influence of Red Yeast Rice on Meridian EPD. We screened 20 healthy volunteers into the study. All of them completed the study. The study flow is presented in Figure 1.

In this study, after volunteers took red yeast rice or water, the EPD of 12 meridians on the left side of volunteers was monitored in real time for 70 min. The results are shown in Figures 2–4. The EPD changes of the control CK group are relatively gentle, and the fluctuation range is within 10 mV. Red yeast rice had obvious effects on the EPD of stomach, heart, small intestine, and liver meridians. After the administration of red yeast rice, the fluctuation range of the meridian EPD of the volunteers exceeded 10 mV, the peaks of the stomach, small intestine, and liver meridians all appeared at 40–50 min, and the peaks of the heart meridians appeared at 50–70 min, as shown in Figure 1. For the lung meridian and pericardium meridian, the fluctuation range of the meridian EPD of the volunteers was about 10 mV (Figure 2).

The EPD fluctuation of the meridians of the large intestine, spleen, bladder, kidney, triple energizer, and gallbladder of volunteers in the red yeast rice group is not different from that in the control CK group, as shown in Figure 3.

3.2. Antioxidant Activity of Red Yeast Rice and Distilled Water. The pH value, REDOX potential value (ORP), ABTS, FRAP, and T-SOD of red yeast rice and distilled water were determined as shown in Table 2. Distilled water, as a solvent, has a certain REDOX potential value [19]. When the REDOX potential value of red yeast rice is lower than that of distilled water, it indicates that red yeast rice presents reductivity.

3.3. Particle Size Distribution of Red Yeast Rice. The average particle size of red yeast rice soup was 108 nm (7.1%) and 398.1 nm (92.9%), respectively.

4. Discussion

In our studies of reactive oxygen species (ROS) distribution in living animals by ROS indicator visualization, a few vertical fluorescent lines were demonstrated on the body. They could be almost perfectly superimposed on a standard human acupuncture meridian network [20, 21]. ROS has a strong connection with REDOX potential (ORP) and antioxidant activity. Moreover, topical application of antioxidants to acupoints was found to result in an

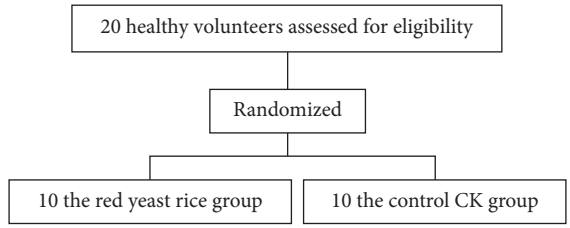

Figure 1: Study flow chart.

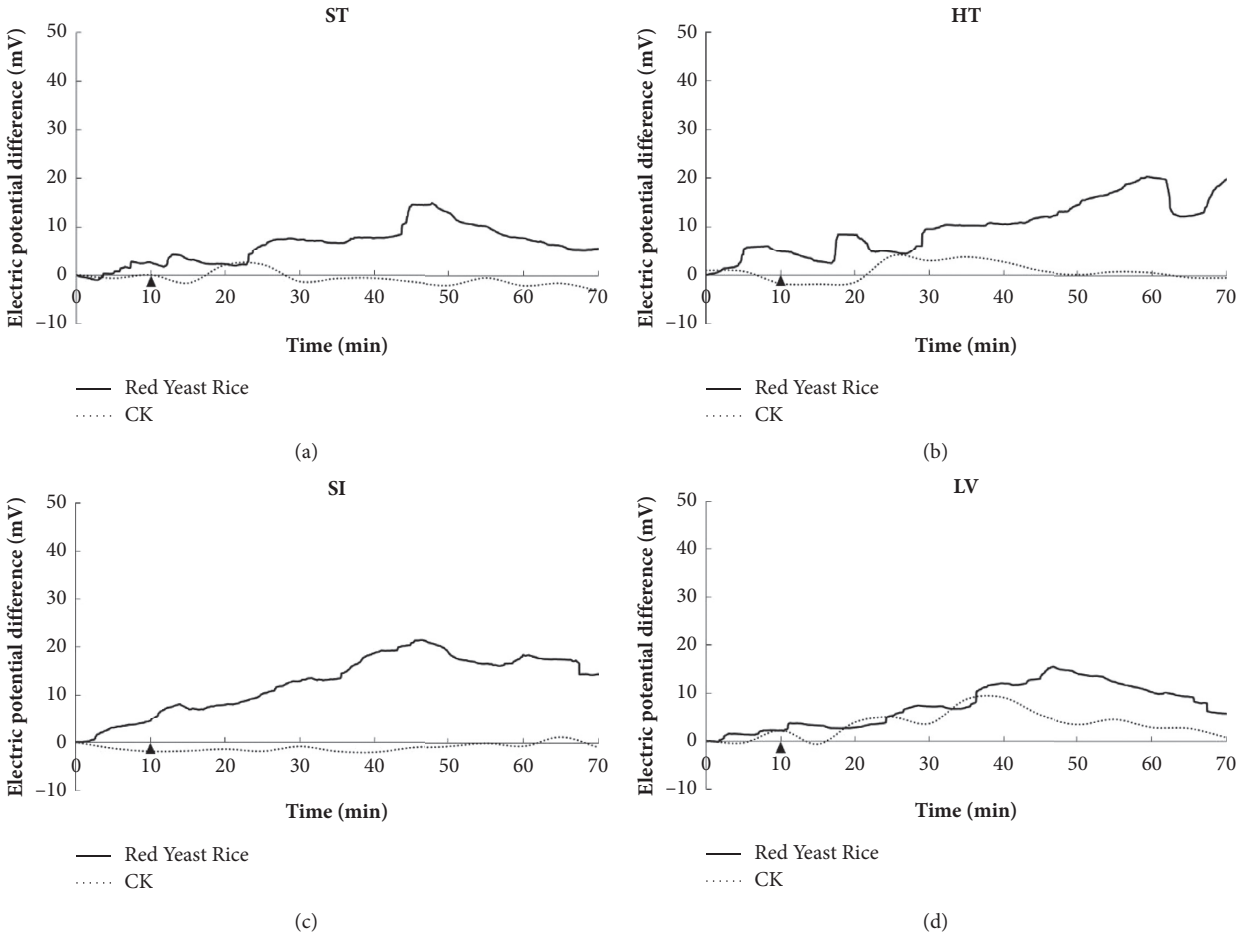

Figure 2: Electric potential difference of the stomach meridian (a), heart meridian (b), small intestine meridian (c), and liver meridian (d).

acupuncture-like action [10, 11, 22, 23]. All those results point to a new applaudable hypothesis of meridians as channels of ROS and ROS modulation along meridians as the acupuncture mechanism.

Although in Table 2, the results of antioxidant activity of red yeast rice in vitro show weak acidity (pH = 4.22 ± 0.19, high H^+ solubility, and partial oxidation), its overall REDOX potential was lower than that of distilled water and showed high reductivity. The results of ABTS, FRAP, and T-SOD all showed that red yeast rice had antioxidant activity. The particle size distribution of red yeast rice soup was determined. The particle size distribution was mainly divided into two components. The main component was 398.1 nm (92.9%), followed by 108 nm (7.1%). The active ingredients isolated from *Semen Armeniacae Amarum* with particle size less than 200 nm had strong biological activity [24]. In addition, enzymatically active nanoparticles of Cu/Zn SOD were simultaneously generated during the reaction, with an average particle size of 175.86 ± 0.71 nm [25]. The nanoparticles isolated from sun-dried *Isatis indigotica* Fort. root decoction were also about 120 nm [26]. The nanoparticles less than 200 nm can enter the macrophages, significantly reduce the oxidative stress level of cells, and show the strong oxidation resistance [27], with the effect of detoxification [28].

When substances with antioxidant activity are introduced into the human body, they will cause changes in the

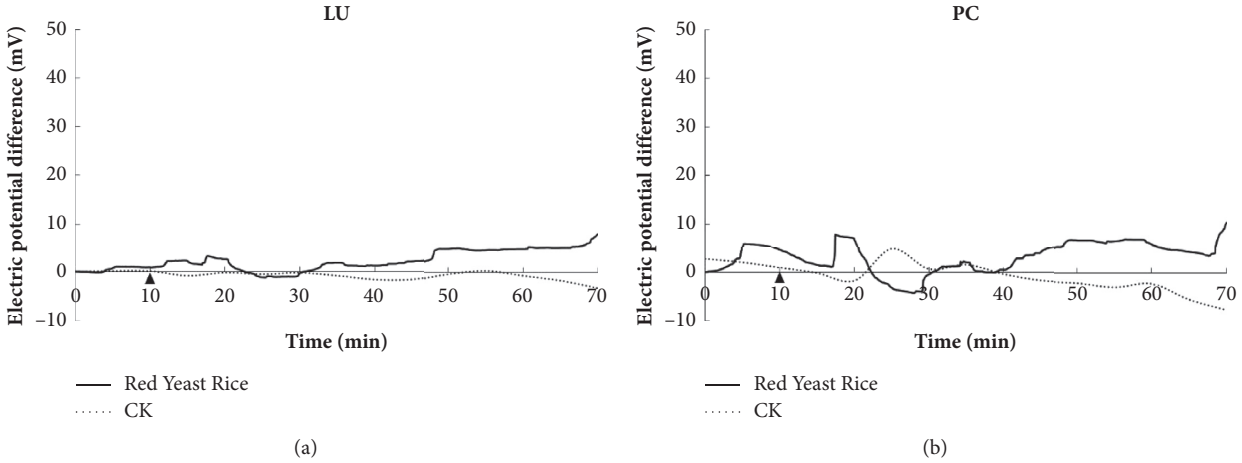

Figure 3: Electric potential difference of the lung meridian (a) and pericardium meridian (b).

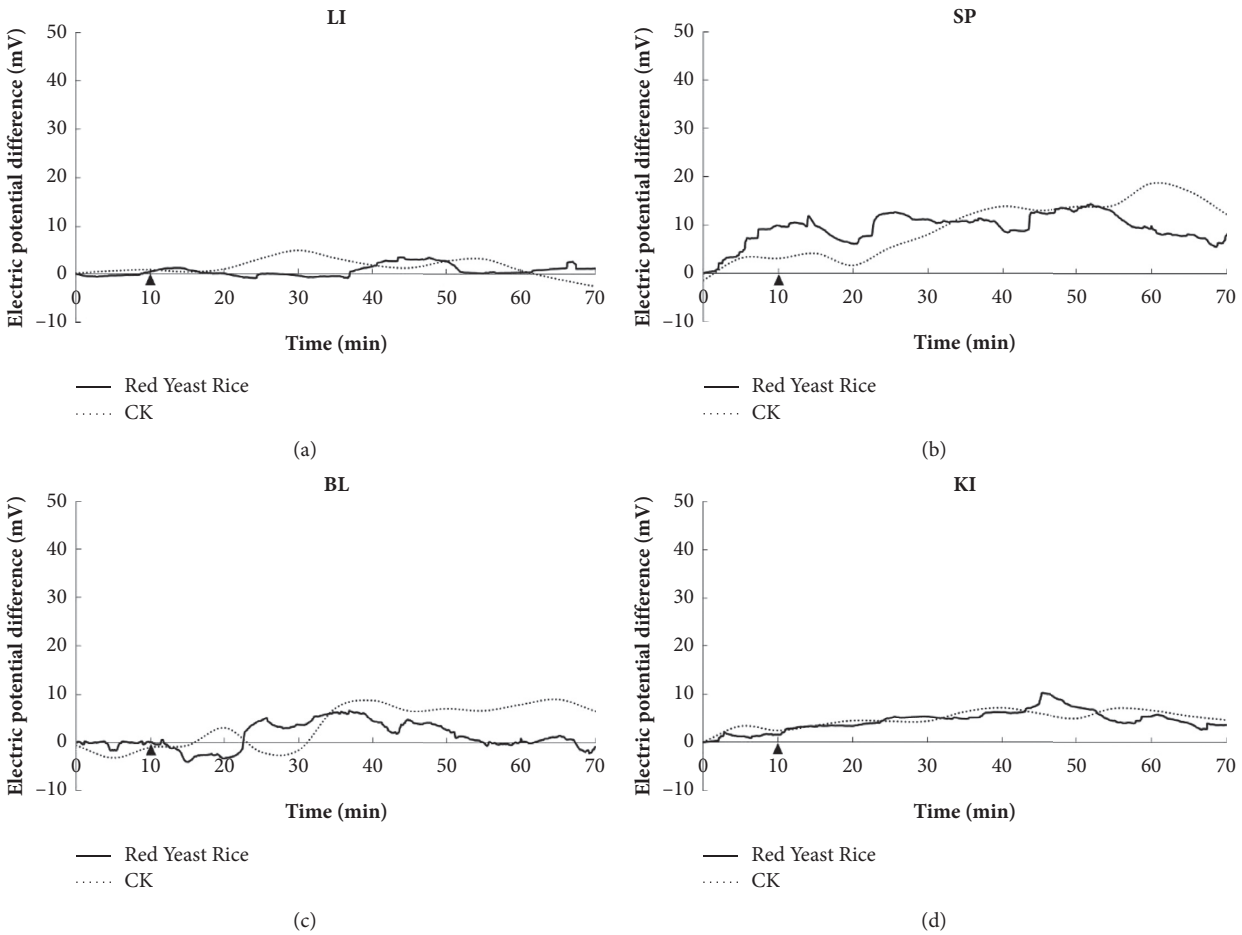

Figure 4: Continued.

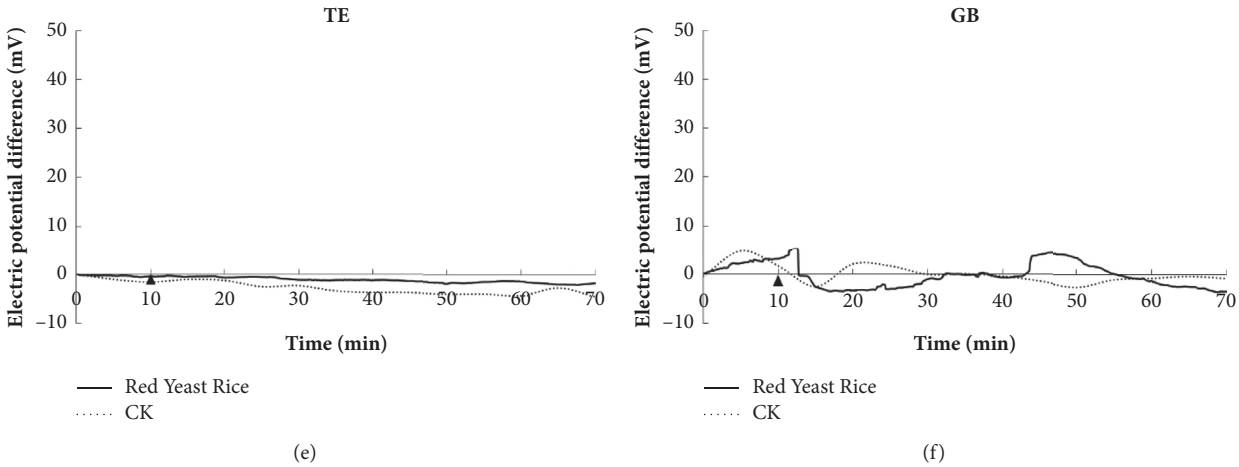

Figure 4: Electric potential difference of the large intestine meridian (a), spleen meridian (b), bladder meridian (c), kidney meridian (d), triple energizer meridian (e), and gallbladder meridian (f).

Table 2: Antioxidant activity of red yeast rice and distilled water.

Determination method	Red yeast rice	Distilled water
PH	$4.22 \pm 0.19^{**}$	7.01 ± 0.01
Redox potential (mV)	$359.63 \pm 6.68^{**}$	512.70 ± 9.36
ABTS (equal to the amount of Trolox standard solution substance) (mmol)	$0.48 \pm 0.11^{**}$	0.02 ± 0.00
FRAP (amount of $FeSO_4$ standard solution substance) (mmol)	$0.080 \pm 0.004^{**}$	0.01 ± 0.00
T-SOD (U)	$4.71 \pm 0.19^{**}$	0.09 ± 0.00

Note: compared with distilled water, $^{*}P < 0.05$, $^{**}P < 0.01$. $n = 5$.

content of some free radicals to give full play to their antioxidant effect, thus causing changes in the meridian EPD value [10–17]. Compared with other acupoints, the EPD signal-to-noise ratio between the 12 meridians on the left side of the Source-Sea (Yuan-He) acupoint is higher and suitable for monitoring [10]. The administration of red yeast rice can cause significant changes in the meridians of the stomach, heart, small intestine, and liver, mild and moderate in the lung meridian and pericardium meridian, but has no obvious effect on the others. Medical scientists in the past dynasties summarized the natural taste and meridian tropism of red yeast rice, concluding that it has sweet taste, smooth nature, and nontoxic. The meridian tropism of red yeast rice is the meridian of the large intestine, spleen, and liver [29]. Modern pharmacology has shown that red yeast rice exerts potential protective effects on the liver, pancreas, blood vessels, and intestines [2], which matches the functions to the meridians of the liver, stomach, heart, and small intestine, respectively. Therefore, the results of this study have reference significance for the treatment of diseases related to stomach, heart, and small intestine meridians by red yeast rice beyond the meridian of the large intestine, spleen, and liver [29].

The meridian orientation of traditional Chinese medicine refers to the selective effect of traditional Chinese medicine on different organs and the specificity of traditional Chinese medicine on meridians based on the theory of meridians [6–9]. The meridian tropism has been proved to be effective in guiding clinical practice, but other than the scientifically mysterious bioenergy or *Qi* concept, there is hardly any clue to what exactly happens immediately after a medication and could be observed precisely. It is still difficult to determine how red yeast rice selectively influences the electrical properties of particular meridians; however, this study attempts to explore the physiological effects of red yeast rice on the human body by monitoring the meridian EPD, so as to provide new ideas for the analysis of the specificity of red yeast rice on the meridian, the application, and development of red yeast rice.

5. Conclusions

In this study, the pH value of the red yeast rice was 4.22, the ORP was 359.63 mV, the ABTS was 0.48 mmol Trolox, the FRAP was 0.08 mmol $FeSO_4$, the T-SOD was 4.71 U, and the average particle size was 108 nm (7.1%) and 398.1 nm (92.9%). The results of 12 acupuncture meridians EPD showed that the red yeast rice can significantly affect the EPD of stomach, heart, small intestine, and liver meridians.

Data Availability

The data that support the findings of this study are openly available in Mendeley Data at https://dxdoi.org/10.17632/txc5g64t6s.1.

Conflicts of Interest

The authors declare no conflicts of interest regarding the publication of this paper.

Acknowledgments

This research was supported by the National Natural Science Foundation of China (31500685); Zhejiang Provincial Natural Science Foundation of China (LY16C050002); Zhejiang University Rockchip United Technologies Center Foundation (ZD20190052); Education Research Project for Young and Middle-Aged Teachers in Fujian Province of China (JAT200947); and Fujian Provincial Innovative Training Programme for College Students (S202013470027 and S202013470029).

References

[1] J. Song, J. Luo, Z. Ma et al., "Quality and authenticity control of functional red yeast rice-a review," *Molecules*, vol. 24, no. 10, p. 1944, 2019.

[2] J. Hu, J. Wang, Q.-X. Gan et al., "Impact of red yeast rice on metabolic diseases: a review of possible mechanisms of action," *Journal of Agricultural and Food Chemistry*, vol. 68, no. 39, pp. 10441–10455, 2020.

[3] Z. Xiong, X. Cao, Q. Wen et al., "An overview of the bioactivity of monacolin K/lovastatin," *Food and Chemical Toxicology*, vol. 131, Article ID 110585, 2019.

[4] L. R. Gomes and P. Leão, "Recent approaches on signal transduction and transmission in acupuncture: a biophysical overview for medical sciences," *Journal of Acupuncture and Meridian Studies*, vol. 13, no. 1, pp. 1–11, 2020.

[5] H. Zhang, G. Han, and G. Litscher, "Traditional acupuncture meets modern nanotechnology: opportunities and perspectives," *Evidence-Based Complementary and Alternative Medicine*, vol. 2019, Article ID 2146167, 2019.

[6] P. Liu, S. Liu, G. Chen, and P. Wang, "Understanding channel tropism in traditional Chinese medicine in the context of systems biology," *Frontiers of Medicine*, vol. 7, no. 3, pp. 277–279, 2013.

[7] M. Zeng, M. Li, L. Zhang et al., "Different meridian tropism in three Chinese medicines: Tinglizi (*Semen Lepidii Apetali*), Yiyiren (*Semen Coicis*), Cheqianzi (*Semen Plantaginis*)," *Journal of traditional Chinese medicine = Chung I Tsa Chih Ying Wen Pan*, vol. 39, no. 2, pp. 213–220, 2019.

[8] L.-L. Wang, W.-W. Li, C.-S. Wu et al., "Relationship between tissue distributions of modified Wuzi Yanzong prescription (加味五子衍宗方) in rats and meridian tropism theory," *Chinese Journal of Integrative Medicine*, vol. 24, no. 2, pp. 117–124, 2018.

[9] N. Zhang, Y. Hua, C. Wang et al., "Distribution study of tryptanthrin in rat tissues by HPLC and its relationship with meridian tropism of indigo naturalis in traditional Chinese medicine," *Biomedical Chromatography*, vol. 28, no. 12, pp. 1701–1706, 2014.

[10] J.-K. Guo, J.-S. Xu, T.-B. Chen et al., "Effects of TAT-SOD at acupoints on essential hypertension by monitoring meridians electrical potential," *Chinese Journal of Integrative Medicine*, vol. 26, no. 9, pp. 694–700, 2020.

[11] M. M. Xu, J. K. Guo, J. S. Xu et al., "Monitoring the effects of acupoint antioxidant intervention by measuring electrical potential difference along the meridian," *Evidence-Based Complementary and Alternative Medicine*, vol. 2015, Article ID 286989, 2015.

[12] P. Rao, H. Chen, H. Zhou et al., "Studies on anti-oxidative capacity, thermal stability and its channel tropism of cordyceps militaris," *Journal of Chinese Institute of Food Science and Technology*, vol. 20, no. 7, pp. 59–64, 2020.

[13] P. Rao, Q. Chen, H. Zhou et al., "Preliminary study on the antioxidant capacity of water extracts derived from *Inonotus obliquus* (Fr.) Pilat and its effect on human meridian voltage," *Journal of Chinese Institute of Food Science and Technology*, vol. 20, no. 6, pp. 88–94, 2020.

[14] S. Yan, J. Guo, M. Xu et al., "Study on the antioxidant activity of Dendrobium officinale Kimura et Migo and its different effects on Zang-Fu organs channel tropism," *Chinese Journal of Integrated Traditional and Western Medicine*, vol. 41, no. 1, pp. 41–45, 2021.

[15] W. Lu, J. Guo, J. Zhou et al., "Hypothesis review: the direct interaction of food nanoparticles with the lymphatic system," *Food Science and Human Wellness*, vol. 1, no. 1, pp. 61–64, 2012.

[16] M. Xu, J. Guo, L. Ni et al., "The effect of infusions of tea soup on electrical potential difference along the meridian," *Journal of Chinese Institute of Food Science and Technology*, vol. 18, no. 11, pp. 27–33, 2018.

[17] Q. Chen, J. Guo, M. Xu et al., "Anti-oxidative analysis of lapsang tea infusion, tea polyphenols, tea polysaccharides and its electrophysiological acupuncture meridian signals," *Journal of Chinese Institute of Food Science and Technology*, vol. 20, no. 10, pp. 43–49, 2020.

[18] World Health Organization Regional Office for the Western Pacific, *WHO Standard Acupuncture Point Locations in the Western Pacific Region*, World Health Organization, Geneva, Switzerland, 2008.

[19] Ż. Król-Kilińska, D. Kulig, I. Yelkin, A. Zimoch-Korzycka, Ł. Bobak, and A. Jarmoluk, "The effect of using micro-clustered water as a polymer medium," *International Journal of Molecular Sciences*, vol. 22, no. 9, p. 4730, 2021.

[20] J. Guo, S. Liu, X. Cheng et al., "Revealing acupuncture meridian-like system by reactive oxygen species visualization," *Bioscience Hypotheses*, vol. 2, no. 6, pp. 443–445, 2009.

[21] J. Guo, H. Xu, S. Liu et al., "Visualising reactive oxygen species in live mammals and revealing of ROS-related system," *Free Radical Research*, vol. 53, no. 11-12, pp. 1073–1083, 2019.

[22] J. Guo, Y. Chen, B. Yuan, S. Liu, and P. Rao, "Effects of intracellular superoxide removal at acupoints with TAT-SOD on obesity," *Free Radical Biology and Medicine*, vol. 51, no. 12, pp. 2185–2189, 2011.

[23] J. K. Guo, M. M. Xu, M. F. Zheng et al., "Topical application of TAT-superoxide dismutase in acupoints LI 20 on allergic rhinitis," *Evidence-Based Complementary and Alternative Medicine*, vol. 2016, Article ID 28119757, 2016.

[24] D. Lin, W. Lin, G. Gao et al., "Purification and characterization of the major protein isolated from *Semen Armeniacae Amarum* and the properties of its thermally induced nanoparticles," *International Journal of Biological Macromolecules*, vol. 159, pp. 850–858, 2020.

[25] L. Cai, C. Lin, N. Yang et al., "Preparation and characterization of nanoparticles made from co-incubation of SOD and glucose," *Nanomaterials (Basel)*, vol. 7, no. 12, p. 458, 2017.

[26] J. Zhou, J. Liu, D. Lin et al., "Boiling-induced nanoparticles and their constitutive proteins from *Isatis indigotica* Fort. root decoction: purification and identification," *Journal of Traditional and Complementary Medicine*, vol. 7, no. 2, pp. 178–187, 2017.

[27] L. Ke, H. Wang, G. Gao et al., "Direct interaction of food derived colloidal micro/nano-particles with oral macrophages," *NPJ Science of Food*, vol. 1, p. 3, 2017.

[28] L. J. Ke, G. Z. Gao, Y. Shen, J. W. Zhou, and P. F. Rao, "Encapsulation of aconitine in self-assembled licorice protein nanoparticles reduces the toxicity in vivo," *Nanoscale Research Letters*, vol. 10, no. 1, p. 449, 2015.

[29] B. Zhu, F. Qi, J. Wu et al., "Red yeast rice: a systematic review of the traditional uses, chemistry, pharmacology, and quality control of an important Chinese folk medicine," *Frontiers in Pharmacology*, vol. 10, p. 1449, 2019.

Hindawi
Evidence-Based Complementary and Alternative Medicine
Volume 2021, Article ID 9902211, 13 pages
https://doi.org/10.1155/2021/9902211

Research Article

Improvement of Presbyopia Using a Mixture of Traditional Chinese Herbal Medicines, Including Cassiae Semen, Wolfberry, and *Dendrobium huoshanense*

Chi-Ting Horng,[1,2] **Jui-Wen Ma**,[3] **and Po-Chuen Shieh**[2]

[1]*Department of Ophthalmology, Fooying University Hospital, Pintung 928, Taiwan*
[2]*Department of Pharmacy, Tajen University, Pingtung 907, Taiwan*
[3]*Unique Biotechnology Co., Ltd., Koahsiung 800, Taiwan*

Correspondence should be addressed to Chi-Ting Horng; h56041@gmail.com

Received 7 June 2021; Revised 29 June 2021; Accepted 21 July 2021; Published 27 July 2021

Academic Editor: Xiaolong Ji

Copyright © 2021 Chi-Ting Horng et al. This is an open access article distributed under the Creative Commons Attribution License, which permits unrestricted use, distribution, and reproduction in any medium, provided the original work is properly cited.

Background. Presbyopia is a primary cause of a decline in near vision. In this study, we developed a new mixed herbal medicine to retard presbyopic progression and increase the amplitude of accommodation (AA), which is beneficial for near vision. *Methods*. A total of 400 participants between the ages of 45 and 70 years were recruited. We designed the mixed herbal drug to include Cassiae Semen (200 mg), wolfberry (200 mg), and *Dendrobium huoshanense* (DD) (40 mg) in one capsule. In experiment 1, the recruited subjects were directed to perform a push-up test to measure their AA; this was then converted to the additional diopters of reading glasses. In experiment 2, 240 subjects took three capsules daily for six months and then stopped medical therapy for a six-month follow-up. In experiment 3, 160 subjects were randomly categorized into four groups: a placebo group, low-dose group (LDG) (1 capsule daily), middle-dose group (MDG) (two capsules daily), and high-dose group (HDG) (three capsules daily). The 160 volunteers took different doses for six months and then stopped treatment, accompanied by another six-month follow-up. In experiments 2 and 3, the change in AA, uncorrected far visual acuity (UFVA), and uncorrected near visual acuity (UNVA) were recorded each month for one year. *Results*. In experiment 1, AA was found to decrease with age and a great deal of additional power was needed in older individuals. In experiment 2, the mean AA reached a maximum value of 2.1D ($P < 0.05$) after six months, while the UNVA improved by about two to three lines of a Jaeger chart in most of the subjects. At nine months, all the means decreased slightly to 2.0 D ($P < 0.05$). This meant that the mixed herbal medicine could still maintain AA for another three months because the herbal therapy was stopped at the seventh month. In experiment 3, the maximal AA was 2.8D, 2.9D, and 3.2D ($P < 0.05$) in the LDG, MDG, and HDG after six-month treatments, respectively. Experiment 3 showed that AA gain occurred in a dose-dependent manner; the higher the dose, the greater the AA value. *Conclusion*. Only two studies on the use of herbal drugs for presbyopia have been reported in PubMed. In our study, we found that taking a mixed herbal drug caused an excellent gain in AA. This is the first study to report that the characteristics of the new herbal regimen could retard and even ameliorate presbyopia.

1. Background

The prevalence of presbyopia in the population is gradually growing worldwide. Its prevalence was estimated to be at 1.7–2.0 billion people globally in 2015. A total of 826 million of those affected do not have sufficient vision correction. In China, ≥12% of patients with vision impairment are a result of uncorrected presbyopia [1]. Presbyopia typically affects people from the 4th decade of life; however, accommodation to it decreases with age, with it nearly finishing after age fifty and impacting almost 100% of people over the age of 65. It is worth noting that, in recent years, the overuse of smartphones and portable computers has led to the rapid progression and onset of presbyopia (around 35 years). The mechanisms of accommodation depend on the contraction of the ciliary muscle and iris; changes in the shape of the lens

and convergence can show a variation in dioptric powers to enable people to see or work easily at near distances [2].

When people gaze at objects intently, the accommodation initiates a series of actions. Accommodation is the ability of the eye to change focus, and the amplitude of accommodation (AA) is the maximum potential increase in diopter that an eye can achieve in adjusting its focus. The accommodative system is controlled by acetylcholine (Ach) from the parasympathetic nerves. The change in biometry that diopters exert and increasing lenticular stiffness are responsible for presbyopia. AA should be measured corresponding to the acuity at the viewing distance. When a human wants to see objects about 40 cm in front of the eyes and the accommodation is functional, the ciliary muscles began to contract, anchor at the scleral spur, and the trabecular meshwork with peripheral cornea comes forward. Lastly, the thickness of the lens increases, and the person is able to view nearby objects. Presbyopia is a physiologic inevitability and aging is the primary etiology. With the development of society, the overuse of portable computers and smartphones has become an important cause of presbyopia [3, 4]. Geographic and sex factors have also been reported [5, 6]. In general, presbyopia manifests at 40–45 years of age due to the gradual loss of accommodation, necessitating the extra-additional (Add) power of reading spectacles. AA generally decreases at a rate of 0.3 D per year. The symptoms of presbyopia usually occur when the AA value decreases to below about 3–4 D. At this point, subjects with presbyopia suffer from blurred vision, asthenopia, ocular pain, and headaches after reading or working at close distances for prolonged periods. In our current understanding of the principles, the add diopter is about 0.097 to 0.105 D/year for presbyopia. When patients are 45 to 50 years of age, the decline in accommodation is around 3 D/year. By the fifth decade of life, there is an obvious reduction in AA. It is not surprising that this accommodation decreases to nearly zero at the age of 70 years [7].

Except for AA, presbyopia occurs due to changes in the chemical composition and physical structure of the lens [8]. There exists a close relationship between the biomechanics of the lens, accommodative system, and presbyopia. The thickness of the elastic capsule of the lens and the flexibility of zonular fibers change during adulthood may impact patients with presbyopia. An increase in the fibrillary materials of zonules reduces the compliance of the posterior insertion of the ciliary muscle. The deterioration of the elastic components of the ciliary body and choroid may result in a decline in AA. Furthermore, vitreous liquefaction occurs and the pressure between the anterior and posterior chamber may change with age [9]. The irregularity of the fibrous morphology of the lens is also noted when humans become older. These findings have been reported as the predisposing factors for presbyopia [10]. Hence, the loss of AA in individuals begins early in life at 40 to 50 years of age and rapidly progresses when people are around 55 years old.

Presbyopia is also believed to reflect a loss of accommodation due to cataract formation and the weakening of the ciliary muscles—the lens zonules apparatus. According to Hemohotz (1855), the ciliary muscles relax and the zonules around the lens are under initial tension. When the eye accommodates, the tractive force from the ciliary muscles enhances and reduces the tension on the zonules. The reduced zonular tension allows the elastic capsule of the lens to contract, causing an increase in the anterior–posterior diameter of the lens, making it more spherical in shape. Finally, it may increase the diopter powers needed for viewing near objects. Therefore, Schachar et al. demonstrated that, during accommodation, the central surface should steepen while the peripheral surface of the crystalline lens flattens [8]. Nandi et al. also proposed two major probable factors related to presbyopia—the contractility of the ciliary muscles and the resistance to deformation of the compacted lenticular sclerosis due to the deposition of damaged fibers and the cross-linking of the α-crystalline protein through the formation of advanced glycation end-products (AGEs) [11]. Hence, the diopter of the lens may reduce gradually because of the excessive accumulation of AGEs for oxidation, which leads to a harder nucleus. On the other hand, Pescosolido and colleagues demonstrated that the ciliary muscles undergo compensatory hypertrophy and AA decreases with age because of the loss of the elasticity and ductility of muscles [12]. There are several procedures available for evaluating the outcomes of treatments of presbyopia. The evaluation parameters include the change in refraction, pupil size, axial length, near vision, depth of the anterior chamber (A/C), lens thickness, and level of AA. Schneider et al. made use of the Hartinger coincidence refractometer to examine the A/C depth and pupillary diameter between accommodative intraocular lenses (IOL) and PMMA IOL of 30 eyes after cataract surgery. The aim of their research was to identify many factors in different IOLs and make a contribution to the development of IOL in humans [13]. Additionally, the change in AA was valuable in assessing the prognosis. For instance, a decrease in the AA of the nondominant eye should be the predictive factor for the success rate of exotropia surgery [14].

When accommodation is not enough for people at near working distances, some auxiliary procedures are necessary for avoiding vision stress and ocular disability. Common strategies for coping with presbyopia are the use of reading glasses and contact lenses. Moreover, other procedures have also been claimed to restore accommodative ability, including orthokeratology, corneal inlays, Supracor laser procedure, cataract surgery with multifocal IOLs, Presby-LASIK, diode laser thermal keratoplasty, surgical expansion of the sclera, and conductive keratopathy [15]. Although spectacles can meet the basic needs of the majority of individuals, they may be inconvenient to use. In addition, some of these surgeries are either undeveloped or controversial and several of the methods are not acceptable because of their invasive and relatively dangerous properties. Therefore, there is a need to develop a relatively safe, new, and effective method to address presbyopia.

Pharmacologic therapy for presbyopia is another choice, which shows the characteristics of reversibility, noninvasiveness, and ease of use. From 2005 to 2016, very few articles about pharmacologic treatment for presbyopia were published. For example, Abdelkader stated that a

combination of eye drops with 3% carbachol (parasympathomimetic agent) and 0.2% brimonidine (α2-adrenergic agonist) was prescribed for 10 subjects with presbyopia between the ages of 42 and 58 years, once daily. Carbachol should promote Ach release and lead to miosis to enhance depth-of-focus (DoF) and the pinhole effect, thus obtaining accommodative capacity in subjects between their forties and fifties. Brimonidine enhances the effects of carbachol and produces a more miotic pupil. A statistically significant improvement in mean near vision (4-lines) was achieved in all persons, while far vision was still preserved [16]. Renna et al. claimed that their ophthalmic formulation with 0.247% pilocarpine (cholinergic agonist), 0.78% phenylephrine (α1-adrenergic agonist), 0.023% nepafenac (NSAID), and 0.003% naphazoline (sympathomimetic agent) can be recommended to patients with presbyopia (28 eyes) twice-a-day binocularly. The mechanisms of the complex formulation are ciliary muscle contraction, lens softening, and miosis. Pilocarpine predominantly stimulates accommodation and enables miosis and ciliary body contraction. It also improves the tear volume by enhancing lacrimal gland secretion, which relieves the effects of ocular fatigue and dry eye. The outcome showed a mean improvement in UNVA of two to three lines by J chart [17].

In recent years, the worldwide use of herbal medicines for eye diseases has become popular and trendy. For example, *Astragalus membranaceus* can be used for diabetic retinopathy, while *Cinnamon cassia* could be beneficial for age-related macular degeneration [18]. We reviewed the topic of herbal treatment for presbyopia from studies reported in PubMed, wherein only two studies were found. Our team has published reports examining the use of cassia seeds and *Lycium barbarum* for eye diseases [19, 20]. In this new study, our mixed formulation of herbal drugs to address presbyopia included Cassiae Semen, *L. barbarum*, and *Dendrobium huoshanense* (DD). We collected the extracted substances, ground them into a fine powder, and mixed them in a capsule according to a specific ratio [21]. In the current study, we attempted to use these three herbal drugs on a large sample of subjects and investigated the therapeutic effects.

2. Methods

In this approved study, we selected 400 consecutive eyes (200 right eyes and 200 left eyes) randomly from 400 adult participants aged 45 to 70 who could not easily perform near work (around 40 cm) in southern Taiwan. We conducted this prospective study in 2016, after obtaining informed consent from all subjects. Then, investigations were conducted in accordance with the Declaration of Helsinki. The ethical approval for the human trial was obtained from the institutional review board of Kaohsiung Armed Forces General Hospital (Kaohsiung City, Taiwan, ROC) (approval number: KAFGH-106-003). All patients with presbyopia underwent a standardized protocol of ocular examination, including slit-lamp biomicroscopy (Haag-Streit IM 900, Clinico. INC), noncontact tonometry (Reichert® 7, Reichert Technol), autorefraction (KA-1000, KOWA), and nonmydriatic retinal photography (Nonmyd AF, KOWA) for checking the cornea, lens, A/C depth, intraocular pressure (IOP), and refraction. An optical coherence tomography system (Zeiss Com.) was applied to evaluate the vitreous, retina, and optic nerve. The horizontal diameter of pupils was measured using Orbscan II Topography (Bausch & Lomb). Only emmetropia (cycloplegic spherical equivalent, ±1.0D; astigmatism ≤0.5D) measured from an autorefractor was used. For example, longer axial myopia has a thicker ciliary body, which impacts the accommodation of presbyopia and adversely affects the results. Hence, only subjects with emmetropic eyes were enrolled to avoid bias [22]. The uncorrected distance visual acuity (UDVA) and uncorrected near visual acuity (UNVA) were examined. Particular attention was given to the UDVA according to the Snellen chart (test distance: 6 mm). UNVA was assessed by the Jaeger Eye Chart (test distance: 40 cm; J score: 1–15), where people with presbyopia were told to read the letters of books until the letters are no longer clearly seen without reading glasses [23]. In our experiments, all the eligible subjects with at least 20/32 UDVA and J6 UNVA were enrolled, according to another study [24]. For easy analyses, UDVA was transferred to LogMAR. Volunteers with ocular pathologies such as glaucoma, history of eye trauma, uveitis, amblyopia, strabismus, severe cataracts (Grade III and IV), severe corneal diseases, optic neuropathy, various retinopathy, s/p any major ocular surgery, receiving correction of presbyopia, and stereopsis less than 400 arc second were excluded. In addition, none of the participants had received any chronic miotic or mydriatic therapy, which could have caused an error in our results.

Several examinations were conducted for all 400 eyes. At each visit monthly, the ocular structure, IOP, and pupil diameter of all the involved eyes were checked. Additionally, we verified the change in AA to evaluate the effectiveness of the herbal treatment. There are many methods for obtaining AA in various conditions [25, 26]. The Donder table and Hofstetter's equation can be used to measure AA easily, although the accuracy of these methods remains controversial due to the omission of some facts [27]. Hence, we adopted the push-up method for assessing the AA of each subject AA using an autorefractometer, which is a more suitable manner for surveying AA. The push-up test is a valuable technique for an estimate of near reading ability because it has the advantages of the rapid and simple measurement of AA [28, 29]. Although the push-up test is a subjective method, its repeatability and validity are highly appreciated [30]. Hence, we used this equipment for a monocular AA check-up. First, the AA from each subject with different ages and conditions was checked at the baseline, in the third, sixth, ninth, and twelfth months (the end of this study). In the initial experiment, each participant sat in a room where the lights were switched off to create a semidark condition. All the measurements were taken twice, and the arithmetic mean of the results was registered. As for the detailed procedures, the refractive correction was prescribed for a far distance if necessary. Subjects had an eye patch placed over their nontested eyes and were asked to focus on a near target consisting of two parallel vertical lines

(designed with a constant angular size) on a standard chart. The chart was brought closer until the target became slightly blurred. This chart was then slowly pushed back until the parallel vertical lines could be clearly seen again, which was considered to be the near point of accommodation. The reciprocal of the closest distance in meters was AA [31]. Throughout the study, all adverse effects were recorded. A questionnaire recording visual satisfaction compliance with taking drugs was administered to patients each month. The definition of success was an improvement in UNVA of at least two lines of the J chart, accompanied by presbyopic symptoms, including ocular fatigue, dry eye, and periocular pain when working at near distances after six months of treatment. The rates of satisfaction of the subjects were collected between the first and twelfth months.

According to our small sample of previous human studies, the ideal formula was a mixture of Cassiae Semen (200 mg), wolfberry (200 mg), and DD (40 mg) in a capsule. The ratio of cassia seeds, goji, and DD was 5 : 5 : 1 (not published yet). The medical plant powders were purchased from herbal drug stores in Taiwan. We manufactured a slow-releasing capsule that included the three herbal rugs together. The special components of this capsule included hydroxylpropyl methylcellulose (HPMC) and pectin. HPMC is a semisynthetic, inert, viscoelastic polymer that is used in eye drops and as an excipient for controlled-delivery compositions in oral medications. Pectin can act as a gelling agent, thickening agent, and stabilizer. In capsules, pectin should resist gastric acid and ensure that the herbal drugs are absorbed in the small intestine for maximal effect. Regarding the choice of criteria cases in our study, people aged ≥45 years were recruited. Wold et al. demonstrated that problems manifest earliest in hyperopes and emmetropes at about 40 years of age [28]. According to our clinical experience in Taiwan, the symptoms of presbyopia get remarkably worse between 40 and 45 years of age. We also found that the average age for requesting added correction for reading spectacles is around 45 years due to the significant reduction in AA. Therefore, we chose subjects whose mean age was 45 for real and exact analysis in this research.

In experiment 1,400 participants with various mean ages (45, 50, 55, 60, 65, and 70 years) were recruited. AA was measured by the push-up test and converted to the presbyopic powers of the individual [32]. In the early stages of presbyopia, residual accommodation remains crucial for achieving the functional near vision. Then, 200 participants with a mean age of 50 years were separated into 40 subjects for experiment 2 and 160 subjects for experiment 3, which will be the subject of another study.

In experiment 2, all 240 participants were categorized into six groups according to their different ages (45, 50, 55, 60, 65, and 70 years), and each group included 40 subjects. We obtained the AA from experiment 1. In the beginning, 240 patients took one capsule three times a day for six months. Afterwards, from the start of the seventh month, all the subjects stopped taking drugs and received a further six-month follow-up (Figure 1). The aim of experiment 2 was to evaluate the efficacy of these mixed herbal drugs in improving accommodation. From the start of experiment 2, the participants were requested to report to our outpatient department and participate in a push-up test to survey their AA every month. We completed the recordings, including UDVA, UNVA, IOP, and pupil diameter. We first compared the results at the baseline and at other time points (i.e., after three, six, nine, and twelve months) using Scheffe's test. We then inspected the change in all parameters at the ninth and twelfth month compared with the results at the sixth month. We also examined the difference after stopping herbal treatment using Scheffe's test. Finally, the mean IOP, horizontal diameter of the pupil, UNVA, and UNVA were analyzed among the six groups.

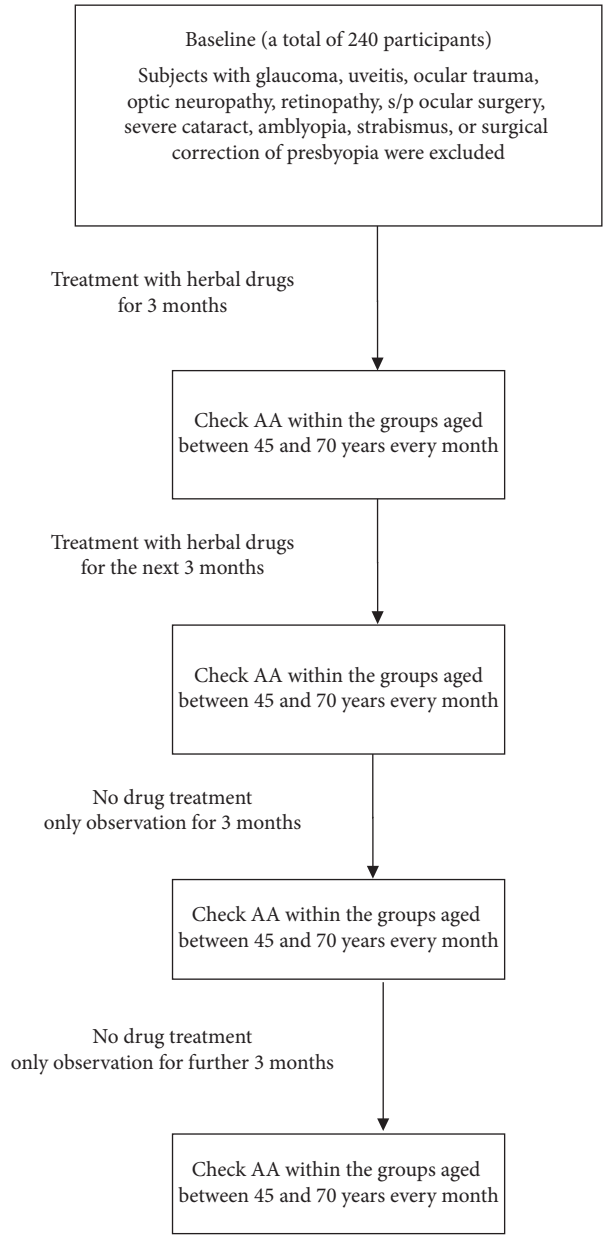

Figure 1: Flowchart of experiment 2.

In experiment 3, 160 presbyopic subjects with a mean age of 50 were randomly categorized into four groups, including a placebo group (taking 10 mg vitamin C daily), low-

dose group (LDG) (1 capsule/day), middle-dose group (MDG) (2 capsules/day), and high-dose group (HDG) (3 capsules/day), respectively. According to our designed flow chart, the procedures used in experiments 2 and 3 were similar. Oral vitamin C was prescribed for placebo group 1. Moreover, in groups 2, 3, and 4, the volunteers took one, two, and three capsules every day, respectively, for six months (Figure 2). When half a year had passed, the presbyopic patients terminated the use of the herbal supplements and received follow-up for the next six months. We compared the parameters, including AA, pupil size, UNVA, and UDVA at the baseline and at other times (third, sixth, ninth, and twelfth months) using Scheffe's test. Then, we checked all the parameters at the ninth and twelfth months and compared them to the sixth month. We inspected the difference after the discontinuation of herbal drugs using Scheffe's test. We also measured the difference in AA and other values between the placebo and other three groups (LCG, MCG, and HCG) at various times (i.e., the baseline and the end of the third, sixth, ninth, and twelfth months) using William's test.

The AA, pupil size, and presbyopic diopters were presented as mean ± standard deviation (SD). We analyzed the data using SAS 9.0 (SAS Institute, Cary, USA). A P value <0.05 was considered statistically significant when compared in all the experiments.

3. Results

A total of 200 males and 200 females participated in our study, and their average age was 54.5 ± 2.8 years (range: 42–72 years). Their IOP remained within a normal range after the oral intake of herbal drugs for one year. In addition, the anatomy of the ocular structure of all participants except the diameters of the pupils were all found to be normal at the sixth month and the end of our study (twelfth month). We observed the lens of every volunteer, and there was no rapid progression to severe cataract formation (grade III or IV). Additionally, there were no significant adverse events or complications—for example, severe diarrhea, red-eye, skin rash, or even convulsion—mentioned by any participants. We did not find overaccommodation-induced headaches from excessive ciliary muscle contractility. In our entire study, the percentage of good compliance and satisfaction after taking herbal capsules was up to 90% (324/360). Forty volunteers in the placebo group in experiment 3 were deductible from the total number of 400 participants. The success rate was nearly 95% (342/360) in the sixth month. In other words, the symptoms and near vision in 95% of presbyopic patients would improve after herbal treatments for a total of six months.

In experiment 1, 400 participants of different ages (45, 50, 55, 60, 65, and 70 years) completed the push-up test, and their AA values were estimated. For example, the mean AA of people aged 60 years was 1.0 ± 0.1 D, and this was converted to the add powers of +2.0 ± 0.1 D by a special formula, showing that they potentially needed reading glasses [33]. Additionally, the AA of people aged 45 and 70 years was 3.6 ± 0.1 D and 0.2 ± 0.1 D, respectively. The decrease in AA with age was verified. The level of AA in presbyopic subjects aged 65 and 70 years was approximately zero (0.2 D~0.3 D) (Table 1). In other words, people aged ≥65 years really need the add power of eyeglasses. Hence, reading spectacles were necessary for older presbyopic persons because of their total loss of accommodative ability. Physical status (i.e., the difference in arm length), visual tasks, and working distance affect the add power for individual patients. In fact, it is a meticulous technique about the procedure of getting a prescription for a pair of reading glasses. However, Taub and

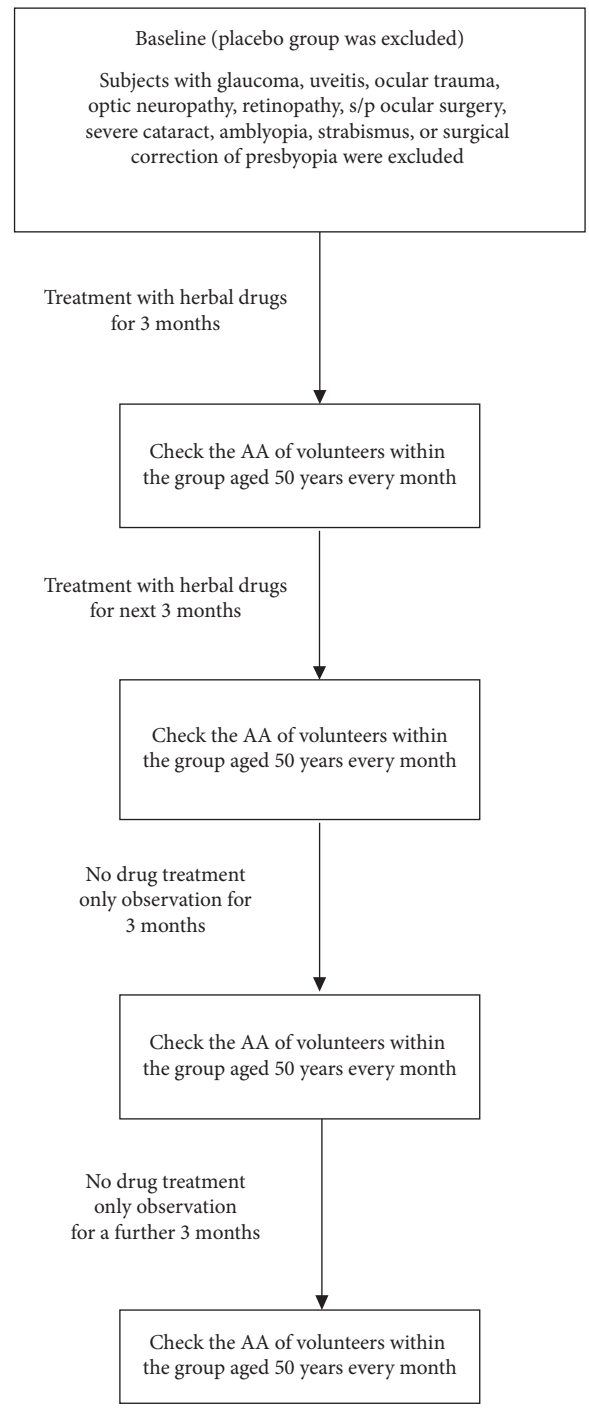

Figure 2: Flowchart of experiment 3.

Table 1: Demographics of the volunteers in experiment 1.

Age	Baseline		
	Numbers	AA	Presbyopic D
45	40	3.6 ± 0.2D	+0.7 ± 0.1D
50	200	2.6 ± 0.1D	+1.2 ± 0.1D
55	40	1.8 ± 0.2D	+1.6 ± 0.1D
60	40	1.0 ± 0.1D	+2.0 ± 0.1D
65	40	0.3 ± 0.1D	+2.4 ± 0.2D
70	40	0.2 ± 0.1D	+2.3 ± 0.1D

(1) Numbers: a total of 400 participants were gathered through an interview in our study aged between 45 and 70 years. Besides this, 240 subjects were enrolled in experiment 2 and 160 participants were separated for experiment 3 for persons with a mean age of 50 years. (2) At first, we gained the AA from subjects with different ages using the subjective push-up method. Subsequently, AA may be converted to the additional diopters of presbyopic reading glasses. (3) Near vision: test at 40 cm in front of the volunteers' eyes. (4) Age (mean age) in years. (5) AA: amplitude of accommodation. (6) D: Diopter.

Shallo-Hoffmann showed that the add power required for working at near distances is provided by a combination of spectacle addition and residual accommodation [34]. In the study, the mean AA (add power) was 3.6 ± 0.2 D (+0.7 ± 0.1 D), 2.6 ± 0.1 (+1.2 ± 0.1 D), and 1.8 ± 0.2 D (+1.6 ± 0.1 D) for people aged 45, 50, and 55 years, respectively. These results of our experiments were in agreement with the earlier published notion of presbyopia beginning at 40–45 years old and lower AA apparently occurring in the mid-fifties [35].

In experiment 2, 240 subjects were categorized into six groups in accordance with their different ages. Experiment 2 aimed to determine the outcome of using the same dose for subjects of different ages. Each patient took three capsules each day for six months and received follow-up for the next six months continuously. The findings from the various groups revealed that AA could reach the maximal level at the sixth month, perhaps because the herbal drugs reached their highest accumulated concentration in the human body in that period (Table 2). We took the subjects aged 55 years as an example. When comparing the results at the baseline, the mean AA reached the maximal level (2.3 ± 1.5 D) at the sixth month ($P < 0.05$). In addition, the highest AA values among all the six groups were around the sixth month. In summary, the herbal drugs were given to volunteers aged 45 to 70 years for six months and the AA value reached a maximum value of 2.1 D in the sixth month ($P < 0.05$) and decreased slightly to 2.0 D in the ninth month ($P < 0.05$). Furthermore, from the seventh month, the AA gradually decreased because of the decayed drug reaction. However, it was interesting to find that AA still maintained significant results in people aged 65 and 70 years in the ninth month ($P < 0.05$). Surprisingly, this was when the participants had already stopped herbal supplementation for three months, thus showing that excellent pharmacologic abilities were still achieved in the ninth month. Therefore, we propose that our designed formula could perhaps maintain valid AA and maintenance effects for patients with presbyopia.

The mean pupil diameter was 4.3 ± 1.1 mm, 5.0 ± 0.9 mm, 5.6 ± 0.8 mm, 4.5 ± 0.7 mm, and 4.2 ± 0.5 mm at the beginning of the study and the third, sixth, ninth, and twelfth months, respectively. We found that the pupil would slowly dilate to the maximal size after six months and then recover slowly to nearly the initial size. The UDVA and UNVA were 0.18 LogMAR and J5.5, 0.09 LogMAR and J3.5, 0.05 LogMAR and J1.5, 0.12 Log MAR and J2.5, and 0.17Log MAR and J5.0 at the initial phase, at the 3rd month, at the third, sixth, ninth, and twelfth months, respectively. Hence, it was verified that far vision was not affected in our treatment. Besides this, in most of the participants, the near vision measured with the Jaeger Eye Chart showed an improvement of around two to three lines. The mean UNVA reached J1.5, which may be beneficial for patients with presbyopia after six-month treatment. The mean UNVA was also maintained at J2.5 (ninth month), even after the herbal supplement was stopped for three months. This meant that the mixed herbal medicine maintained its effects for good near visual acuity. Meantime, mydriasis showed the largest pupil size (5.6 ± 0.8 mm) at the sixth month ($P < 0.05$), and the diameter of the pupil showed a mild decrease (4.5 ± 0.7 mm) at the ninth month ($P < 0.05$) when compared with the baseline. The parasympathetic functions after taking our mixed herbal drugs were predominant in terms of pupillary dilation. Besides this, the maintenance doses from our herbal drugs were also appreciated for at least three months. A smaller pupil enhances the DoF and improves human near vision [36]. However, mydriasis and excellent near vision were noted after our herbal drug supplementations. We propose that the mechanisms of improvement of near visual acuity may be due to accommodation rather than miosis-induced DoF and the pinhole effect in our subjects.

In experiment 3, 160 participants with a mean age of 50 years were randomly categorized into four groups for different treatments. In this experiment, we wanted to realize the appropriate doses for patients with presbyopia. During our observation, the AA of the subjects in the placebo group who took vitamin C remained unchanged. On the other hand, we found that the maximal AA was 2.8 ± 0.4 D, 2.9 ± 0.8 D, and 3.2 ± 0.5 D in the LDG, MDG, and HDG in the sixth month (Table 3). Only the elevation of AA in HDG showed a significant difference when compared with the baseline ($P < 0.05$). The increase in AA in LDG and MDG was also apparent. Furthermore, the AA (3.0 ± 0.5 D) in HDG was still elevated at the ninth month; this difference was also significant when compared with the baseline ($P < 0.05$) using Scheffe's test. To our surprise, the AA remained good in the HDG after the subjects had stopped the treatment for three months. This meant that the residual effects of the herbal treatment in the human body still maintained a therapeutic function after the subjects had stopped continuous herbal therapy for three months. In experiment 2, we had a similar outcome and associated conclusions. We compared the results between the placebo group and the other three groups (LDG, MDG, and HDG) using William's test. It was revealed that taking any dose of herbal drugs will improve the AA; however, only the frequency of prescription of about three capsules/day could significantly improve the levels of AA ($P < 0.05$). We conclude that that AA gain occurs in a dose-dependent manner; the higher the dose taken, the greater the AA value. We

Table 2: The changes in AA of various ages after talking herbal drugs in experiment 2.

Age	Times				
	Baseline	3rd month	6th month	9th month	12th month
45	3.6 ± 0.2D	3.8 ± 1.4D	4.2 ± 1.5D*	4.0 ± 1.9D	3.7 ± 1.5D#
50	2.6 ± 0.1D	2.9 ± 0.5D	3.1 ± 0.9D*	2.9 ± 0.9D	2.7 ± 2.0D#
55	1.8 ± 0.2D	2.0 ± 0.8D	2.3 ± 1.5D*	2.3 ± 1.1D	1.9 ± 1.2D#
60	1.0 ± 0.1D	1.2 ± 0.6D	1.6 ± 0.9D*	1.3 ± 0.6D	1.0 ± 0.6D#
65	0.3 ± 0.1D	0.5 ± 0.2D	1.0 ± 0.5D*	0.9 ± 0.6D*	0.4 ± 0.2D#
70	0.2 ± 0.1D	0.3 ± 0.2D	0.6 ± 0.3D*	0.5 ± 0.2D*	0.2 ± 0.2D#

(1) All 240 participants were recruited in experiment 2, and a total of 40 volunteers with various ages took part in each group between 45 and 70 years. (2) All the volunteers took the capsules three times daily for six months and stopped treatment at the end of the sixth month. Afterward, we followed up the parameters and questions for a further six months. (3) A herbal capsule included 200 mg Cassiae Semen, 200 mg wolfberry, and 40 mg *Dendrobium huoshanense* (DD). (4) At first, we compared the results (at the third, sixth, ninth, and twelfth months) with the baseline. Second, we inspected the data (at the ninth and twelfth months) with the results of the sixth month. In all comparisons, the method of Scheffe's test was used for analysis. (5) When the p value was less than 0.05, it was considered as a significant difference. Hence, in the first comparison, it will be marked as *, and in the second comparison, it will be marked as#.

Table 3: The outcomes after taking various amounts of herbal drugs in experiment 3.

Age	Times				
	Baseline	3rd month	6th month	9th month	12th month
Placebo	2.6 ± 0.1D	2.6 ± 0.4D	2.6 ± 0.5D	2.6 ± 0.5D	2.5 ± 0.6D
1 cap/day	2.6 ± 0.1D	2.7 ± 0.8D	2.8 ± 0.4D	2.8 ± 0.9D	2.6 ± 0.4D
2 cap/day	2.6 ± 0.1D	2.8 ± 1.1D	2.9 ± 0.8D	2.9 ± 0.6D	2.7 ± 0.8D
3 cap/day	2.6 ± 0.1D	2.9 ± 0.9D	3.2 ± 0.5%*	3.0 ± 0.5D*	2.7 ± 0.7D#

(1) In experiment 3, 120 volunteers with a mean age of around 50 years were involved, and they were randomly divided into four groups. (2) Group 1 (placebo group) ($n = 20$): only 10 mg vitamin C daily was taken. Group 2 ($n = 20$): all subjects took one capsule/day. Group 3 ($n = 20$): all victims took two capsules daily. Group 4 ($n = 20$): total volunteers were fed with three capsules in each day. (3) All volunteers took the various doses of mixed herbal capsules for six months in groups 2, 3, and 4 and stopped treatment at end of the sixth month. Then, the participants received follow-up for the next six months. The associated parameters and questions were collected. (4) At first, we compared the AA of at the third, sixth, ninth, and twelfth months with the baseline using Scheffe's test. Moreover, the results at the ninth and twelfth months were recorded and compared with the outcome of the sixth month by Scheffe's test. Third, the mean AA in group 2 (1 cap/day), group 3 (2 cap/day), and group 4 (3 cap/day) was compared with the placebo group using William's test. (5) A P value less than 0.05 was considered significantly different. Hence, in the first comparison, it will be marked as*, in the second comparison, it will be marked as#, and in the third comparison, it will be marked as %. (6) Cap/day: capsule(s)/day.

suggested that the components of mixed herbal drugs may enhance the elevation of AA [36, 37].

4. Discussion

Currently, nearly 2.1 billion people worldwide are estimated to suffer from presbyopia. In 2019, more than 30% of the total population in their mid-to-late 40s were reported to be affected to some degree. Surprisingly, in developing countries, the most prevalent ocular disease was found to be presbyopia in 92.5% of patients, compared with the 34% of patients reported in developed countries. With the increasing longevity of the population, most of the global population is expected to spend roughly half their lives with presbyopia [38].

Presbyopia is loss of the ability of the eye to focus sharply on nearby objects, resulting from the age-related loss of AA. The ability of the eye to accommodate or adjust its focus diminishes with age. Most of the facilities to accommodate will be lost by 55 years of age. In experiment 1, we demonstrated that the mean AA was 1.8 D in subjects aged 55 years. In 60-year-old subjects, the mean AA was 1.0 D, which dropped to 0.2 D (nearly zero) in those aged 70 years. Our examination of the Taiwanese population showed similar results to those of many other studies. Likewise, Boccardo stated that AA declined from 40 to 83 years of age in the Spanish population [39]. When the eye is at rest and focused on the distance, the ciliary muscle is relaxed. If a person wants to view objects at a close distance, the ciliary muscle contracts and induces a forward movement of the lens. This phenomenon causes the bulk of the anterior ciliary body to move forward and toward the axial length, further increasing the vitreous pressure, resulting in a release in tension in the zonular fibers around the lens equator [7]. The elastic lens capsule is able to mold the young and soft lens into a more spherical form (increasing the lens thickness) for AA gain. However, these mechanisms are subject to a series of pathologic changes during aging. We could observe the hypertrophy of the ciliary muscle, loss of the elasticity of zonular fibers and lens capsule, insertion of the ciliary muscles becoming more tangential to the lens surface, shallow A/C, IOP elevation, and hardening of the lens. Presbyopia may also occur due to the crowing of the posterior chamber and a reduction in the tension of zonules fibers at the lens equator. Therefore, the primary cause of the onset of presbyopia is the subject of aging. At times, it has also been connected to long-term reading or working at near distances, geographic latitude, higher environmental temperature, race, gender, excessive ultraviolet radiation, chronic deficiency of essential amino acids, and exposure to

hair dye [39–41]. In addition, people with uncorrected hyperopia and anisometropia and contact lens wearers have shorter times until the onset of presbyopia [42]. It appears that nutrient intake—for example, vitamin C supplementation—may delay the occurrence of early age-related lens opacity and loss of accommodation. Early-onset presbyopia was recently studied in special groups, including computer workers and smartphone overusers, who were around 35 years old. Moreover, we demonstrated that the relationship between ocular floater and posterior vitreous detachment (PVD) is close. PVD may lead to symptomatic vitreous opacity, which is also related to the onset of presbyopia because of vitreous liquefaction. The peak incidence of PVD occurs between 45 and 65 years, which is when a higher prevalence of presbyopia also occurs [43].

Presbyopia is believed to occur due to a loss of visual accommodation due to the weakening of the ciliary muscle-lens zonules apparatus and the stiffening of the lens with age. In other words, an abnormal change in the configuration of the ciliary body leads to a change in lens thickness and elasticity of the lens capsule and crystalline lens; these associated ocular pathologies result in the development of presbyopia. In clinics, we could measure the variation in the AA for the evaluation of presbyopia. In fact, dynamic AA varies in different people, ages, ocular diseases, and treatments. If human AA is not suitable for users performing near-distance tasks, presbyopia develops, and extra AA from reading glasses or other methods is necessitated.

In experiment 1, the decline in accommodation in the subjects aged between 45 and 50 years was not obvious. The add diopters between the two groups were almost +0.70 D and +1.2 D (Table 1). In clinics, when the add power is around +1.0 D, the use of extra-additional reading glasses is not indicated. Our results were similar to the report of Pescosolido's research team [13]. In experiment 2, in the ninth month, we unexpectedly found that the mean AA still showed significant results for people aged between 65 and 70 years, who had gone without treatment for three months ($P < 0.05$) (Table 2). Why did only older people retain the apparent AA and why did most of the people from the groups aged from 65 to 70 years have improved near vision? We hypothesize that the chemical substances of herbal drugs may be metabolized in younger people rapidly; however, the pharmacologic functions remained effective in much older people. In the meantime, their near vision also remained at J 2.5 (baseline: J 5.5), and the pupil size was maintained at 4.5 mm (baseline: 4.3 mm), which, on comparison, showed significant differences. The previously mentioned findings suggest that the parasympathetic functions that were beneficial for accommodation were still functional at this point. Hence, we suggest that the oral herbal drugs from our designed formula could offer a valid improvement in AA, which would be beneficial for people with presbyopia. In experiment 3, we found an elevation in the maximal AA in the three groups with various treatments. Although the only elevated AA value in the HDG in the sixth month was remarkable ($P < 0.05$), the maximal AA in LDG and MDG also showed an elevation. This meant that taking any capsules would be good for obtaining an improved AA. According to the outcomes mentioned in Table 3, the ideal prescription indicates that the subjects should take three capsules each day for at least six months.

There are many methods for the treatment of presbyopia in patients. The strategies for dealing with presbyopia include using a separate optic device before the visual system (reading spectacle), change in the gaze to view through optical zones of different optical powers (bifocal, trifocal, or progressive spectacles), monovision (contact lenses, IOLs, and laser refractive surgery), simultaneous images (corneal inlays), pinhole depth focus expansion (IOLs, corneal inlays, and pharmaceuticals), crystalline lens softening (lasers or pharmaceuticals), and restored dynamics (accommodating IOLs, and scleral expansion) [44–46]. After various management efforts, presbyopic people feel comfortable working at near distances. The use of reading glasses is the most common and acceptable method for the correction of presbyopia. Traditional single-vision, bifocal, and progressive eyeglasses are acceptable for humans and are relatively simple [47]. Nevertheless, the associated problems included inconvenience in performing daily or athletic activities. Optically similar, simultaneous-image contact lenses are another choice. However, age-dependent ocular changes such as the decreased muscle tonus of both the upper and lower eyelids reduced palpebral aperture, and diminished lacrimal production and tear stability may influence one's experience of wearing contact lenses. Besides this, the relatively higher infectious rate decreased stereopsis, and contrast sensitivity may limit the desire of patients to use this method [48]. Considering invasive techniques, cataract surgeries combined with multifocal IOL appear to offer the most consistent and reliable choice for presbyopia [49]. Other approaches also show promise, but as yet no method has demonstrated reliable and long-term effectiveness. Besides this, some unexpected adverse reactions and possible perpetual damage may irreversibly impact the intention of people to use these methods [44].

Pharmacologic methods are another choice for presbyopia. Most eye drops given to presbyopic patients are mixed and include compounding agents. We searched for the treatment of presbyopia in the PubMed system. To our surprise, only a few articles on topical eye drops have been published in journals until 2021. Eye drops for presbyopic subjects have become popular due to several advantages, such as their ease of use, effectiveness, and noninvasiveness, and they also do not limit patients' daily activities [50]. The pharmacological mechanisms of the drugs are to enhance the contraction of the ciliary muscle, pupil control, and management of DoF. Some eye drops may gain AA for the compensation of presbyopic loss, which should improve near vision. For example, Benoozzi and coworkers used a combination of pilocarpine (1%) and diclofenac (0.1%) (NSAID) for presbyopia. The cholinergic drug, pilocarpine, would act on the muscarinic receptors of the ciliary muscle and iris and then restore near visual acuity. In addition, the pharmaceutical form used was devoid of any inflammatory or other collateral effects through the inhibition of prostaglandin synthesis by NSAIDs [38]. The eye drops comprise several components, including pilocarpine, dapiprazole, and

naphazoline, which are used alone or in combination for presbyopia. Pilocarpine can be used topically for stimulating accommodation for presbyopic subjects. Nevertheless, various concentrations have different results. One-percent pilocarpine could facilitate pupil constriction and ciliary body contraction, thus stimulating accommodation and improving tear production by stimulating lacrimal gland secretion. On using the eye drops containing the combination of 4% pilocarpine and 10% phenylephrine, the subjects' AA may even reach the maximal 14 D. It was verified that pilocarpine 6% should be at a higher concentration relative to a clinical therapeutic dose. Pilocarpine could also induce an increase in the lens thickness [51, 52]. Unfortunately, the use of pilocarpine has many side effects, such as headache, dizziness, nausea, flushing, acute-angle closure glaucoma, and retinal detachment [53]. Dapiprazole is an adrenergic α1 blocker that counteracts the effects of 1% tropicamide and 2.5% phenylephrine. It should reverse the mydriatic function. Hence, the presumed effects could diminish the haloes after excimer keratectomy. Moreover, dapiprazole could also increase the level of AA, DoF, and comfortable reading ability in patients with presbyopia [54]. However, we must pay attention to its side effects, such as photophobia, corneal endothelial toxicity, and poor near vision. Finally, naphazoline is a direct-acting sympathomimetic amine with vasoconstrictive activity. Upon ocular administration, naphazoline exerts a rapid effect by acting on alpha-adrenergic receptors at the conjunctiva to produce the vasoconstriction of ocular arterioles, resulting in decreased conjunctival congestion, itching, irritation, and redness. For presbyopic subjects, naphazoline intensifies the relaxing effect of pilocarpine on the dilator pupillae, increasing the Ach level and reducing norepinephrine release. Hence, it is also one type of eye drop recommended for presbyopia [55].

We also reviewed the publications on herbal treatments for presbyopia on PubMed and found only two papers. Biswas et al. conducted one herbal drop preparation to be applied by patients with various ocular diseases for six months. They found that cataracts and presbyopia became better [56]. However, the contents of the herbal drug were not mentioned, and the detailed usage was also not clear. Likewise, Khan et al. demonstrated that the "Ocucure" tablet (500 mg), including *Foeniculum vulgare* (150 mg), *Paeonia officinalis* (150 mg), *Coriandrum sativum* (100 mg), and *Benincasa hispida* (100 mg), and two tablets were prescribed daily for six to eight weeks. Presbyopic symptoms in only 17 cases (28.8%) improved when compared with the control group (six patients; 11.5%). Nevertheless, the sample size in their research was relatively small and the subjects were too young (mean age was about 33.5 years) [57]. In this research, we tried to design a new mixed herbal drug to improve AA for good near vision. During our experiments, we made mixed herbal capsules, and the pharmacological effects of each traditional Chinese drug were analyzed.

Cassiae Semen is a well-known traditional medicine that has been used for improving eyesight, liver function, and various types of inflammation in China since ancient times. Of late, cassia seeds have been used to treat headaches, obesity, periocular pain, constipation, hypertension, hyperlipidemia, Alzheimer's disease, ischemic stroke, and bronchospasm, as well as some ocular diseases such as dry eye and retinitis pigmentosa [58]. A total of 55 chemical compounds in Cassiae Semen were identified, including flavonoids, emodin, chrysophanol, physcion, obtusin, rhein, aurantio-obtusin, chryso-obtusin, and anthraquinones—which showed various pharmacological functions, including anticoagulant, antiangiogenic, antimicrobial, and antioxidant abilities. For example, physcion belongs to polyphenol, which has antioxidative and anti-inflammatory properties. Aloe-emodin regulates the apoptosis of retinal ganglion cells and prevents glaucoma. Besides this, obtusin and aurontio-obtusin may enhance vasodilation and diuresis. Chrysophanol and physcion were suggested to decrease IOP in our study in 2013 [19]. We know that shallow A/C and the elevation of IOP may be found during accommodation, resulting in periocular pain and even headaches. Therefore, the ability of cassia seeds to lower the IOP function could relieve the symptoms of presbyopia. Furthermore, obtusifolin and emodin are important in accommodation due to acetylcholinesterase (AChE) activity in the cholinergic nervous system through the activation of the muscarinic receptors [59]. We believed that the contractility of the ciliary muscle, relaxation of zonules, more curved lenses, mydriasis, increase in the thickness of the lens, and modification of the shape and position of the lens during accommodation due to parasympathetic functions may be due to the effects of cassia seed extracts. Hence, taking Cassiae Semen may help to obtain AA and good near vision. The real mechanisms behind accommodative pathways need to be investigated more exhaustively in the future.

The fruit of *L. barbarum* or goji berries has been used as an antiaging herb to maintain good health for a long time. Goji can also improve "Kidney Yang Deficiency Syndrome" and balance the "yin" and "yang" in the body. There are various primary extracts of goji berries, including carotenoids, phenolic acid, flavonoids, betaine, taurine, β-sitosterol, polysaccharides, scopoletin, and vitamins [60]. Goji berries exhibit cytoprotective, immunomodulatory, antifatigue, neuroprotective, anti-inflammatory, antiradiation, antiapoptotic, anticoagulant, antiplatelet, cardioprotective, antiproliferative, antimicrobial, and antioxidant effects. These berries can also improve arterial compliance, skeletal muscle power, renal function, and hemopoiesis and ameliorate anemia, asthma, metabolic syndrome, diabetes mellitus, various types of cancers, and Parkinson's disease [61]. A recent study showed that the use of goji berries led to a change in serum metabolic profiles, including energy metabolism (lactic acid), lipid metabolism (cholesterol), and biosynthesis of catecholamine (norepinephrine). Furthermore, Guo et al. demonstrated that *L. barbarum* polysaccharides could increase the level of cortisol and epinephrine [62]. In the ophthalmic field, wolfberries are known to be beneficial for presbyopia-induced dry eye, blurred vision, ocular fatigue, age-related macular degeneration, diabetic retinopathy, UV light-induced retinal degeneration, retinitis pigmentosa, and even glaucoma [63].

Dendrobium, known as "Shihu," is a Chinese traditional medicinal herb that belongs to the *Orchidaceae* family. The stem has been traditionally used for centuries for treating diseases such as throat inflammation and chronic superficial gastritis, strengthening the body, and prolonging life. Dendrobium is widely famous since ancient times for its medical value in treating cataracts. The ingredients extracted from DD are alkaloids, stilbenoids, anthracene, polysaccharides, fluorine, flavone, phenanthrene, and gigantol that have several pharmacological functions, including enhancing immune activities, controlling blood sugar, inhibiting tumor growth, and protecting the liver from oxidative stress [64]. DD is also used for several ophthalmic diseases, such as dry eye and diabetic and ischemic retinopathy. Accumulating evidence indicates that all improvements in ocular conditions are due to the plant's anti-inflammatory and antioxidant abilities. DD also shows significant hypoglycemic and anticataract activities through its inhibition of nitric oxide (NO), aldose reductase, protein glycation, and advanced glycation end products (AGEs) [65]. During aging, the cortex thickens, the lens becomes more curved, and the nucleus becomes less deformed. The pharmacologic mechanisms of DD include the prevention of the development of cataracts and improvement in AA. Except for DD, cassia seeds and wolfberries also contribute to slowing down the formation of cataracts through their antioxidants. For example, cassia seeds contain polysaccharides, emodin, and flavonoids that may resist oxidase stress and decrease the maturation of cataracts. The anthraquinones have inhibitory activity in protein glycation and aldose reductase, preventing the formation of cataracts [66]. As for *L. barbarum*, it can induce the activation of suituin 1 and thereby decrease cataract formation [67]. The extracts from goji berries, including polysaccharides, phenolic acid, and flavonoids, can help in preventing free radicals from attacking the lens fibers. Therefore, goji berry and cassia seeds have a stronger antioxidant ability, which may retain lens clarity and prevent presbyopia.

In this study, we administered mixed herbal drugs to subjects aged 45 to 70 years for six months. The mean AA reached a maximum value of 2.1 D after the sixth month ($P < 0.05$), and this decreased to 2.0 D at the ninth month without herbal treatments ($P < 0.05$). This indicates that these drugs could still exert positive effects after taking them for six months and further for at least three months without drug intake. The outstanding pharmacologic effects are prolonged because of the increased AA gain. Besides this, pupil size and near vision reached their maximal levels (5.6 mm and J 1.5) in the sixth month. The effective ability of mydriasis and near vision (4.2 mm and J 2.5) was also noted after the ninth month. We suggest that the parasympathetic function is predominant even in the ninth month. The primary pharmacological effects of the improvement in near vision were due to accommodation rather than miosis. A smaller pupil-enhanced DoF (sympathetic function) and good accommodative ability may increase the AA more (parasympathetic function). Cassiae Semen could enhance the accommodation by the parasympathetic effects that obtain AA. Besides this, intake of cassia seeds leads to miosis, followed by the pinhole effect and DoF, and goji berries supply sympathetic effects for dilated pupils. It is interesting that cassia seeds have parasympathetic effects; however, *L. barbarum* in our herbal capsule showed sympathetic effects. We conducted several previous studies and found that the ideal ratio of cassia seeds and *L. barbarum* was 5 : 5, to affect the presbyopic participants to have the best near visual acuity, with dilated pupils. In other words, the parasympathetic function is predominant when taking the designed herbal capsules, while the ratio of cassia seeds and *L. barbarum* was 5 : 5 in our previous small sample of studies after many adjustments (not published yet). The partial ability of the sympathetic function of goji berries may be counteracted by the parasympathetic function from Cassiae Semen. However, just the combined concentrations of two herbal drugs could enhance the near vision at around J 1.5. DD has an anticataract ability. In this study, we used three herbal drugs to offset the decrease in AA in presbyopic subjects. According to past studies, the best-estimated ratio of cassia seeds and *L. barbarum* was 5 : 5. When we added DD, we found the golden ratio of cassia seeds, goji berries, and DD to be 5 : 5:1. The final weight was 200 mg of cassia seeds, 200 mg of goji berries, and 40 mg of DD in one capsule, which may aid in improved AA of the participants.

In general, the symptoms of presbyopic patients worsen significantly between 40 and 50 years of age, with patients complaining about blurred vision at their usual reading distance, ocular strain, and periocular pain. Sometimes, dry eye, diplopia, chromatic aberrations, and even headaches may worsen under dim environments (named night presbyopia). At present, 90% of smartphone users are prone to digital eye strain (so-called computer vision syndrome; CVS) and presbyopia in modern society. Recently, Iqbal et al. reported that smartphone misuse is the main cause of the development and prevalence of CVS among users. Furthermore, through their documented multifocal electroretinogram (mfERG) examinations, they also proved that CVS elicits screen-induced foveal dysfunction. These visual sequelae might also cause simulated near vision troubles related to presbyopia [72]. The occurrence of digital eye strain is similar to presbyopic problems. When viewing examinations, or something, especially for a long period of time, the presbyopic symptoms easily developed and were accompanied by the weakness of the orbicularis oculi muscle and decreased lacrimal gland secretion, which eventually leads to a reduction in blinking reflex and in dry eyes [68–70]. The highest prevalence of presbyopia is in middle-aged patients with decreasing lacrimal function. These individuals always read or work at near distances for long periods of time, which leads to a diminished blinking rate and worsened dry eyes. The pathological mechanisms include the instability of the tear film, tear hyperosmolarity, oxidative stress, and inflammation of the ocular surface [71]. Hence, the administration of both artificial tears and anti-inflammatory drug is prescribed for dry eyes. We propose that polysaccharides in goji berries can enhance the anti-inflammatory functions, inhibiting free radicals and reducing oxidase stress, while betaine protects the cornea from environmental stress and improves the moisture and

nutritional levels in eyes experiencing presbyopia and associated symptoms in our research [20].

Our study also had a few limitations. First, because the number of participants was so large (400), we adopted the subjective method such as push-up test for measuring AA, which was simple and rapid during the experiments. Indeed, various subjective techniques are inadequate for the evaluation of the AA; objective ways such as dynamic retinoscopy may aid in achieving more exact AA. However, it wastes time and involves high technology of performance, which is not suitable for the large sample study. If possible, we could take the subjective and objective AAs simultaneously and average to obtain more exact data. Second, we categorized the participants according to age intervals of five years (between 45 and 70 years), although the changes in presbyopia sometimes varied. Clinically, for some subjects with long-term near work, their AA changes within two to three years rather than five years, and we could not take that into consideration and could only adopt the five-year interval for rough average.

Finally, in our series of experiments, we formulated a mixed herbal capsule that seems to benefit the younger groups that use smartphones and older groups with long-term work and loss of the accommodation ability. We have the desire to manufacture the capsules to help the subjects with difficulty in near working in the future.

5. Conclusion

Presbyopia describes the progressive loss of accommodation, weakness of the contraction of the ciliary muscles, reduction in the elasticity of zonules and lens capsules, and increased stiffness of the lens. The mechanism of our designed treatment is based on enhancing the accommodative ability and pupil control. Besides this, ameliorating the developing cataract formation is also important.

In this study, we proposed a novel herbal combination including Cassiae Semen, wolfberry, and DD for use in presbyopia. The parasympathetic function of cassia seeds could enhance the accommodative system, and the goji berry could supply appropriate effects for the sympathetic nervous system and moisturizing effects for the presbyopic symptoms and associated dry eyes. DD diminishes the progression of cataracts through the inhibition of sorbitol and AGE accumulation, and Cassiae Semen and wolfberry exhibit strong antioxidant abilities. The success rate was approximately 95% after six months of therapy. Therefore, we suggest that herbal drug supplements may be another choice because of their convenience, safety, and persistence of their beneficial pharmacologic functions.

Data Availability

The datasets used during the current study are available from the corresponding author.

Conflicts of Interest

All the authors declared they have no conflicts of interest.

Authors' Contributions

Chi-Ting Horng drafted the manuscript including discussion, performed this study, and corrected all the data. Jui-Wen Ma and Po-Chuen Shieh designed and performed the materials and methods. Moreover, all authors read and approved the final manuscript.

Acknowledgments

A part of this study's flowcharts were supported and designed by Masaru Takeuchi, Chairman and Professor, Department of Ophthalmology, National Defense Medical College, Japan.

References

[1] T. R. Fricke, N. Tahhan, S. Resnikoff et al., "Global prevalence of presbyopia and vision impairment from uncorrected presbyopia," *Ophthalmology*, vol. 125, no. 10, pp. 1492–1499, 2018.

[2] C. Wang, X. Wang, L. Jin et al., "Influence of presbyopia on smartphone usage among Chinese adults: A population study," *Clinical & Experimental Ophthalmology*, vol. 47, no. 7, pp. 909–917, 2019.

[3] G. Sharma, S. Chiva-Razavi, D. Viriato et al., "Patient-reported outcome measures in presbyopia: A literature review," *BMJ Open Ophthalmology*, vol. 5, no. 1, Article ID e000453, 2020.

[4] Y. Bababekova, M. Rosenfield, J. E. Hue, and R. R. Huang, "Font size and viewing distance of handheld smart phones," *Optometry and Vision Science*, vol. 88, no. 7, pp. 795–797, 2011.

[5] O. Idowu, O. Aribaba, A. Onakoya, A. Rotimi-Samuel, K. Musa, and F. Akinsola, "Presbyopia and near spectacle correction coverage among public school teachers in Ifo Township, South-West Nigeria," *Nigerian Postgraduate Medical Journal*, vol. 23, no. 3, pp. 132–136, 2016.

[6] Y. D. Sapkota, S. Dulal, G. P. Pokharel et al., "Prevelance and correction of near vision impairment at Ksaki, Nepal," *Nepalese Journal of Ophthalmology*, vol. 4, no. 1, pp. 17–22, 2012.

[7] S. Kasthurirangan and A. Glasser, "Age-related changes in accommodative dynamics in human," *Vision Research*, vol. 46, no. 8-9, pp. 1507–1519, 2006.

[8] R. A. Schachar, "Cause and treatment of presbyopia with a method for, increasing the amplitude of accoimmodation," *Annals of Ophthalmology*, vol. 24, no. 12, pp. 445–452, 1992.

[9] J. Cumming, SG. Slade, and A. Chayet A, "Clinical evaluation of the model AT-45 silicone accommodating intraocular lens Results of feasibility and the initial phase of a food and drug administration clinical trial," *Ophthalmology*, vol. 108, no. 11, pp. 2005–2009, 2001.

[10] K. Wang and B. K. Pierscionek, "Biomechanics of the human lens and accommodative system: functional relevance to physiological states," *Progress in Retinal and Eye Research*, vol. 71, pp. 114–131, 2019.

[11] S. K. Nandi, J. Rankenberg, M. A. Glomb, and R. H. Nagaraj, "Transient elevation of temperature promotes cross-linking of α-crystallin-client proteins through formation of advanced glycation endproducts: a potential role in presbyopia and cataracts," *Biochemical and Biophysical Research Communications*, vol. 533, no. 4, pp. 1352–1358, 2020.

[12] N. Pescosolido, A. Barbato, R. Giannotti et al., "Age-related changes in the kinetics of human lenses: prevention of the catartact," *International Journal of Ophthalmology*, vol. 9, no. 10, pp. 1506–1517, 2016.

[13] H. Schneider, O. Stachs, K. Göbel, and R. Guthoff, "Changes of the accommodative amplitude and the anterior chamber depth after implantation of an accommodative intraocular lens," *Graefe's Archive for Clinical and Experimental Ophthalmology*, vol. 244, no. 3, pp. 322–329, 2006.

[14] D. Somer, S. Demirci, and F. G. Duman, "Accommodative ability in exotropia: predictive value of surgical success," *Journal of American Association for Pediatric Ophthalmology and Strabismus*, vol. 11, no. 5, pp. 460–464, 2007.

[15] D. Damien Gatinel, "Presbyopia surgery," *La Revue du praticien*, vol. 58, no. 10, pp. 1049–1054, 2008.

[16] A. Abdelkader and HE. Kaufman, "Clinical outcomes of a combined versus separate carbachol and brimonidine drops in correcting presbyopia," *Eye and Vision (Lond)*, vol. 3, 31 pages, 2016.

[17] A. Renna, L. F. Vejarano, E. De la Cruz, and J. L. Alió, "Pharmacological treatment of presbyopia by novel binocularly instilled eye drops: a pilot study," *Ophthalmology and Therapy*, vol. 5, no. 1, pp. 63–73, 2016.

[18] C. Zhang, L. Fan, S. Fan et al., "Cinnamomum cassia presl: a review of its traditional uses, phytochemistry, pharmacology and toxicology," *Molecules*, vol. 24, no. 19, p. 3473, 2019.

[19] C.-T. Horng, M.-L. Tsai, S.-T. Chien et al., "The activity of lowering intraocular pressure of Cassiae seed extract in a DBA/2J mouse glaucoma model," *Journal of Ocular Pharmacology and Therapeutics*, vol. 29, no. 1, pp. 48–54, 2013.

[20] K. J. Chien, C. T. Horng, Y. S. Huang et al., "Effects of *Lycium barbarum* (goji berry) on dry eye diesase in rats," *Molecular Medicine Reports*, vol. 17, no. 1, pp. 809–818, 2013.

[21] J.-P. Luo, Y.-Y. Deng, and X.-Q. Zha, "Mechanism of polysaccharides fromDendrobium huoshanense. On streptozotocin-induced diabetic cataract," *Pharmaceutical Biology*, vol. 46, no. 4, pp. 243–249, 2008.

[22] O. Muftuoglu, B. M. Hosal, and G. Zilelioglu, "Ciliary body thickness in unilateral high axial myopia," *Eye*, vol. 23, no. 5, pp. 1176–1181, 2009.

[23] S. Jacob, D. A. Kumar, A. Agarwal, A. Agarwal, R. Aravind, and A. I. Saijimol, "Preliminary evidence of successful near vision enhancement with a new technique: PrEsbyopic allogenic refractive lenticule (PEARL) corneal inlay using a SMILE lenticule," *Journal of Refractive Surgery*, vol. 33, no. 4, pp. 224–229, 2017.

[24] H. Machačová, E. Vlková, L. Michalcová et al., "Supracor, laser correction of mpresbyopia: one year follow-up outcome," *Ceska a Slovenska Oftalmologie*, vol. 70, no. 4, pp. 146–150, 2014.

[25] R. P. Rutstein, P. D. Fuhr, and J. Swiatocha, "Comparing the amplitude of accommodation determined objectively and subjectively," *Optometry and Vision Science*, vol. 70, no. 6, pp. 496–500, 1993.

[26] E. Long and H. Lin, "Research progress in measurement of human accommodation amplitude," *Eye Science*, vol. 30, no. 3, pp. 110–115, 2015.

[27] GO. Ovenseri-Ogbomo and O. A. Oduntan, "Comparision of measured with calculated of accommodation ion Nigerian children aged 6 to 16 years," *Clinical and Experimental Optometry*, vol. 101, no. 4, pp. 571–577, 2018.

[28] J. E. Wold, A. Hu, S. Chen, and A. Glasser, "Subjective and objective measurement of human accommodative Amplitude," *Journal of Cataract and Refractive Surgery*, vol. 29, no. 10, pp. 1878–1888, 2003.

[29] N. M. Sergienko and D. P. Nikonenko, "Measurement of amplitude of accommodation in young persons," *Clinical and Experimental Optometry*, vol. 98, no. 4, pp. 359–361, 2015.

[30] M. Rosenfield and A. S. Cohen, "Repeatability of clinical measurements of the amplitude of accommodation," *Ophthalmic and Physiological Optics*, vol. 16, no. 3, pp. 247–249, 1996.

[31] A. Faramarzi, A. Bagheri, F. Karimian, H. Shaianfar, M. R. Razzaghi, and S. Yazdani, "Correlation between ocular biometry and amplitude of accommodation in early presbyopia," *European Journal of Ophthalmology*, vol. 25, no. 4, pp. 298–301, 2015.

[32] H. Hashemi, P. Nabovati, M. Khabazkhoob, A. Yekta, M. H. Emamian, and A. Fotouhi, "Does Hofstetter's equation predict the real amplitude of accommodation in children?" *Clinical and Experimental Optometry*, vol. 101, no. 1, pp. 123–128, 2018.

[33] M. Millodot and S. Millodot, "Presbyopia correction and the accommodation in reserve," *Ophthalmic and Physiological Optics*, vol. 9, no. 2, pp. 126–132, 1989.

[34] M. B. Taub and J. Shallo-Hoffmann, "Comparison of three clinical tests of accumulation amplitude Hofstetter's norms to guild diagnosis and treatment," *Optometry & Vision Development*, vol. 43, no. 3, pp. 180–190, 2012.

[35] S. D. Mathebula, M. D. Ntsoane, N. T. Makgaba et al., "Comparison of the amplitude of accommodation determined subjectively and objectively in South African university students," *African Vision and Eye Health*, vol. 77, no. 1, Article ID a431, 2018.

[36] L.-H. Pan, B.-J. Feng, J.-H. Wang, X.-Q. Zha, and J.-P. Luo, "Structural characterization and anti-glycation activityin vitroof a water-soluble polysaccharide *Fromdendrobium huoshanense*," *Journal of Food Biochemistry*, vol. 37, no. 3, pp. 313–321, 2013.

[37] Y. S.-Y. Hsieh, C. Chien, S. K.-S. Liao et al., "Structure and bioactivity of the polysaccharides in medicinal plant *Dendrobium huoshanense*," *Bioorganic & Medicinal Chemistry*, vol. 16, no. 11, pp. 6054–6068, 2008.

[38] G. Benozzi, C. Perez, J. Leiro, S. Facal, and B. Orman, "Presbyopia treatment with eye drops: an eight year retrospective study," *Translational Vision Science & Technology*, vol. 9, no. 7, p. 25, 2020.

[39] L. Boccardo, "Viewing distance of smartphones in presbyopic and non-presbyopic age," *Journal of Optometry*, vol. 14, no. 2, pp. 120–126, 2021.

[40] P. F. Jacques, L. T. Chylack Jr., S. E. Hankinson et al., "Long-term nutrient intake and early age-related nuclear lens opacities," *Archives of Ophthalmology*, vol. 119, no. 7, pp. 1009–1019, 2001.

[41] M. A. Stenvens and J. P. Bergmansom, "Does sunlight casue premature aging of the crystalline lens?" *Journal of the American Optometric Association*, vol. 60, no. 9, pp. 660–663, 1989.

[42] I. K. O. K. Kragha and H. W. Hofstetter, "Bifocal adds and environmental temperature," *Optometry and Vision Science*, vol. 63, no. 5, pp. 372–376, 1986.

[43] M. Takeuchi, P.-C. Shieh, and C.-T. Horng, "Treatment of symptomatic vitreous opacities with pharmacologic vitreolysis using a mixure of bromelain, papain and ficin supplement," *Applied Sciences*, vol. 10, no. 17, p. 5901, 2020.

[44] J. S. Wolffsohn and L. N. Davies, "Presbyopia: Effectiveness of correction strategies," *Progress in Retinal and Eye Research*, vol. 68, pp. 124–143, 2019.

[45] W. N. Charman, "Developments in the correction of presbyopia I: Spectacle and contact lenses," *Ophthalmic and Physiological Optics*, vol. 34, no. 1, pp. 8–29, 2014.

[46] W. N. Charman, "Developments in the correction of presbyopia II: Surgical approaches," *Ophthalmic and Physiological Optics*, vol. 34, no. 4, pp. 397–426, 2014.

[47] H. H. Park, I. K. Park, N. J. Moon, and Y. S. Chun, "Clinical feasibility of pinhole glasses in presbyopia," *European Journal of Ophthalmology*, vol. 29, no. 2, pp. 133–140, 2019.

[48] L. Remón, P. Pérez-Merino, R. J. Macedo-de-Araújo, A. I Amorim-de-Sousa, and J. M González-Méijome, "Bifocal and multifocal contact lenses for presbyopia and myopia control," *Journal of Ophthalmology*, vol. 2020, Article ID 8067657, 2020.

[49] J. L. Alio, A. B. Plaza-Puche, R. Férnandez-Buenaga, J. Pikkel, and M. Maldonado, "Multifocal intraocular lenses: an overview," *Survey of Ophthalmology*, vol. 62, no. 5, pp. 611–634, 2017.

[50] R. H. Breyer, H. Kaymak, T. Ax et al., "Multifocal intraocular lenses and extended depth of focus intraocular lenses," *Asia-Pacific Journal of Ophthalmology (Phila)*, vol. 6, no. 4, pp. 339–349, 2017.

[51] A. Renna, J. L. Alió, and L. F. Vejarano, "Pharmacological treatments of presbyopia: a review of modern perspectives," *Eye and Vision*, vol. 4, no. 1, p. 3, 2017.

[52] B. Gilmartin, M. A. Rosenfield, B. Winn, and H. Owens, "Pharmacological effects on accommodative adaptation," *Optometry and Vision Science*, vol. 69, no. 4, pp. 276–282, 1992.

[53] D. H. Abramson, S. Chang, and J. Coleman, "Pilocarpine therapy in glaucoma," *Archives of Ophthalmology*, vol. 94, no. 6, pp. 914–918, 1976.

[54] C. Kulkani, UR. Chaudhuri, and A. Jagathesan, "Bilateral acute angle-closure glaucoma following with topiramate for headache," *Neurology and Therapy*, vol. 2, no. 1-2, pp. 57–62, 2013.

[55] N. Nyman and L. Reich, "The effect of dapirazole on accommodative amplitude in eyes dilated with 0.5 percent tropicamide," *Journal of the American Optometric Association*, vol. 64, no. 9, pp. 625–628, 1993.

[56] J. V. Greiner and I. J. Udell, "A comparison of the clinical efficacy of pheniramine maleate/naphazoline hydrochloride ophthalmic solution and olopatadine hydrochloride ophthalmic solution in the conjunctival allergen challenge model," *Clinical Therapeutics*, vol. 27, no. 5, pp. 568–577, 2005.

[57] N. R. Biswas, S. Beri, G. K. Das et al., "Comparative double blind multicentric readomised placebo controlled clinical trial of a herbal preparation of eye drops in some ocular aliment," *Journal of Indian Medical Association*, vol. 94, no. 3, pp. 101-102, 1996.

[58] MM. Khan, K. Usmanghani, H. Nazar et al., "Clinical efficacy of herbal coded formulation ocucure for the imprevement of presbyopia: a randomized comparative clinical trial," *Pakistan Journal of Pharmaceutical Sciences*, vol. 27, no. 2, pp. 317–320, 2014.

[59] J. Y. Huang, P. T. Yeh, and Y. C. Hou, "A randomized, double-blind, placebo-controlled study of oral antooxidant supplement therapy in patients with dry eye syndrome," *Clinical Ophthalmology*, vol. 10, pp. 813–820, 2016.

[60] S. Ali, M. S. Watson, R. H. Osborne et al., "The stimulant cathartic, emodin, contracts the rat isolated ileum by triggering release of endogenous acetylcholine," *Autonomic and Autacoid Pharmacology*, vol. 24, no. 4, pp. 103–105, 2004.

[61] H. Amagase, B. Sun, and C. Borek, "*Lycium barbarum* (goji) juice improves in vivo antioxidant biomarkers in serum of healthy adults," *Nutrition Research*, vol. 29, no. 1, pp. 19–25, 2009.

[62] X.-f. Guo, Z.-h. Li, H. Cai, and D. Li, "The effects of *Lycium barbarum* L. (L. barbarum) on cardiometabolic risk factors: a meta-analysis of randomized controlled trials," *Food & Function*, vol. 8, no. 5, pp. 1741–1748, 2017.

[63] M. Yang, J. Ding, X. Zhou et al., "Effects of *Lycium barbarum* polysaccharides on neuropeptide Y and heat-shock protein 70 expression in rats exposed to heat," *Biomedical Reports*, vol. 2, no. 5, pp. 687–692, 2014.

[64] K. Neelam, S. Dey, R. Sim, J. Lee, and K.-G. Au Eong, "Fructus lycii: A natural dietary supplement for amelioration of retinal diseases," *Nutrients*, vol. 13, no. 1, p. 246, 2021.

[65] X.-Q. Zha, X.-L. Li, J.-F. Wang, L.-H. Pan, and J.-P. Luo, "The core structure of a *Dendrobium huoshanense* polysaccharide required for the inhibition of human lens epithelial cell apoptosis," *Carbohydrate Polymers*, vol. 155, pp. 252–260, 2017.

[66] Y. Q. Yi, Q. H. Yang, J. F. Su et al., "Experimental study on preclinical qualiuty control, urgent posion and irrritation of *Dendrobium aurantiacum* eye drops, a class I new drug aganist diabetic cataract," *Zhongguo Zhong Yao Zhi*, vol. 38, no. 7, pp. 1061–1066, 2013.

[67] D. S. Jang, G. Y. Lee, Y. S. Kim, Y. M. Kim, J. L. Yoo, and J. S. Kim, "Anthraquinones from the seeds of *Cassia tora* with inhibitory activity on protein glycation and aldose reductase," *Biological and Pharmaceutical Bulletin*, vol. 30, no. 11, pp. 2207–2210, 2007.

[68] Q. Yao, Y. Zhou, Y. Yang et al., "Activation of Sirtuin1 by *Lyceum barbarum* polysaccharides in protection against diabetic cataract," *Journal of Ethnopharmacology*, vol. 261, Article ID 113165, 2020.

[69] W. Jaschinski, M. König, T. M. Mekontso, A. Ohlendorf, and M. Welscher, "Computer vision syndrome in presbyopia and beginning presbyopia: Effects of spectacle lens type," *Clinical and Experimental Optometry*, vol. 98, no. 3, pp. 228–233, 2015.

[70] J. Valle-Sole, "Spontaneous, voluntary and reflex blinking in clinical practice," *Journal of Clinical Neurophysiology*, vol. 36, no. 6, pp. 415–421, 2019.

[71] C. Coles-Brennan, A. Sulley, G. Young et al., "Management of digital eye strain," *Clinical and Experimental Optometry*, vol. 102, no. 1, pp. 18–29, 2019.

[72] M. Iqbal, O. Said, O. Ibrahim, and A. Soliman, "Visual sequelae of computer vision syndrome: a cross-sectional case-control study," *Journal of Ophthalmology*, vol. 2021, Article ID 6630286, 16 pages, 2021.

Hindawi
Evidence-Based Complementary and Alternative Medicine
Volume 2021, Article ID 4812068, 10 pages
https://doi.org/10.1155/2021/4812068

Research Article

Characterization of a Tumor-Microenvironment-Relevant Gene Set Based on Tumor Severity in Colon Cancer and Evaluation of Its Potential for Dihydroartemisinin Targeting

Bo Liang[1], **Biao Zheng**[1], **Yan Zhou**[2], **Zheng-Quan Lai**[3], **Citing Zhang**[3], **Zilong Yan**[4], **Zhangfu Li**[4], **Xuefei Li**[5], **Peng Gong**[1], **Jianhua Qu**[1,4] and **Jikui Liu**[4]

[1]*Department of General Surgery & Carson International Cancer Research Center, Shenzhen University General Hospital/Shenzhen University Clinical Medical Academy, Shenzhen, Guangdong 518055, China*
[2]*Department of Obstetrics and Gynecology & Carson International Cancer Research Center, Shenzhen University General Hospital/Shenzhen University Clinical Medical Academy, Shenzhen, Guangdong 518055, China*
[3]*Department of Pharmacy, Shenzhen University General Hospital/Shenzhen University Clinical Medical Academy, Shenzhen University, Shenzhen, Guangdong, China*
[4]*Department of Hepatobiliary Surgery, Peking University Shenzhen Hospital, Shenzhen, Guangdong Province, China*
[5]*College of Stomatology, Dalian Medical University, Dalian, Liaoning, China*

Correspondence should be addressed to Peng Gong; doctorgongpeng@hotmail.com, Jianhua Qu; qjh@pkuszh.com, and Jikui Liu; liu8929@126.com

Received 6 May 2021; Accepted 9 June 2021; Published 18 June 2021

Academic Editor: Li Zhang

Copyright © 2021 Bo Liang et al. This is an open access article distributed under the Creative Commons Attribution License, which permits unrestricted use, distribution, and reproduction in any medium, provided the original work is properly cited.

Colon cancer (COAD) is a leading cause of cancer mortality in the world. Most patients with COAD die as a result of cancer cell metastasis. However, the mechanisms underlying the metastatic phenotype of COAD remain unclear. Instead, particular features of the tumor microenvironment (TME) could predict adverse outcomes including metastasis in patients with COAD, and the role of TME in governing COAD progression is undeniable. Therefore, exploring the role of TME in COAD may help us better understand the molecular mechanisms behind COAD progression which may improve clinical outcomes and quality of patients. Here, we identified a Specific TME Regulatory Network including AEBP1, BGN, POST, and FAP (STMERN) that is highly involved in clinical outcomes of patients with COAD. Comprehensive *in silico* analysis of our study revealed that the STMERN is highly correlated with the severity of COAD. Meanwhile, our results reveal that the STMERN might be associated with immune infiltration in COAD. Importantly, we show that dihydroartemisinin (DHA) potentially interacts with the STMERN. We suggest that DHA might contribute to immune infiltration through regulating the STMERN in COAD. Taken together, our data provide a set of biomarkers of progression and poor prognosis in COAD. These findings could have potential prognostic and therapeutic implications in the progression of COAD.

1. Introduction

Colon cancer (COAD) is a common gastrointestinal cancer which is one of the leading causes of cancer deaths in the world. Although the early diagnosis and therapeutic strategy have substantially improved, the COAD-related mortality is still high [1, 2]. Current treatment options for COAD mainly contain surgery resection, radiation therapy, chemotherapy, and immunotherapy. The prognosis predictions for COAD generally rely on biomarkers with a cancer-cell-centric focus, such as the TNM staging system [3, 4]. Recent studies have pointed to the influence of the TME on the development of COAD. Thus, the TME-related factors might have the potential to serve as diagnosis and therapeutic biomarkers.

The tumor microenvironment (TME), as the niche of tumor cells, mainly contains immune infiltration cells, stromal infiltration cells, and many others [5]. Each of the components takes various roles in tumor progression. The crosstalk of

tumor cells with the TME plays a crucial role in tumor progression and treatment efficacy. The impact of the TME has been extensively explored to date, including COAD. Assessment of the TME is confirmed to be a crucial biomarker for the TNM staging system of COAD [6–8]. Immune cell infiltration is proposed as a biomarker for the prognosis and contributes to clinical outcomes of COAD [4]. In the literature, the immune infiltration cells are of great prognostic value in COAD [7, 9, 10]. Furthermore, recent studies have proposed that the TME plays a crucial role in COAD development. Taken together, the TME-related factors might be a potential source of novel diagnostic, prognostic, and therapeutic biomarkers.

Dihydroartemisinin (DHA) is semiartificial synthetic derivative of artemisinin extracted from *Artemisia annua* L. [11]. In a previous study, DHA was shown to exhibit significant antitumor activity across human cancers through inhibition of cancer cell proliferation, migration, and invasion capabilities [11–15]. Although the antitumor function of DHA has been proposed recently, the precise mechanisms underlying antitumor function of DHA are still not as well understood. The role of DHA in the TME has only been reported in few studies. DHA was proposed to prevent progression of head and neck cancer via regulating macrophages in TME [16]. However, whether DHA can influence cancer progression through regulating the TME in COAD is still not well characterized. Therefore, investigation of the correlation between DHA and the TME in COAD might provide a new direction toward novel therapeutic strategies for patients with COAD.

With a goal of improving diagnosis, prognosis, and effective treatment for the patients with COAD, in the present study, we employed the bioinformatic analysis to explore the TME-related biomarkers in COAD. Our results uncovered a Specific TME Regulatory Network (STMERN) that is highly involved in clinical outcomes of patients with COAD. Furthermore, we found that DHA might contribute to progression of COAD through the STMERN. Our study proposed potential correlations among DHA, the TME, and COAD progression which might be exploited in therapeutic approaches in COAD.

2. Materials and Methods

2.1. Survival-Associated Gene Analysis. The GEPIA2 web server was used for survival analysis in COAD [17]. The most differential survival genes were calculated using survival analysis in GEPIA2. The 500 survival-associated genes were screened and arranged according to p values ($p < 0.05$, genes were arranged in ascending order).

2.2. Gene Ontology Analysis (GO). Metascape webtool was used for GO [18]. The 500 survival-associated genes were used as input to perform GO and pathway analyses using Metascape webtool.

2.3. Kaplan–Meier Survival Curve. The GEPIA2 web server was used for Kaplan–Meier Survival Analysis in COAD [17]. The median value of gene expression level was used as the group cutoff.

2.4. Protein-Protein Interaction Analysis (PPI). The protein-protein interactions in Figure 1(b) were predicted using multiple protein interaction function of the STRING database. The gene list contains 11 survival-associated TME genes used as input for PPI analysis.

2.5. Spearman's Correlation Analysis. The GEPIA2 web server was used for comprehensive gene expression analysis [17]. Spearman's correlation coefficients among POSTN, BGN, FAP, and AEBP1 expression levels in COAD were calculated using the correlation analysis function of GEPIA2.

2.6. Correlation between Gene Expression and Clinical Feature. The relationships between target genes and clinical features were examined and visualized using MEXPRESS (Figure 2(b)) and UALCAN (Figures 2(a) and 2(c)) web servers [19, 20].

2.7. Immune Infiltration Analysis. Tumor IMmune Estimation Resource [21, 22] was used for comprehensive analysis of tumor-infiltrating immune cells. The results in Figure 3 were generated using the web server.

2.8. Protein-Ligand Docking. The protein-ligand docking analysis was performed using discovery studio. The protein structures of POSTN, FAP, and BGN were downloaded from the Protein Data Bank [23]. The chemical structure of dihydroartemisinin was downloaded from PubChem [24].

3. Results

3.1. Identification of a Specific TME Regulatory Network (STMERN) in COAD. To explore the relevance of biomarkers to survival in COAD, the genes with the most 500 significant association with patient survival were identified and arranged in COAD using the Most Differential Survival Genes analysis in GEPIA webtool (Figure 4(a)) [17]. To further investigate the biological roles of the survival-associated genes, we then performed gene ontology analysis. The 500 survival-associated genes were used as input to perform the GO and pathway analyses using Metascape webtool. As shown in Figure 4(b), the GO terms showed that a proportion of survival-associated genes was significantly involved in extracellular environment (NABA matrisome associated and extracellular structure organization) alterations which is a major structural component of the TME. These results revealed that the TME might contribute to survival of patients with COAD. In order to deeply explore the functions of the TME in survival of patients with COAD, we identified a set of survival-associated TME genes by taking the intersection from the COAD survival-related genes and extracellular structure organization-related genes from pathway hits of Metascape analysis. As shown in Figure 4(c), a survival-associated TME gene list containing 11 genes was identified. We then carried out Kaplan–Meier overall survival analysis to validate the correlations between

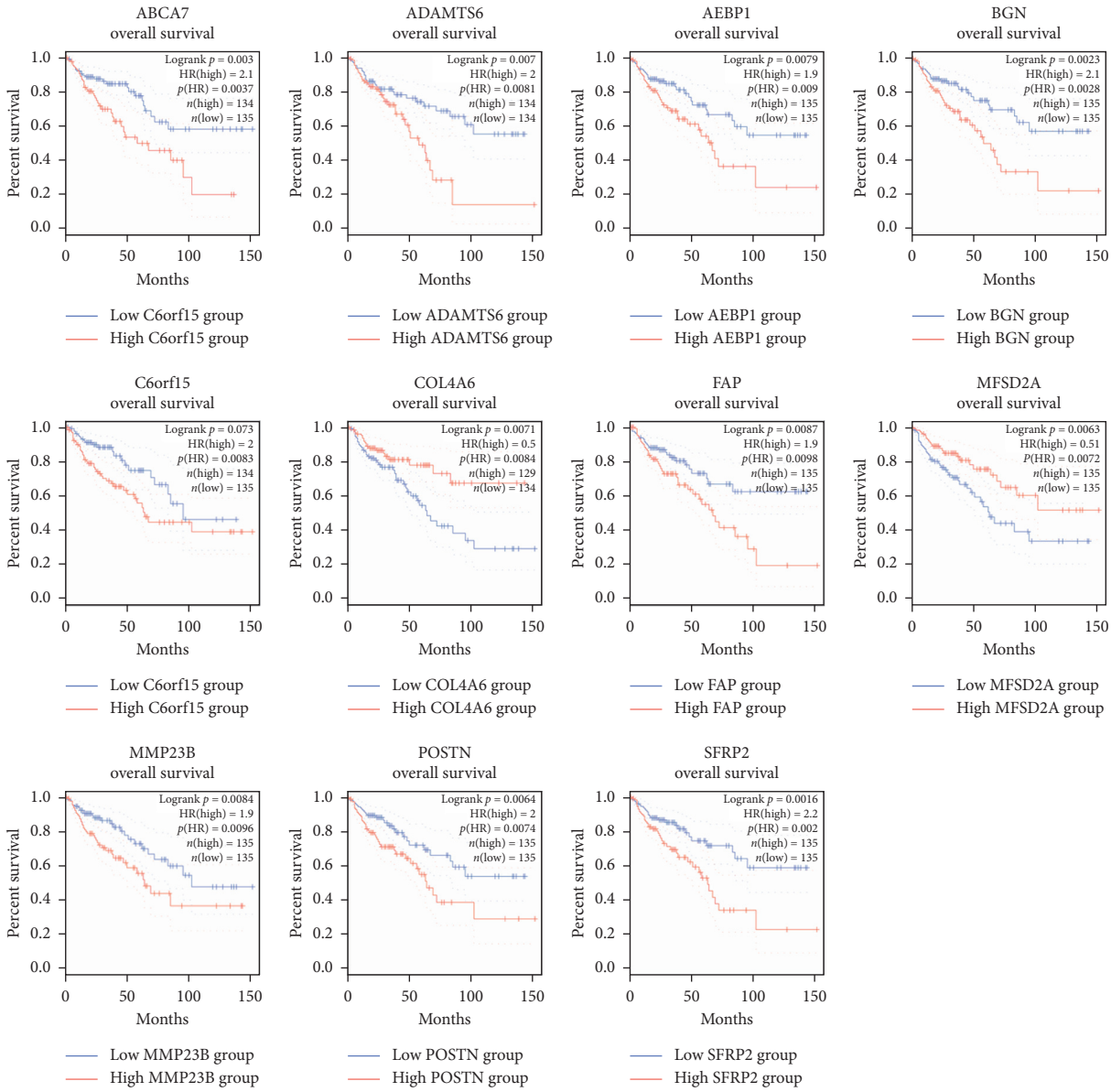

Figure 1: Continued.

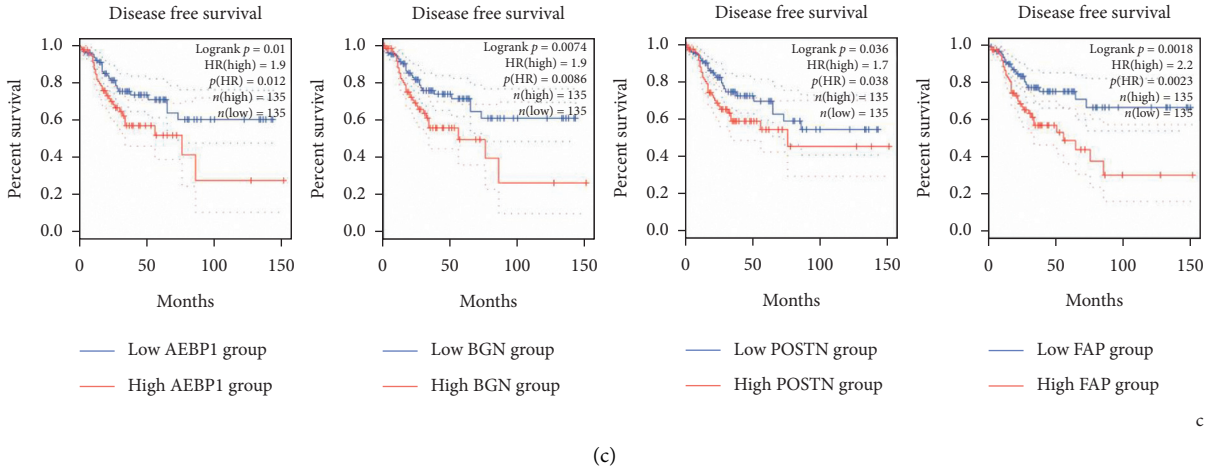

(c)

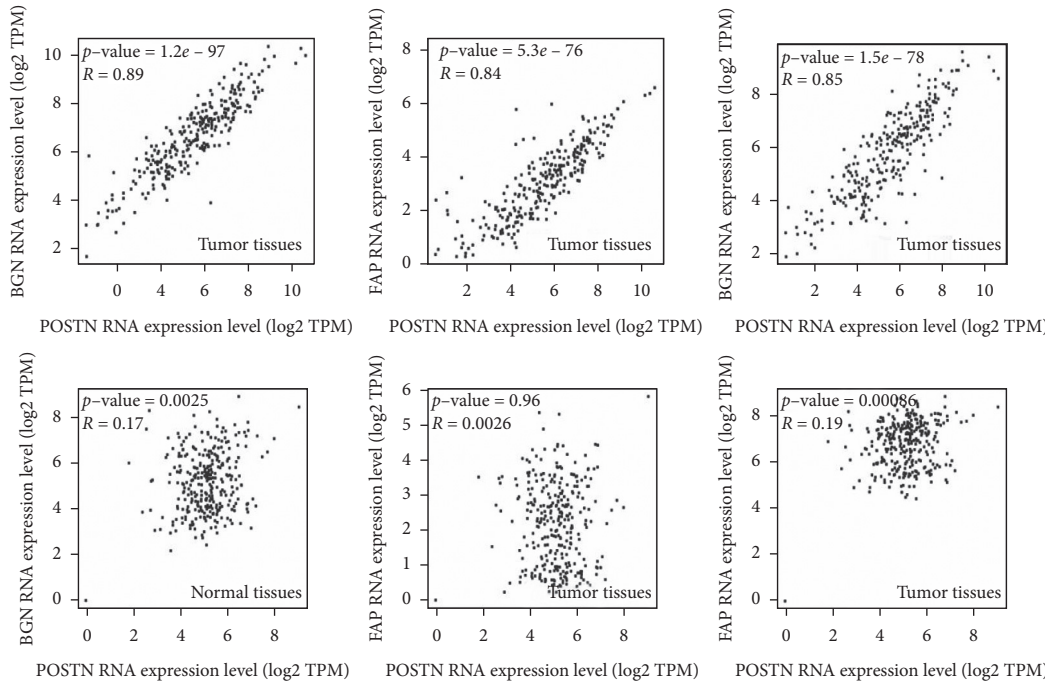

(d)

Figure 1: (a) Kaplan–Meier overall survival analysis of the 11 survival-associated TME genes in COAD. Differences were tested using the log-rank test. The median value of gene expression level was used as the group cutoff. Significant differences between the high-expression group and low-expression group of the 11 survival-associated TME genes in COAD were observed. (b) PPI analysis was carried out using the 11 survival-associated TME genes as the input. A PPI network was identified, including AEBP1, BGN, POSTN, and FAP. (c) Kaplan–Meier disease-free survival analysis of the STMERN in COAD. Differences were tested using the log-rank test. The median value of gene expression level was used as the group cutoff. Significant differences between the high-expression group and low-expression group of the 5 genes of the STMERN in COAD were observed. (d) Spearman' s correlation analysis among the 5 genes of the STMERN in COAD tissues and normal tissues. Significantly higher correlations were observed among the 5 genes of the STMERN in COAD tissues compared to normal tissues.

11 TME-related genes and survival of patients with COAD [17]. Significant differences in survival were observed between high-expression and low-expression groups of the 11 TME-related genes (Figure 1(a)). To further investigate the interactions among the 11 genes, we then performed Protein-Protein Interaction Assay (PPI). As shown in Figure 1(b), we identified a Specific TME Regulatory Network including AEBP1, BGN, POST, and FAP (STMERN). To further validate the correlations between the STMERN and survival of patients with COAD, the Kaplan–Meier disease-free survival was performed. We observed that higher expression of AEBP1, BGN, POST, and FAP was accompanied by worse survival of patients with COAD compared to the lower-expression group (Figure 1(c)). Next, we examined the correlations among the genes in the STMERN. The correlation coefficients were calculated among the expressions of AEBP1, BGN, POST, and FAP in COAD tissues and normal tissues. Intriguingly, as shown in Figure 1(d), we observed extremely highly positive correlations among AEBP1, BGN, POST, and FAP in COAD

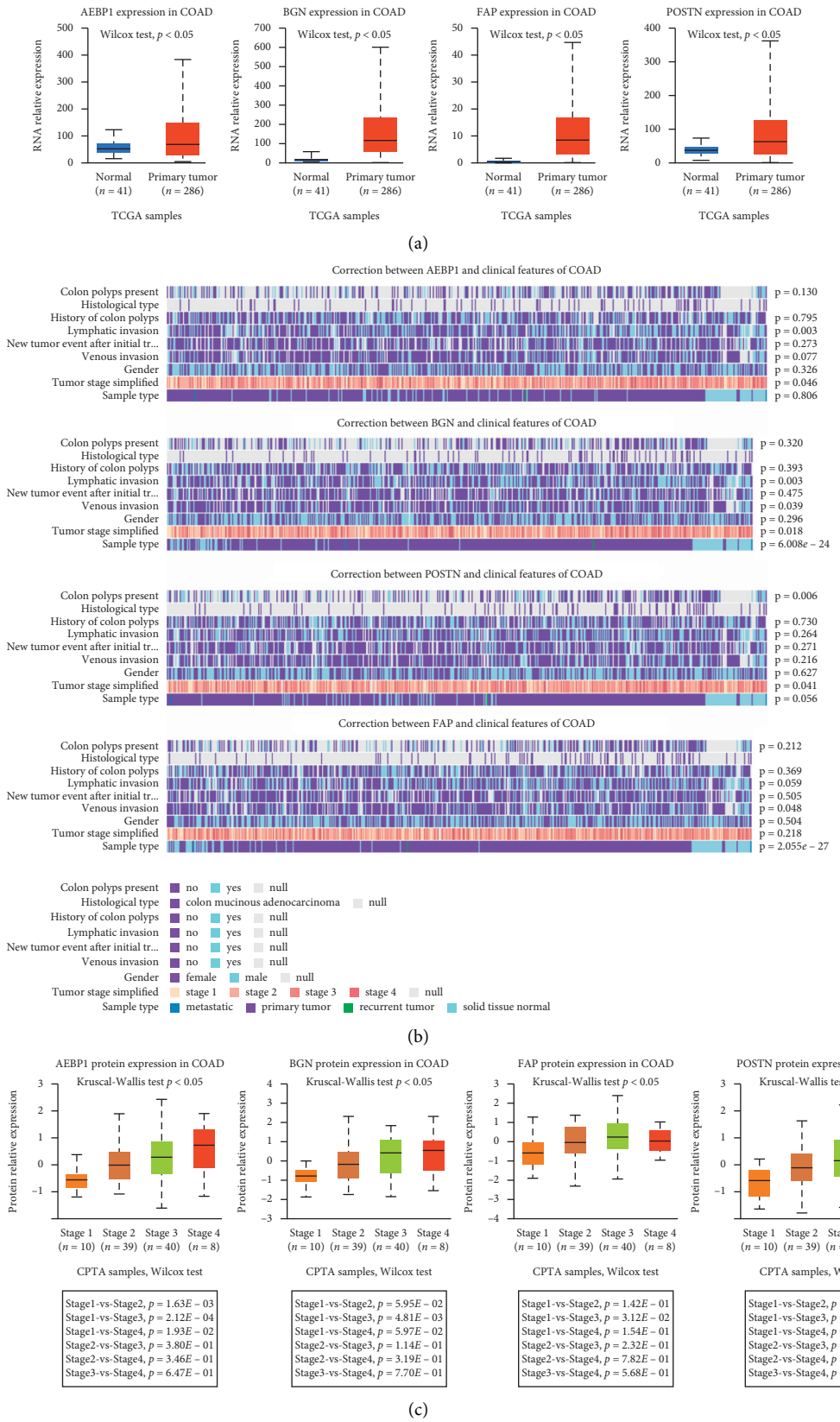

Figure 2: (a) RNA expression patterns of the 5 genes of the STMERN in COAD tissues and normal tissues. (b) The relationships between the RNA expression level of the STMERN and clinical features. (c) The correlations between the protein expression level of the STMERN and tumor stage.

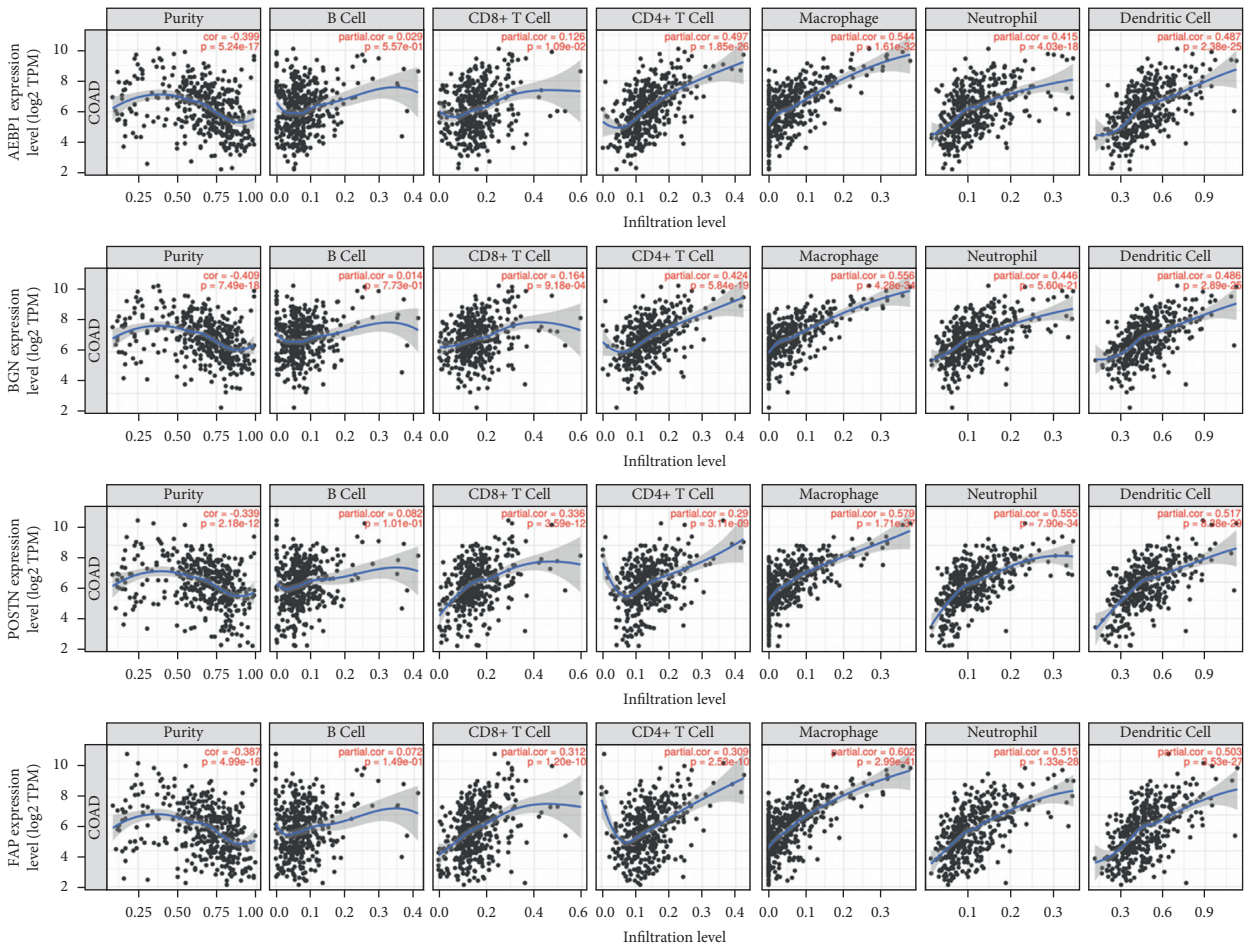

(a)

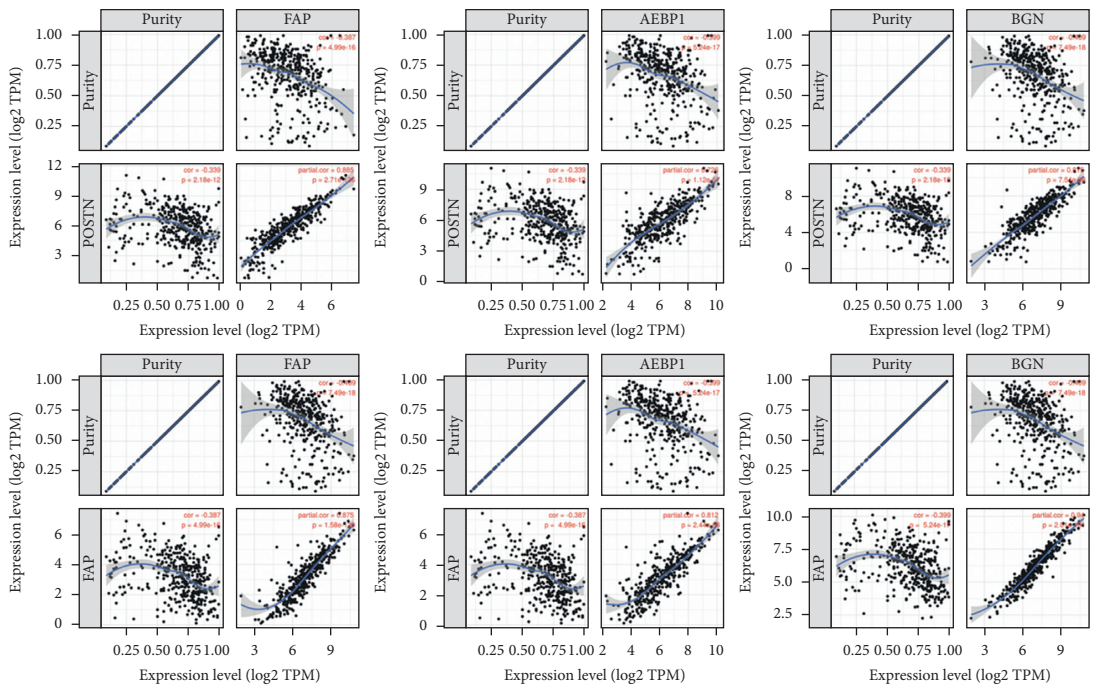

(b)

Figure 3: (a) Correlations between the STMERN and tumor immune infiltration cells in COAD. (b) Correlations among the genes in the STMERN.

tissues. However, compared to COAD tissues, no significant correlations were observed in the network in normal tissues. Taken together, we identified a Specific TME Regulatory Network, which contains AEBP1, BGN, POST, and FAP (STMERN) in COAD. Meanwhile, the extremely highly positive correlations in COAD tissues compared to normal tissues suggest that the STMERN shares a common regulatory mechanism, specifically in COAD.

3.2. Correlations between the STMERN and Clinical Features in COAD. To further explore the clinical role of the STMERN in COAD, the expression pattern of the STMERN was examined in COAD. As shown in Figure 2(a), we examined the expression pattern of the STMERN in both COAD tissues and normal tissues using UALCAN. We observed that AEBP1, BGN, POST, and FAP were highly expressed in COAD tissues at the RNA level (Figure 2(a)) [20]. We then examined the correlations between STMERN expression and clinical features of patients with COAD using MEXPRESS [19]. We found that the STMERN RNA expression pattern was significantly correlated to COAD clinical features including lymphatic invasion, tumor stage, and tumor metastasis (Figure 2(b)). To further validate the correlations between the STMERN expression pattern and clinical features, we then examined the STMERN protein expression pattern using CPTAC analysis [20]. As shown in Figure 2(c), AEBP1, BGN, POST, and FAP expressions were highly positively correlated with tumor stage of patients with COAD at the protein level. We give a brief summary here, and we identified an overexpressed STMERN in COAD, which is highly associated with tumor severity.

3.3. STMERN Was Highly Involved in Immune Cell Infiltration in COAD. To further investigate the regulatory mechanism of the STMERN in TME, we examined the relationship between the STMERN and immune infiltrates using TIMER [21, 22]. We observed quite high correlations between the STMERN and immune infiltration cells (Figure 3(a)), suggesting that the STMERN was associated with immune infiltration in COAD. We then validated the correlations among the genes in the STMERN using TIMER. As shown in Figure 3(b), extremely strong correlations were observed among AEBP1, BGN, POST, and FAP expressions. We also observed a negative correlation between the STMERN and tumor purity. Our results revealed that the STMERN might contribute to the TME through regulating immune cell infiltration.

3.4. Dihydroartemisinin (DHA) Is Potentially Involved in COAD TME Regulating through Targeting the STMERN. DHA is a semiartificial synthetic product originated from Chinese herbal medicine. DHA has potential antitumor therapeutic effects across human cancers through inhibition of cancer cell proliferation, migration, and invasion capabilities. DHA was proposed to regulate the TME in head and neck cancer, breast cancer, and melanoma [16, 25, 26]. However, the effect of DHA in the TME of COAD has not been previously described. In the present study, we assume that DHA might contribute to COAD TME through the STMERN that we identified. To clarify and investigate the interaction between DHA and the STMERN, we performed protein-ligand docking analysis between DHA and the STMERN. The protein structures of BGN, POST, and FAP were downloaded from the PDB website. The DHA structure was downloaded from PubChem. Discovery studio was used for protein-ligand docking. As shown in Figures 5(a)–5(c), BGN, POST, and FAP showed proper docking abilities to DHA. Based on the high correlations between the STMERN and immune infiltration in our study, as well as the docking abilities between DHA and the STMERN, we suggest that DHA might regulate the TME through targeting the STMERN in COAD.

4. Discussion

COAD is one of the deadliest and aggressive forms of cancer in the world. The mechanism underlying progression of COAD remains unclear. Previous studies proposed that the TME could predict adverse outcomes including metastasis in patients with COAD, while the precise function of the TME in governing COAD progression is still uncertain. Thus, exploring the underlying mechanisms of the TME in COAD progression will assist us develop a more sophisticated understanding of the molecular mechanisms underlying COAD progression and, particularly, may improve clinical outcomes and survival quality of patients with COAD. In the present study, we identified a Specific TME Regulatory Network including AEBP1, BGN, POST, and FAP that is highly involved in clinical severity of COAD. Importantly, compared to normal tissues, extremely high correlations were observed among AEBP1, BGN, POST, and FAP in COAD, suggesting that the STMERN specifically formed in tumor tissues. Also, these results proposed a possibility that the formation of the STMERN in COAD might be associated with the changes of the TME in COAD compared to normal tissues. Notably, our results revealed that the STMERN was highly associated with immune infiltration in COAD. Particularly, the STMERN was highly positively correlated with tumor-associated macrophages, neutrophil, and dendritic cells. Significantly, we show that DHA potentially interacts with the STMERN. Therefore, we propose that DHA might be involved in immune infiltration via regulating the STMERN. In summary, our study provides a STMERN which contains biomarkers for severity prediction of patients. Our study provides potential prognostic and therapeutic biomarkers of progression for COAD.

Tumor-associated macrophages is a type of innate immune cells that constitute a plastic and heterogeneous cell population of the TME. Tumor-associated macrophages and their impact on the TME contribute to tumor progression and resistance to therapy [27]. Studies showed that high level of infiltration of tumor-associated macrophages is correlated with poor clinical outcomes, including prognosis and resistance to therapies [28]. Therefore, targeting tumor-associated macrophages is considered as a potential therapeutic strategy in cancer treatment. Tumor-associated

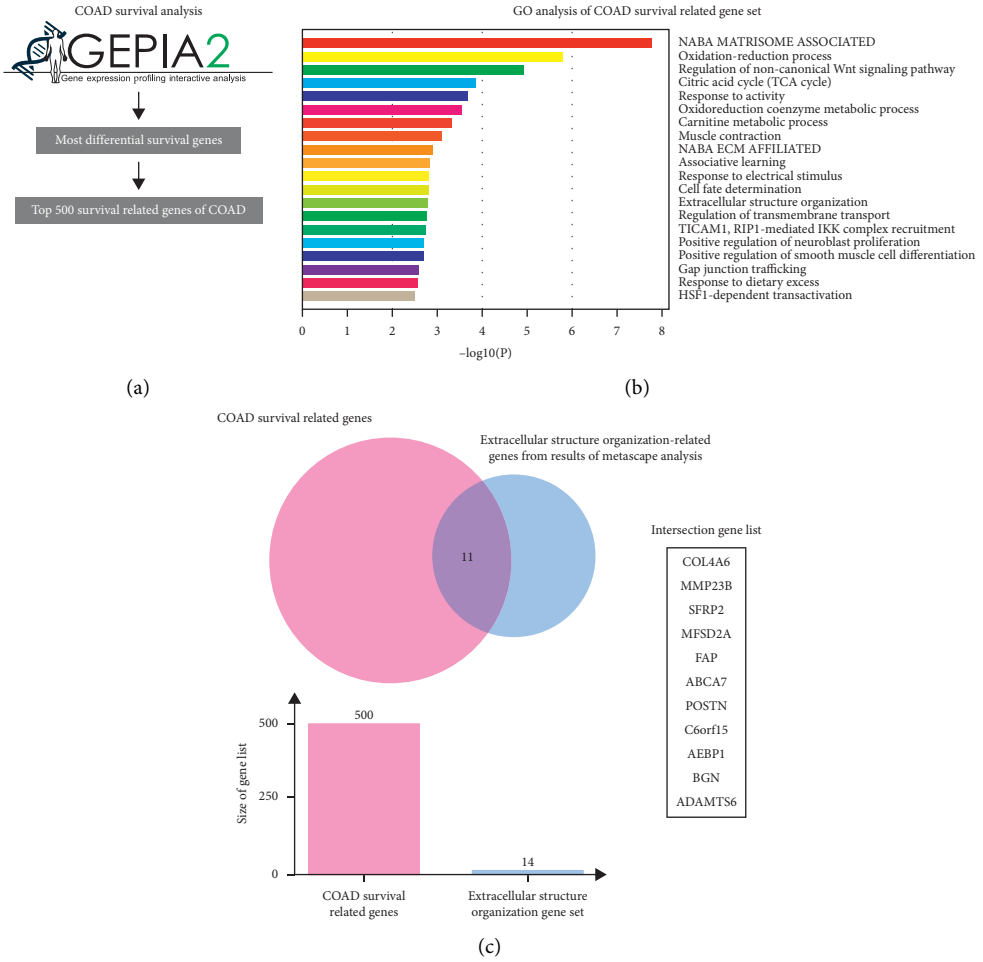

Figure 4: (a) The most differential survival genes were calculated in COAD using GEPIA2. The 500 survival-associated genes were screened and arranged according to p values. (b) GO analysis was performed using the most 500 survival-associated genes as the input. The GO terms showed that a proportion of survival-associated genes were concentrated in extracellular environment alterations which is a major structural component of the TME. (c) Venn analysis was carried out to take the intersection between survival-associated genes and extracellular structure organization-related genes from pathway hits of Metascape analysis in COAD.

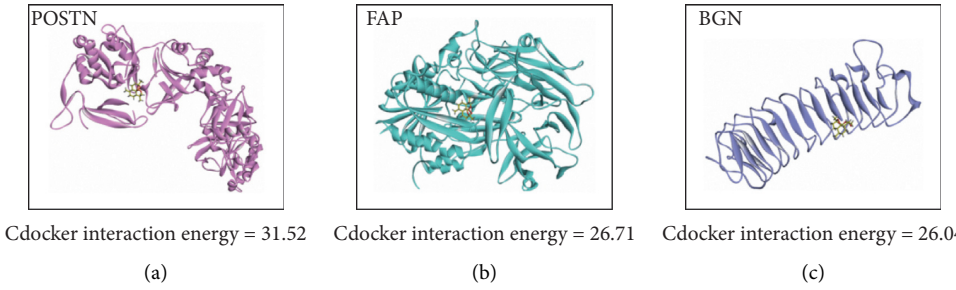

Figure 5: Protein ligand docking. The three-dimensional protein docking models between DHA and POSTN (a), FAP (b), and BGN (c).

dendritic cells are a type of antigen-presenting cells with crucial functions in initiating innate and adaptive immune responses [29, 30]. Recent studies have shown that tumor-associated dendritic cells contribute to cancer progression and can potentially be used as biomarkers and therapeutics [31, 32]. Tumor-associated macrophages and dendritic cells were identified as key mediators of cellular crosstalk in the TME of COAD, which can be harnessed for therapeutics development [33]. Tumor-associated neutrophils are the first response factor to inflammation and infection, which contribute to prognosis and survival, as well as correlate with progression and metastasis in cancer [34, 35]. Accumulating evidence described

tumor-associated neutrophils as key drives of cancer progression via interactions with the TME [36]. Particularly, studies have shown that neutrophils are associated with prognostication and tumor severity in COAD [37–39]. It is, therefore, important to determine the mechanisms under which COAD cells initiate tumor progression through the TME. As the clinical importance of tumor-associated immune cells [4], due to the high correlations between the STMERN and tumor-associated macrophages and neutrophil, as well as dendritic cells, the STMERN might inform novel immune-centered approaches to cancer therapies.

Dihydroartemisinin (DHA) is the primary of artemisinin extracted from *Artemisia annua*, which has been extensively used in treatment of malaria. Increasing studies have indicated that DHA also exhibits anticancer activity [40, 41]. However, the precise mechanisms of DHA underlying cancer treatment are still largely unknown. Previous studies showed that DHA could inhibit COAD cell viability through regulating cell proliferation and apoptosis [15, 42].

The data presented above, in addition to many studies in the literature, indicate that DHA is involved in regulating the TME of cancer [16, 26]. However, there is no publicly available information about the role of DHA in the TME of COAD. STMERN overexpression in aggressive COAD and its correlations with immune infiltration, as well as the interactions of the STMERN to DHA, provide good prospects to our study. Not only does our work provide insights into the association of the STMERN with advanced COAD but also it holds the promise of yielding potential biomarkers and therapeutic strategies for an improved management of COAD. We proposed that DHA potentially contributes to COAD severity by changing the TME through interacting with the STMERN.

5. Conclusions

In the study, we identified a Specific TME Regulatory Network including AEBP1, BGN, POST, and FAP that is highly involved in clinical outcomes of patients with COAD. Furthermore, our results revealed that the STMERN might be associated with immune infiltration in COAD. Importantly, we showed that DHA potentially interacts with the STMERN. Therefore, we suggested that DHA might contribute to immune infiltration via regulating the STMERN in COAD. Our findings have therapeutic implications for the progression of COAD. These results encouraged us to further perform the studies. Future questions arising from our current study will be the direct and indirect interactions between DHA and the STMERN, and we will explore if the STMERN could be identified as a candidate pharmaceutical target in patients with COAD.

Data Availability

The data used to support the results in this manuscript are included within the article.

Conflicts of Interest

The authors declare that there are no conflicts of interest regarding the publication of this study.

Authors' Contributions

Bo Liang, Biao Zheng, and Yan Zhou contributed equally to this article.

Acknowledgments

This work was supported by the Sanming Project of Medicine in Shenzhen (No. SZSM201612021).

References

[1] G. Yothers, M. J. O'Connell, M. Lee et al., "Validation of the 12-gene colon cancer recurrence score in NSABP C-07 as a predictor of recurrence in patients with stage II and III colon cancer treated with fluorouracil and leucovorin (FU/LV) and FU/LV plus oxaliplatin," *Journal of Clinical Oncology*, vol. 31, no. 36, pp. 4512–4519, 2013.

[2] N. W. Wilkinson, G. Yothers, S. Lopa, J. P. Costantino, N. J. Petrelli, and N. Wolmark, "Long-term survival results of surgery alone versus surgery plus 5-fluorouracil and leucovorin for stage ii and stage iii colon cancer: pooled analysis of NSABP C-01 through C-05. a baseline from which to compare modern adjuvant trials," *Annals of Surgical Oncology*, vol. 17, no. 4, pp. 959–966, 2010.

[3] H. Hu, A. Krasinskas, and J. Willis, "Perspectives on current tumor-node-metastasis (TNM) staging of cancers of the colon and rectum," *Seminars in Oncology*, vol. 38, no. 4, pp. 500–510, 2011.

[4] R. Zhou, J. Zhang, D. Zeng et al., "Immune cell infiltration as a biomarker for the diagnosis and prognosis of stage I–III colon cancer," *Cancer Immunol. Immunother.*vol. 68, no. 3, pp. 433–442, 2019.

[5] Z. Xiao, Z. Dai, and J. W. Locasale, "Metabolic landscape of the tumor microenvironment at single cell resolution," *Nature Communications*, vol. 10, no. 1, p. 3763, 2019.

[6] F. Pagès, B. Mlecnik, F. Marliot et al., "International validation of the consensus immunoscore for the classification of colon cancer: a prognostic and accuracy study," *Lancet (London, England)*, vol. 391, no. 10135, pp. 2128–2139, 2018.

[7] J. Galon, A. Costes, F. Sanchez-Cabo et al., "Type, density, and location of immune cells within human colorectal tumors predict clinical outcome," *Science*, vol. 313, no. 5795, pp. 1960–1964, 2006.

[8] Y. Wang, H.-C. Lin, M.-Y. Huang et al., "The immunoscore system predicts prognosis after liver metastasectomy in colorectal cancer liver metastases," *Cancer Immunol. Immunother.*vol. 67, no. 3, pp. 435–444, 2018.

[9] T. Saito, H. Nishikawa, H. Wada et al., "Two FOXP3 + CD4 + T cell subpopulations distinctly control the prognosis of colorectal cancers," *Nature Medicine*, vol. 22, no. 6, pp. 679–684, 2016.

[10] C. Mirjolet, C. Charon Barra, S. Ladoire et al., "Tumor lymphocyte immune response to preoperative radiotherapy in locally advanced rectal cancer: the LYMPHOREC study," *Oncoimmunology*, vol. 7, no. 3, Article ID e1396402, 2018.

[11] C. Z. Zhang, H. Zhang, J. Yun, G. G. Chen, and P. B. S. Lai, "Dihydroartemisinin exhibits antitumor activity toward hepatocellular carcinoma in vitro and in vivo," *Biochemical Pharmacology*, vol. 83, no. 9, pp. 1278–1289, 2012.

[12] J. D. Paccez, K. Duncan, D. Sekar et al., "Dihydroartemisinin inhibits prostate cancer via JARID2/miR-7/miR-34a-dependent downregulation of axl," *Oncogenesis*, vol. 8, no. 3, p. 14, 2019.

[13] Y. Liu, S. Gao, J. Zhu, Y. Zheng, H. Zhang, and H. Sun, "Dihydroartemisinin induces apoptosis and inhibits proliferation, migration, and invasion in epithelial ovarian cancer via inhibition of the hedgehog signaling pathway," *Cancer Medicine*, vol. 7, no. 11, pp. 5704–5715, 2018.

[14] B. Yuan, F. Liao, Z.-Z. Shi et al., "Dihydroartemisinin inhibits the proliferation, colony formation and induces ferroptosis of lung cancer cells by inhibiting PRIM2/SLC7a11 axis," *OncoTargets and Therapy*, vol. 13, pp. 10829–10840, 2020.

[15] Z.-H. Lu, J.-H. Peng, R.-X. Zhang et al., "Dihydroartemisinin inhibits colon cancer cell viability by inducing apoptosis through up-regulation of PPARγ expression," *Saudi Journal of Biological Sciences*, vol. 25, no. 2, pp. 372–376, 2018.

[16] R. Chen, X. Lu, Z. Li, Y. Sun, Z. He, and X. Li, "Dihydroartemisinin prevents progression and metastasis of head and neck squamous cell carcinoma by inhibiting polarization of macrophages in tumor microenvironment," *OncoTargets and Therapy*, vol. 13, pp. 3375–3387, 2020.

[17] Z. Tang, B. Kang, C. Li, T. Chen, and Z. Zhang, "GEPIA2: an enhanced web server for large-scale expression profiling and interactive analysis," *Nucleic Acids Research*, vol. 47, no. W1, pp. W556–W560, 2019.

[18] Y. Zhou, B. Zhou, L. Pache et al., "Metascape provides a biologist-oriented resource for the analysis of systems-level datasets," *Nature Communications*, vol. 10, no. 1, p. 1523, 2019.

[19] A. Koch, J. Jeschke, W. Van Criekinge, M. Van Engeland, and T. De Meyer, "MEXPRESS update 2019," *Nucleic Acids Research*, vol. 47, no. W1, pp. W561–W565, 2019.

[20] D. S. Chandrashekar, B. Bashel, S. A. H. Balasubramanya et al., "UALCAN: a portal for facilitating tumor subgroup gene expression and survival analyses," *Neoplasia*, vol. 19, no. 8, pp. 649–658, 2017.

[21] T. Li, J. Fan, B. Wang et al., "TIMER: a web server for comprehensive analysis of tumor-infiltrating immune cells," *Cancer Research*, vol. 77, no. 21, pp. e108–e110, 2017.

[22] B. Li, E. Severson, J. C. Pignon et al., "Comprehensive analyses of tumor immunity: implications for cancer immunotherapy," *Genome Biology*, vol. 17, no. 1, p. 174, 2016.

[23] G. Fermi, M. F. Perutz, B. Shaanan, and R. Fourme, "The crystal structure of human deoxyhaemoglobin at 1.74 Å resolution," *Journal of Molecular Biology*, vol. 175, no. 2, pp. 159–174, 1984.

[24] S. Kim, J. Chen, T. Cheng et al., "PubChem in 2021: new data content and improved web interfaces," *Nucleic Acids Research*, vol. 49, no. D1, pp. D1388–D1395, 2021.

[25] S. Noori and Z. M. Hassan, "Dihydroartemisinin shift the immune response towards Th1, inhibit the tumor growth in vitro and in vivo," *Cellular Immunology*, vol. 271, no. 1, pp. 67–72, 2011.

[26] R. Yu, L. Jin, F. Li et al., "Dihydroartemisinin inhibits melanoma by regulating CTL/Treg anti-tumor immunity and STAT3-mediated apoptosis via IL-10 dependent manner," *Journal of Dermatological Science*, vol. 99, no. 3, pp. 193–202, 2020.

[27] I. Vitale, G. Manic, L. M. Coussens, G. Kroemer, and L. Galluzzi, "Macrophages and metabolism in the tumor microenvironment," *Cell Metabolism*, vol. 30, no. 1, pp. 36–50, 2019.

[28] K. K. Goswami, T. Ghosh, S. Ghosh, M. Sarkar, A. Bose, and R. Baral, "Tumor promoting role of anti-tumor macrophages in tumor microenvironment," *Cellular Immunology*, vol. 316, pp. 1–10, 2017.

[29] S. K. Wculek, F. J. Cueto, A. M. Mujal, I. Melero, M. F. Krummel, and D. Sancho, "Dendritic cells in cancer immunology and immunotherapy," *Nature Reviews Immunology*, vol. 20, no. 1, pp. 7–24, 2020.

[30] K. F. Bol, G. Schreibelt, K. Rabold et al., "The clinical application of cancer immunotherapy based on naturally circulating dendritic cells," *Journal for ImmunoTherapy of Cancer*, vol. 7, no. 1, p. 109, 2019.

[31] Y. L. Hsu, Y.-J. Chen, W.-A. Chang et al., "Interaction between tumor-associated dendritic cells and colon cancer cells contributes to tumor progression via CXCL1," *International Journal of Molecular Sciences*, vol. 19, no. 8, 2018.

[32] C. E. Bryant, S. Sutherland, B. Kong, M. S. Papadimitrious, P. D. Fromm, and D. N. J. Hart, "Dendritic cells as cancer therapeutics," *Seminars in Cell and Developmental Biology*, vol. 86, pp. 77–88, 2019.

[33] L. Zhang, Z. Li, K. M. Skrzypczynska et al., "Single-cell analyses inform mechanisms of myeloid-targeted therapies in colon cancer," *Cell*, vol. 181, no. 2, pp. 442–459, 2020.

[34] F. Mollinedo, "Neutrophil degranulation, plasticity, and cancer metastasis," *Trends in Immunology*, vol. 40, no. 3, pp. 228–242, 2019.

[35] J. Park, R. W. Wysocki, Z. Amoozgar et al., "Cancer cells induce metastasis-supporting neutrophil extracellular DNA traps," *Science Translational Medicine*, vol. 8, no. 361, Article ID 361ra138, 2016.

[36] P. Lecot, M. Sarabi, M. P. Abrantes et al., "Neutrophil heterogeneity in cancer: from biology to therapies," *Frontiers in Immunology*, vol. 102155 pages, 2019.

[37] S. Rashtak, X. Ruan, B. R. Druliner et al., "Peripheral neutrophil to lymphocyte ratio improves prognostication in colon cancer," *Clinical Colorectal Cancer*, vol. 16, no. 2, pp. 115–123, Article ID e3, 2017.

[38] J. Mazaki, K. Katsumata, K. Kasahara et al., "Neutrophil-to-lymphocyte ratio is a prognostic factor for colon cancer: a propensity score analysis," *BMC Cancer*, vol. 20, no. 1, p. 922, 2020.

[39] R. Mizuno, K. Kawada, Y. Itatani, R. Ogawa, Y. Kiyasu, and Y. Sakai, "The role of tumor-associated neutrophils in colorectal cancer," *International Journal of Molecular Sciences*, vol. 20, no. 3, 2019.

[40] T. Wang, R. Luo, W. Li et al., "Dihydroartemisinin suppresses bladder cancer cell invasion and migration by regulating KDM3A and *p*21," *Journal of Cancer*, vol. 11, no. 5, pp. 1115–1124, 2020.

[41] F. Zhang, Q. Ma, Z. Xu et al., "Dihydroartemisinin inhibits TCTP-dependent metastasis in gallbladder cancer," *Journal of Experimental and Clinical Cancer Research*, vol. 36, no. 1, 2017.

[42] D. Wang, B. Zhong, Y. Li, and X. Liu, "Increases apoptosis of colon cancer cells through targeting Janus kinase 2/signal transducer and activator of transcription 3 signaling," *Oncology Letters*, vol. 15, no. 2, pp. 1949–1954, 2018.